Pectinate ligament dysplasia and primary glaucoma in dogs: investigating prevalence and identifying genetic risk factors

James Andrew Clive Oliver

A thesis submitted for the degree of Doctor of Philosophy

Animal Health Trust and

UCL Institute of Ophthalmology

2018

Declaration

I, James Oliver, confirm that the work presented in this thesis is my own. Where information has been derived from other sources, I confirm that this has been indicated in the thesis.

James Oliver

Acknowledgements

The inception of this project sprung from my experience in treating canine primary glaucoma. The inability to save both the sight and the eyes of affected dogs and provide hope to their owners is a source of continued frustration. My quest, therefore, was to seek help in investigating the genetics of this devastating disease because, as they say, "prevention is better than cure". At the culmination of this frustration, I was lucky to be practising at the Animal Health Trust (AHT), where Cathryn Mellersh, my primary PhD supervisor, and her world renowned Canine Genetics Research team reside. Without Cathryn's encouragement, support and devotion to collaborative research to enhance animal welfare, none of this research would have been possible. Thank you Cathryn.

I must also thank my UCL supervisor Alison Hardcastle who has always been there in the background to offer support and encouragement. I am also indebted to Paul Foster and David Sargan for performing my first year viva and providing their constructive criticisms which helped shape the direction of the project.

My heartfelt thanks extend to Sally Ricketts, Louise Burmeister, Louise Pettitt and Rebekkah Hitti at the AHT for their patience and help in instructing a simple vet in the laboratory and statistical methodology required to perform this work which was an incredibly enjoyable, although at times steep, learning curve.

I also need to thank all the owners who allowed me to examine their dogs and collect DNA from them. Sincere gratitude also extends to Hannes Lohi, Markus Kuehn and Tosso Leeb who shared DNA samples which were used in the GWAS.

Finally, this project would not have been possible without the financial support of Dogs Trust who funded my PhD, and of PetPlan, the European College of Veterinary Ophthalmologists, the British Association of Veterinary Ophthalmologists, the American Kennel Club and the Welsh Springer Spaniel, Flatcoated Retriever and Dandie Dinmont Terrier breed clubs and societies.

Abstract

Canine primary glaucoma is a painful and blinding disease associated with pathologically high intraocular pressure. The two main recognised forms are primary closed angle glaucoma (PCAG) and primary open angle glaucoma (POAG). Pectinate ligament dysplasia (PLD), an abnormality of the iridocorneal angle, is a consistent risk factor for canine PCAG. PCAG and PLD have been shown previously to be highly heritable although inheritance is considered complex. Gonioscopy was performed in > 1100 dogs of seven breeds to provide current estimates of PLD prevalence between September 2013 and March 2016. PLD was associated with age ($P < 0.01$) and there was inter-examiner variability in performing PLD grading ($P = 0.05$). These results have influenced the policy making of the United Kingdom's canine hereditary eye disease scheme. Genome-wide association studies (GWAS) were performed to identify regions of the genome associated with PCAG in four dog breeds. Two loci (chr24:17,381,226-18,739,902 and chr37:24,747,131-24,958,250) were associated with PCAG in the Basset Hound, the former being syntenic with a region previously reported to be associated with primary glaucoma in humans. Meta-analysis of summary data from the Welsh Springer Spaniel and Dandie Dinmont Terrier GWAS analyses revealed an additional (shared) PCAG locus (chr28:18,835,904-19,358,417). Whole genome sequencing was used to interrogate PCAG loci for candidate causal variants and RNA sequencing was used to investigate candidate genes for PCAG in the Basset Hound. For POAG, a candidate gene approach was used to screen *ADAMTS17* for causal mutations in three different dog breeds. POAG was shown to be an autosomal recessive trait associated with a different *ADAMTS17* mutation in each breed (c.193_211del in Basset Hound, c.1552G>A in Basset Fauve de Bretagne and c.3070_3075del in Shar Pei). DNA tests have been developed to enable a reduction in the incidence of POAG in these breeds and a controlled elimination of each mutation over time.

Impact statement

This PhD will deliver considerable positive effects both inside and outside academia that cumulatively will lead to the prevention of inherited forms of glaucoma in multiple populations of purebred dogs, thus positively impacting animal welfare in the short term, and also contributing to an improved understanding of the genetic aetiology of glaucoma in dogs and, potentially, other species in the longer term.

Short term benefits to animal welfare have been achieved through the development of genetic tests to assay for disease-associated mutations and by the generation of current prevalence data for PLD - a risk factor for glaucoma. Thus far, the AHT has tested >400 dogs for the POAG mutations reported in this thesis which will enable breeders to eliminate POAG from their breeds while maintaining genetic diversity. Furthermore, all of the POAG mutations reported are in *ADAMTS17* which emphasises this gene's importance in canine glaucoma, make it a potential candidate for human glaucoma and, potentially, a therapeutic target of the future. The PLD prevalence data will aid breed clubs and veterinary health schemes in future surveillance of this abnormality and will be informative of the benefit of screening for PLD prior to breeding. Previous PLD prevalence data had only been published for the Flatcoated Retriever some 20 years ago and so the current data suggest that the widespread use of gonioscopy testing in this breed has been very successful in reducing PLD (and possibly glaucoma) prevalence in this breed. The PLD data have also influenced the stance of the United Kingdom's canine hereditary eye disease scheme, with regard to recommendations regarding the necessity to perform gonioscopy in certain breeds, the frequency of gonioscopy testing and how PLD can be better graded than the existing system.

In the longer term, publication of the PCAG loci identified in multiple dog breeds will provide a springboard to facilitate identification of candidate genes and variants through further work both by the AHT and by other groups. The significant findings regarding

the genetics of PCAG, a complex disease, will lead to an improved understanding of the underlying genetic architecture of this disease in dogs, offering the potential for improved prevention and/or treatment strategies across species.

Table of contents

List of figures

List of tables

List of abbreviations

x g	Measurement of relative centrifugal force
λ	Lambda – genomic inflation factor
A	Adenine
ADAMTS17	A disintegrin and metalloproteinase with thrombospondin type 1 motifs
AFLP	Amplified fragment length polymorphism
AH	Aqueous humour
AHT	Animal Health Trust
b	Bases (e.g. Mb)
BAM	Binary Aligment/Map
BC	Border Collie
BFdB	Basset Fauve de Bretagne
BH	Basset Hound
bp	Base pairs
BVA	British Veterinary Association
BWA	Burrows-Wheeler Alignment
C	Cytosine
cDNA	Complementary DNA
CFA	*Canis familiaris* chromosome
CI	Confidence interval
DBVD	Dog biomedical variant database
ddNTP	Dideoxynucleotide triphosphate
DDT	Dandie Dinmont Terrier
df	Degree(s) of freedom
DNA	Deoxyribose nucleic acid
dNTP	Deoxyribose nucleoside triphosphate
ECM	Extracellular matrix
ECVO	European College of Veterinary Ophthalmologists
EDTA	Ethylenediaminetetraacetic acid
FAM	Carboxyfluorescein
FPKM	Fragments Per Kilobase Million
FCR	Flatcoated Retriever
g	Gram
G	Guanine
GATK	Genome Analysis Toolkit
GEMMA	Genome-wide Efficient Mixed Model Association
GCL	Ganglion cell layer
gDNA	genomic DNA
GMT	Greenwich Mean Time
GR	Golden Retriever
GWAS	Genome-wide association study (or studies)
HapMap	Haplotype Map
H&E	Haematoxylin and eosin
HTG	High Throughput Genomics (University of Oxford)
HV	Hungarian Vizsla
ICA	Iridocorneal angle
IGV	Integrated Genomics Viewer
Indel	Insertion or deletion
INL	Inner nuclear layer
IOP	Intraocular pressure

- ISDS — International Sheep Dog Society
- KC — Kennel Club
- L — Litre
- m — minutes
- MAF — Minor allele frequency
- MDS — Multi-dimensional scaling
- MMP — Matrix metalloproteinase
- MQ — Milli Q (ultrapure water)
- NFL — Nerve fibre layer
- NA — Not applicable
- No. — Number
- NP — Not performed
- NGS — Next-generation sequencing
- OD260/280 — Optical density at 260nm/280nm wavelength
- OMIM — Online Mendelian Inheritance in Man
- ONH — Optic nerve head
- PACG — Primary angle-closure glaucoma
- PCAG — Primary closed angle glaucoma
- PCR — Polymerase chain reaction
- PL — Pectinate ligament
- PLD — Pectinate ligament dysplasia
- PLL — Primary lens luxation
- POAG — Primary open angle glaucoma
- qPCR — Quantitative polymerase chain reaction
- Q-Q plot — Quantile-quantile plot
- qRT-PCR — Quantitative reverse transcriptase polymerase chain reaction
- RIN — RNA integrity number
- s — Seconds
- SAM — Sequence Alignment/Map
- SD — Standard deviation
- SIFT — Sorting Intolerant from Tolerant
- SNP — Single nucleotide polymorphism
- SP — Shar Pei
- SPARC — Secreted protein acidic and rich in cysteine
- SVP — Scleral venous plexus
- T — Thymine
- TGF — Transforming growth factor
- Tm — Melting temperature
- UCSC — University of California, Santa Cruz
- VCF — Variant Call Format
- VEP — Variant Effect Predictor
- WGS — Whole genome sequence
- WSS — Welsh Springer Spaniel

Metric prefixes

- p — Pico (10^{-12})
- n — Nano (10^{-9})
- µ — Micro (10^{-6})
- m — Milli (10^{-3})
- k — Kilo (10^{3})
- M — Mega (10^{6})

Publications and presentations

Publications

Oliver JAC, Forman OP, Pettitt L, Mellersh CS (2015) Two independent mutations in *ADAMTS17* are associated with primary open angle glaucoma in the Basset Hound and Basset Fauve de Bretagne breeds of dog. *PLoS One*; 11(5):e0156192

Oliver JAC, Ekiri A, Mellersh CS (2016) Prevalence and progression of pectinate ligament dysplasia in the Welsh springer spaniel. *Journal of Small Animal Practice*; 57(8):416-21

Oliver JAC, Ekiri A, Mellersh CS (2016) Prevalence of pectinate ligament dysplasia and associations with age, sex and intraocular pressure in the Basset hound, Flatcoated retriever and Dandie Dinmont terrier. *Canine Genetics and Epidemiology*; 3:1 (doi 10.1186/s40575-016-0033-1)

Oliver JAC, Ekiri A, Mellersh CS (2017) Pectinate ligament dysplasia in the Border Collie, Hungarian Vizsla and Golden Retriever. *Veterinary Record*; 180(11):279

Oliver JAC, Cottrell BC, Newton JR, Mellersh CS (2017) Gonioscopy in the dog: inter-examiner variability and the search for a grading scheme. *Journal of Small Animal Practice*; 58:652-658

Oliver JAC, Rustidge S, Pettitt L, Jenkins CA, Farias FHG, Giuliano EA, Mellersh CS (2018) Evaluation of ADAMTS17 in Chinese Shar-Pei with primary open-angle glaucoma, primary lens luxation, or both. *American Journal of Veterinary Research*; 79:98-106

Oliver JAC, Ricketts SL, Kuehn MH, Mellersh CS (2019) Primary closed angle glaucoma in the Basset Hound: Genetic investigations using genome-wide association and RNA sequencing strategies. *Molecular Vision*; 25: 93-105

Presentations (oral)

Oliver JAC (2014) Goniodysgenesis and glaucoma in the Welsh Springer Spaniel: a candidate gene study. 45th Annual Meeting of the American College of Veterinary Ophthalmologists, Texas, USA.

Oliver JAC (2015) Prevalence of pectinate ligament dysplasia and associations with age, sex and IOP in the Basset Hound, Flatcoated Retriever and Dandie Dinmont Terrier. Annual Meeting of the European College of Veterinary Ophthalmologists, Helsinki, Finland.

Oliver JAC (2015) Prevalence and progression of pectinate ligament dysplasia in the Welsh Springer Spaniel. Annual Meeting of the European College of Veterinary Ophthalmologists, Helsinki, Finland.

Oliver JAC (2015) Two independent mutations in *ADAMTS17* are associated with primary open angle glaucoma in the Basset Hound and Basset Fauve de Bretagne breeds of dog. 8th International Conference on Advances in Canine and Feline Genomics and Inherited Disease, Cambridge, UK.

Oliver JAC (2017) A novel *ADAMTS17* mutation is associated with primary open angle glaucoma and primary lens luxation in the Shar Pei. 9th International Conference on Advances in Canine and Feline Genomics and Inherited Disease, St Paul, USA.

Oliver JAC (2017) Multi-breed genome-wide association studies reveal a novel locus for canine primary closed angle glaucoma. 9th International Conference on Advances in Canine and Feline Genomics and Inherited Disease, St Paul, USA.

Oliver JAC (2018) Primary closed angle glaucoma in the Basset Hound: Genetic investigations using genome-wide association and next-generation sequencing strategies. Annual Meeting of the European College of Veterinary Ophthalmologists, Florence, Italy.

1 Introduction

1.1 Anatomy and physiology of the canine aqueous humour outflow pathways

1.1.1 Aqueous humour and intraocular pressure

Aqueous humour (AH) is the fluid that fills the anterior and posterior chambers of the eye and is secreted by the epithelium of the ciliary processes of the ciliary body which are located in the posterior chamber. AH functions to deliver nutrients to and remove metabolic waste from the intraocular tissues and it is the constant balance between AH production and drainage that maintains intraocular pressure (IOP) within a physiological range which, in the dog, is generally considered to be 10 - 25 mmHg[1-3]. IOP values may vary in relation to time of day, breed and age. Canine IOP follows a similar circadian phase as humans, with highest IOP values occurring in the morning and lowest in the evening[2,3]. Advancing age is associated with a decrease in IOP in the dog[1]. The reason for this is unknown but most likely relates to a reduction in AH production as AH outflow is thought to reduce with age[4].

1.1.2 Aqueous humour outflow pathways

AH may leave the eye via two main routes:

- The conventional outflow pathway
- The unconventional outflow pathway

Conventional outflow occurs down a pressure gradient and is pressure-dependent[5]. This form of outflow accounts for approximately 85 % of total AH outflow from the normal canine eye[6]. Unconventional outflow is passive and largely independent of IOP being regulated mostly by osmotic gradients[7]. This form of outflow accounts for approximately 15 % of AH outflow from the normal canine eye[6]. Compromise of AH

outflow leads to increased IOP which is considered a constant risk factor in canine glaucoma and a major risk factor in human glaucoma. In simple terms, elevated IOP in the anterior segment is transmitted to the posterior segment leading to death of retinal ganglion cells and their axons (**Figure 1.1**).

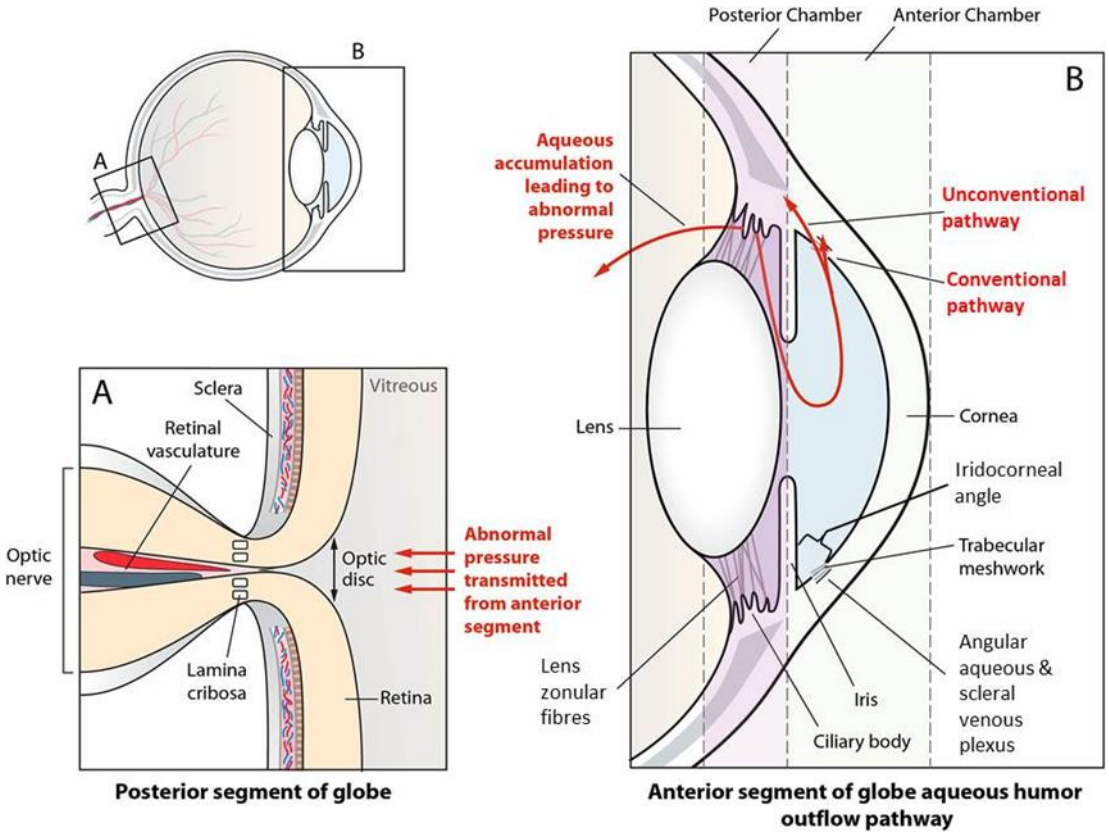

Figure 1.1. Schematic of the eye.

Sub-image A demonstrates the elevated intraocular pressure transmitted to the posterior segment of the globe in the glaucomatous eye where retinal ganglion cells and their axons reside. Sub-image B reflects the aqueous humour outflow pathways (modified from Danford et al.[8]).

1.1.2.1 The conventional outflow pathway

The majority of AH drains peripherally from the anterior chamber via the iridocorneal angle (ICA) into the sieve-like trabecular meshwork of the ciliary cleft before entering a plexus of channels which drains into the eye's venous system. The histological appearance of the normal canine ICA is depicted in **Figure 1.2**. The ICA is bordered

anteriorly by the peripheral cornea and perilimbal sclera and posteriorly by the iris base and anterior ciliary body musculature. The normal canine ICA is spanned by numerous, fine, branching stands of iris tissue which connect the anterior iris base to the posterior cornea. These 'fibres' are collectively termed the pectinate ligament (PL). A single PL fibre is composed of a collagen core which is completely encased in cells (melanocytes and fibroblasts) which are confluent with the iris surface[9]. The PL fibres branch frequently and anastomose with the trabecular beams within the anterior ciliary cleft. The ciliary cleft is the peripheral circumferential region posterior to the ICA and contains the trabecular meshwork through which AH drains via bulk flow down a pressure gradient[5]. The trabecular meshwork is composed of the anterior uveal and the posterior corneoscleral meshworks. The trabeculae, like the PL fibres, also have a collagen core, but this is interspersed with modified elastin and other extracellular matrix (ECM) proteins including laminin and fibronectin[10]. The trabeculae are lined by cells (trabeculocytes) which are thought to play an important role in regulating outflow and therefore IOP. Trabeculocytes have phagocytic properties allowing them to digest trapped particles and they also have the ability to increase ECM turnover in response to mechanical strain[11]. Trabeculocytes also produce several non-structural proteins that regulate ECM turnover and remodelling including transforming growth factor beta-2 (TGFβ-2), myocillin, stromelysin, secreted protein acidic and rich in cysteine (SPARC), thrombospondin -1 and -2, bone morphogenetic protein-7, tenascin C and matrix metalloproteinases and their inhibitors[12-19]. From interior to exterior, the trabeculae become smaller and more closely approximated to each other allowing the trabecular meshwork to act like a sieve, reducing the particle size within the AH as it filters from the uveal to the corneoscleral trabecular meshworks.

From the corneosceral trabecular meshwork, AH must then traverse the juxtacanalicular tissue before entering the vascular network that is the angular aqueous plexus (similar to

the Schlemm's canal of primates). The juxtacanalicular tissue is a thin layer (5 - 20 μm thick) containing fibroblast-like cells within an ECM of proteoglycans (including versican and perlecan) and their associated glycosaminoglycans (including dermatan sulphate, chondroitin sulphate and hyaluronic acid). Structural and functional proteins present include fibrillar and non-fibrillar collagen, elastin, fibronectin and laminin[20]. This ECM is thought to be critically important in providing resistance to AH outflow and therefore IOP regulation[21]. Evidence for this comes from experimental treatment with hyaluronidase which resulted in reduction of IOP[22]. It is thought that the glycosaminoglycans of the ECM assist in IOP regulation by altering the state of their polymerisation which controls their capacity for hydration.

AH must then move from the juxtacanalicular tissue across the endothelium (inner wall) of the angular aqueous plexus before subsequent drainage into the distal outflow vessels. AH makes the transition into the plexus via the formation of endothelial vacuoles and intercellular and intracellular pores. The plexus interconnects with radial collector vessels which, in turn, drain into the anterior ciliary veins or the scleral venous plexus. Longitudinal ciliary muscle fibres insert on the elastic fibre system (composed of an elastin core with surrounding microfibrils composed of fibrillin-1 and microfibrillar-associated proteins -1 and -2) of the trabecular meshwork and juxtacanalicular tissue. Furthermore, myofibroblastic cells have been observed within the inner, posterior region of the corneoscleral and outer, posterior region of the uveal trabecular meshworks. These findings suggest that these cells and the smooth muscle cells of the ciliary body along the same plane of orientation function to facilitate the removal of AH by maintaining opening of the spaces of the angular aqueous plexus[23].

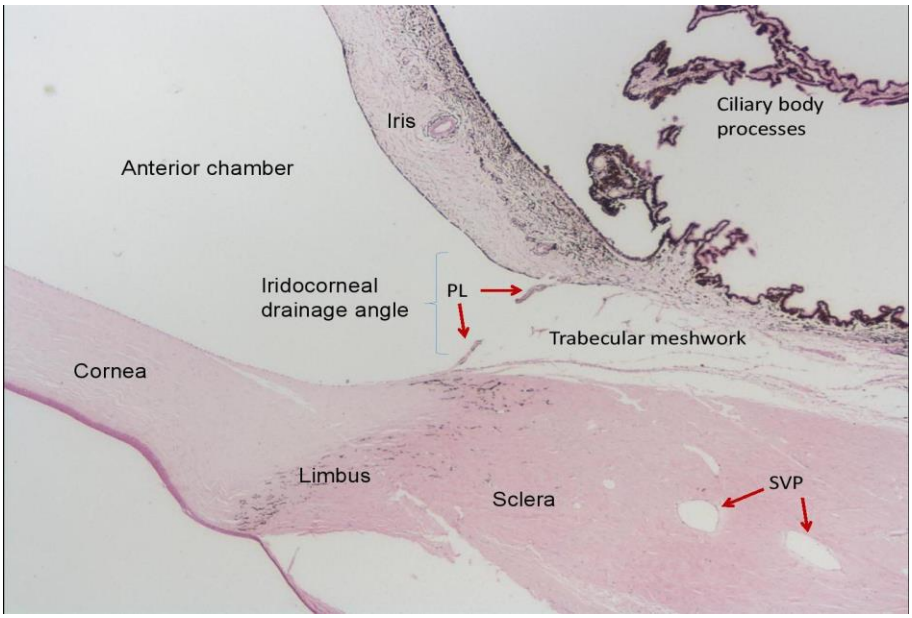

Figure 1.2. Histological appearance of the normal canine ICA (H&E x 20).

PL = pectinate ligament fibres. SVP = scleral venous plexus. Photograph courtesy of Emma Scurrell, CytoPath Ltd.

1.1.2.2 The unconventional outflow pathway

In the unconventional route, AH still traverses the trabecular meshwork but, instead of moving anteriorly across the juxtacanalicular tissue and into the angular aqueous plexus, it is directed posteriorly through ciliary body. AH passes through the connective tissue between the longitudinal muscle fibres of the ciliary body (which attach to the ICA trabeculae) before collecting in the potential uveoscleral space. From here, AH enters the suprachoroidal space before entering choroidal and scleral blood vessels. AH flow via this pathway is thought to be relatively independent of IOP being instead driven by a difference in osmotic pressure created between the colloids within the choroidal and scleral blood vessels and the ciliary body tissue[24].

1.1.2.3 Embryology of the ICA and pectinate ligament dysplasia

Development of the ICA occurs in three sequential steps:

1. Separation of anterior mesenchyme into corneoscleral and uveal regions followed by differentiation of ciliary muscle and folding of neuroectoderm into the ciliary processes.
2. Enlargement of corneal trabeculae and development of spaces within the trabecular meshwork, accompanied by regression of the corneal endothelium that covers the opening to the ICA.
3. Postnatal remodeling of the ICA aided by cellular necrosis and macrophage-mediated phagocytosis. This results in further opening of the spaces within the trabecular meshwork and the outflow pathways.

In the dog, a species born with fused eyelids, the peripheral iris and cornea are in contact at birth. As in other species, differential growth occurs with posterior movement of the iris and ciliary body relative to the cornea revealing the trabecular meshwork and outflow pathways as the ICA deepens[25]. Early studies in the Beagle have described maturation of the ICA in dogs reporting its morphology to be complete by eight weeks after birth[26,27]. Specifically, the fibres which collectively form the PL are thought to form by a process of rarefaction of an initial sheet of mesenchymal tissue spanning the ICA[27,28]. Pectinate ligament dysplasia (PLD) describes the broad sheets of tissue which span the ICA (extending from the base of the anterior surface of the iris to the periphery of the posterior cornea) thought to result from a lack of this rarefaction during this time frame (**Figure 1.3**). PLD is thus a form of goniodysgenesis, which is defined as abnormal development of the ICA, and is considered a risk factor for the development of canine primary closed angle glaucoma (PCAG) based on the finding that severe PLD is associated with PCAG in affected eyes in numerous breeds[29-33].

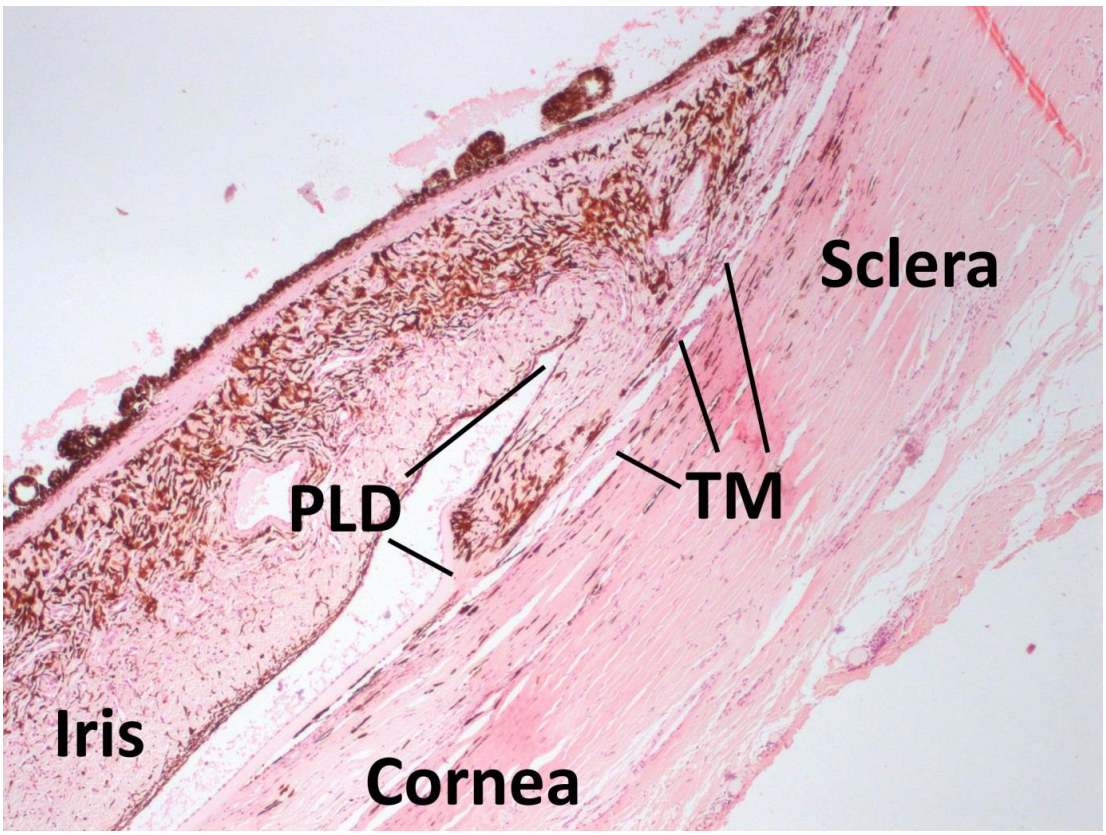

Figure 1.3. Histological appearance of PLD in a dog without PCAG (H&E x 40).

Beams of the trabecular meshwork can be seen within the extremely narrowed ciliary cleft. Photograph courtesy of Emma Scurrell, CytoPath Ltd.

1.1.2.4 The effect of aging on the aqueous humour outflow pathways

Numerous changes associated with advancing age have been documented to occur within the outflow pathways most of which confer increased resistance to AH outflow. Age-related narrowing of the canine ICA has been documented in more than one breed with progressive reduction in the width of the ciliary cleft being associated with an increasingly shallow anterior chamber[29,34]. Progression of PLD in individual dogs over time has also recently been demonstrated, which challenged the original theory that this anomaly is always a congenital one. In a study of 96 Flatcoated Retrievers (FCR), 39 (40.6 %) demonstrated progression of PLD 1.92 - 12.58 years later (mean 6 years, median 5.75 years) with 12 (12.5 %) demonstrating progression to severe PLD and

being considered at risk of glaucoma development[35]. PLD progression over time in other breeds had not yet been reported.

It is known that the beams of the trabecular meshwork become thicker with age in dogs but other changes are not well described in this species[22,36]. In primates, several changes within the trabecular meshwork and juxtacanalicular tissue have been documented. There is age-related trabeculocyte loss which appears to occur at a higher rate in primates with primary open angle glaucoma (POAG) than in age-matched controls[37,38]. As trabeculocytes have phagocytic properties, such loss may result in an accumulation of debris within the trabecular meshwork leading to an increased resistance to outflow. It is known that fibronectin, a major component of the trabecular meshwork, accumulates with age although the significance of this is not fully understood[39]. There is also increased cross-linking of the fibres of the trabecular meshwork's elastin system which leads to reduced compliance of the tissue and potential capacity for modulation of outflow[40]. This increased stiffness of the ECM is likely to be most important in the juxtacanalicular tissue – a region thought to be pivotal in IOP determination.

1.2 Classification and pathophysiology of canine primary glaucoma

The glaucomas constitute a heterogeneous group of diseases characterised by retinal ganglion cell apoptosis and optic neuropathy (**Figure 1.4** and **Figure 1.5)**. Primary glaucoma in dogs refers to those glaucomas which are thought to occur as a result of inherent defects in the AH outflow pathways which lead to IOP dysregulation. Primary glaucoma is generally considered to be a bilateral condition and occurs in the absence of any other identifiable intraocular disease such as haemorrhage, inflammation, neoplasia and lens luxation[41]. Canine primary glaucoma is relatively poorly characterised which likely relates in part to the late presentation of affected dogs. Affected eyes usually have very advanced disease associated with markedly elevated IOP, blindness and pain. Painless forms are not recognised. Canine primary glaucomas are traditionally divided

into two categories based on the appearance of the ICA as seen on gonioscopy. These are PCAG and POAG. Exact diagnostic criteria for canine PCAG and POAG are not published. For the purposes of this study, the following diagnostic criteria were employed:

PCAG

- Closed ICAs on gonioscopy
- Elevated IOP > 50mmHg
- The absence of any possible cause of secondary glaucoma
- The finding of severe PLD (>90 % of the ICA affected) in the contralateral eye

POAG

- Open ICAs on gonioscopy
- Elevated IOP > 25mmHg
- The absence of any possible cause of secondary glaucoma
- The absence of PLD in the contralateral eye
- Buphthalmos
- Lens subluxation

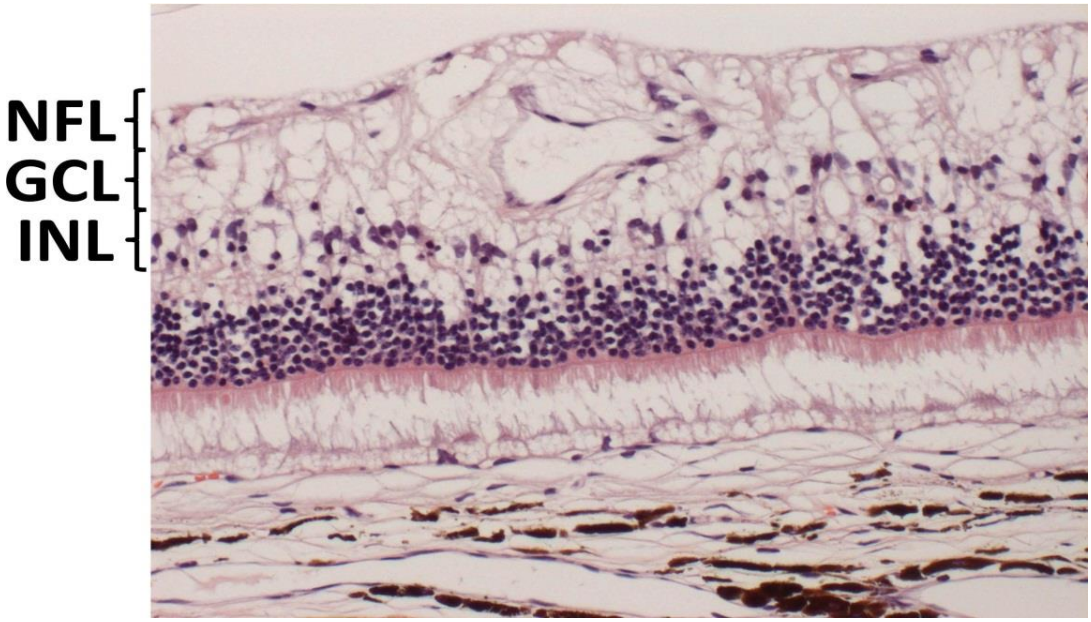

Figure 1.4. Histological appearance of the retina in a dog with PCAG (H&E x 100).

There is atrophy of the inner retinal layers. NFL = nerve fibre layer, GCL = ganglion cell layer, INL = inner nuclear layer. Photograph courtesy of Emma Scurrell, CytoPath Ltd.

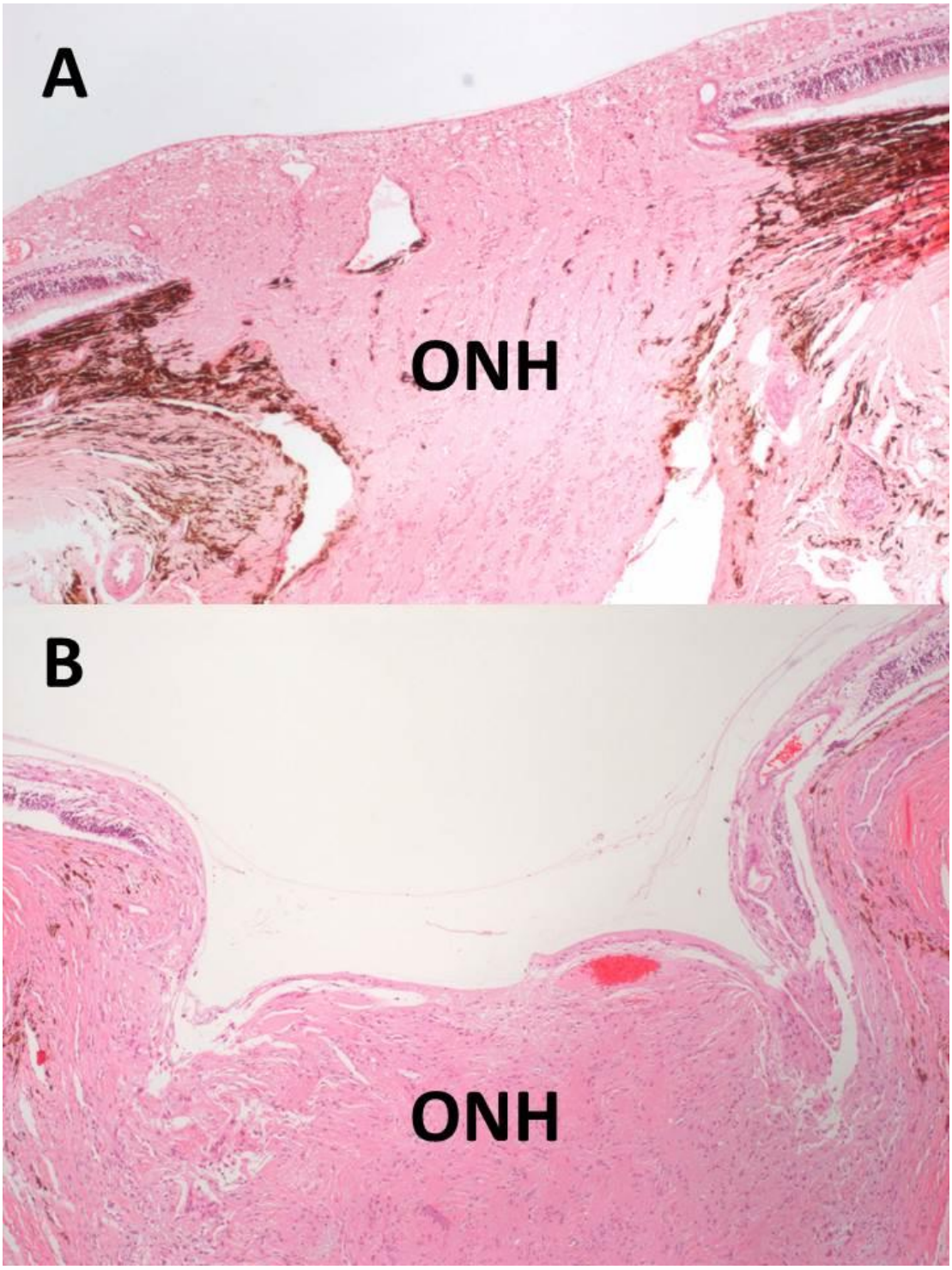

Figure 1.5. Histological appearances of the optic nerve head (ONH) (H&E x 40).

A) The appearance of a normal ONH in a normotensive canine eye. B) The ONH in a canine eye with PCAG. The ONH is posteriorly displaced ('cupped') as a result of chronic IOP elevation. Courtesy of Emma Scurrell, CytoPath Ltd.

1.2.1 Gonioscopy

Gonioscopy describes the examination of the anterior ICA and ciliary cleft, and normal gonioscopic findings in the dog are presented in **Figure 1.6**[42]. Like many species, the canine ICA cannot be directly visualised as it is obscured by the scleral shelf. If examination at an oblique angle is attempted, the ICA cannot be visualised owing to the phenomenon of total internal reflection of light rays which occurs when light rays pass from a medium of higher refractive index (1.376 for the cornea) to one of lower refractive index (1.00 for air). The application of a contact lens (goniolens) removes the cornea-air interface creating a new contact lens-air interface and overcomes this phenomenon. Goniolenses may be direct or indirect. In dogs, direct goniolenses are most commonly employed and overcome the phenomenon of total internal reflection by virtue of their relative convexity. The Koeppe lens is an example of a commonly used direct goniolens[43]. Following topical anaesthesia of the cornea and application of a coupling gel to the concave side of the lens, it is placed onto the surface of the cornea in the conscious dog (**Figure 1.7).** The lens is held in place by a combination of vacuum forces and a small flange which surrounds the lens and sits in the conjunctival fornices under the eyelids. The ICA is then examined with the aid of a light source and, usually, magnification. A portable slit-lamp biomicroscope is most practical for these combined purposes in the dog. The entire ICA and ciliary cleft opening are then systematically evaluated giving attention to PL conformation and ICA width. As described above, the normal PL consists of fine strands of iris tissue which extend from the iris base to the corneal endothelium. The line of insertion is referred to as the deep pigmented line[44]. A

more superficial and less densely pigmented zone represents the pigmentation of the corneoscleral limbus and is known as the superficial pigmented line. The presence and thickness of these two lines varies from dog to dog (being correlated with coat colour) and also even between different quadrants of the same eye[42]. The appearance of the PL itself is variable, particularly between breeds[42]. Dogs with darkly pigmented irides usually have darkly pigmented and obvious PL fibres, whereas in dogs with pale or blue irides, the PL fibres may be extremely fine and difficult to visualise. Fibrae latae describe the presence of broad PL fibres and a small percentage of these within a given ICA is deemed normal variation which is in contrast to the sheets of tissue which represent PLD (**Figure 1.8**).

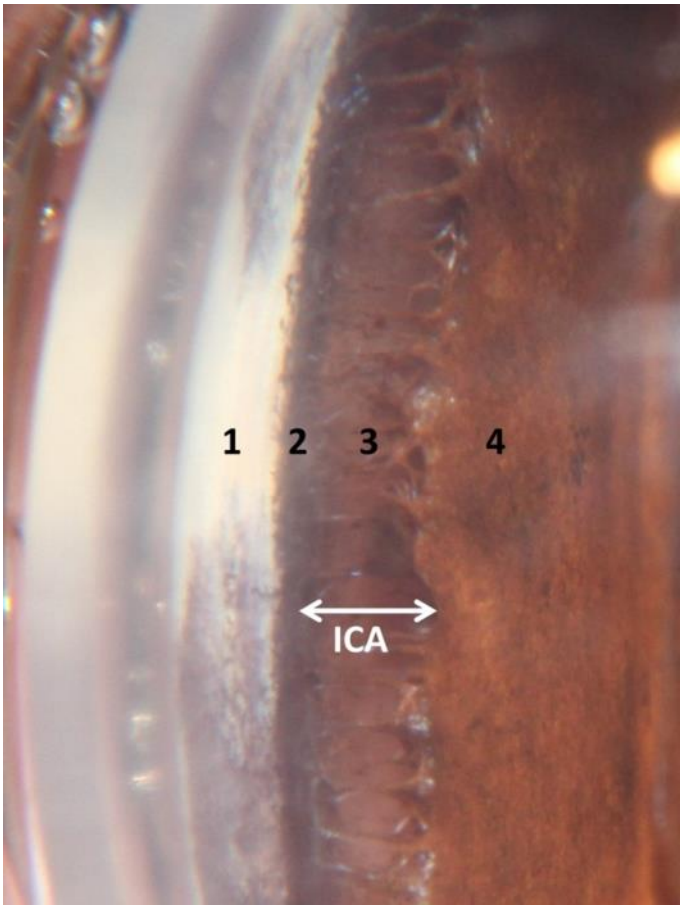

Figure 1.6. The gonioscopic view of a normal ICA as viewed through a Koeppe goniolens.

1 = corneoscleral limbus (superficial pigmented line), 2 = site of insertion of pectinate ligament (PL) fibres (deep pigmented line), 3 = PL fibres and 4 = iris. The double-headed white arrow delineates the opening of the ICA.

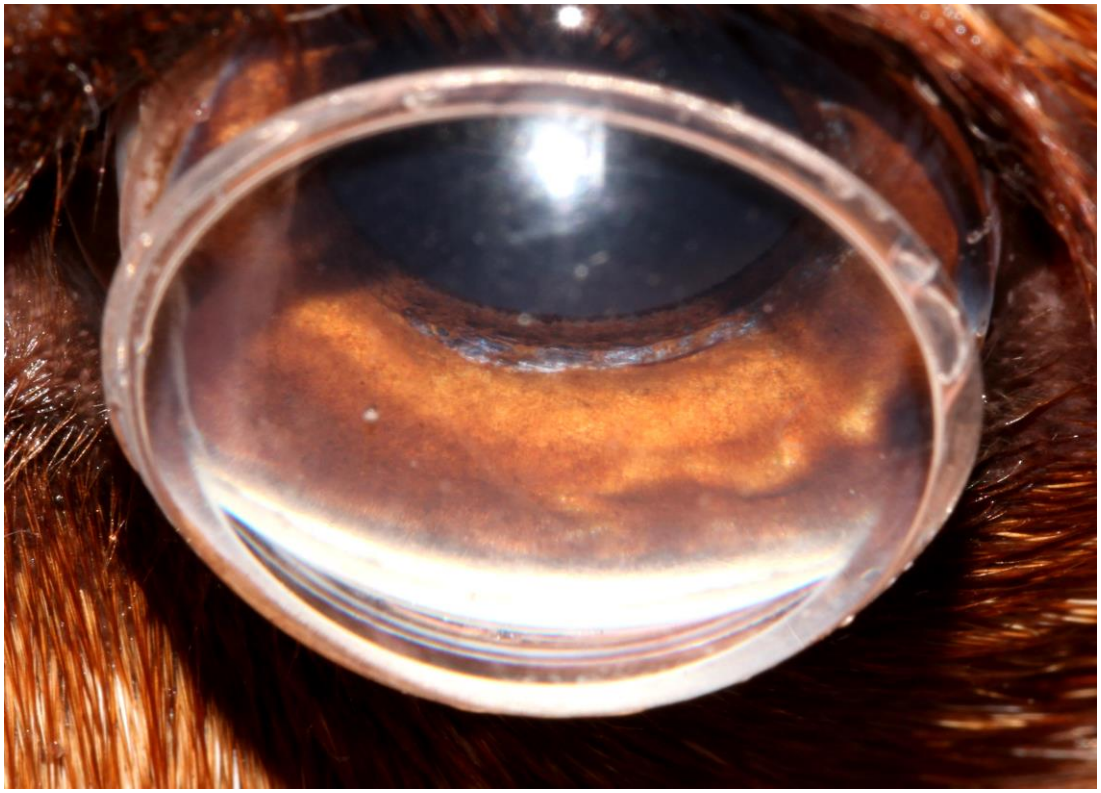

Figure 1.7. Application of a Koeppe goniolens to the cornea of a dog.

Following application of topical anaesthetic to the ocular surface and coupling gel to the lens, the Koeppe lens has been directly applied to the corneal surface being held in place by a flange and vacuum forces. In the photograph, the ventral ICA can be visualised.

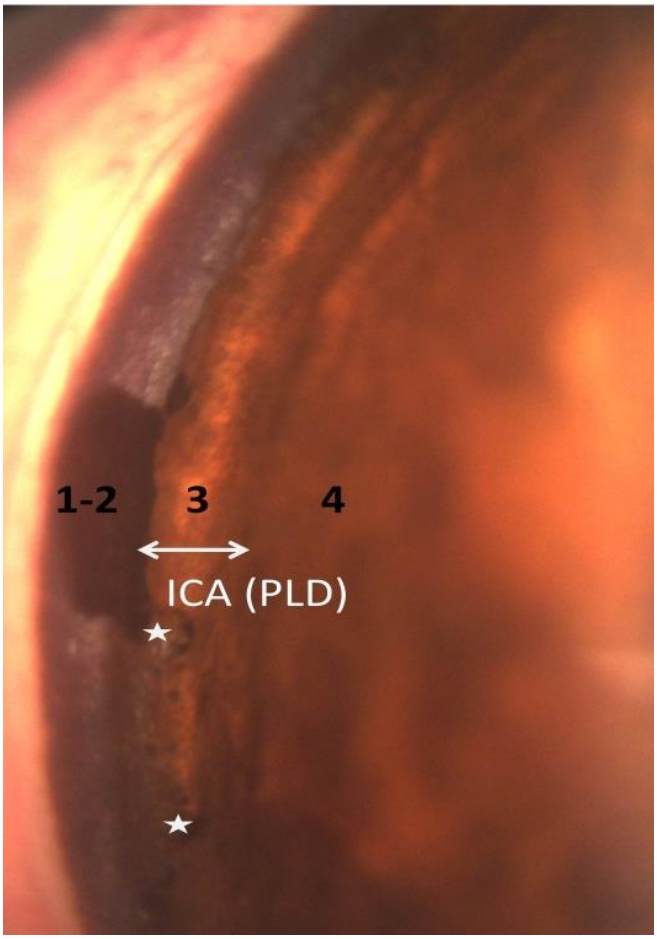

Figure 1.8. The gonioscopic view of a canine ICA demonstrating PLD as seen through a Koeppe goniolens.

1-2 = corneoscleral limbus (no distinction between superficial and deep pigmented lines), 3 = PLD and 4 = iris. The double-headed white arrow delineates the opening of the ICA which is spanned by broad sheets of tissue (PLD). No pectinate ligament fibres are discerned but 'flow holes' are present (white stars).

The United Kingdom's BVA/KC/ISDS Eye Scheme is based on eye examination and is a means of identifying inherited and non-inherited ocular conditions in dogs. Under the Eye Scheme, predisposition to PCAG is assessed by gonioscopy by a certified veterinary ophthalmologist. The ophthalmologist is required to estimate the proportion (or percentage) of PLD that affects the entire circumference of the ICA along with a subjective interpretation of ICA width (BVA unpublished data). Interpreting the width is especially challenging and can vary significantly even within regions of an individual eye and between the eyes of normal dogs and thus it is common for investigators not to

consider width assessment when evaluating goniodysgenesis in scientific studies[31,35,45,46]. Dispute also occurs as to what constitutes a 'normal' level of PLD with different investigators suggesting that figures of between 6.25 % and 25 % may constitute normal, or at least, acceptable levels of variation[31,35,47,48]. Before the publication of the studies reported in this thesis, the BVA/KC/ISDS Eye Scheme considered a dog to be either 'unaffected' or 'affected' by PLD (referring to the condition as *goniodysgenesis* or *primary glaucoma*) but did not employ any further grading beyond this binary classification. A dog was deemed 'unaffected' if both eyes exhibited < 20 % PLD for the entire circumference of the ICA and 'affected' if either or both eyes exhibited ≥ 20 % PLD[35]. Anecdotally, however, estimation of the percentage of PLD is thought to be open to a high degree of subjectivity with the potential for individual examiners to judge the same ICA very differently. This anecdotal suspicion has led to the application of 'gonioscopy grading schemes' in research as an attempt to reduce the influence of subjectivity on examination findings[31,35,47,48]. All of the above referenced schemes involve initial estimation of the percentage of ICA circumference affected by PLD before assignment to one of four - eight different ordinal grades depending on the scheme employed as summarised in **Table 1.1**. At the time of project outset, the scheme by Pearl et al. was the most recently published (in online format) and was adopted in estimating PLD prevalence and progression in the dog breeds investigated. This scheme was employed in the studies enclosed in this thesis because it is composed of four relatively broad grades making it more likely to be able to categorise different eyes similarly than schemes with larger numbers of narrow grades. In this scheme, the boundaries between the different grades are unequally divided. The proposed benefit of this scheme is that it allows the identification of PLD at both ends of the spectrum i.e. those eyes which had absolutely no evidence of PLD and those with > 90 % PLD and being considered at risk of PCAG[31,35].

Table 1.1. Details of four previously published gonioscopy grading schemes.

Ordinal grade	Read et al. (1998)[31]	Ekesten & Narfström (1992)[49]	Pearl et al. (2015)[35]	Fricker et al. (2015)[48]
	PLD as a percentage of the circumference of the ICA			
0	< 25 %	< 6 %	0 %	< 25 %
1	25.0 %	6 – 25 %	5 – 15 %	25 – 50 %
2	37.5 %	26 – 50 %	20 – 90 %	55 – 75 %
3	50.0 %	51 – 75%	> 90 %	> 75 %
4	62.5 %	> 75 %	N/A	N/A
5	75.0 %	N/A	N/A	N/A
6	87.5 %	N/A	N/A	N/A
7	100.0 %	N/A	N/A	N/A

Gonioscopy only allows examination of the entrance of the ICA and visualisation of the ciliary cleft (abnormalities of which are likely to be important in the pathogenesis of PCAG) is not possible at all if PLD is extensive[50]. Additional techniques such as high-resolution ultrasound and ultrasound biomicroscopy are currently being evaluated and may, to some extent, eventually replace gonioscopy[51,52].

1.2.2 Primary closed angle glaucoma

PCAG is by far the most common form of primary glaucoma in the dog affecting over 40 breeds worldwide[28,53]. In contrast to POAG, but similar to human primary angle closure glaucoma (PACG)[54-56], female dogs of certain breeds are more likely to be affected by PCAG than male dogs[29,53,57-59]. Female American Cocker Spaniels, Cocker Spaniels, Basset Hounds (BH), Welsh Springer Spaniels (WSS) and Samoyeds have been reported to be affected more frequently with PCAG than males[53,60]. A sex

difference has also been described for PLD in the American Cocker Spaniel but not in the English Springer Spaniel, FCR or Samoyed[29,34,61]. The reason for the sex predisposition for PCAG is unknown but may relate to gender differences in anterior chamber morphology as female dogs and humans tend to have shorter axial globe lengths and narrower ICA openings[62,63]. In humans, females are affected by PCAG more frequently than males[54-56].

As mentioned previously, PLD is known to be a risk factor, and a prerequisite, for PCAG in dogs and has been shown to have high heritability[29-32,64]. This, together with a relatively high prevalence of PLD and PCAG in a number of purebred dog breeds is suggestive of a genetic aetiology. The BVA/KC/ISDS Eye Scheme lists the following dog breeds to be either *certifiable* or *under investigation* for PLD (http://www.bva.co.uk/Canine-Health-Schemes/Eye-scheme):

- American Cocker Spaniel
- BH
- Border Collie (BC)
- Cocker Spaniel
- Dandie Dinmont Terrier (DDT)
- English Springer Spaniel
- FCR
- Golden Retriever (GR)
- Great Dane
- Hungarian Vizsla (HV)
- Leonberger
- Japanese Shiba Inu
- Siberian Husky
- Spanish Water Dog

- WSS
- Welsh Terrier

In predisposed breeds, risk of PCAG disease is associated with the percentage of ICA affected by PLD with only eyes with a very high percentage (> 90 %) PLD being at risk[29,31,65]. The vast majority of dogs with PLD, however, do not go on to develop PCAG and thus, PLD alone, is insufficient for PCAG[41]. It has been suggested that PLD may be a marker for other inherent defects of the AH outflow pathways, but these are yet to be characterised[31].

The degree of PLD present does not appear to be correlated with IOP in normotensive dogs[30,31,48]. PCAG presents as an acute onset disease with clinical signs of markedly elevated IOP (typically > 50 mmHg), pain, corneal oedema, mydriasis and blindness[28,66]. A diagnosis is usually made when these characteristic signs are present in the affected eye with no evidence of other intraocular disease and where gonioscopic abnormalities of the contralateral unaffected eye are present[41].

Other than PLD being a prerequisite for PCAG, the pathogenesis of this form of glaucoma is poorly understood. Collapse of the ciliary cleft is the most obvious histological finding (**Figure 1.9)**, but whether this occurs secondary to increased IOP being generated elsewhere (for example in the juxtacanalicular tissue) or is a progressive narrowing primarily generated within the ciliary cleft itself is unknown[41]. A histological diagnosis of PLD is challenging in the face of chronic glaucoma owing to the collapse of the ciliary cleft emphasising the importance of gonioscopic evaluation of the contralateral eye[67].

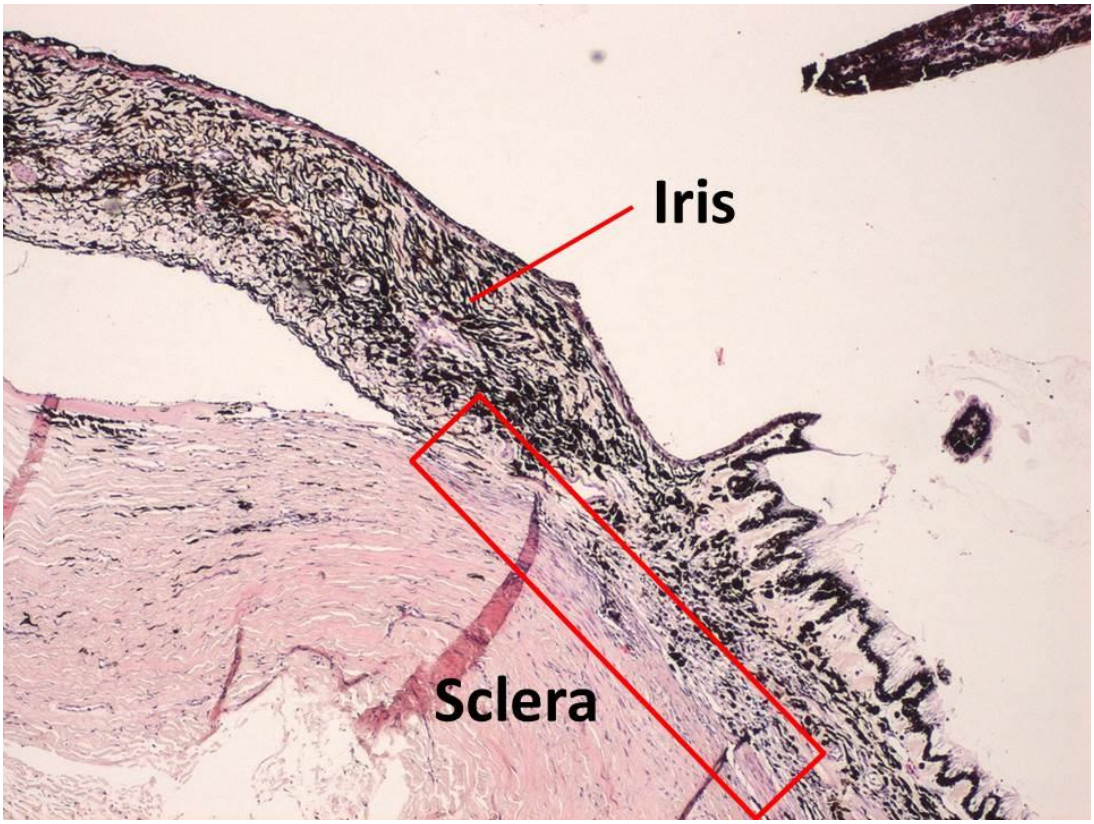

Figure 1.9. The ICA of a dog with PCAG (H&E X 40).

The ciliary cleft (boxed in red) is collapsed. Photograph courtesy of Emma Scurrell, CytoPath Ltd.

1.2.3 Primary open angle glaucoma

POAG is less common than PCAG in the dog and, at the time of project outset, had only been reported in two breeds - the Beagle and the Norwegian Elkhound[68-70]. In both of these, POAG is an autosomal recessive trait.

In POAG, the ICA appears normal on gonioscopy in the very early stages of disease but becomes progressively narrow, and eventually closes, in association with chronic IOP elevation[41,71]. POAG has a relatively insidious onset in dogs and typical clinical signs include buphthalmos, mydriasis, lens subluxation, corneal oedema and vascularisation, visual deficits and elevated IOP (> 25 mmHg)[28,66,72,73]. Age of onset varies but clinical signs may occur as early as 6 months in Beagles – the breed in which this form of glaucoma has been most extensively studied[73]. Owing to the insidious and slowly

progressive nature of POAG, however, clinical diagnosis is usually made only in very advanced cases[41]. The exact pathogenesis of canine POAG is unknown. Excluding the studies reported in this thesis, all reported forms of canine POAG have been linked to mutations in *ADAMTS10* or *ADAMTS17*[68-70,74,75]. These mutations are thought to result in altered processing of the ECM and/or defects in microfibril structure which lead to decreased AH outflow and increased IOP.

Before commencing this project, POAG had been diagnosed by myself in several Shar Pei (SP) and anecdotally by other veterinary ophthalmologists. Although POAG in the SP had not been published, there was a publication describing primary lens luxation (PLL) in this breed, although the description of the phenotype of some of the affected dogs was more consistent with a diagnosis of POAG rather than PLL[76]. Differential diagnosis between POAG and PLL can be difficult owing to the coexistence of increased IOP, lens subluxation and an apparently normal globe size in some dogs at initial clinical presentation[77]. PLL almost exclusively affects terriers in which the disease is caused by another mutation in *ADAMTS17*. In terriers with PLL, the lens is usually acutely displaced into the anterior chamber causing glaucoma through obstruction of the pupil and/or ICA[77]. In the SP, however, the most common clinical sign of PLL has been reported to be iridodonesis with some dogs presenting with buphthalmos. This is not consistent with the classic presentation of PLL and is more consistent with POAG[76]. For this project, genetic investigation of POAG in three breeds was performed: BH, Basset Fauve de Bretagne (BFdB) and SP.

1.3 Genetics of canine primary glaucoma

Where primary glaucoma occurs with an increased prevalence in a certain canine breed, a genetic component is suspected[78]. Several techniques are available to further investigate the genetic basis of inherited disease, including glaucoma, which will be

briefly discussed before an appraisal of the previous investigations into canine primary glaucoma.

1.3.1 Techniques used to investigate the genetics of primary glaucoma

1.3.1.1 Pedigree analysis

Compilation of a pedigree is particularly useful in determining the mode of inheritance when the disease results from a mutation in a single gene leading to a simple Mendelian trait. The disease should be seen to segregate within the family and, if the disease is well phenotyped (in particular with reference to age of onset), it is usually relatively straightforward to identify whether inheritance is autosomal dominant, autosomal recessive or sex-linked. This is the case for POAG in the Beagle, which was first established to be an autosomal recessive condition by test matings and pedigree analysis in 1981[79]. Pedigree analysis has also been employed to study the mode of inheritance of canine PCAG. Originally, autosomal dominant and autosomal recessive mechanisms of inheritance of PCAG were reported in the WSS and Siberian Husky respectively although it is now generally accepted that canine PCAG is inherited as a complex trait, where the disease results from the effects of multiple genetic and possibly environmental factors[60,78]. PLD and narrowing of the ICA are forms of goniodysgenesis and are considered risk factors for PCAG in multiple breeds[29-31,33,48,60,65,80,81]. In the Bouvier des Flandres, pedigree analysis has suggested PLD to be inherited as a recessive trait and, in the FCR, English Springer Spaniel, Samoyed and Great Dane, PLD and ICA narrowing increase in severity with degree of kinship[29,30,32,33,65]. Molecular techniques are, however, required to identify the genetic cause of disease.

1.3.1.2 Molecular genetic markers

A molecular genetic marker is a region of DNA with a known location on a chromosome that varies between individuals and populations. Microsatellites and single

nucleotide polymorphisms (SNPs) are examples of molecular genetic markers that are, in combination, commonly used in molecular applications ranging from forensic identification, parentage testing, creation of genetic maps and disease mapping. Regions of DNA that are in close proximity tend to be inherited together, and genetic markers are therefore commonly used to investigate the relationship between an inherited disease and the genetic mutations that cause it.

1.3.1.2.1 Microsatellites

A microsatellite is a tract of repetitive DNA in which certain DNA motifs (ranging in length from 2 – 5 base pairs) are repeated, typically 5 - 50 times. Microsatellites occur at thousands of locations in the canine genome and are notable for their high mutation rate and diversity in the canine population. Diversity of each microsatellite arises from the number of DNA motif repeats, allowing for multiple alleles to exist within a given population.

A few considerations are required for suitable microsatellite selection. Microsatellites composed of dinucleotide repeats occur more frequently than longer motifs and are more stable than tetranucleotides and are, therefore, preferred[82]. Microsatellites composed of the dinucleotides CA or GT are also preferable as they tend to be more mutatable (polymorphic). The microsatellite should be as long as possible with the dinucleotide being found to repeat at least 12 times in the reference sequence. In candidate gene studies (described below), to maximise the likelihood that the microsatellite, and by implication the gene and any disease-causing mutations, will be in linkage disequilibrium (LD) with one another, the microsatellite should be located as close to the gene in question as possible. LD varies from breed to breed but averages around 2 Mb in the dog and thus microsatellites occurring within 500 kb of the candidate gene should be selected where possible[82-84]. Two microsatellites should be

selected to closely flank the gene and, once selected, a pair of primers must be designed with which to amplify each microsatellite (**section 2.2.5**).

1.3.1.2.2 Single nucleotide polymorphisms

A single nucleotide polymorphism (SNP) represents a change at a specific genomic position from one nucleotide to another. SNPs are generally bi-allelic and tend to be less informative than microsatellites. However, SNPs occur at a much higher density across the canine genome occurring, on average, every 1 kb[85]. This high density makes them very useful for whole genome mapping strategies.

1.3.1.3 The candidate gene approach

A candidate gene approach is particularly useful when the disease is inherited as a simple Mendelian trait. This approach identifies specific genes that are considered good candidates to harbour mutations causing the disease in question, and assesses the association of markers within those genes with the disease in a set of affected and unaffected individuals.

1.3.1.3.1 Selection of candidate genes

Candidate genes are often selected on the basis of previous association with a phenotypically identical or similar disease in other species or breeds or from knowledge of their function. Novel candidate genes may also be selected on the basis of their presence in genomic loci identified to be associated with the disease in question. Such genes become of particular interest when their known function or activity in affected tissues implicates their involvement further[82].

A list of candidate genes is often formed by an appraisal of the scientific literature surrounding the condition, for example by the use of online tools such as PubMed (http://www.ncbi.nlm.nih.gov/pubmed) or online databases such as OMIM (https://www.omim.org/). Once a list has been established, the chromosomal location of

the gene, or its canine orthologue, must be established within the canine genome. This is usually performed by using a publicly available genome database such as Ensembl (http://www.ensembl.org).

1.3.1.3.2 Association analysis of candidate genes

Once the chromosomal location of a candidate gene is known, polymorphic markers (e.g. microsatellites) within close proximity of or within the candidate gene can be identified. These markers are then genotyped in both affected animals (cases) and unaffected animals (controls). Following genotyping, statistical association analyses are performed to test for association between the markers and the disease in question. If the candidate gene contains a pathogenic mutation, there should be significant association of the investigated markers with disease and the candidate gene may then be investigated in more detail. On the other hand, if the markers show no association with disease, the candidate gene is unlikely to contribute to disease and is usually excluded from further investigation[82].

Such an approach was used to identify mutations in *HSF4* in three different dog breeds by screening 20 candidate genes known to be associated with inherited cataract in humans[86]. Prior to the studies described in this thesis, the candidate gene approach had been less successful in identifying causal mutations for cases of canine primary glaucoma. In humans, mutations in the myocillin gene (*MYOC*) have been associated with multiple primary glaucoma phenotypes in particular POAG[87-91]. Using a candidate gene approach, POAG in the Beagle was shown not to be associated with mutations in *MYOC* and, indeed, no mutations in this gene have been associated with any form of canine primary glaucoma to date[92,93]. A candidate gene approach did reveal associations between mutations in *SRBD1* and PCAG in Shiba Inu and Shih Tzu dogs, however, although the exact causative mutations remain elusive[94].

1.3.1.5 Whole-genome locus mapping

For inherited diseases which do not share a close phenotypic description with a disease in another breed or species which has already been molecularly characterised and/or for which inheritance is thought to be complex, or where the list of candidate genes is prohibitively long, more sophisticated molecular techniques are required. Whole genome approaches have the advantage of not being limited to a list of proposed candidate genes and do not require prior knowledge of a target locus.

DNA sequences (i.e. genetic markers and mutations) that are located close to one another on a chromosome are likely to be inherited together during meiosis. The further apart they are the more likely it is that recombination will occur between them, and they will not be inherited together. Genotyping of markers across the entire genome in cases and controls, and comparison of marker allele segregation with the disease in question can identify the likely loci harbouring the disease causal mutation. These studies can be conducted using a family-based approach (linkage analysis) or using 'unrelated' cases and controls in an association-based analysis – i.e. genome-wide association study.

1.3.1.5.1 Linkage analysis

Linkage analysis can be performed in many different ways but traditionally has involved the evaluation of genetic markers (microsatellites or SNPs) across a pedigree (or family) in which the disease has been shown to segregate[95]. The power to detect linkage is proportional to the number of individuals affected within families and the total number of families. Once linkage to a specific chromosomal locus is identified, analysis of genes contained within the region is conducted. Traditional linkage analysis has been widely and successfully used to identify genetic variants with Mendelian inheritance, including primary glaucoma in humans. Linkage studies have led to the identification of *MYOC* and *OPTN* as genes implicated in Mendelian POAG in humans and were used to identify the POAG locus in the Beagle[69,96,97]. Canine linkage analysis

tends to work very well in experimental colonies but presents more of a challenge 'in the field' as it is more difficult to collect cases and controls and information is often incomplete which reduces study power. Since the establishment and availability of a canine reference genome and the development of newer technologies such as SNP genotyping arrays, traditional linkage analysis is less commonly used in the molecular investigation of canine inherited disease. Furthermore, linkage analyses have proven less successful in the investigation of complex traits, of which canine PCAG is thought to be an example.

1.3.1.5.2 Genome-wide association studies

Genome-wide association studies (GWAS) involve the use of a SNP genotyping array - a dense array of genetic markers which capture a substantial proportion of common variation in the genome sequence[98]. The aim of GWAS is to map susceptibility loci through the detection of associations between genotype and phenotype using cases and controls. Over the last decade, GWAS has improved the understanding of the genetic basis of numerous complex traits by revealing susceptibility loci and providing insights into the allelic architecture of multifactorial traits[99,100].

A number of canine SNP arrays have been developed and used over the years, containing SNP markers based on the 7.8X canine reference sequence derived from a Boxer dog[85]. The CanineHD BeadChip (Illumina) containing 172,115 SNPs has been most widely used to date, although this has recently been updated to a denser array containing 220,853 SNPs[101,102]. Furthermore, ThermoFisher has recently launched a canine genotyping array containing over 670,000 SNPs. In the CanineHD BeadChip, each chip contains millions of 3 micron beads which are covalently bound to hundreds of thousands of copies of a single locus-specific 50-mer oligonucleotide. Single base, allele-specific extension of the oligonucleotide with subsequent fluorescent staining of the extension product enables identification of the allele at that locus. Once allele

identification has been performed at each SNP locus for each sample, the genotype of that sample can be determined. Analysis software packages are then used to test the data for associations between SNPs and the trait in question once filtering has been conducted to exclude poorly performing individuals and markers. Significant association of a SNP or SNPs allows identification of a locus for further investigation. A positional candidate approach may then be performed with or without fine-mapping to refine the associated locus.

The number of samples required for GWAS to be informative in locus identification depends on the inheritance pattern of the investigated trait. For simple Mendelian recessive traits, as few as 20 cases and 20 controls, and perhaps even less, may be required[103]. For complex traits, in which more than one gene or mutation may be involved, a larger number of samples is required. For example, in dogs, it has been predicted that a fivefold risk allele can be detected with 100 cases and 100 controls but a twofold risk allele would require approximately 500 cases and 500 controls to be identified. This is in distinct contrast to human studies, in which as many as 6,000 samples may be needed to detect a twofold risk allele as a result of the relatively short LD in this species[104]. The dog has a unique pattern of LD, extending over several megabases (Mb) within breeds (10 – 100 X further than in humans), but only tens of kilobases (kb) between breeds[85]. LD patterns can vary greatly between breeds, with a general trend of greater LD in breeds that have experienced significant population bottlenecks[105].

GWAS have previously been used to investigate the genetic basis of glaucoma in dogs. In their investigation of POAG (an autosomal recessive trait) in the Norwegian Elkhound, Ahonen et al. performed GWAS in 9 cases and 8 controls (using the 172,115 SNP CanineHD array) to map the glaucoma gene to a 750 kb region on canine chromosome 20[70]. This region was found to contain *ADAMTS10*, which had previously

been reported to be associated with POAG in another breed, and thus was an excellent candidate gene for further investigation. Ahonen et al. also performed GWAS in the DDT to investigate PCAG, which is thought to be a complex trait, using the Illumina Canine SNP20 BeadChip array (Illumina)[106]. There was an association between PCAG and a 9.5 Mb locus on canine chromosome 8 although no SNPs reached Bonferroni significance.

1.3.1.6 Sequencing

Sequencing strategies may be employed in mutation mapping, fine-mapping and identification of disease-causing mutations.

1.3.1.6.1 Sanger sequencing

Sanger sequencing, also known as the chain termination method, is a technique for DNA sequencing based upon the selective incorporation of chain-terminating dideoxynucleotides (ddNTPs) by DNA polymerase during in vitro DNA replication. It was developed by Frederick Sanger and colleagues in 1977. It was the most widely used sequencing method for approximately 25 years before it was replaced by next-generation sequencing (NGS) methods. However, the Sanger method remains in wide use, for smaller-scale projects, validation of NGS results and for obtaining especially long contiguous DNA sequence reads (> 500 nucleotides). The classical chain-termination method requires a single-stranded DNA template, a DNA primer, DNA polymerase, dNTPs and modified fluorescently labelled ddNTPs. The ddNTPs lack a 3'-OH group which is necessary for the formation of a phosphodiester bond between two nucleotides. Thus, incorporation of a ddNTP instead of a dNTP, causes DNA elongation to terminate.

1.3.1.6.2 Next-generation sequencing

NGS is based on massively-parallel, high throughput sequencing of millions of short nucleotide sequences. Targeted NGS may be used to sequence a genomic locus identified by a previous whole-genome scan or to sequence the exons of a gene, for example in a candidate gene analysis. NGS may also be used in a non-targeted fashion in whole-genome and RNA sequencing.

NGS has already been used in the investigation of canine POAG and PCAG but has only successfully led to the identification of mutations associated with POAG thus far[69,107].

1.3.2 Previous studies of the genetics of human and canine glaucoma

The high prevalence of PCAG in certain dog breeds implies a genetic link. Despite this, the genetics of the disease have received relatively little scientific attention. This, however, is changing as molecular techniques to investigate genetic disease, in particular GWAS and whole-genome sequencing, become increasingly available and affordable. The genetics of human primary glaucoma have been extensively studied, however, serving as a useful learning resource for those researching the canine disease equivalents.

In humans, glaucoma is the most common cause of irreversible blindness worldwide[59]. POAG is by far the most common form of primary glaucoma followed by PACG (the human equivalent of canine PCAG) and genetic studies of these diseases are most relevant to the investigation of canine primary glaucoma and this project[108,109]. Primary congenital glaucoma, exfoliative glaucoma and pigment dispersion glaucoma have all been, and continue to be, investigated but are less relevant to the canine situation.

Most forms of human primary glaucoma appear to be genetically complex – likely involving a large number of grouped or independently inherited genes along with environmental factors[8,110,111]. However, Mendelian forms of POAG have been reported

in humans in association with mutations in *MYOC*, *OPTN*, *CYP1B*, *TBK1* and *WDR36*[112-115]. Of these genes, *MYOC* has gained most interest from researchers investigating canine primary glaucoma. MYOC protein has been found to be elevated in the AH of dogs with POAG and PCAG but, to date, no *MYOC* mutations have been discovered in dogs with primary glaucoma[92,93,116,117]. Numerous other genes have been implicated in human POAG with GWAS helping to elucidate genes involved in the more complex forms. A large GWAS of 3,853 POAG patients and 33,480 matched control subjects revealed associations for three novel susceptibility loci for POAG: *TXNRD2*, *FOXC1* and *ATXN2*[118]. The functions of these genes suggest that studies of ocular development (*FOXC1*), neurodegeneration (*ATXN2*) and mitochondrial dysfunction (*TXNRD2*) may help define the biological pathways that contribute to POAG[118]. Another study reported seven novel POAG susceptibility loci (*FNDC3B*, *ANKRD55-MAP3K1*, *LMX1B*, *LHPP*, *HMGA2*, *MEIS2* and *LOXL1*) and GWAS have also been used to identify loci associated with IOP, improving risk prediction for primary glaucoma[119-121]. Recently, a bioinformatics study resulted in the compilation of 542 genes with confirmed associations with POAG and its related phenotypes (normal tension glaucoma, ocular hypertension, juvenile open-angle glaucoma, and primary congenital glaucoma)[8]. In this study, functional annotation and pathway analyses of these genes were performed which revealed that no single molecular pathway encompasses the pathophysiology of POAG and suggested that inflammation and senescence may play pivotal roles in POAG with the TGF-β signaling pathway being repeatedly implicated.

All cases of canine POAG investigated to date are Mendelian, showing simple autosomal recessive inheritance, and have been associated with mutations in *ADAMTS10* or *ADAMTS17*[68-70,74]. Interestingly, mutations in *ADAMTS10* and *ADAMTS17* have also been associated with reduced scleral rigidity and PLL (equivalent

to ectopia lentis in humans) respectively in certain dog breeds, further highlighting the importance of these genes in connective tissue biology in the mammalian eye[122-124]. Secondary, but not primary, glaucoma has been reported in humans with Weill-Marchesani, Weill-Marchesani-like and Marfan syndromes as a result of mutations in *ADAMTS10, ADAMTS17* and *FBN-1* (*fibrillin-1*)[125-131], and autosomal-recessive ectopia lentis caused by a homozygous mutation in *ADAMTSL4*[132]. These genes, all expressed within the trabecular meshwork, are involved in microfibril formation and maintenance, and diseases as a result of mutations in these genes are often referred to as microfibrillopathies[133-135]. In these human microfibrillopathies, glaucoma occurs in conjunction with other ocular phenotypes such as spherophakia and ectopia lentis and systemic phenotypes relating to connective tissue disorders including brachydactyly and heart defects[125,136-139]. The pathogenesis of canine POAG as a result of mutations in *ADAMTS10* and *ADAMTS17* is unknown. Microfibrils are components of elastic fibres which are important structural units within the trabecular meshwork and are likely to be involved in assisting AH movement into the distal outflow pathways as previously discussed[137]. Furthermore, microfibrils are involved in ECM metabolism, for example through the binding and storage of TGF-β which is known to contribute to increased trabecular outflow resistance[21,133,134,137,140,141]. Increased resistance to AH outflow may also be caused by the accumulation of various products within the trabecular meshwork[9]. Evidence for this comes from the identification of plaque-formation in the trabecular meshwork of humans and Beagles with POAG[19,20,142,143]. Furthermore, ADAMTS4 has been shown to be important in AH outflow in human and porcine eyes[144]. These studies suggest that the *ADAMTS* and *ADAMTSL* gene families play an important role in intraocular physiology and demonstrate how mutations within the same gene can cause multiple ocular phenotypes.

Human PACG is characterised by a shallow anterior chamber, increased lens thickness, complete or partial ICA closure, short axial globe length, hyperopia and optic nerve injury[58,145,146]. Reduced anterior chamber depth and narrowing of the ICA are important risk factors for PACG and correlate with age, sex and ethnicity[146-148]. Risk for PACG increases with age, and females are at higher risk than males[54,58]. Furthermore, PACG is more prevalent in Chinese, Malay, Asian Indian and Eskimo populations[149-152]. Human GWAS, typically involving thousands of cases and controls, have helped identify numerous genetic loci associated with PACG including the *PCMTD1-ST18*, *COL11A1* and *PLEKHA7* loci[153-155]. Although many genes underlying PACG remain undiscovered, several have been proposed. These include *MMP-9* (matrix metalloproteinase-9) which is involved in ECM metabolism[154,156,157]. PACG has also been associated with genes involved in regulation of axial globe length and connective tissue remodeling such as *MFRP* (membrane type frizzled related protein), *MTHFR* (methylenetetrahydrofolate reductase) and *CHX10* (retinal homeobox)[158-160]. Other genes implicated in PACG pathogenesis include *eNOS* (endothelial nitric oxide synthase), *HSP70* (heat-shock protein 70), *HGF* (hepatocyte growth factor), *GSTT1* (glutathione S-transferase T1), *GSTM1* (glutathione S-transferase M1), *CALCR* (calcitonin receptor-like receptor), *APOE* (apolipoprotein E), *TNFA* (tumour necrosis factor A), *TNFR1* (tumor necrosis factor-α receptor 1) and *SPARC*[158,159,161-168]. SPARC protein is found within the trabecular meshwork and is involved in ECM remodelling making it an attractive candidate gene for PACG. The list of genes associated with human PACG is being added to all the time, further highlighting the complexity of the disease. Recently, a large multi-ethnic GWAS meta-analysis involving 10,503 PACG cases and 29,567 controls drawn from 24 countries revealed five new genetic loci: *EPDR1*, *CHAT*, *FLIS3*, *FERMT2*, and *DPM2-FAM102A*[169].

Genetic studies of canine PCAG have been far more limited, nevertheless susceptibility loci have been identified and some candidate genes postulated. PCAG genetics have been studied in most detail in the BH owing to the establishment of an affected breeding colony. In this breed three genetic loci have been identified leading to the proposal of the three positional candidate genes *COL1A2*, *NEB* and *RAB22A*, which are all expressed in the anterior segment of the eye[170,171]. Based on their function, *COL1A2* and *NEB* appear to be promising candidate genes. *COL1A2* encodes for the pro-alpha2 chain of collagen type 1 – an important component of the trabecular meshwork. *NEB* encodes the muscle contractility regulating protein, nebulin, which is expressed in the ciliary body musculature, and the belief that muscle-related mechanisms are involved in the AH humour outflow pathways makes *NEB* a feasible candidate. *RAB22A*, is known to be an oncogene, and thus its potential role in primary glaucoma is more difficult to explain.

SRBD1 (S1 RNA-binding domain 1) has been associated with primary glaucoma in humans and has also been identified as a PCAG risk gene in the Shih Tzu and Shiba Inu[94]. In a study reporting findings of GWAS of PCAG in the DDT, although an association was found between PCAG and a region on canine chromosome 8, no candidate gene or causal mutations have been identified[106].

1.4 Aims and objectives

This study was conceived with three main aims:

1. To provide robust and current PLD prevalence data for seven dog breeds known to be affected by PLD and PCAG: FCR, BH, DDT, WSS, GR, BC and HV.
2. To investigate the genetic basis of PLD and PCAG in four dog breeds: BH, FCR, DDT and WSS.
3. To investigate the genetic basis of POAG in three dog breeds: BH, BFdB and SP.

2 Materials and methods

2.1 Determination of pectinate ligament dysplasia prevalence

2.1.1 Animals used

Canine breeds at risk of PCAG were identified on the basis of scientific publications and/or inclusion on the BVA/KC/ISDS Eye Scheme (**1.2.2**). Health representatives from relevant breed clubs were contacted, informed of the study and their clubs invited to participate. Participation involved setting up gonioscopy screening sessions for each breed to identify dogs affected with PLD (cases) and unaffected dogs (controls). The breeds investigated were the FCR, BH, DDT, WSS, BC, HV and GR. These seven breeds of dog were enrolled in gonioscopy screening sessions at different locations across the United Kingdom between September 2013 and March 2016 between the hours of 10:00 and 16:00 GMT. The sessions were promoted by a variety of different mechanisms, including correspondence from the KC to the owners of KC registered dogs of each breed, via breed club websites and via social media. All dogs that were volunteered for screening were accepted, regardless of their age, ancestry or KC registration status.

2.1.2 Examination procedure

All experiments were conducted in accordance with the ARVO statement for the Use of Animals in Ophthalmic and Vision Research and approved by the AHT's Research and Ethical Approval Committee. All dogs were pets and ophthalmological examination was only performed after informed and written owner consent. All examinations were performed by myself, a board-certified veterinary ophthalmologist of the European College of Veterinary Ophthalmologists (ECVO).

IOP was estimated using rebound tonometry with a TonoVet Tonometer (TonoVet, Kruuse). Tonometry was performed immediately prior to topical anaesthesia and gonioscopy. This tonometer takes six consecutive measurements, discards the highest and lowest readings and averages the remaining four. Only readings with a maximum standard deviation of 5 % were recorded. Three averaged readings were taken for each eye and the average of these three readings was then calculated and used for subsequent analyses.

Gonioscopy was performed bilaterally in conscious dogs following topical anaesthesia achieved by application of 0.5 % proxymetacaine (Bausch & Lomb, Chauvin Pharmaceuticals Ltd.) using a 17 or 19 mm Koeppe goniolens (Ocular Instruments) filled with 2 mg/g carbomer gel (Viscotears; Alcon) before placing onto the cornea. The entire 360^{o} of the ICA was then examined using a handheld slit-lamp biomicroscope (Keeler PSL Classic; Keeler) for the presence of PLD which was quantified according to the percentage of the ICA circumference affected, estimating this to the nearest 5 %. Regions of ICA were judged to be affected by PLD where they exhibited abnormally broad PL fibres or solid sheets of tissue as previously described in **section 1.2.1**[31]. No attempt to measure ICA width was made as this was considered too subjective in line with previous publications[31,35,48].

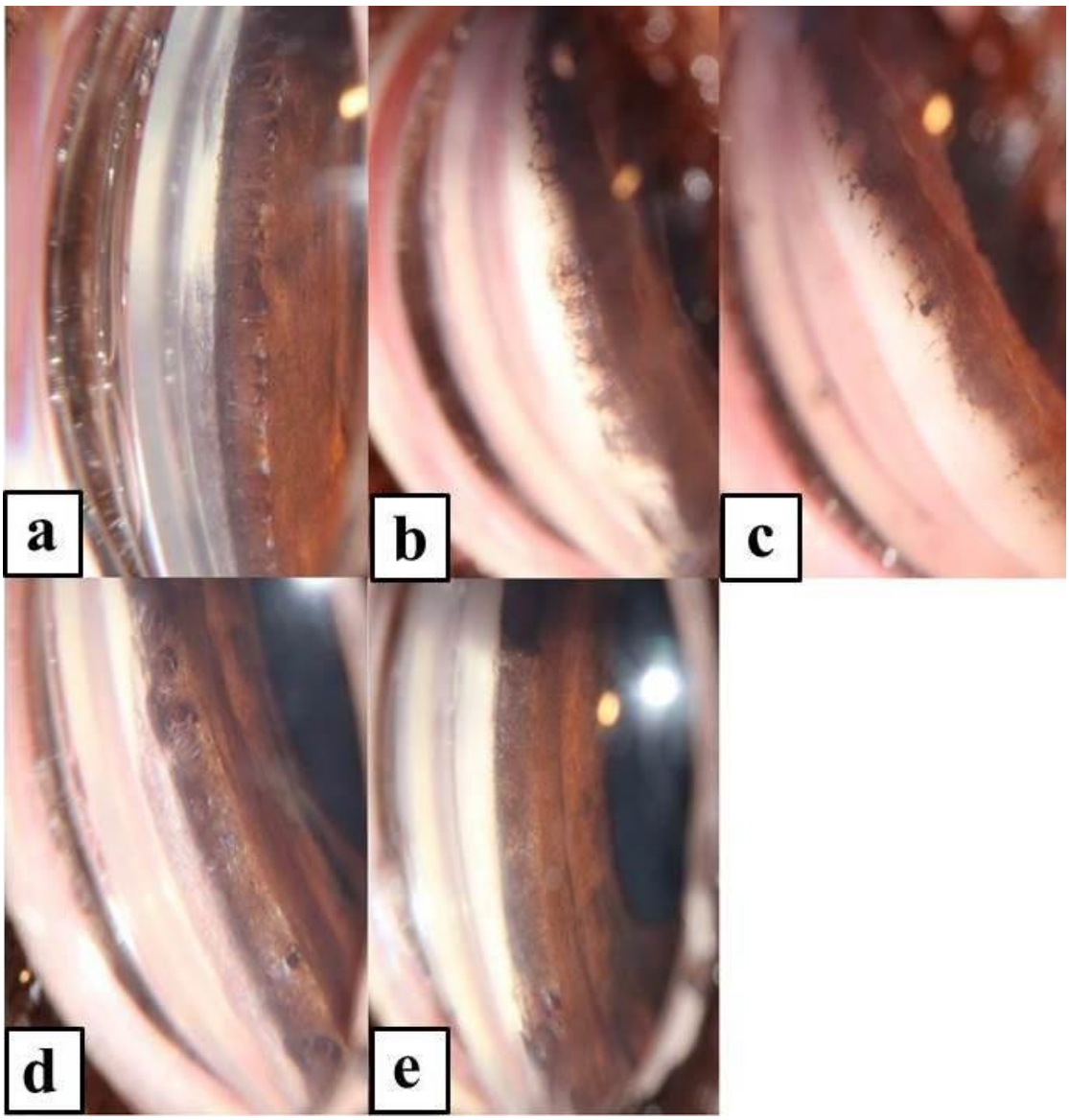

Figure 2.1. A series of gonioscopy photographs to illustrate the PLD grading system used.

The grading system has been applied assuming the photographs are representative of the entire 360^{o} of ICA in each case. (a) Normal appearance of the ICA and PL. Unaffected (grade 0). (b) Approximately 15 % of the ICA is affected by abnormally thickened PL fibres. Mildly affected (grade 1). (c) Approximately 25 % of the ICA is affected by PL 'sheeting'. Moderately affected (grade 2). (d) Approximately 75 % of the ICA is affected by PL 'sheeting'. Moderately affected (grade 2). (e) Over 90 % of the ICA is affected by 'sheeting'. Severely affected (grade 3).

2.1.4 Analyses pectinate ligament dysplasia data

2.1.4.1 Pectinate ligament dysplasia: prevalence, progression and associations with age, sex and intraocular pressure

For each dog examined, data were collected on breed, sex, age at time of examination and, for each eye, percentage ICA affected by PLD and IOP. The mean percentage of ICA affected by PLD and mean IOP for the left and right eyes were averaged for each dog. To reduce the influence of subjectivity on estimation of PLD (percentage of ICA circumference affected to the nearest 5 %), PLD results were assigned to one of four ordinal scale grades, based on the percentage of ICA circumference affected (**Table 2.1**) as previously described[35]. Eyes were classified as 'unaffected' if 0 % of the ICA was affected by PLD (ordinal grade 0), 'mildly affected' if < 20 % was affected (grade 1), 'moderately affected' if 20 - 90 % was affected (grade 2) and 'severely affected' if > 90 % was affected (grade 3) (**Table 2.1**). The continuous variables age and IOP were not normally distributed and so were converted into ordinal variables with four ranks based on quartile values. The following statistical analyses were performed:

- The variables IOP and age were examined for normal distribution using the Shapiro-Wilk test, and the overall pattern of the data and deviations from the pattern were examined using scatterplots.
- For each breed, the prevalence of PLD was determined by calculating proportions of dogs graded as 0, 1, 2, and 3.
- The linear relationships between the ordinal variable PLD grade and age, and PLD grade and IOP were evaluated using Spearman's correlation coefficient (rho).
- The proportions of male and female dogs affected with PLD were compared using the Chi-square test of independence.

- The variables IOP and age were not normally distributed for the three breeds, and therefore the linear relationship between IOP and age was assessed using Spearman's correlation coefficient.
- The difference in average IOP between male and female dogs was assessed using the Mann-Whitney U test.
- The variables age and IOP were compared between breeds using the Kruskal-Wallis test.
- The proportions of male and female dogs in the three breeds were compared using the Chi-square test of independence.

Table 2.1. Degree of PLD estimated by gonioscopy as percentage of total ICA circumference affected and equivalent ordinal grade as published by Pearl et al.[35].

Percentage of ICA affected by PLD	Definition	Ordinal grade
0 %	Unaffected	0
5 - 15 %	Mildly affected	1
20 – 90 %	Moderately affected	2
> 90 %	Severely affected	3

2.1.4.2 Pectinate ligament dysplasia: progression

In the WSS, PLD progression in individual dogs was investigated. This was not performed in the other breeds owing to insufficient historic data. In the WSS, following examination as part of the cross-sectional study above, Eye Scheme certificates of any previous gonioscopic examination were sought and obtained where available for each dog. Only dogs with certificates that clearly documented the degree of PLD at this

earlier examination and dogs that were previously examined by a single examiner (Beverley Cottrell) were included in this study (n = 65). This allowed comparison of gonioscopy results over time. As only two examiners (Beverley Cottrell and myself) were involved, it was thought that subjectivity would be reduced whilst ensuring the second examiner was masked as to the result of the first examiner.

For the analyses described in **2.1.4.1** and **2.1.4.2**, a P value of < 0.05 was considered statistically significant, and all analyses were performed by Dr Abel Ekiri using IBM SPSS statistical software (version 22).

2.1.4.3 Gonioscopy in the dog: inter-examiner variability and the search for a grading scheme (section 3.2)

Both eyes of 49 Welsh springer spaniel dogs (98 eyes) were examined by two panellists of the BVA/KC/ISDS Eye Scheme on the same day (Beverley Cottrell and myself). The two examiners had never worked together and were trained at different institutions under different mentors. Each examiner was masked to the findings of the other examiner and to those of any previous examinations. Gonioscopy was performed as detailed in **2.1.2**. For the purpose of this study, left and right eyes were classified independently. Data were first analysed for individual examiners to provide descriptive statistics of percentage of PLD assigned to examined eyes. Kernel density plots were then created to allow visualisation of the distribution of data for each examiner. The relationship between the results of the two examiners was assessed with a scatterplot and simple linear regression with degree of association between the two examiners' results being assessed using Pearson's product moment correlation coefficient. The non-parametric Wilcoxon signed rank test was used to test the null hypothesis that there was no difference between the percentages of PLD assigned to each eye by the two examiners with a $P < 0.05$ considered statistically significant and allowing rejection of

the null hypothesis. The signed rank test was applied to both the full set of 98 paired observations and to the subset of eyes for which both examiners considered PLD to be present. A Bland-Altman plot was created to further characterise any inter-examiner discrepancy of PLD percentage scores. Following assignment of percentage scores of PL to the four different ordinal grading schemes, quantification of agreement beyond that expected by chance alone between the two examiners for each scheme was assessed using the Cohen's kappa statistic. The level of agreement based on the kappa statistic was interpreted as follows: ≤ 0.20 = 'poor', > 0.20 - ≤ 0.40 = 'fair', > 0.41 – ≤ 0.60 = 'moderate', > 0.60 – ≤ 0.80 = 'good' and > 0.80 – 1.00 = 'very good'[172]. For the purposes of this study, only grading schemes which resulted in a 'good' or 'very good' level of agreement were considered acceptable. All of these analyses were performed by myself using the internet-based software GraphPad (https://www.graphpad.com/).

2.2 Mutation mapping and identification

2.2.1 DNA collection and extraction

DNA samples were collected from all dogs examined as part of the PLD prevalence study and also from clinical cases of PCAG and POAG. All DNA samples were collected from privately owned pet dogs following fully informed and written owner consent. Samples were collected in the form of five buccal mucosal swabs from each dog, which were air dried and then stored at -20 ^{o}C until DNA extraction. DNA samples received from collaborators were either received as buccal mucosal swabs, blood samples collected in EDTA or as DNA in solution. All samples were stored at -20 ^{o}C.

DNA was extracted from buccal mucosal swabs using a QIAamp® DNA Blood Midi Kit (Qiagen) following a modified protocol. Briefly, buccal cells were lysed by incubation of four of the five swabs in a solution of 1,600 μL phosphate buffered saline (PBS), 1,600 μL Lysis Buffer (Qiagen) and 80 μL Proteinase K (Qiagen) in a 15 mL

conical tube (Falcon) at 56 ^{o}C for 20 minutes. After 10 minutes of incubation, each sample was mixed by vortexing for 10 seconds. Following incubation, DNA was precipitated by the addition of 1,600 μL absolute ethanol and mixed by vortexing. Precipitated DNA was collected via passage of the solution through supplied filter columns (Qiagen) by centrifugation at 1,620 x g for 3 minutes (5804/5804 R, Eppendorf). DNA collected on the filter was then purified with two separate wash steps using 2 mL of each of the supplied two wash buffers AW1 and AW2, followed by centrifugation at 4,500 x g for 1 minute and 15 minutes respectively. DNA was eluted by addition of 150 μL AE elution buffer followed by centrifugation at 4,500 x g for 1 minute. The elution step was performed a total of three times to result in a DNA solution approaching 450 μL in volume.

DNA was extracted from whole blood stored in EDTA using a protocol based on the Nucleon BACC2 Genomic DNA Extraction Kit (Tepnel Life Sciences). Briefly, up to 5 mL of blood was added to a 50 mL polypropylene tube (Falcon). Nucleon Reagent A (stored at 4 ^{o}C) was then added to make up a total volume of 25 mL and the tube inverted 10 times to lyse red blood cells. White blood cells were collected by centrifugation of the sample at 4,500 x g for 10 minutes followed by removal of the supernatant. To lyse the white blood cells in the pellet, 10 mL of Nucleon Reagent B was then added and the pellet broken up by shaking, followed by overnight incubation at 37 ^{o}C. The lysis mix was then transferred to a 15 mL polypropylene tube (Falcon), and 800 μL of 5M sodium perchlorate added, followed by mixing by inversion to achieve protein precipitation. Two millilitres of chloroform was then added and the sample mixed by inversion for 4 minutes before centrifugation at 4,500 x g for 5 minutes. This step resulted in the formation of three distinct layers within the sample: a bottom layer of chloroform; a middle layer of precipitated protein; and a top layer of DNA-containing aqueous solution. The DNA-containing layer was transferred using a

sterile pastette to a new 15 mL tube. The protein precipitation stage was then repeated (addition of chloroform and centrifugation) followed by removal of the DNA-containing aqueous phase. Finally, 5 mL ice cold absolute ethanol was added and the DNA-containing solution gently inverted until the precipitated DNA could be observed. The DNA spool was captured using a sealed glass hook and air-dried before transfer to a microcentrifuge tube containing 300 μL 1X TE buffer (**Appendix I**).

2.2.2 DNA normalisation and concentration

DNA concentration and purity were determined using a spectrophotometer (NanoDrop™ 1000 Spectrophotometer, Thermo Scientific) and fluorometer (Qubit™ Fluorometer used in conjunction with the Qubit™ dsDNA BR Assay Kit, Invitrogen). Samples for genome-wide association mapping were normalised in ultrapure water (MQ; Ultra Clear UV Plus Water System, SG) to a final concentration of 20 ng/μL and a final volume of 25 μL. Samples for pre-NGS QC were normalised in MQ to a final concentration of 30 - 80 ng/μL and a final volume of 50 μL. Samples used for microsatellite genotyping and Sanger sequencing were normalised with MQ to concentrations of 20 ng/μL. For samples in need of concentration, DNA was precipitated using MultiScreen$_{HTS}$ PCR filter plates (Millipore) before resuspension in a smaller volume of MQ.

2.2.4 Polymerase chain reaction

The polymerase chain reaction (PCR) is used to amplify a specific region of DNA. A standard PCR mix comprises: DNA template; two primers complimentary to the 3' end of the sense and antisense DNA fragments to be amplified; deoxynucleotide triphosphates (dNTPs); a heat stable DNA polymerase (e.g. Taq polymerase); and buffer solution. A standard PCR protocol requires cycling through a series of thermally controlled steps, comprising an initiation phase, 30 - 45 cycles of three sequential steps (denaturation, annealing and elongation/extension), followed by a final elongation phase and an infinite holding step:

1. **Initiation step:** Required to activate Hot Start polymerases at 94 - 98 ^{o}C for 5 - 10 minutes.
2. **Denaturation:** The reaction is first heated to 95 ^{o}C for 30 seconds to denature the double-stranded DNA template. This step disrupts the hydrogen bonds between the strands and yields single-stranded DNA.
3. **Annealing:** The reaction is cooled to 50 - 60 ^{o}C for approximately 30 seconds to allow the primers to hybridise to the complementary single stranded DNA. The annealing temperature varies according the melting temperature (Tm) of the primers but is typically 3 - 5 ^{o}C below the primer Tm. If annealing temperature is too low then non-specific binding may occur. DNA polymerase then binds to the DNA-primer hybrid so that elongation may begin.
4. **Elongation:** DNA polymerase synthesises a new strand of DNA complementary to the strand to which the primer has bound using the dNTPs in the reaction mix. Extension occurs in the 5' to 3' direction by condensing the 5'-phosphate group of the complimentary dNTP onto the 3'-hydroxyl group of the nascent DNA strand. The temperature used varies according to the optimum temperature of the DNA polymerase. For Taq polymerase, a temperature of 72 ^{o}C is typically

selected. Under optimal conditions, target DNA amplification occurs in an exponential fashion. Steps 2 - 4 are repeated 30 - 45 times.

5. **Final elongation:** This step is performed to ensure that any remaining single-stranded DNA is fully extended. It is performed at the same temperature as the elongation phase (typically 72 ^{o}C) and for 5 - 30 minutes.
6. **Final hold.** This step is performed for an indefinite amount of time to safely store the final PCR reaction for a short period. A temperature of 7 - 12 ^{o}C is usually employed.

The thermal cycling reactions and parameters used varied from experiment to experiment and are presented in **Appendix II** and **III**. For allelic discrimination assays, an additional step was incorporated to measure fluorescent emissions (allelic reads) in the reaction. PCR amplification for microsatellite genotyping consisted of two three-step cycles. The first was used to amplify from the tailed forward primer and reverse primer and another, at a lower annealing temperature, for annealing of the tailed primer and the tailed fluorescent primer. Unless stated otherwise, HotStarTaq Plus DNA Polymerase (Qiagen) was used for all PCR reactions. For DNA templates with high GC content, an additive, Q solution (Qiagen) was added to facilitate double-stranded DNA denaturation. For each PCR experiment, a non-template control was included as a quality control measure. Thermal cycling for PCR and microsatellite genotyping was carried out on a T100^{TM} thermal cycler (Bio-Rad) and for allelic discrimination on a StepOnePlus^{TM} Real-Time PCR System (Applied Biosystems).

2.2.5 Primer design

All primers for microsatellite genotyping, Sanger sequencing and mutation detection by allelic discrimination assays were designed using Primer3 (http://bioinfo.ut.ee/primer3-0.4.0/primer3/) and details can be found in **Appendix IV**[173-175]. All primers were designed to meet the following criteria:

- **Primer length:** 16 - 24 bp with an optimum length of 21 bp.
- **Primer melting temperature (Tm):** 57 - 63 ^{o}C with an optimum of 60 ^{o}C.
- **Maximum Tm difference:** 2 ^{o}C between each primer of a pair in order that both primers will anneal with similar efficiency at the experimental temperature.
- **Guanine-cytosine (GC) content:** Minimum 40 % and maximum 60 %. High GC content leads to stable imperfect hybrids and low GC depresses the Tm of perfect hybrids. In GC-rich regions, this parameter was relaxed to a minimum of 20 % and maximum of 80 %.
- **Maximum allowable length of a mononucleotide repeat (Max Poly-X):** 3 - increasing this reduces the specificity of the primer.
- **Consecutive guanine and cytosine bases at primer 3' end (CG clamp):** 2 - increasing this provides tighter primer binding but at the expense of reducing suitable primers.

Each primer pair was 'blasted' (BLAST = Basic Local Alignment Search Tool) against the canine reference assembly (CanFam3.1) using the Ensembl genome browser (http://www.ensembl.org/index.html), to ensure that primers were specific to the targeted DNA fragment. Primers with more than 100 alignments were discarded and new ones designed. For primer pairs designed for microsatellite genotyping, an 18 bp tail (TGACCGGCAGCAAAATTG) was added to the 5'-end of the forward primer as previously reported[176]. A third primer with sequence complementary to the tail was labelled with a fluorescent molecule, FAM (with blue fluorescence), to allow detection of fragments on an ABI 3130xl genetic analyser (Applied Biosystems).

For allelic discrimination assays (SNP genotyping), a pair of primers was designed along with two allele-specific probes. One probe was labelled with 6-FAM and the other with HEX reporters and both were labelled with a Black Hole Quencher®. The design criteria for the probes were as follows:

- The targeted nucleotide should be within the middle third of the probes
- Tm 4 – 5 ^{o}C > than Tm of primers
- Product size as small as possible
- The 5' nucleotide should not be guanine

All primers and probes were purchased from Integrated DNA Technologies (IDT, Belgium).

2.2.6 Agarose gel electrophoresis

Following PCR amplification of the initial DNA templates (and a non-template control), an aliquot of the product was run on an agarose gel to ensure the presence of expected PCR product. Molecular grade agarose (Bioline) was used to make a 1.5 % gel (1.5 g agarose in 100 mL 1X TAE buffer (National Diagnostics)). The agarose was dissolved by heating and 3 μL of 0.625 mg/mL ethidium bromide was added prior to casting. Once set, the gel was completely submerged in 1X TAE buffer in an electrophoresis tank (PerfectBlue^{TM} Gel System Mini L, PeqLab). An aliquot (2 μL) of each PCR product was mixed with 5 μL STOP loading dye before loading into lanes of the gel. A 2-Log DNA Ladder (10 μL; New England Biolabs) was loaded as a size control. Electrophoresis was performed at 120 V for 45 minutes. The gels were analysed under ultraviolet light using a fluorochemistry imager (FluorChem^{TM} 5500 Imager, Alpha Innotech). Samples for which a single band of the expected size was visible, and when the band was absent from the non-template control lane, were considered suitable for microsatellite genotyping or sequencing (following purification).

2.2.7 Microsatellite genotyping

Microsatellite genotyping was used to investigate associations between candidate genes and PLD and PCAG. Microsatellites were identified and selected as described in **1.3.1.2.1** and primers were designed as described above with resulting products between

200 and 400 bp in size. After amplification with the third fluorescent primer, PCR products were separated by size on an ABI 3130xl Genetic Analyzer using the GeneScan 400HD Rox size standard (Applied Biosystems). Data were analysed and alleles assigned to each sample using GeneMapper v4.0 software (Life Technologies Ltd.).

2.2.8 Sanger sequencing

2.2.8.1 Purification of PCR products

Following initial PCR and successful amplification, as assessed by agarose gel electrophoresis, PCR product purification was performed to remove excess primers and PCR reagents. PCR products were purified using 96-well MultiScreen$_{HTS}$ PCR filter plates (Millipore), according to the manufacturer's instructions. Briefly, 100 µL MQ was added to each well containing PCR product. Following this, each sample was transferred into the corresponding well on the filter plate. The filter plate was then assembled onto a vacuum manifold and a vacuum of 15 inches Hg was applied for 10 - 20 minutes until each well appeared empty. The filter plate was then removed from the manifold, 20 µL MQ was added to each well and the DNA was resuspended by gentle agitation for 20 minutes on a rocking table (Luckham Ltd.). The purified products were then transferred to a 96-well PCR plate for storage and further use.

2.2.8.2 Sequencing reaction

The same primers used for initial PCR amplification were also used for Sanger sequencing. Sequencing was performed in both the forward and reverse directions (by performing reactions with forward and reverse primers separately). Sanger sequencing was performed using Bigdye v3.1 chemistry (Life Technologies Ltd). The reaction and cycling parameters used are presented in **Table 2.2** and **Table 2.3**.

Table 2.2. Recipe for Sanger sequencing.

Reaction component	Volume/reaction (μL)	Final concentration
Template (PCR product)	2	
2.5 X Bigdye Ready Reaction Mix	0.5	0.2 X
10 X SBDD Buffer	1	1.7 X
Primer (1.6 μM)	1	0.27 μM
Ultrapure water (MQ)	1.5	

Table 2.3. Thermal cycling parameters for Sanger sequencing.

Step	Temperature	Duration	Cycles
Initial denaturation	96 ^{o}C	30 s	
Denaturation	92 ^{o}C	4 s	X44
Annealing	55 ^{o}C	4 s	
Extension	60 ^{o}C	110 s	

Following sequencing, excess reagents were removed by isopropanol precipitation. Briefly, 60 μL of 80 % isopropanol was added to each reaction in the 96-well PCR plate to precipitate the DNA. The plate was then centrifuged at 2,254 x g for 30 minutes to collect the DNA at the bottom of each well. The supernatant was discarded by tipping the plate upside-down, and blotting the inverted plate on tissue to prevent cross-contamination. Further purification was performed by the addition of 100 μL of 60 % isopropanol followed by centrifugation at 2,254 x g for 10 minutes to collect the DNA at the bottom of each well. The supernatant was discarded as above, and excess isopropanol was removed by placing the plate upside-down on tissue, followed by

centrifugation at 141 x g for 1 minute. To ensure all isopropanol was removed and the DNA pellet was as pure as possible, the plate was dried in a 37 ^{o}C oven for 10 minutes. Finally, precipitated DNA was resuspended in 10 µL Hi-Di Formamide (Applied Biosystems). The sequencing products were then separated on an ABI 3130xl genetic analyser and data analysed using the Staden software package (http://staden.sourceforge.net/)[177]. The raw sequencing data were first processed using Pregap4 to determine if sequence quality was sufficient for alignment, to convert data from ABI to ZTR format and to create experiment files. Gap4 was then used to assemble and compare sequence reads, align and compare them to a reference sequence and view the sequence traces.

2.2.9 Genome-wide association studies

GWAS were used to investigate the genetics of PLD and PCAG in four dog breeds: BH, FCR, DDT and WSS. DNA samples were used from dogs with the following phenotypes:

1. Dogs with normal appearing ICAs aged five years and above (controls).
2. Dogs with PLD affecting at least 50 % of the ICA of each eye as assessed by gonioscopy (PLD cases).
3. Dogs with PCAG (PCAG cases). Criteria for a diagnosis of PCAG included elevated IOP > 50 mmHg, the absence of any possible cause of secondary glaucoma and the finding of severe PLD (> 90 % of the ICA affected) in the contralateral eye.

Dogs were designated as controls or PLD cases based on the results of gonioscopy performed by myself. Dogs were classified as PCAG cases following examination by board-certified veterinary ophthalmologists and included many samples from both national and international collaborators.

All DNA was extracted and normalised in house before submitting to an external laboratory for genotyping (Neogen). Cases and controls were randomly intercalated at the normalisation stage and, where possible, also at the DNA extraction stage. This was to preserve data quality and avoid any impact of between-chip variability in processing. GWAS were all performed using the CanineHD BeadChip (Illumina) which contains 172,115 SNPs (based on the CanFam2.0 reference sequence)[101]. Samples were submitted for genotyping in three batches over two years (corresponding with sample collection). New genotyping data were merged with previous data and reclustered in GenomeStudio (Illumina) to preserve data quality before analysis. Any SNPs that were found to be associated with disease were also checked for expected clustering in GenomeStudio. GWAS data were analysed using the freely available software package PLINK (http://zzz.bwh.harvard.edu/plink/)[178]. Data were filtered for quality control parameters including sample call rate, SNP call rate and minor allele frequency (MAF). SNPs were excluded from analysis if they were not polymorphic, had a MAF < 0.05 or had a call rate of < 97 %. Individuals were excluded if > 10 % SNP genotypes were missing.

SNPs were not excluded on the basis of Hardy-Weinberg equilibrium due to the inbred nature of purebred dogs, the small sample size of the studies, and the non-population-based sampling methods, making it more likely that truly associated SNPs could be filtered out using Hardy-Weinberg. Clustering/assay performance of associated SNPs were checked in GenomeStudio. GWAS analyses were conducted using a standard unadjusted allelic chi-squared test for association (1 degree of freedom (df)). Genome-wide Manhattan plots were created to display the GWAS findings with respect to their genomic positions to highlight any signals of potential interest. Manhattan plots represent the P-values of the entire GWAS on a genomic scale. The P-values are represented in genomic order by chromosome and position on the chromosome (x-axis).

The value on the y-axis represents the $-\log_{10}$ of the P-value. Because of local correlation of the genetic variants, arising from infrequent genetic recombination/LD, groups of significant P-values tend to rise up high on the Manhattan plot, making the graph look like a Manhattan skyline.

For each individual breed, the following analyses were performed:

1. PCAG cases and controls
2. PCAG and PLD cases combined and controls
3. PLD cases and controls
4. PCAG cases and PLD cases
5. PCAG cases and PLD cases and controls combined

2.2.9.1 Assessment and correction of population stratification

As part of all GWAS conducted, quantile-quantile (Q-Q) and multi-dimensional scaling (MDS) plots of cases and controls were created using PLINK (**Appendix VI**). MDS is a means of visualising the level of similarity (homogeneity) between the cases and controls and refers to a set of related ordination techniques to display the information from the GWAS genotypes in a distance matrix. Cases and controls should be intercalated in the plot with little evidence of separate clustering. The MDS plot allows visualisation of potential outlier samples, for example if an incorrect breed was included in the analysis, which would then be excluded from subsequent analyses.

Q-Q plots were created in Excel using summary association statistics (χ^2 values from unadjusted PLINK analysis and χ^2 values converted from P-values of score test in GEMMA (Genome-wide Efficient Mixed-Model Association, www.xzlab.org/software.html)[179]. The Q-Q plot is used to assess the number and magnitude of observed associations between genotyped SNPs and the disease compared to the association statistics expected by chance because of the large number of statistical tests performed. Observed association statistics are ranked from smallest to largest on

the y-axis against the null hypothesis of no association on the x-axis. General deviations from the null line suggest that there is bias in the study set, such as population stratification. Deviation of observed associations from the end of the null line is suggestive of true association of genotype with phenotype. Inflation of observed statistics due to relatedness or population substructure can be estimated by genomic control (λ). Genomic control is defined as the median χ^2 (1 df) association statistic across SNPs divided by its theoretical median under the null distribution and is proportional to sample size[180]. A value of $\lambda \approx 1$ indicates no stratification, whereas $\lambda > 1$ indicates stratification or other confounders such as family structure of cryptic relatedness, or differential bias. $\lambda < 1.05$ is generally considered benign.

Data were subsequently corrected for population stratification using the mixed model GEMMA. A mixed model is a class of statistical model in which phenotypes are modelled using both fixed effects such as GWAS SNPs and fixed covariates and random effects (the genotypic covariate matrix). GEMMA takes into account the familial and pedigree structure of the case-control sample set by calculating kinship matrices directly from the genome-wide SNP data and its application results in a reduction in the λ which becomes visually evident on the Q-Q plot as the observed statistics more closely approximate to the null line.

2.2.9.2 Statistical association of variants with disease

P-values derived from GEMMA were used to create a Manhattan plot for each analysis. A P-value of 0.05 after correction for multiple testing using the Bonferroni correction (0.05/number of tests) was the threshold for significant statistical association in all studies (typically $-\log_{10}P = 6.3$) and prompted further investigation of associated SNPs.

Associations between GWAS SNPs and candidate variants and disease were assessed using the Fisher's exact test and logistic regression using an additive model to compute an odds ratio and confidence interval for the association of SNPs with disease. Logistic

regression and log-likelihood ratio tests were used to assess the shape of the association between variants and disease by comparing a general inheritance model with a linear per allele model. The variance in disease risk explained by one or more SNPs was obtained from the pseudo R^2 value from the regression model.

Logistic regression and log-likelihood ratio tests were also used to examine the independence of SNPs statistically associated with disease risk. This was done by comparing the log likelihood of a nested model (2 df) with that of a full model (3 df) by adding the other SNP (coded in a linear 1 df) into a model containing the strongest associated SNP (coded as a general inheritance 2 df form). This analysis was also repeated reciprocally.

2.2.9.3 Meta-analysis studies

In the meta-analysis studies, summary estimates (beta coefficients and standard errors) from each individual breed association analysis (using GEMMA) were combined using meta-analysis for SNPs that were informative in all breeds and that had passed individual-breed QC filters (MAF and call rate) in all breeds. Effect allele designation was harmonised amongst studies prior to analysis by beta coefficient flipping where required. A fixed effects model and inverse-variance weighted averages of beta coefficients to obtain a combined estimate of the overall association between SNPs and disease was used. Heterogeneity was assessed using the Q statistic. An inflation factor (λ) was calculated for the meta-analysis which was estimated from the median of the chi-squared tests generated on all SNPs that were tested. The above statistical analyses described in **2.2.9.2** and **2.2.9.3** were conducted using STATA 10.0 (College Station, TX, USA) and were performed by Dr Sally Ricketts.

2.2.9.4 Genome-wide haplotype analysis

In addition to standard GWAS, multi-SNP haplotype analysis methods for association analysis were performed using unadjusted association data in PLINK. The disadvantage

of this approach was that the data had not been corrected for population stratification. The potential advantage of this approach is that it might reveal certain associations not detected by single SNP analysis because haplotypes may capture a causal variant more effectively than any single measured SNP. Genome-wide sliding windows of 1 – 8 SNPs were selected and Manhattan plots of association of these SNP windows with phenotype were created. The threshold for genome-wide significance for haplotype analysis was also set using Bonferroni correction. Haplotype permutation analyses were also performed in PLINK using 100,000 permutations. Permutation procedures provide a computationally intensive approach to generating significance levels empirically. Such values have desirable properties: for example, relaxing assumptions about normality of continuous phenotypes and Hardy-Weinberg equilibrium, dealing with rare alleles and small sample sizes, providing a framework for correction for multiple testing, and controlling for identified substructure or familial relationships by permuting only within cluster.

The threshold for significance for haplotype permutation association analysis was set at $\log_{10}0.05$ (1.3). Haplotype association and permutation plots are presented in **Appendix VII** rather than in the main text as they did not reveal any additional significant associations of SNPs with disease that were not detected by standard GWAS.

2.2.10 Next-generation sequencing of DNA

All NGS was performed on the Illumina sequencing platforms. Whole-genome sequencing (WGS) of all samples was outsourced to the High Throughput Genomics (HTG) group at the Welcome Trust Centre for Human Genetics (WTCHG, University of Oxford), Cambridge Genomic Services (CGS, University of Cambridge) or Edinburgh Genomics (University of Edinburgh). The amount of DNA, library preparation, read length and depth, and sequencing platforms used varied, particularly for early samples (**Table 2.4**).

Targeted NGS was performed in-house on a MiSeq platform. The NGS process is made up of three parts that are broadly similar for WGS and targeted sequencing: library preparation, cluster generation and sequencing. The description that follows applies specifically to targeted sequencing as it was performed in-house.

Table 2.4. Summarised details of DNA amount, library preparation, sequencing laboratory, read length and coverage and sequencing platform for samples submitted for WGS.

Sample ID	Mass, volume of DNA sent	Library preparation	Sequencing laboratory	Read length, coverage	Platform
WSS_24604	4nM, 18uL (pooled)	In-house, TruSseq LT PCR free	CGS	150 bp PE, 20x	NextSeq
WSS_25078	4nM, 18uL (pooled)	In-house, TruSeq LT PCR free	CGS	150 bp PE, 20x	NextSeq
FCR_25382	1000 ng, 60 uL	WTCHG, PCR FREE	WTCHG	100 bp PE, 20x	HiSeq4000
FCR_25384	1000 ng, 60 uL	WTCHG, PCR FREE	WTCHG	100 bp PE, 20x	HiSeq4000
BaH_28502	2500 ng, 55 uL	Edinburgh Genomics, TruSeq Nano	Edinburgh Genomics	150 bp PE, 30x	HiSeqX
BaH_29716	2500 ng, 55 uL	Edinburgh Genomics, TruSeq Nano	Edinburgh Genomics	150 bp PE, 30x	HiSeqX
BaH_31929	2500 ng, 55 uL	Edinburgh Genomics, TruSeq Nano	Edinburgh Genomics	150 bp PE, 30x	HiSeqX
DD_26698	2500 ng, 55 uL	Edinburgh Genomics, TruSeq Nano	Edinburgh Genomics	150 bp PE, 30x	HiSeqX
DD_27784	2500 ng, 55 uL	Edinburgh Genomics, TruSeq Nano	Edinburgh Genomics	150 bp PE, 30x	HiSeqX
WSS_25165	2500 ng, 55 uL	Edinburgh Genomics, TruSeq Nano	Edinburgh Genomics	150 bp PE, 30x	HiSeqX
WSS_7617	2500 ng, 55 uL	Edinburgh Genomics, TruSeq Nano	Edinburgh Genomics	150 bp PE, 30x	HiSeqX
DD_14598	764 ng, 40 uL	Edinburgh Genomics, TruSeq Nano	Edinburgh Genomics	150 bp PE, 30x	HiSeqX

2.2.10.1 Library preparation

DNA libraries were prepared using the Nextera XT DNA Library Preparation Kit (Illumina). The Nextera DNA Sample Preparation Kit uses an engineered transposome to simultaneously fragment and tag ("tagment") input DNA, adding unique adapter sequences in the process (**Figure 2.2**). A limited-cycle PCR uses these adapter sequences to amplify the insert DNA. The PCR also adds index sequences on both ends of the DNA, thus enabling dual-indexed sequencing of pooled libraries.

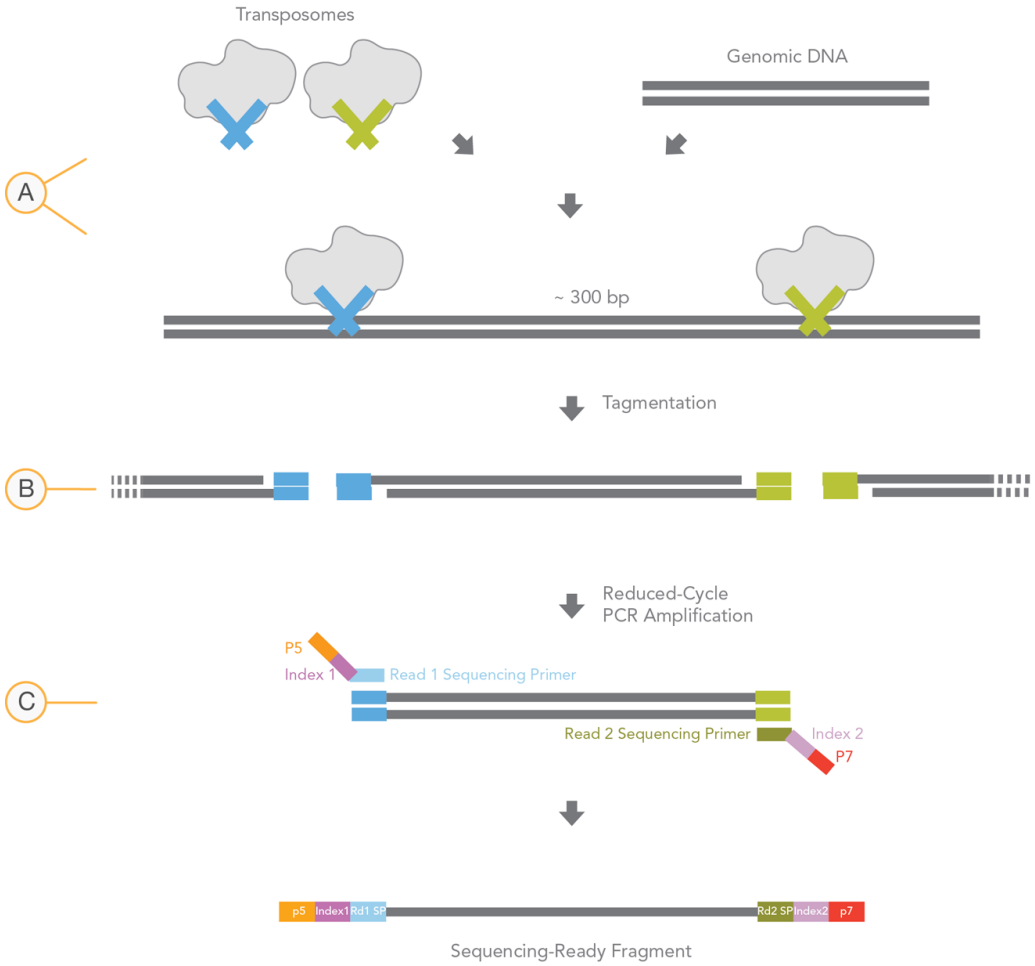

Figure 2.2. Nextera XT library preparation.

A - Nextera XT transposome with adapters is combined with template DNA. B - Tagmentation to fragment and add adapters. C - limited cycle PCR to add sequencing primer sequences and indicies. (http://support.illumina.com).

Library preparation was performed according to the manufacturer's recommendations, with some modifications. Briefly, 5 μL of 0.2 ng/μL input DNA was combined with 10 μL supplied Tagment DNA Buffer and 5 μL of Amplicon Tagment Mix, and the solution was mixed by pulsing. The tagmentation solution was incubated at 55 ^{o}C for 5 minutes, followed by the addition of 5 μL of Buffer NT and mixing. Tagmented DNA was then purified using AMPure XP (Beckman Coulter Life Sciences) beads and the purified tagmented DNA eluted in MQ. PCR was then performed by combining 5 μL of index primer 1, 5 μL of index primer 2, 15 μL purified tagmented DNA and 25 μL KAPA HIFI HS RM to individual wells of a PCR plate and thermal cycling performed according to the conditions in **Table 2.5**.

Table 2.5. Thermal cycling parameters for Nextera XT library preparation.

Step	Temperature	Duration	Cycles
Initiation	72 ^{o}C	3 m	
Initial denaturation	98 ^{o}C	30 s	
Denaturation	98 ^{o}C	10 s	X12
Annealing	63 ^{o}C	30 s	
Extension	72 ^{o}C	3 m	
Hold	10 ^{o}C	∞	

Purification with AMPure XP beads was repeated and the purified DNA library was resuspended in 25 μL MQ. Eluted libraries were quantified by quantitative PCR (qPCR), using the KAPA Library Quantification Kit for the Illumina Genome Analyser Platform (KAPA Biosystems), on an Eco Real-Time PCR System (Illumina). Briefly, a 10 μL reaction volume was used, made up of 6 μL 2X KAPA SYBR FAST qPCR

Master Mix containing primer premix, 2 μL MQ and 2 μL Library DNA (diluted 1:1,000 with Library Dilution Buffer) or 2 μL DNA standard or 2 μL MQ (non-template control). Thermal cycling was then performed as below (**Table 2.6**). Experimental DNA library reactions were performed in triplicate whereas those of DNA standards and non-template controls were performed in duplicate.

Table 2.6. Quantitative PCR cycling conditions.

Step	Temperature	Duration	Cycles
Initial denaturation	95 ^{o}C	5 m	
Denaturation	95 ^{o}C	30 s	
Annealing, extension and data acquisition	60 ^{o}C	45 s	X 35

Average concentrations determined by qPCR were then adjusted to account for differences in the average length of the DNA library and the length of the DNA standards (452 bp). The following formula was used: $C = A \times \frac{452}{S} \times D$, where C = concentration to be determined (pM) , A = average concentration (pM) determined by qPCR, S is the size of the fragments (bp) as determined by Bioanalyser analysis (outsourced to CGS, University of Cambridge) and D is the dilution factor (1,000) used in the qPCR reaction. Finally, all captured libraries were diluted to 3,000 pM (3 nM) and pooled in equimolar amounts for multiplexed sequencing.

2.2.10.2 Cluster generation

Cluster generation is performed by the sequencing platform (e.g. Miseq) prior to sequencing. The pooled library is first immobilised on the surface of a flow-cell; the single-stranded DNA library fragments first randomly bind to oligonucleotides on the

surface of the flow-cell, via the complimentary adapters added during library preparation. Unlabelled nucleotides and enzyme are then added and the bound fragments are then extended to form double-stranded DNA and the adapter on the unattached end also binds covalently to the flow-cell surface to form a bridge. Through a series of expansions, bridge amplification and denaturation, each library fragment is clonally amplified to create millions of unique clusters. The reverse strands are removed to leave single-stranded DNA molecules attached at one end to the flow-cell. The free ends are then blocked and sequencing primers hybridise to the DNA templates.

2.2.10.3 Sequencing

The Illumina systems use sequencing by synthesis (SBS) technology in which DNA templates are sequenced in parallel, base by base. Four fluorescently-labelled nucleotides compete to bind to millions of templates simultaneously. The labelled nucleotides are reversibly terminated so that the templates only extend by a single base in each round of synthesis. After each round of synthesis, a laser is applied to excite the clusters with the resultant colour of fluorescence denoting the identity of the newly bound base. After this, cleavage of the terminator molecule and fluorescent label occurs, allowing the commencement of the next round of base addition to the DNA template.

Targeted NGS was performed in-house on the MiSeq platform, and the first 100 bases of each fragment were sequenced from one end only, resulting in 100 bp single end reads. Initial data quality control was performed by the MiSeq, generating the raw sequencing data in FASTQ format. For WGS (outsourced to commercial sequencing laboratories), the first 100 or 150 bases of each fragment were sequenced from both ends of the fragment to result in 100 bp or 150 bp paired-end reads. Initial quality control was conducted by the commercial laboratories to include the Illumina base-calling pipeline and Illumina tag identification.

2.2.10.4 Data analysis

Raw sequencing data were received as FASTQ files containing millions of sequence reads 100 or 150 bp in length. The FASTQ files were run through the AHT pipeline which was designed by Dr Mike Boursnell. This pipeline is made up of a number of analytical tools. The BWA (Burrows-Wheeler-Alignment) tool aligns short sequences to the reference sequence (CanFam3.1) by assigning chromosomal coordinates to each read, creating a read file in SAM (Sequence Alignment/Map) format[181]. Picard was used to manipulate SAM files to create BAM (Binary Alignment/Map) files in which the reads were sorted according to chromosomal coordinates. The BAM files could be directly analysed at this stage using the Integrated Genomics Viewer (IGV) if desired (for example if a strong candidate gene had already been identified)[182,183].

SAMtools was used to manipulate both SAM and BAM files, removing PCR duplicate reads and retaining only read pairs of the highest quality. SAMtools was also used to index the reference FASTA files and read BAM files. GATK (Genome Analysis Toolkit) provides a Java programming framework for writing tools for the analysis of NGS data[184]. The pipeline included various built-in tools including base quality score recalibration, identification of indels and SNPs and depth coverage calculations. Variants were filtered by effect of variant using the Ensembl Variant Effect Predictor (VEP) to provide an 'effect score' for variants giving rise to new annotated files (VCF_VEP) before conversion into Excel files[185,186]. The effect score is a scoring system (graded 1 to 5) developed by the AHT to rank the variants by their anticipated effect on proteins. For example, coding deletions, coding insertions and nonsense variants were assigned the highest effect score of 5, whereas intergenic variants were assigned the lowest effect score of 1. To further aid in variant filtration, segregation scores were also assigned by comparing WGS data between affected and unaffected dogs. The higher the score, the better the variant segregated with disease status, with the highest possible score equal to the number of individuals used in the analysis.

Depending on the nature of the disorder being investigated, effect scores and segregation scores are used to filter out variants unlikely to be pathogenic, thereby reducing the number of candidate variants to a practical and manageable level for further investigation.

2.2.11 Identification of candidate variants

A next-generation WGS approach was used to identify variants that segregated with PCAG in loci determined by GWAS. Associated loci were defined based on pair wise linkage disequilibrium estimates ($R^2 \geq 0.5$) of the SNPs using the Tagger program embedded in Haploview[187,188]. A list of SNPs in LD with the top GWAS SNP was generated which could denote a region tagged by the GWAS association signal. SNPs were excluded from analysis if they had a minor allele frequency < 0.05 or had a call rate of < 97 %. but were not excluded on the basis of Hardy-Weinberg equilibrium. As canine PCAG is thought to be a complex disease, possibly involving a combination of risk alleles, effect score was set at the minimum. However, to reduce the number of variants to a practical level, the highest possible segregation score was selected. In **section 4.2**, candidate variants were searched within susceptibility loci in breed-specific analyses using a single WGS from one PCAG case and 97 controls of other breeds without PCAG and belonging to breeds not thought to be predisposed to PLD or PCAG. Identified variants were further explored using WGS from 465 canids, held by the Dog Biomedical Variant Database (DBVD) consortium to which the AHT belongs. Only variants that were private to the breed in question were further investigated.

2.2.12 Variant screening

The method used to screen samples for candidate variants varied, depending on the nature of the variant and number of samples being screened and all raw genotyping results are presented in **Appendix VIII**. Insertion or deletion (indel) mutations result in a change in PCR amplicon size which was generally assessed by amplified fragment

length polymorphism (AFLP) analysis. This was achieved using capillary electrophoresis of 5' 6FAM-labelled PCR products on an ABI 3130xl genetic analyser and data were analysed with GeneMapper v4.0 (Life Technologies Ltd.). Sanger sequencing (as described in **section 2.2.8**) was employed to screen small sample cohorts for indel or SNP variants. Allelic discrimination was used to identify SNP variants in larger sample cohorts. This method makes use of allele-specific fluorescently labelled probes, with each probe labelled with a unique fluorescent reporter (6-FAM or HEX) on the 5'-end and a quencher on the 3'-end. As long as the reporter and quencher are in close proximity to each other, as they are when not hybridised to the mutation, the quencher absorbs the fluorescence emitted by the reporter dye. During PCR, however, the probe hybridises to the target SNP and is cleaved by the 5'- to 3'-exonuclease activity of polymerase. This results in spatial separation of the reporter and quencher increasing the fluorescence of the reporter dye. By determining which reporter dye is fluorescing, the allele-specific primer that is hybridising with the DNA template, and therefore allele, can be identified.

2.3 Gene expression studies

2.3.1 Tissue collection and RNA extraction

Most dogs with primary glaucoma require eye removal (enucleation) on welfare grounds when the eyes are irreversibly blind, painful and there is no response to therapy. When possible, and following informed written owner consent, tissue samples were collected and stored immediately following enucleation. Following enucleation, each globe was transected along the sagittal plane into two equal halves. Each half globe was immersed in 15 mL RNA*later* solution (Ambion) before storing at -80 ^{o}C until later use as previously described[189,190]. RNA was extracted from selected tissue samples using the Qiagen RNeasy Midi Kit (Qiagen). Following thawing of each half globe, a section of ICA was dissected under an operating microscope with microsurgical

instrumentation aiming for approximately 200 - 250 mg tissue. The posterior boundary of the dissected tissue was the posterior pars plana and the anterior boundary was the corneoscleral limbus. No lens tissue was included in the dissection but the sclera was included. Adherent conjunctiva and episcleral tissues were removed. The resultant tissue section was weighed on an electronic balance to ensure a final weight of 150 - 250 mg tissue. The tissue was placed in a 15 mL centrifuge tube (Falcon) and 80 µL 2M DDT (dithiothreitol) and 4 mL RLT buffer before homogenisation using a motorised rotor-stator homogeniser (Omni International). The lysate was then centrifuged for 10 minutes at 4,500 x g to remove debris and prevent subsequent filter clogging. The supernatant (3 - 4 mL) was then transferred by pipetting into a clean 15 mL tube. To the supernatant was added one volume of 70 % ethanol before mixing by vigorous shaking, followed by the addition of 4 mL of sample to an RNeasy Midi column on a supplied 15 ml centrifuge tube and centrifugation for 5 minutes at 4,500 x g. The flow-through was discarded and the step was repeated with any remaining sample, followed by the addition of 4 mL Buffer RW1 to the spin column and centrifugation for 5 minutes at 4,500 x g, discarding the flow-through. In order to eliminate any contaminating DNA, 20 µL DNAase was added to 140 µL RDD and gently mixed before pipetting gently onto the spin column filter and left to stand at room temperature for 15 minutes. Biomolecules such as carbohydrates and proteins were removed by the addition of 2 mL Buffer RW1 to the column, which was left to stand for 5 minutes and then centrifuged for 5 minutes at 4,500 x g. The flow-through was discarded and traces of salts were removed by the addition of 2.5 mL Buffer RPE to the column before centrifugation for 2 minutes at 4,500 x g. The flow-through was discarded and a further 2.5 ml Buffer RPE was added before centrifugation for 5 minutes at 5,000 rpm. The spin column was then transferred to a new 15 mL centrifuge tube and 250 µL RNase free water was added to elute, left to stand for 1 minute then centrifuged for 3 minutes at 4,500 x g.

This step was then repeated and the eluted RNA transferred to a 1.5 mL eppendorf tube. RNA concentration and purity was assessed by Nanodrop with a target final concentration of 20 – 80 ng/µL. RNA integrity was initially assessed by agarose gel electrophoresis (**section 2.2.6**). Intact total RNA run on an ethidium bromide denaturing gel has clear 28S and 18S rRNA bands. The 28S rRNA band should be approximately twice as intense as the 18S band. Partially degraded RNA has a smeared appearance. RNA was stored at -20 ^{o}C for up to 2 weeks or at -80^{o}C for long-term storage.

2.3.2 Quantitative reverse transcriptase PCR

Quantitative reverse transcriptase PCR (qRT-PCR) was used to compare gene expression between normal and affected tissues. Two step qRT-PCR was performed using complementary DNA (cDNA) synthesised by the reverse transcription of tissue-extracted RNA.

2.3.2.1 Reverse transcription of RNA

Reverse transcription was performed using the QuantiTect Reverse Transcription Kit (Qiagen) according to the manufacturer's instructions. Template RNA was thawed on ice and the supplied gDNA Wipeout Buffer, Quantiscript Reverse Transcriptase, Quanitiscript RT Buffer, RT Primer Mix and RNase-free water were thawed at room temperature. Each solution was mixed by gentle flicking and brief centrifugation before keeping on ice. Before reverse transcription, a genomic DNA elimination reaction was performed using 2 µL 7x gDNA Wipeout Buffer and 12 µL template RNA (up to 1 µg). The reaction was performed with incubation for 2 minutes at 42 ^{o}C before placing on ice. A reverse-transcription reaction was performed for each sample, which included 1 µL Quantiscript Reverse Transcriptase, 4 µL 5x Quantiscript RT Buffer, 1 µL RT Primer Mix and the entire genomic DNA elimination reaction (14 µL). The reaction was mixed, stored on ice and then incubated for 15 minutes at 42 ^{o}C. Incubation was then

performed at 95 ^{o}C to inactivate Quantiscript Reverse Transcriptase. The reaction (cDNA) was stored at -20 ^{o}C until subsequent use for sequencing or qPCR.

2.3.2.2 Quantitative PCR

Forward primer, reverse primer and assay probe were designed using the IDT PrimerQuest design tool (https://eu.idtdna.com/Primerquest/Home/Index). To avoid amplification of any contaminating genomic DNA, primers were designed so that one primer hybridises to the 3' end of one exon and the other to the 5' end of the adjacent exon, thereby flanking the exon splice sites. Such primers ensure that only cDNA synthesised from spliced mRNAs is amplified, but genomic DNA is not. Desired amplicon parameters were adjusted as follows: minimum amplicons size = 60, maximum amplicon size = 120, optimum amplicon size = 90. A sequence specific fluorescently labelled probe (5'FAM), complimentary to sequence between the two primers, was incorporated in each assay. In addition to the qPCR assay, PrimeTime® Gene Expression Master Mix (IDT) and template cDNA were required. The PrimeTime® Gene Expression Master Mix is a ready-to-use 2X concentrated master mix designed for use in probe-based, real-time quantitative PCR. It contains an antibody-mediated, Hot Start DNA polymerase, dNTPs, $MgCl_2$, enhancers and stabilisers and a reference dye. The template cDNA samples generated by reverse transcriptase were normalised to 20 ng/µL (as assessed by Nanodrop). qPCRs were performed in 10 µl reactions using a StepOnePlus^{TM} Real-Time PCR System (Applied Biosystems) as detailed in **Table 2.7** and **Table 2.8**.

Table 2.7. Thermal cycling recipe for qPCR.

Reaction component	Volume/reaction (µL)	Final concentration
cDNA template (20 ng/µl)	4	8 ng/µl

PrimeTime® Gene Expression Master Mix (2 X)	5	1 X
PrimeTime® qPCR assay (10 X)	1	1 X

Table 2.8. Thermal cycling parameters for qPCR.

Step	Temperature	Duration	Cycles
Polymerase activation	95 ^{o}C	3 m	
Denaturation	92 ^{o}C	15 s	X 40
Annealing/extension	60 ^{o}C	1 m	
Hold	4 ^{o}C	Up to 24 h	

cDNA derived from normal and affected tissues were used in each experiment with reactions performed in triplicate and with a no template control. To enable relative quantification of real-time PCR products, the ratio between the amounts of target gene and a house-keeping gene was determined using the ΔΔCT method[191]. Unless otherwise stated, the house-keeping gene used for the reference assay was TATA box binding protein (*TBP*).

The methodology behind this technique is as follows: during the annealing stage of the PCR both probe and primers anneal to the DNA target. Polymerisation of a new DNA strand is initiated from the primers, and once the polymerase reaches the probe, its 5'-3'-exonuclease degrades the probe, physically separating the fluorescent reporter from the quencher, resulting in an increase in fluorescence. Fluorescence is detected and measured in the real-time PCR machine, and its geometric increase corresponding to exponential increase of the product is used to determine the threshold cycle (C_T – the precise cycle at which the level of fluorescence exceeds a desired threshold) in each

reaction. C_T values were averaged for each sample/probe triplicate for both the target gene and house-keeping gene and the difference between the two was calculated (ΔC_T). The difference between the average ΔC_T value of the sample of interest (cDNA from affected tissue) and the average ΔC_T of the reference sample (cDNA from unaffected tissue) was then calculated ($\Delta\Delta C_T$). An unpaired t-test was performed and the gene was defined as differentially expressed where a statistically significant change in expression level, measured as fold change (FC), was observed and where FC was ≥ 2 or ≤ -2.

2.3.3 Next-generation RNA sequencing

The integrity and purity of total RNA were assessed using an Agilent Bioanalyzer 2100 at CGS (University of Cambridge), and OD260/280 using Nanodrop. Total RNA (20ng - 1μg per sample, at a concentration of ≥ 20ng/uL with RIN ≥ 8.0 and OD260/280 ≥ 1.8) was submitted to Otogenetics Corporation for library preparation and sequencing: 1 - 2 μg of cDNA was generated using Clontech Smart cDNA kit (Clontech Laboratories) from 100ng of total RNA. cDNA was fragmented using Covaris (Covaris) and profiled using an Agilent Bioanalyzer 2100. Libraries were prepared using NEBNext reagents (New England Biolabs, Catalog No. 634925): mRNAs were purified using Poly(A) selection from the total RNA sample, and then fragmented. cDNA was then synthesised using random priming, followed by end repair, phosphorylation, A-tailing, adapter ligation and finally PCR amplification. The quality, quantity and size distribution of the Illumina libraries were determined using an Agilent Bioanalyzer 2100. The libraries were then loaded on an Illumina HiSeq2500 for clustering and sequencing according to the standard operation. Paired-end 90-100 nucleotide reads were generated and data quality was assessed using FASTQC (Babraham Institute, Cambridge, UK). After achieving optimum QC results, samples were analysed. The bioinformatics workflow for RNA-Seq, was performed by Otogenetics, and is summarised as follows:

- Sequence reads trimmed to remove adapters and low quality bases at the ends. After trimming, sequence reads shorter than 30 nucleotides were discarded.
- FASTQC quality control of Fastq file per sample.
- Sequence reads mapped to CanFam3.1 reference genome.
- Calculation of read count values of gene expression (FPKM – Fragments Per Kilobase Million).
- Differential gene expression analysis with unique read counts among samples.

2.3.3.1 Statistical analysis of transcriptome data

Sufficient samples were collected from five BH PCAG cases and four non-BH controls to allow for differential gene expression studies between these two groups in the loci identified in **4.2.2.1.6**. Differential expression of FPKM (read counts) between PCAG cases and controls was calculated as the base 2 log of fold change of controls/PCAG cases ($\log_2$ (FPKM of PCAG cases/FPKM of controls)). Differential gene expression could not be performed for genes with insufficient alignments or insufficient read depth. The test statistic was used to compute significance of the observed change in FPKM. The P-value represents the uncorrected P-value of the test statistic and the Q-value represents the False Discovery Rate-adjusted P-value of the test statistic. Significance of differential gene expression ('yes' or 'no') was based on whether the P-value was statistically greater than the Q-value.

2.3.3.2 Assessment of gene function and candidacy

For genes shown to be differentially expressed, their functions and associated phenotypes (for potential candidacy for canine PCAG) were assessed using VarElect GeneCards® (http://varelect.genecards.org). GeneCards is a searchable, integrative database that provides comprehensive information on all annotated and predicted human genes. It automatically integrates gene-centric data from approximately 125 web

sources, including genomic, transcriptomic, proteomic, genetic, clinical and functional information. .

3 Pectinate ligament dysplasia: prevalence and a study of inter-examiner variability in performing pectinate ligament dysplasia grading

3.1 Pectinate ligament dysplasia: prevalence, progression and associations with age, sex and intraocular pressure

3.1.1 Introduction

Gonioscopy is performed to identify PLD, which is advised in predisposed breeds prior to breeding. At the time of project outset, the BVA/KC/ISDS Eye Scheme recommended gonioscopy to be performed as a 'once in a lifetime test' as PLD was considered a congenital and static abnormality. There was, however, emerging evidence that this might not be the case with a single report of PLD progression over time in individual FCR[35].

The aims of the following studies were to:

1. Estimate the prevalence of PLD in BH, FCR, DDT, WSS, BC, GR and HV.
2. Investigate possible associations between IOP and sex, age and PLD in BH, FCR, DDT and WSS.
3. Investigate possible associations between PLD and sex and age in BH, FCR, DDT, WSS, BC, GR and HV.
4. Investigate PLD progression in individual WSS.

3.1.2 Results

In total, gonioscopy was performed in 198 BH, 170 FCR, 95 DDT, 227 WSS, 102 BC, 112 HV and 230 GR by myself. For each dog, data were collected on PLD, sex and age at time of examination. In the BH, FCR, DDT and WSS, IOP measurements were also recorded.

3.1.2.1 BH, FCR & DDT

These three breeds were examined as part of a single study. Investigations into PLD prevalence and possible associations of PLD with age and sex and associations between IOP and sex and age were conducted. Of the dogs examined gonioscopically, IOP was estimated using rebound tonometry in 198 BH, 137 FCR and 95 DDT. This study has since been published[46].

3.1.2.1.1 BH

Of the 198 BH examined, 72 (36.4 %) were male and 126 (63.6 %) were female. The median age at examination was 43.1 months (minimum = 4.0 months, maximum = 152.9 months). One hundred and forty-five of 198 (73.2 %) of BH were affected by PLD (ordinal grades 1 - 3): 69 (34.8 %) were mildly affected (grade 1), 72 (36.4 %) were moderately affected (grade 2), and 4 (2 %) were severely affected (grade 3) (**Table 3.1**). A significant positive correlation was observed between PLD and age (rho = 0.26, $P < 0.01$). No correlation was observed between PLD and IOP (rho = 0.14, $P = 0.06$). The proportion of female dogs affected by PLD (grades 1 - 3) was higher compared to male dogs ($P = 0.004$). The normality test revealed that the variables IOP ($P < 0.001$) and age ($P < 0.001$) were not normally distributed and as such, the relationship between IOP and age was examined using Spearman's correlation coefficient. No correlation was observed between IOP and age (rho = 0.043, $P = 0.55$). Average IOP was not significantly different between male and female dogs ($P = 0.53$).

3.1.2.1.2 FCR

Of the 170 FCR examined, 67 (39 %) were male and 103 (61 %) were female. The median age at examination was 48.3 months (minimum = 7.5 months, maximum = 147.6 months). One hundred and six of 170 (62.4 %) FCR were affected by PLD (ordinal grades 1 - 3): 70 (41.2 %) were mildly affected (grade 1), 36 (21.2 %) were moderately affected (grade 2) and 0 were severely affected (grade 3) (**Table 3.1**). A

significant positive correlation was observed between PLD and age (rho = 0.34, P < 0.01). No correlation was observed between PLD and IOP (rho = -0.02, P = 0.85). The proportion of dogs affected by PLD (grades 1 - 3) was not significantly different between male and female dogs (P = 0.34). The variables IOP and age were not normally distributed (P < 0.001 for both) and as such, the relationship between IOP and age was examined using Spearman's correlation coefficient. No correlation was observed between IOP and age (rho = -0.14, P = 0.095). Average IOP was not significantly different between male and female dogs (P = 0.34).

3.1.2.1.3 DDT

Of the 95 DDT examined, 35 (36.8 %) were male and 60 (63.2 %) were female. The median age at examination was 47.5 months (minimum = 4.9 months, maximum = 165.3 months). Fifty-two of 95 (54.7 %) DDT were affected by PLD: 31 (32.6 %) were mildly affected (grade 1), 20 (21.1 %) were moderately affected (grade 2) and 1 (1.1 %) was severely affected (grade 3) (**Table 3.1**). A positive linear relationship was observed between PLD and age (rho = 0.57, P < 0.001). A significant negative correlation was observed between PLD and IOP (rho = -0.35, P = 0.001). The proportion of dogs affected by PLD (grades 1 - 3) was not significantly different between male and female dogs (P = 0.86). The variables IOP and age were not normally distributed (P = 0.01 and P < 0.001 respectively) and as such, the relationship between IOP and age was examined using Spearman's correlation coefficient. A moderately strong and significant negative correlation was observed between IOP and age in DDT dogs (rho = - 0.578, P < 0.0001).

Table 3.1. Frequency of PLD in BH, FCR and DDT.

PLD grade	BH			FCR			DDT		
	No.	**%**	**95% CI**	**No.**	**%**	**95% CI**	**No.**	**%**	**95% CI**
0	53	26.8	20.6, 32.9	64	37.6	30.4, 44.9	43	45.3	35.3, 55.3
1	69	34.8	28.2, 41.5	70	41.2	33.8, 48.6	31	32.6	23.2, 42.1
2	72	36.4	29.7, 43.1	36	21.2	15.0, 27.3	20	21.1	12.9, 29.3
3	4	2.0	0.1, 3.9	0	0		1	1.1	0.0, 3.1
Total	198			170			95		

No. = number of dogs, CI = confidence interval

3.1.2.1.4 Interbreed comparison

The prevalence of PLD was significantly higher in BH (145/198) compared to FCR (106/170, P = 0.025) or DDT (52/95, P = 0.002). No significant difference was observed in the distribution of age and sex among the three dog breeds (**Table 3.2**). However, average IOP among the three dog breeds was significantly different (P < 0.001). Average IOP in DDT was significantly higher compared to BH (P = 0.039) or FCR (P < 0.001).

Table 3.2. Comparison of distribution of mean age, sex, and mean IOP in BH, FCR and DDT.

Variable	Breed			P-value
	BH	FCR	DDT	
Age at examination Median (months)	43.1	48.3	47.5	0.20
Sex				
Male	72 (36.4%)	67 (39%)	35 (36.8%)	0.82
Female	126 (63.6%)	103 (61%)	60 (63.2%)	
IOP Median (mmHg)	13.50	12.50	14.17	<0.001

3.1.2.2 WSS

In the WSS, PLD prevalence and potential associations of PLD with sex, age and IOP and of IOP with sex and age were investigated. In addition, the progression of PLD over time in individual dogs was investigated. The results of this study have since been published[45].

3.1.2.2.1 Prevalence and associations of PLD

Of the 227 dogs examined by gonioscopy, 79 (34.8 %) were male and 148 (65.2 %) female. The median age (± SD) was 48.6 months ± 41.7 (minimum = 5.8 months, maximum = 170.8 months). One hundred and thirty-nine dogs (61.2 %) were affected with PLD (grades 1 - 3): 57 (25.1 %) were mildly affected (grade 1), 78 (34.4 %) were moderately affected (grade 2) and 4 (1.8 %) were severely affected (grade 3) (**Table 3.3**). A weak but statistically significant positive correlation was observed between PLD and age (rho = 0.22, P = 0.002). No correlation was observed between PLD and IOP

(rho = -0.03, P = 0.68). The proportion of dogs affected by PLD (of any grade) was not significantly different between male and female dogs (P = 0.49). During examination of the relationship between IOP and age, the normality test revealed that IOP was normally distributed (P = 0.166) but age was right skewed (P < 0.0001). As such, the relationship between IOP and age was examined using Spearman's correlation coefficient. No correlation was observed between IOP and age (rho = -0.092, P = 0.19).

Table 3.3. Frequency of PLD in WSS.

PLD grade	WSS		
	No.	**%**	**95% CI**
0	88	38.8	32.4, 45.1
1	57	25.1	19.5, 30.8
2	78	34.4	28.2, 40.5
3	4	1.8	1.0, 3.5
Total	227		

No. = number of dogs, CI = confidence interval

3.1.2.2.2 Progression of PLD

Gonioscopy had been performed prior to this study in 65/227 dogs comprising 17 males and 48 females. All 65 dogs (100 %) were classified as unaffected under the Eye Scheme at first examination with clear documentation that no PLD was present (0 % ICA affected by PLD, grade 0) and had all been examined by a single examiner (Beverley Cottrell). These same 65 dogs were examined by myself at a later time point. The median age at first examination was 11.2 months (range = 64.7 months, minimum = 4.2 months, maximum = 68.9 months), while the median age at second examination was 76 months (range = 140.2 months, minimum = 21.9 months, maximum = 162.1

months). At second examination, 35/65 dogs (53.8 %) were classified as affected (grades 1 - 3): 10 (15.4 %) dogs progressed to become mildly affected (grade 1), 24 (36.9 %) dogs became moderately affected (grade 2), and 1 (1.5 %) dog became severely affected (grade 3) (**Figure 3.1**). The proportion of dogs affected by PLD was significantly different ($P < 0.0001$) at first examination (0/65) compared to second examination (35/65). The proportion of dogs affected by PLD (of any grade) was not significantly different between male (7/17) and female (28/48) dogs ($P = 0.22$).

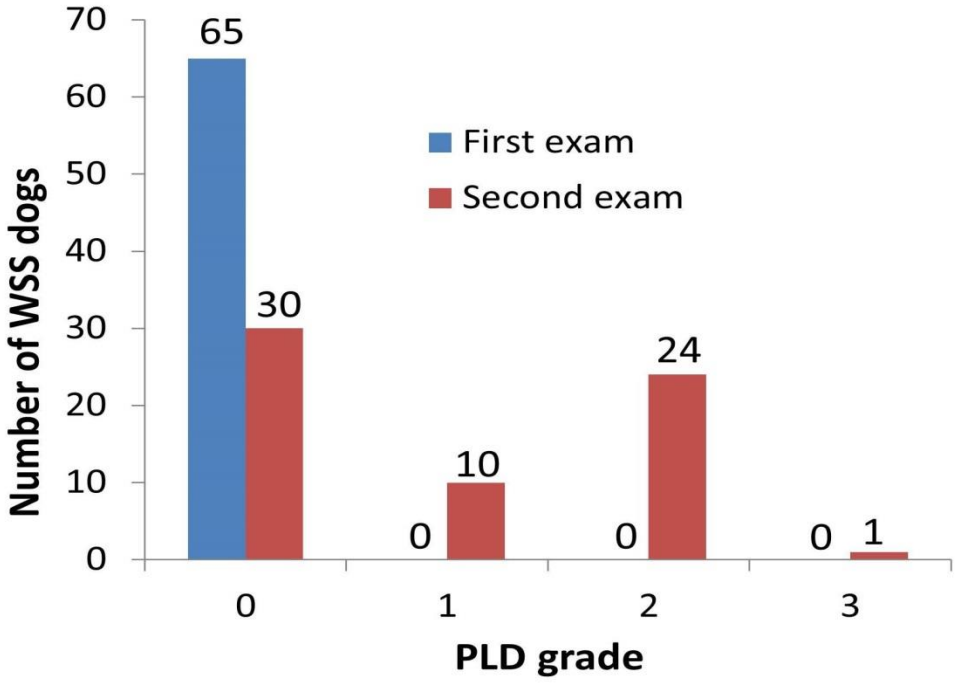

Figure 3.1. Comparison between number of dogs with PLD at first and second gonioscopy examinations.

3.1.2.3 BC, HV & GR

Before publication of these studies, these three breeds were listed as 'under investigation' for PLD under the BVA/KC/ISDS Eye Scheme. Thus, an estimation of PLD prevalence in these breeds was considered important as the result may influence

the Eye Scheme's future policy making decisions. The results of this study have since been published[192].

3.1.2.3.1 BC

Of the 102 BC examined, 49 (48 %) were male and 53 (52 %) were female. The median age ± SD of BC was 43.7 months ± 46.4 (minimum = 2.0 months, maximum = 172.8 months). Eighteen of 102 (17.6 %) BC were PLD affected (ordinal grades 1 - 3): 7 (6.9 %) were mildly affected (grade 1), 7 (6.9 %) were moderately affected (grade 2), and 4 (3.9 %) were severely affected (grade 3) (**Table 3.4**). No significant correlation was observed between PLD and age (rho = -0.015, P = 0.879). The proportion of male and female dogs affected by PLD (grades 1 - 3) was not significantly different (P = 0.169).

3.1.2.3.2 HV

Of the 112 HV examined, 35 (31.3 %) were male and 77 (68.8 %) were female. The median age ± SD of HV dogs examined was 44.5 months ± 37.7 (minimum = 3.1 months, maximum = 145.2 months). Thirty eight of 112 (33.9 %) HV were affected by PLD (ordinal grades 1 - 3): 22 (19.6 %) were mildly affected (grade 1), 14 (12.5 %) were moderately affected (grade 2) and 2 (1.8 %) were severely affected (grade 3) (**Table 3.4**). A weak but significant positive correlation was observed between PLD and age (rho = 0.366, P < 0.01). The proportion of dogs affected by PLD (grades 1 - 3) was not significantly different between male and female dogs (P = 0.957).

3.1.2.3.3 GR

Of the 230 GR examined, 93 (40.4 %) were male and 137 (59.6 %) were female. The median age ± SD of GR examined was 41.4 months ± 38.6 (minimum = 4.8 months, maximum = 173.8 months). One hundred and eleven of 230 (48.3 %) GR were affected by PLD: 51 (22.2 %) were mildly affected (grade 1), 51 (22.2 %) were moderately affected (grade 2) and 9 (3.9 %) were severely affected (grade 3) (**Table 3.4**). A weak

but significant positive linear relationship was observed between PLD and age (rho = 0.173, P = 0.009). The proportion of dogs affected by PLD (grades 1 - 3) was not significantly different between male and female dogs (P = 0.114).

Table 3.4. Frequency of PLD in BC, HV and GR.

PLD grade	BC			HV			GR		
	No.	**%**	**95% CI**	**No.**	**%**	**95% CI**	**No.**	**%**	**95% CI**
0	84	82.4	74.5, 89.2	74	66.1	57.1, 75.0	119	51.7	45.2, 58.3
1	7	6.9	2.9, 11.8	22	19.6	12.5, 26.8	51	22.2	17, 27.4
2	7	6.9	2.0, 11.8	14	12.5	6.3, 18.8	51	22.2	17, 27.8
3	4	3.9	1.0, 7.8	2	1.8	0.0, 4.5	9	3.9	1.7, 6.5
Total	102			112			230		

No. = number of dogs, CI = confidence interval

3.1.2.3.4 Interbreed comparison

The prevalence of PLD (grades 1 - 3) was significantly higher in HV (38/112, 33.9 %) and GR (111/230, 48.3 %) compared to BC (18/102, 17.6 %, P = 0.007 and P < 0.001 respectively), and higher in GR (111/230, 48.3 %) compared to HV (38/112, 33.9 %, P = 0.011). Age distribution among the three breeds was not significantly different (P = 0.494, **Table 3.5**). Distribution of male and female dogs among the three breeds was significantly different (P = 0.042). The proportion of males and females was significantly different between BC and HV dogs: the proportion of males was higher in BC (49/102, 48 %) compared to HV (35/112, 31 %; P = 0.012). The proportion of males and females was not significantly between BC and GR dogs (P = 0.196), or HV and GR dogs (P = 0.100).

Table 3.5. Comparison of distribution of mean age and sex in BC, HV and GR.

Variable	Breed			
	BC	**HV**	**GR**	**P-value**
Age at examination				
Median ± SD (months)	43.7 ± 46.4	44.5 ± 37.7	41.4 ± 38.6	0.494
Sex				
Male	49 (48 %)	35 (31.3%)	93 (40.4 %)	0.042
Female	53 (52 %)	77 (68.8%)	137 (59.6 %)	

3.1.3 Discussion

3.1.3.1 Prevalence

These studies provide current prevalence data for PLD in United Kingdom populations of BH, FCR, DDT, WSS, BC, HV and GR. Under the BVA/KC/ISDS Eye Scheme, and at the time these studies were performed, dogs were considered to be 'affected' if 20 % or more of the entire ICA circumference was affected by PLD[35]. Thus, those dogs classified as ordinal grades 2 or 3 ('moderately' or 'severely' affected, respectively) would be classified as 'affected' under the Eye Scheme (**Table 2.1**). Previous PLD prevalence data for six of the breeds are lacking, but Read et al. reported 34.7 % FCR to be moderately or severely affected by PLD[31]. This is much higher than the 21.2 % reported here; the most likely explanation for the reduction in prevalence of PLD in this breed is increased awareness of the anomaly amongst FCR breeders since the initial report and subsequent increased uptake in gonioscopic screening of dogs before breeding with exclusion of affected individuals from the breeding population. Another possible explanation for the different prevalence rates is a possible difference in age between the two groups. PLD has been shown to be progressive in this breed and Wood

et al. also found a significant positive association between PLD and age[32,35]. This seems an unlikely explanation, however, as, although Wood et al. did not report mean age of the population they investigated, 77.6 % of the dogs studied were < 60 months when examined whereas the mean age of the population reported here was 58.7 months.

PLD was particularly prevalent in the BH and WSS with 38.4 % and 36.2 % affected by moderate or severe PLD respectively. This is most likely due to a higher frequency of the genetic factor(s) responsible for PLD in these breeds, which could in turn be a result of the use of popular sires that carry these factors and/or a reduced uptake of gonioscopic screening within these breeds. PLD prevalence in the DDT, FCR, GR was similar to that previously reported in the English Springer Spaniel (25.5 %) and FCR (34.7 %) and is much higher than the 6 % prevalence reported by Read et al. in a control sample of 100 dogs of other breeds[29,31]. PLD prevalence in the BC (17.6 %) was significantly lower than in the other breeds studied potentially owing to a reduced frequency of the genetic risk factors for PLD in this breed in the United Kingdom.

PLD prevalence was 26.1 % in GR in these studies. A previous study reported a much higher PLD prevalence in GR in Switzerland with 56.5 % dogs affected; these dogs would have to be excluded from a breeding program according to the guidelines of the ECVO[193]. Although PLD prevalence may be genuinely higher in Swiss than in United Kingdom GR, it is important to note, however, that the ECVO scheme differs from the BVA/KC/ISDS Eye Scheme and so direct comparison of the results of the two studies is not possible. At the time the Swiss study was performed, and under the ECVO scheme, an eye with *any* degree of pectinate ligament 'sheeting' (also known as *laminae*) would be classed as affected rather than only eyes with ≥ 20 % which might, in part, explain the greater apparent PLD prevalence in Swiss GR.

Before publication of the aforementioned studies, four of the breeds investigated (DDT, BC, HV and GR) were 'under investigation' for PLD by the BVA/KC/ISDS Eye

Scheme. The results of these studies have been informative to the Eye Scheme and the DDT is now listed as breed which should be certified for PLD status before breeding. These studies support the BC and HV to continue to be 'under investigation' but that the GR should also be certified for PLD under the Eye Scheme. Any decision to make PLD certifiable should be as evidence-based as possible and should be guided by knowledge of PLD prevalence in the wider canine population. In their study in FCR, Wood et al. (1998) estimated the degree of PLD in 100 dogs of 30 different breeds as a control samples. In this study, 11 % of dogs were classified as 'affected' and this figure may serve as a useful bench mark in making such decisions.

3.1.3.2 Associations between PLD and sex and IOP

There was no association between IOP and degree of PLD in the absence of glaucoma in the WSS which is in line with previous studies in other breeds[29,32]. These findings are in consensus with the general clinical observation that dogs with severe PLD appear to maintain normal IOP until the acute onset of PCAG, rather than demonstrating a progressive increase in IOP. However, dynamic changes in IOP over an extended period in dogs with and without PLD have not been investigated to date and are required to fully demonstrate a lack of association between IOP and PLD. There was also no association between IOP and sex which was unsurprising and in line with previous studies in other breeds[29,32].

This study showed that female BH were more likely to have PLD than male BH, but the same was not true of any of the other six breeds. A sex predisposition for goniodysgenesis/PLD has previously been reported in the American Cocker Spaniel, but not in the English Springer Spaniel, FCR or Samoyed[29,31,47,61]. This suggests that genetic risk factors for PLD might well vary between breeds. In humans, females are affected by PACG more frequently than males[54-56]. This is likely due to differences in anterior chamber morphology between the sexes. A shallow anterior chamber is the

major risk factor for development of PACG in humans, and women have shallower anterior chambers than men[58,147,148]. The effect of sex on PCAG in dogs seems to vary with breed. A sex predisposition has been reported in American Cocker Spaniels, Cocker Spaniels, BH, WSS and Samoyeds[53,60]. Currently, there is no clear explanation for a predisposition to PCAG in female dogs which is consistent between breeds. In Beagles, a breed not typically considered to be affected by PCAG, females have been shown to have differences in anterior chamber morphology compared to males[63]. The ICA width was significantly smaller for female dogs than male dogs[63]. However, in the Samoyed and English Springer Spaniel, breeds known to be affected by PCAG, there was no difference in ICA width between female and male dogs[29,49]. A previous study reported female WSS to be affected by PCAG more frequently than males at a ratio of 2.4:1[60]. If such a sex predisposition were true, then it would have been a reasonable expectation to have found a similar female predisposition to PLD in WSS in these studies, as PLD is known to be significantly associated with PCAG, but this was not the case. Alternatively, it is possible that additional risk factors that contribute to PCAG risk (but not to PLD) are more frequent in females than males.

3.1.3.3 Associations between IOP and sex and age

Possible associations between IOP and PLD, age and sex in the three breeds (BH, FCR and DDT) included in this study were also investigated. IOP is known to be influenced by a number of factors in dogs, including diurnal variations and age. To reduce the possible influence of diurnal variations in these studies, all tonometric measurements were performed between the hours of 10:00 and 16:00 GMT. An association of IOP with age has already been reported in the Samoyed where a significantly higher IOP was demonstrated in dogs less than 1 year old compared to older dogs and, in animals seven years or older, there was a pronounced decrease in IOP[49]. These studies failed to show any association between IOP and age in the BH or FCR. However, the DDT was

similar to the Samoyed in that a moderately strong negative correlation was observed between IOP and age (i.e. higher IOPs were observed in younger dogs). The reason for this finding is unknown although, in other species, has been proposed as physiological being correlated with ocular growth[194]. In humans, IOP has been shown to decrease with age in Japanese but an increasing IOP with age has been shown in Europeans and Americans with both genetic and environmental factors (e.g. blood pressure, cardiovascular disease and obesity) likely being influential[195-197].

Previous studies have shown no association between IOP and the degree of PLD in the FCR and English Springer Spaniel[29,32]. The studies described in this thesis demonstrated a similar lack of association in the FCR and BH. However, a significant association was found between IOP and degree of PLD in the DDT. The median IOP, counterintuitively, decreased gradually with increasing degree of PLD (i.e., grades 0, 1, 2, 3). Explanations for the different associations between breeds may lie in differences in the anatomy of the ICA between the different breeds which, in turn, may be influenced by genetic variations.

3.1.3.4 Evidence of PLD progression

A significant positive linear relationship was observed between PLD and age in all breeds studied apart from the BC. Age-related narrowing of the ICA has been a generally accepted phenomenon for some time, but only recently has PLD been formally recognised as progressive when Pearl et al. reported that 39 of 96 (40.6 %) FCR demonstrated PLD progression over time[29,35,49]. An association with age would not be expected for a congenital, non-progressive disorder, and thus the studies reported here both support the previous finding in the FCR and provide cross-sectional evidence of a similar progressive nature of PLD in other breeds. The reason for the lack of an association between PLD and age in the BC is unknown. It may be because either PLD is not progressive in this breed or, alternatively and more likely, the sample size was too

small to detect a correlation in this breed, which appears to have a relatively low PLD prevalence in the United Kingdom.

In these studies, not only was *cross-sectional* evidence of an association between PLD and age demonstrated but it was also possible to demonstrate *longitudinal* evidence of PLD progression in individual WSS over time. Sixty-five WSS were previously examined under the BVA/KC/ISDS Eye Scheme by a single examiner and found to be unaffected for PLD (grade 0) and were subsequently available for reexamination. Of these, 35 (53.8 %) demonstrated PLD progression with 38.4 % becoming moderately or severely affected. This is similar to the 40.6 % progression rate reported in the FCR. In the FCR, multiple examiners were involved and inter-examiner agreement was not addressed. In contrast, in the study reported here only two examiners were involved and the second examination was performed by a different examiner thereby effectively masking the results of the previous examination. Other explanations for the apparent progression of PLD in WSS are possible. These include grader differences, as the first examiner was shown in a subsequent study to grade from leniently then the second examiner (**section 3.2.3**), and also the possibility of grader drift.

As PLD was originally thought to be a congenital abnormality[60], it was previously thought that eradication of PLD, and thus PCAG, would be relatively straightforward, by gonioscopic examination of dogs before breeding and the subsequent elimination of affected individuals from the breeding population. The continued high prevalence of PLD in the majority of the breeds studied here suggests that this strategy has not been entirely effective. This is likely, in part at least, due to the progressive nature of PLD which goes unnoticed in those dogs only examined once in early life. Increasing the frequency of gonioscopic examinations of individual dogs during and beyond their breeding lives should increase the rate of identification of affected dogs and their offspring. Additionally, further reduction in the prevalence of PLD may be made

possible by the identification of genetic factors responsible for the diseases, and the subsequent development of DNA tests which breeders can utilize as a tool for selective breeding. However, identification of such factors is likely to be challenging because both PLD and PCAG are thought to be multigenic traits[78]. Furthermore, complete eradication of PCAG is unlikely to be possible by these means alone as risk factors other than PLD, such as progressive narrowing of the ICA and deeper, unidentified abnormalities within the ICA, may continue to exist. PLD itself may be an imperfect biomarker of abnormalities within the trabecular meshwork which cannot be assessed by standard gonioscopy. Further characterisation of these deeper outflow pathways by high resolution ultrasonography and ultrasound biomicroscopy is required in both normal dogs and those which go on to develop PCAG. It is likely that such examination techniques will prove more sensitive indicators of an individual dog's risk of developing PCAG than gonioscopy.

3.1.4 Conclusion

These studies provide current prevalence data for PLD in seven breeds in which PLD/PCAG is known or is suspected to have an inherited aetiology. Cross-sectional and/or longitudinal evidence of PLD progression in six of these breeds is provided, which may account for the continued high prevalence of the condition despite routine gonioscopic testing before breeding. There were no consistent associations between PLD and IOP or PLD and sex in the breeds studied.

3.2 Gonioscopy in the dog: inter-examiner variability and the search for a grading scheme

3.2.1 Introduction

When performing gonioscopy as part of the BVA/KC/ISDS Eye Scheme, the examiner is required to estimate the proportion (or percentage) of PLD that affects the entire

circumference of the ICA. Anecdotally, this estimation of the percentage of PLD is considered to be susceptible to subjectivity. This anecdotal suspicion has led to the application of 'gonioscopy grading schemes' in research as an attempt to reduce the influence of subjectivity on examination findings[31,35,47,48]. In this study, level of inter-examiner agreement when applying gonioscopy findings to two recently published gonioscopy grading schemes and simplifications of these schemes was performed[35,48]. This study was performed opportunistically and after the performance of the aforementioned studies in this chapter.

The objectives of this study were to i) assess inter-examiner variability in estimating the percentage of PLD in canine eyes and ii) assess what level of inter-examiner agreement could be achieved by applying four different gonioscopy grading schemes to the assigned percentage scores. This study has since been published[198].

Table 3.6. Details and results of the four gonioscopy grading schemes tested in the study.

Scheme 2 is a simplification of published scheme 1, and Scheme 4 is a simplification of published Scheme 3[35,48].

Ordinal grade	**Scheme 1[35]**	**Scheme 2**	**Scheme 3[48]**	**Scheme 4**
	Percentage of ICA affected by PLD			
0	0 %	< 20 %	< 25 %	< 25 %
1	5 – 15 %	20 – 90 %	25 – 50 %	25 – 75 %
2	20 – 90 %	> 90 %	55 – 75 %	> 75 %
3	> 90 %	N/A	> 75 %	N/A

3.2.2 Results

3.2.2.1 Scoring of percentage of PLD

The mean percentage (± SE) of PLD to affect an individual eye was 12.1 % (± 2.4) for Examiner 1 (James Oliver) and 8.7 % (± 1.7) for Examiner 2 (Beverley Cottrell). The percentage range of PLD was 0 – 95 for Examiner 1 and 0 – 80 for Examiner 2. The median and mode percentage of PLD was 0 % for both examiners and both data sets exhibited positive kurtosis and skewness (data not shown) reflecting the majority of ICAs that were judged to be entirely normal (0 % PLD) by both examiners. Kernel density plots for both examiners were visually assessed and showed similar skewed distributions (**Figure 3.2**). A scatterplot representing the relationship of the PLD scores assigned by the two examiners is shown in **Figure 3.3**. The Pearson's product-moment correlation coefficient (R) was 0.91 indicating a strong positive relationship between the results of the two examiners.

There was evidence for statistically significant non-random differences in percentage scores for PLD assigned to individual eyes between the two examiners. Examiner 1 scored 34/98 eyes (34.7 %) higher than Examiner 2 when all eyes were included (P = 0.05). This difference was most marked in the subset of eyes in which both examiners considered PLD to be present; Examiner 1 scored 22/30 eye (73.3 %) higher than Examiner 2 (P = 0.0005) (**Figure 3.4** and **Figure 3.4**). These data were also examined using a Bland-Altman plot (**Figure 3.5**). The plot highlights that the majority of the data represent low PLD percentage scores and, for these, inter-examiner agreement was strongest. The eight data points above the upper line represent the outliers for which inter-examiner agreement was lowest and further illustrates the systematic non-random bias with most data points appearing above the red line as the mean of the scores increases.

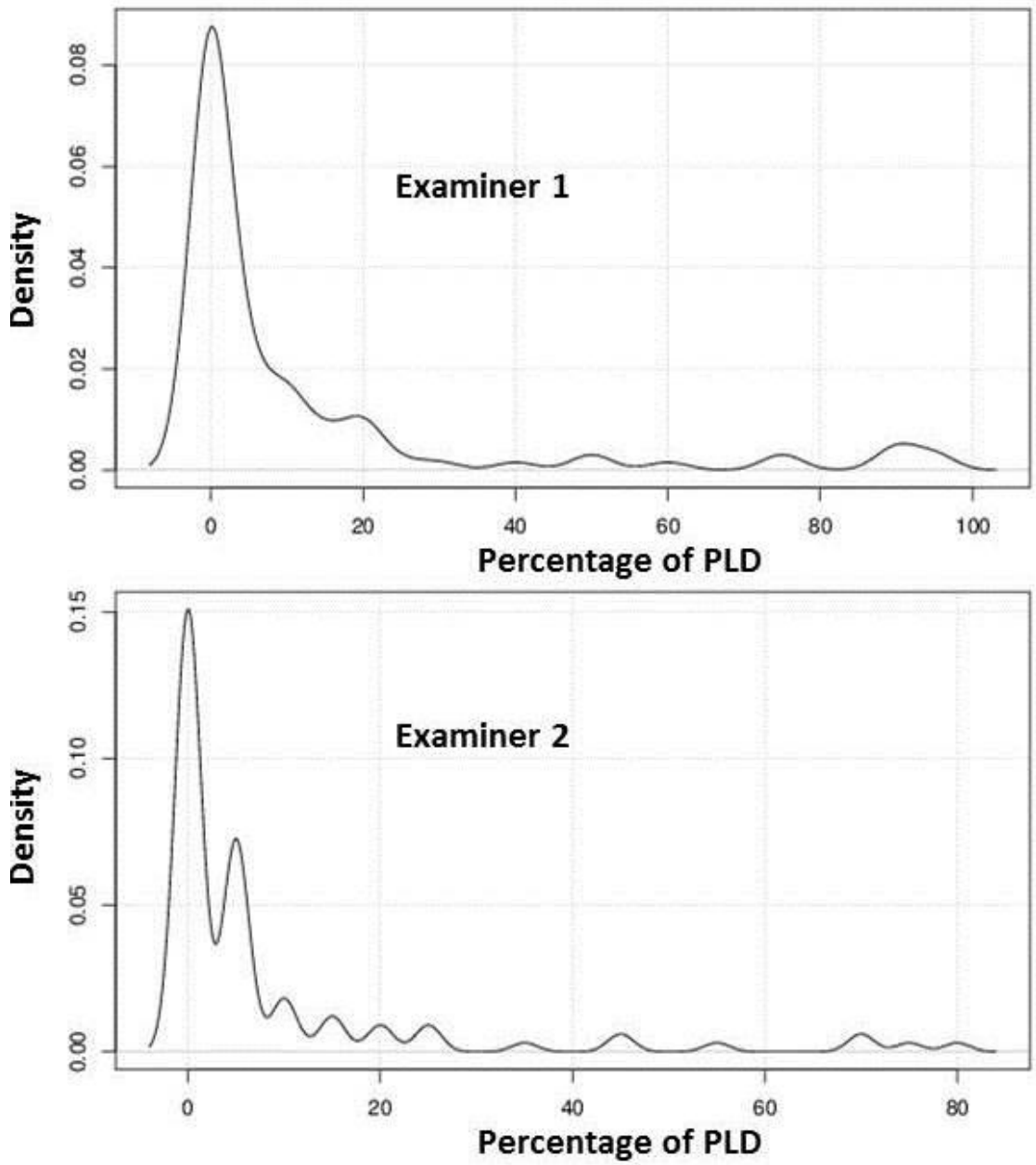

Figure 3.2. Kernel density plots of percentage of PLD assigned to eyes for the two examiners.

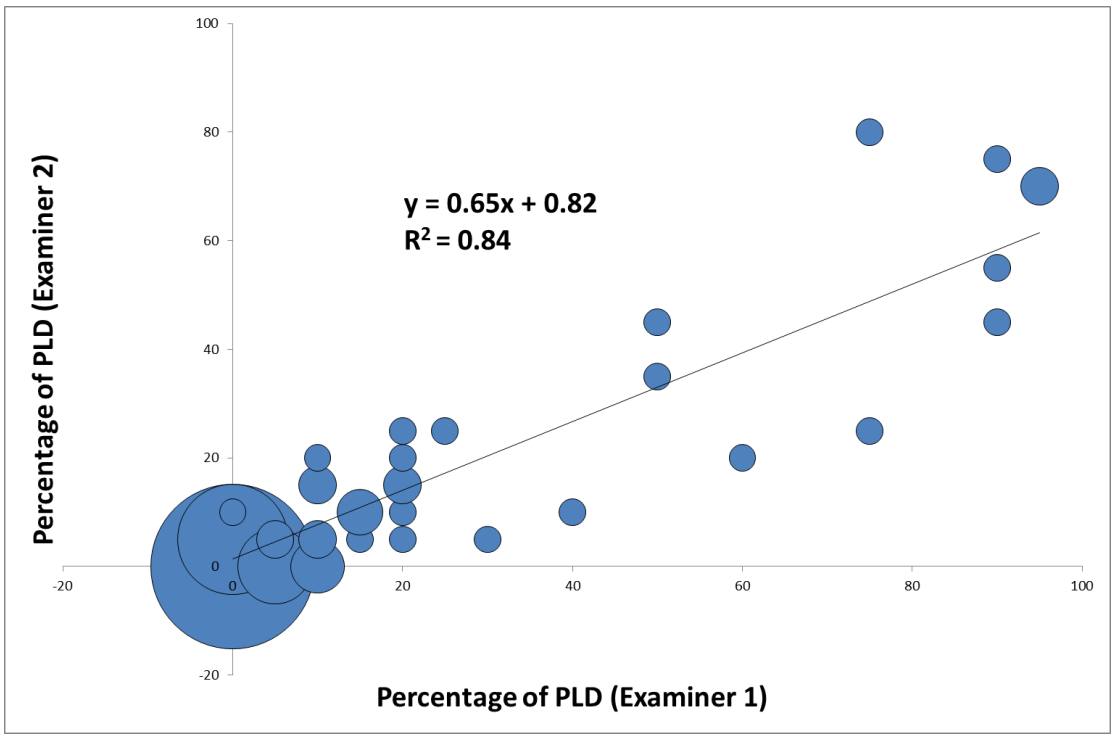

Figure 3.3. Bubble scatterplot and linear regression of the relationship between percentage scores of PLD for individual eyes assigned by the two examiners.

The Pearson's product-moment correlation coefficient (R) was 0.91 indicating a strong positive relationship between the two sets of results. NB Not all 98 data points are seen owing to overlapping of many data points. Instead, proportionally sized bubbles are used to give indication of number of data points present.

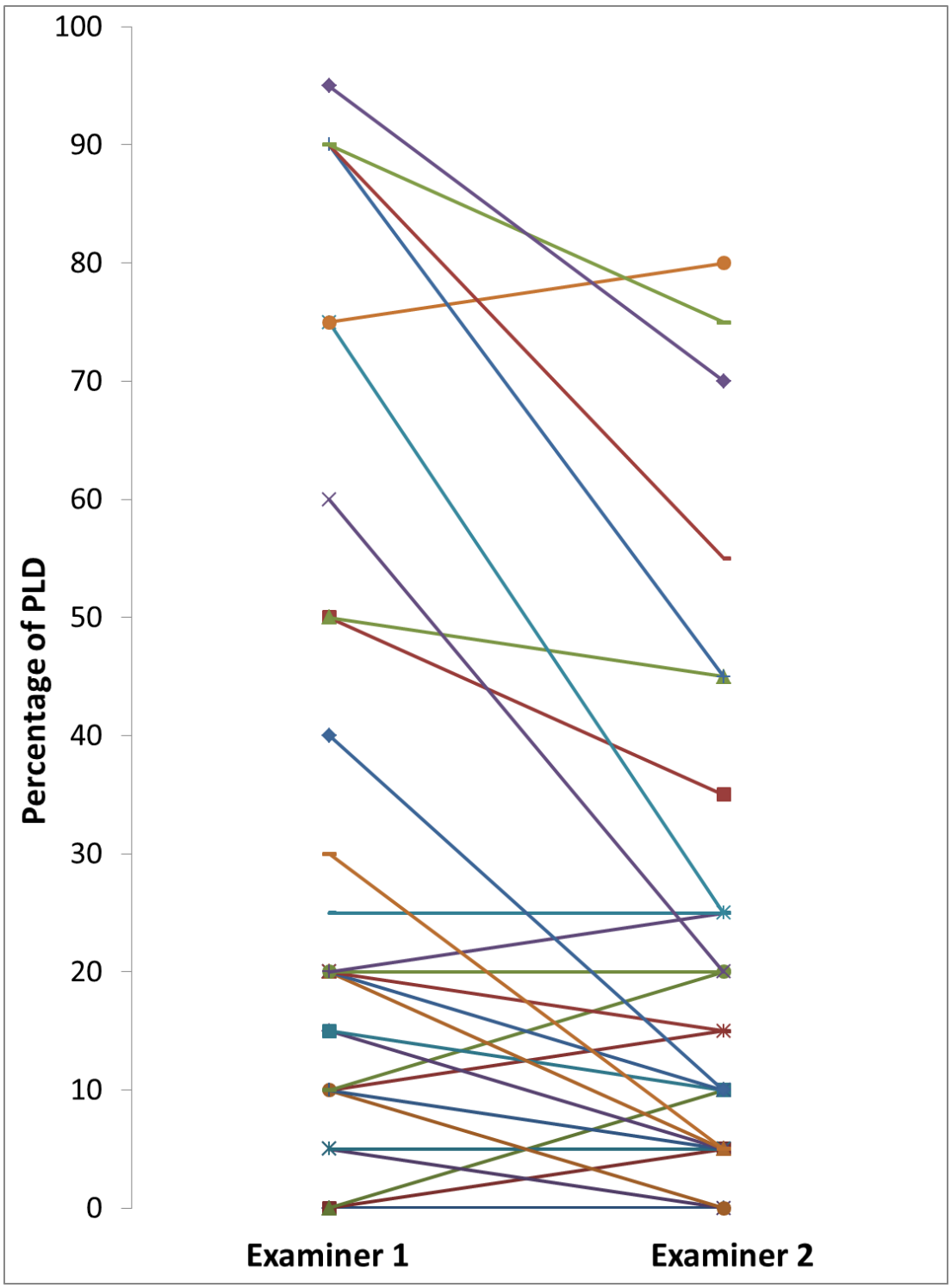

Figure 3.4. Paired data of PLD scores for Examiners 1 and 2 in WSS.

In general, Examiner 1 tended to score a higher percentage PLD than Examiner 2. Not all paired data points owing to overlapping, particularly at low PLD percentages.

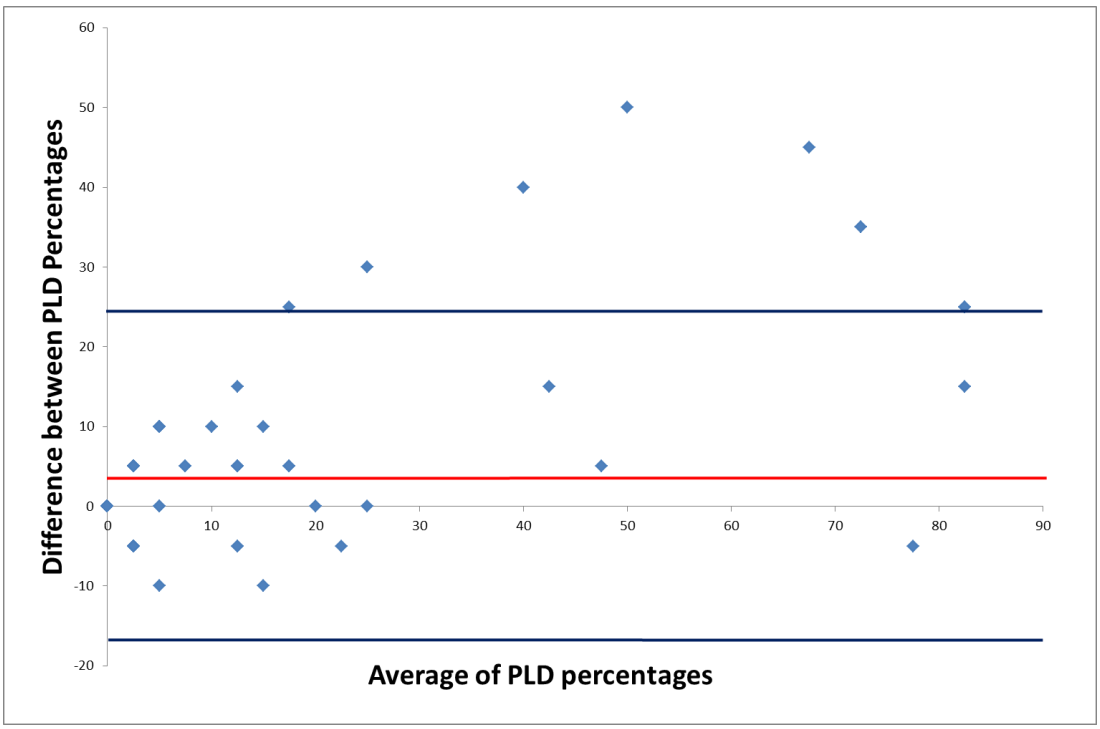

Figure 3.5. Bland-Altman plot of paired data for Examiners 1 and 2.

The averages of PLD percentages of Examiners 1 and 2 are on the X axis and the differences between PLD percentages between Examiners 1 and 2 are on the Y axis. The lines corresponding to the mean of the difference between scores (red line, +3.4) and 95% limits of agreement at ±1.96xSD (blue lines, +24.6 and -17.8) are marked to allow simple assessment of outlying observations. NB Not all 98 data points are seen owing to overlapping of many data points.

3.2.2.2 Ordinal grade assignment

A summary of the ordinal grade scores assigned by the two Examiners for all four schemes is provided in **Table 3.7**. Inter-examiner agreement of ordinal scores was first quantified for level of agreement beyond that expected by chance alone using kappa statistic for each of the schemes:

Scheme 1: There were 60 (61.2 %) observed agreements and 38 (38.8 %) observed disagreements. The kappa statistic (± SE) was 0.35 (± 0.08) and the level agreement was considered ‘fair’. This scheme (which was used in the previously performed PLD prevalence studies) in its current form was therefore considered unacceptable. This somewhat disappointing level of agreement might be explained by the narrow

boundaries between grades 0 and 1 in this scheme and the subsequent inability for examiners to differentiate between such small percentage differences. To further assess this hypothesis, inter-examiner agreement within grades 0 and 1 in Scheme 1 was also analysed separately with eyes being graded as 2 or 3 by either or both examiners being excluded from the analysis. The two examiners both categorised 79 of the 98 eyes as either grades 0 or 1, which represented 49 (62.8 %) observed agreements and 30 (27.2 %) observed disagreements. The resulting kappa statistic (± SE) of 0.12 (± 0.12), representing a 'poor' level of agreement above that expected by chance alone, provided evidence for this hypothesis.

Scheme 2 (a simplification of Scheme 1): There were 89 (90.8 %) observed agreements and 9 (9.2 %) disagreements. The kappa statistic (± SE) was 0.68 (± 0.09) and the level agreement was again considered 'good'. This scheme was considered acceptable.

When this study was conducted, the BVA/KC/ISDS Eye Scheme considered dogs to be unaffected' if both eyes exhibit < 20 % PLD and 'affected' if either or both eyes exhibit ≥ 20% PLD. This, in essence, represents a further simplification of Scheme 2 in which grades 1 and 2 are merged. Application of this simple 'two-tier' grading scheme to the same data presented in the current study was subsequently performed and resulted in a kappa statistic of 0.83 (95 % CI = 0.61 to 0.99) which can be considered a 'very good' level of agreement beyond that which would be expected to occur by chance.

Scheme 3: There were 87 (88.78 %) inter-examiner agreements and 11 (11.22 %) disagreements. The kappa statistic (± SE) was 0.50 (± 0.09) and the level agreement was considered 'moderate'. Although the level of agreement was higher, this scheme in its current form was also considered unacceptable.

Scheme 4 (a simplification of Scheme 3): There were 88 (89.8 %) observed agreements and 10 (10.2 %) disagreements. The kappa statistic (± SE) was 0.54 (± 0.09)

and the level agreement was again considered 'moderate'. This scheme was considered unacceptable.

Table 3.7. Ordinal grades assigned by each examiner for each of four grading schemes.

		Scheme 1			Scheme 2			Scheme 3			Scheme 4		
Examiner		**1**	**2**	☺	**1**	**2**	☺	**1**	**2**	☺	**1**	**2**	☺
Ordinal Grade	**0**	56	53	40	79	84	78	85	87	84	85	87	84
	1	23	31	9	17	14	11	5	6	3	8	10	4
	2	17	14	11	2	0	0	3	4	0	5	1	0
	3	2	0	0	NA	NA	NA	5	1	0	NA	NA	NA
κ value		0.35			0.68			0.50			0.54		
Agreement		Fair			Good			Moderate			Moderate		

☺ columns denote number of eyes where examiners were in agreement on ordinal grade provided. NA = not applicable. κ = kappa statistic.

3.2.3 Discussion

In this prospective study, the results of how two different ophthalmologists evaluated the same ICAs of 98 different canine eyes for degree of PLD were compared. The results for each examiner appeared similar on examination of descriptive statistics and kernel density plots. Furthermore, a strong positive relationship between the two examiners was found on a scatterplot with simple linear regression. These results were encouraging and showed that as one examiner scored an ICA with a higher percentage of PLD, so did the other. Although there was strong association between results, however, it did not necessarily follow that each examiner assigned similar percentage PLD scores to each ICA. The analysis of inter-observer agreement was meaningful since the percentage scoring of PLD is considered to be subjective and has led to the proposal of several different grading systems with the goal to reach improved consistency[31,35,47,48]. When paired results were analysed overall, a statistically

significant non-random difference was found between percentage scores assigned by the two examiners, and which was markedly different when restricted to eyes in which both examiners considered PLD was present. Thus, for the first time, evidence for inter-examiner subjectivity when performing gonioscopy has been provided. Examiner 1 consistently scored higher than Examiner 2, which is to be expected as inter-scorer difference is common when measurement involves subjective judgment of a characteristic. Scores are affected by bias with a tendency of scores to drift towards what is expected by the examiner. The tendency for Examiner 2 to be more 'lenient' may also explain why 100 % of the 65 dogs previously examined by Examiner 2 were graded 0.

It is important to note, however, that this does not detract from the importance of performing gonioscopy as a means of detecting dogs with PLD *per se*. Before this study was published, the BVA/KC/ISDS Eye Scheme operated a simple 'two-tier' gonioscopy grading scheme. When the data derived from the current study were applied to this situation, a 'very good' level of agreement was attained[45].

More sophisticated grading of PLD than a simple 'two-tier' scheme is desirable for several reasons. Firstly, it would allow a more detailed level of monitoring of PLD progression in individual dogs over time than is currently afforded by the current 'affected' vs 'unaffected' categorisation. This is important because, although PLD was originally thought to be a near congenital anomaly, there is now evidence of PLD progression over time in several breeds[35,45,46,48]. PLD grading could help veterinary ophthalmologists identify those dogs more likely to be at risk of PCAG as well as contribute to the understanding of the pathogenesis of the disease. It should be noted, however, that only dogs with severe PLD are considered to be at risk of PCAG and indeed the majority of dogs with PLD will not develop glaucoma. Secondly, a multi-tiered grading scheme may help breeders to make informed decisions on appropriate

matings. This would be particularly pertinent to those breeds which are numerically small and have a high prevalence of PLD. In these breeds, it would be undesirable to eliminate all dogs with PLD as this would restrict the gene pool which may, in turn, lead to the selection of other undesirable inherited characteristics. However, although there is sufficient evidence that PLD is inherited, the precise mode of inheritance is unknown and no causative mutations for PLD have yet been identified[78].

In this study, inter-examiner agreement in PLD estimation was assessed using two recently published gonioscopy grading schemes along with simplifications of these scheme[35,48]. These published schemes were chosen because they were composed of four relatively broad grades and it was considered that two different examiners would be more likely to categorise eyes similarly than schemes with larger numbers of narrow grades. In Scheme 1, the boundaries between the different grades were unequally divided (**Table 3.6**). The proposed benefit of this scheme is that it allows the identification of PLD at both ends of the spectrum i.e. those eyes which had absolutely no evidence of PLD and those with > 90 % PLD and being considered at risk of PCAG[31,35]. When Scheme 1 was applied to the percentage scores, however, only a 'fair' level of agreement was found between the two examiners. This study of inter-examiner agreement was performed following the studies of PLD prevalence which had employed Scheme 1 (the most recently published scheme at the time). In hindsight, it could be argued that because this Scheme showed the lowest level of inter-examiner agreement it was a suboptimal choice for the previous studies. Having, said this, the inclusion of a single examiner in these studies, should have reduced the influence of subjectivity and, at the very least, allowed for relative PLD grading.

When grades 0 and 1 were merged, however, giving rise to the three-tiered Scheme 2 agreement improved to 'good' which led us to conclude that this scheme provided an acceptable level of agreement between the two examiners. The large intermediate

bandwidth of this scheme, however, would only allow detection of dogs with very marked progression of PLD to involve > 90 % of the circumference of the ICA. Although the relationship between the degree of PLD and incidence of glaucoma is not precisely understood, the identification of dogs with PLD affecting > 90 % of the ICA is likely to be clinically important. In a previous study, dogs with PLD affecting an estimated 87.5 % of the ICA had a 60 % probability of developing glaucoma and those dogs with 100 % PLD all developed glaucoma[32].

At face value, Scheme 3 appeared the most desirable of the schemes because the grades were divided into four equally sized categories. If inter-examiner agreement could be shown to be good, then this scheme should better allow for detection of gradual progression of PLD in individual dogs over time and also be a useful tool for breeders in mating selection in particular for those breeds in which PLD is most prevalent. Unfortunately, however, only a 'moderate' level of agreement was achieved with this Scheme. Furthermore, and rather surprisingly, the level of agreement beyond chance only marginally improved and remained at 'moderate' when this scheme was simplified in Scheme 4 which had a much broader intermediate grade than the original scheme. These findings suggested that the two examiners were in agreement when scoring eyes at the unaffected end of spectrum but had difficulty in agreeing on eyes which were considered to be more severely affected by PLD.

In this study, the two examiners were not asked to assess ICA width by gonioscopy as this was considered too subjective, as has been suggested by authors of previous gonioscopy studies[31,35,45,46]. Read et al. (1998) considered ICA width to be too variable between normal dogs, between eyes of individual dogs and even within the same eye and Fricker et al. (2015) commented that position of the goniolens and angle of photographic image capture to be important sources of variability[31,170]. Some authors, however, have included ICA width in their studies[29,30]. Although correlations have been

shown between ICA width and PLD and glaucoma[29,30], inter-examiner variability in assessing ICA width and the validity of width grading schemes have not yet been assessed. Estimation of ICA width remains an important evaluation, however, and with increasing research into and availability of high resolution imaging, validated and objective methods of measuring ICA width will likely become available in the future.

There are, of course, some study limitations which must be discussed. Firstly, the 98 eyes examined in this study were not truly independent with two eyes being derived from each dog. PLD is known to have high heritability and clinical experience is that left and right eyes are similarly affected by degree of PLD[32]. It is therefore possible that, although each examiner was blinded to the results of the other examiner and to those of any previous examinations, he or she may have been influenced by his or her own examination findings of the first eye when examining the second. Both examiners, however, examined the eyes of each dog consistently and examination of both eyes was thus equally subject to such bias and, for the practical purposes of this study, this was considered an acceptable limitation. Secondly, it is possible that the differences and agreements found between the two examiners in this study might not be representative of the general panel membership of the BVA/KC/ISDS Eye Scheme. The two examiners involved in this study are, however, both active panellists of the Eye Scheme being both experienced in performing gonioscopy in the WSS and having published on the technique in this breed and, as such, were considered suitable examiners for the purpose of the study[45,60]. It would be interesting, however, to perform a similar study involving multiple, and perhaps less experienced, examiners to assess if inter-examiner results become even more variable.

3.2.4 Conclusion

In conclusion, inter-examiner variability in gonioscopic evaluation of PLD in dogs for the first time was investigated. Although, there was a strong positive correlation

between the results of the two examiners, there was a statistically significant, non-random difference in the results when the examiners were asked to estimate PLD to the nearest 5 %, with Examiner 1 tending to score higher than Examiner 2. The level of inter-examiner agreement beyond chance alone for four different gonioscopy grading schemes was also investigated. A good level of agreement could only be achieved with a scheme of no more than three categories and with a large intermediate bandwidth which would limit the ability to monitor PLD progression. Furthermore, the level of agreement for all assessed grading schemes fell short of the 'very good' level of agreement offered by the currently employed two-tiered scheme. Thus, it appears that increasing the complexity of any grading scheme will likely come at the expense of inter-examiner agreement.

4 Pectinate ligament dysplasia and primary closed angle glaucoma in four dog breeds: genetic investigations

4.1 Pectinate ligament dysplasia and primary closed angle glaucoma in the Welsh Springer Spaniel: a candidate gene approach

4.1.1 Introduction

PCAG was first reported in the WSS in 1998, when 28 cases of PCAG were reported[60]. Females were affected more frequently than males (2.1:1) and the average age of onset was 2 years 9 months. PCAG was found to be familial and an autosomal dominant mode of inheritance was suggested. To date, no genes have been reported to be associated with PCAG or PLD in this breed. This study sought to investigate possible associations between 11 candidate genes and PCAG and PLD in the WSS.

4.1.2 Materials and methods

4.1.2.1 Sample collection and DNA extraction

DNA samples from 77 WSS were used in this study. These samples derived from dogs examined in **3.1.2.2.1** as part of the PLD prevalence study as well as those collected from clinical cases of PCAG examined at the AHT and received from collaborators. DNA, collected either as buccal mucosal swabs or blood collected in EDTA, was extracted as outlined in **2.2.1**. The 77 samples used consisted of 28 dogs with PCAG (PCAG cases), 31 dogs with moderate or severe PLD (PLD cases) and 20 dogs which were unaffected or mildly affected (controls). For the purposes of this study, only PLD cases with PLD affecting 50 % or more of the ICA were included. The control dogs were at least five years of age at the time of examination to allow for possible PLD progression and PLD affected < 10 % of the ICA of each eye.

4.1.2.2 Candidate gene selection

Eleven candidate genes were selected based on previously published associations with primary glaucoma in humans and/or dog (**Table 4.1**).

4.1.2.3 Microsatellite identification and primer design

The chromosomal coordinates in the canine reference assembly (CanFam3.1) of each candidate gene, or its canine orthologue, were first established in Ensembl (http://www.ensembl.org)[185,186]. Following this, a pair of microsatellites (all dinucleotide repeats) flanking the gene was identified using the UCSC genome browser (https://genome.ucsc.edu/) and a pair of primers flanking the microsatellite was then designed, as described in **2.2.5**[174,175]. PCR and sequencing reaction components, thermal cycling parameters and primer details can be found in **Appendices II**, **III** and **IV**. Alleles and allele frequencies were compared between PCAG cases and controls and PLD cases and controls and were assessed for association with disease using the Chi square test of independence. Statistical significance was set at P = 0.05/number of candidate gene microsatellites tested (0.05/22 = 0.002).

4.1.2.4 Further investigation of *ADAMTS17*

Amplification and sequencing of *ADAMTS17* exons was performed in two PCAG cases, two PLD cases and four unaffected controls. These samples were chosen on the basis of microsatellite genotyping results. All PCAG and PLD cases were homozygous for the disease-associated alleles and three of the four controls were not (**Table 4.3**). The fourth control (25200) was homozygous for the disease-associated alleles.

Table 4.1. PCAG candidate genes: genes associated with primary glaucoma in humans and dogs.

Candidate gene	Canine orthologue (where different)	Genomic coordinates of gene (CanFam3.1)	Species	Phenotype(s)	Reference
ADAMTS10		chr20:53,089,604-53,107,084	Dog	POAG	[68-70]
ADAMTS17		chr3:40,613,857-40,939,685	Dog	POAG	[75,107]
CHX10		chr8:47,455,430-47,473,918	Human	PACG	[199]
COL1A2		chr14:19,883,733-19,920,718	Dog	PCAG	[170]
CYP1B1		chr17:30,269,745-30,278,554	Human	Congenital glaucoma	[200]
eNOS	*NOS3*	chr16:15,053,167-15,072,277	Human	PACG	[164]
HGF		chr18:21,329,616-21,410,296	Human	PACG	[158]
MFRP	*C1QTNF5*	chr5:14,528,039-14,562,907	Human	PACG	[158]
MMP-9		chr24:33,273,918-33,281,411	Human	PACG & POAG	[157,201-203]
RABB22A		chr4:43,108,891-43,157,949	Dog	PCAG	[170]
SRBD1		chr10:47,742,907-47,939,042	Human & dog	PCAG (dog) POAG (human)	[94,204]

POAG = primary open angle glaucoma, PCAG = primary closed angle glaucoma and PACG = primary angle closure glaucoma

4.1.3 Results

4.1.3.1 Microsatellite genotyping

Sixteen out of 22 of the microsatellites genotyped were polymorphic in the cohort of WSS and therefore informative for allele allocation studies. The microsatellite upstream of *ADAMTS17* was significantly associated with both PCAG and PLD and the microsatellite downstream of *ADAMTS17* was significantly associated with PCAG (**Table 4.2**). No other microsatellites were associated with PCAG or PLD. Individual genotyping results are presented in **Appendix V**.

Table 4.2. Microsatellite allele genotyping association results.

Microsatellite	Study cases	Study controls	df	χ^2 value	P-value
ADAMTS10_M1	PCAG cases	Controls	7	7.01	0.4278394
ADAMTS10_M1	PLD cases	Controls	7	2.82	0.9011394
ADAMTS17_M1	PCAG cases	Controls	3	19.95	0.0001738*
ADAMTS17_M1	PLD cases	Controls	1	12.02	0.0005263*
ADAMTS17_M2	PCAG cases	Controls	2	12.63	0.001809*
ADAMTS17_M2	PCAG cases	Controls	2	9.10	0.0105672
C1QTNF5_M1	PLD cases	Controls	1	0.64	0.4237108
C1QTNF5_M1	PCAG cases	Controls	1	0.00	1
C1QTNF5_M2	PLD cases	Controls	1	0.06	0.806496
C1QTNF5_M2	PCAG cases	Controls	1	0.01	0.9203444
CHX10_M1	PCAG cases	Controls	3	3.05	0.3839802
CHX10_M1	PLD cases	Controls	3	3.83	0.2804159
COL1A2_M2	PCAG cases	Controls	4	1.86	0.7614887

Microsatellite	Study cases	Study controls	df	χ^2 value	P-value
COL1A2_M2	PLD cases	Controls	4	5.19	0.2683519
CYP1B1_M1	PCAG cases	Controls	2	0.08	0.9607894
CYP1B1_M1	PCAG cases	Controls	2	0.69	0.7082204
HGF_M1	PLD cases	Controls	3	2.71	0.4385306
HGF_M1	PCAG cases	Controls	3	3.98	0.2636319
MMP_M1	PLD cases	Controls	3	3.69	0.2969428
MMP_M1	PCAG cases	Controls	3	2.34	0.5049013
MMP_M2	PCAG cases	Controls	1	3.07	0.0797495
MMP_M2	PLD cases	Controls	1	0.05	0.8230633
NOS3_M1	PCAG cases	Controls	2	0.64	0.726149
NOS3_M1	PLD cases	Controls	2	2.49	0.2879409
NOS3_M2	PCAG cases	Controls	1	1.46	0.2269301
NOS3_M2	PCAG cases	Controls	1	6.28	0.0122108
RAB22A_M2	PLD cases	Controls	1	0.66	0.4165599
RAB22A_M2	PCAG cases	Controls	1	0.78	0.3771411
SRBD1_M1	PLD cases	Controls	2	6.50	0.0387742
SRBD1_M1	PCAG cases	Controls	2	2.95	0.2287787
SRBD1_M2	PCAG cases	Controls	2	0.75	0.6872893
SRBD1_M2	PLD cases	Controls	2	1.63	0.4426393

*denotes statistical significance ($P < 0.002$)

4.1.3.2 Further investigation of *ADAMTS17*

Owing to the strong association between *ADAMTS17* flanking microsatellites and PCAG and PLD, this candidate gene was investigated more closely for candidate variants. Following *ADAMTS17* exon resequencing in eight WSS samples, a total of 11 SNPs were identified but none fully segregated with either of the disease statuses (PCAG or PLD) (**Table 4.3**). Partial segregation for some SNPs was observed but these SNPs were either synonymous or intronic variants. Intronic variants were assessed using the Variant Effect Predictor (Ensembl) and were considered unlikely to be pathogenic.

Table 4.3. Candidate SNP genotyping results.

AHT No.	Phenotype	*ADAMTS17* microsatellite genotype		SNP position on chromosome 3 (CanFam3.1) and genotype in each sample										
		M1	M2	40615055	40748328	40748330	40748377	40808242	40830948	40831201	40831380	40858537	40858704	40858943
17170	PCAG case	154/154	180/180	T/T	T/T	T/T	T/T	G/G	G/G	C/C	G/G	T/T	C/C	A/A
25165	PCAG case	154/154	180/180	T/T	T/T	T/T	T/T	G/G	G/G	C/C	G/G	T/T	C/C	A/A
25056	PLD case	154/154	180/180	T/T	T/T	T/T	T/T	G/G	G/G	C/C	G/G	T/T	C/C	A/A
25211	PLD case	154/154	180/180	T/T	T/T	T/T	T/T	G/G	G/G	C/C	G/G	T/T	C/C	A/A
25036	Control	150/150	171/171	T/C	T/T	T/T	T/T	G/G	G/G	C/C	G/G	C/T	C/C	A/A
25075	Control	150/154	171/180	T/C	T/T	T/T	T/T	G/G	A/G	C/T	A/G	C/T	C/T	A/G
25185	Control	150/154	172/182	C/C	T/T	T/T	T/T	G/G	A/G	C/T	A/G	C/C	C/T	A/G
25200	Control	154/154	180/180	T/T	T/T	T/T	T/T	G/G	G/G	C/C	G/G	T/T	C/C	A/A

4.1.4 Discussion

This study investigated possible associations between 11 candidate genes and PCAG and PLD in the WSS. A microsatellite-based candidate gene association approach was chosen in this study for a few reasons. Firstly, this approach made advantage of previously performed studies conducted in humans and, to a lesser extent, in dogs which had already identified plausible candidate genes. Secondly, this approach is relatively affordable for modest sized laboratories compared to relatively expensive GWAS. Thirdly, a previous report of PCAG in the WSS suggested an autosomal dominant mode of inheritance (although admittedly evidence for this was very limited)[60]. If PCAG in the WSS is indeed a single gene disease, then a candidate gene approach should have the power to detect significant associations with disease with the number of samples available in this study (provided the correct candidate gene was investigated). A disadvantage of a candidate gene approach is that it introduces significant bias as it is based on *a priori* knowledge of a gene's function or association with disease. Thus, success of such an approach, relies on the presence of phenotypically similar diseases which share similarities at the molecular level[82]. PACG in humans has been very well characterised phenotypically but the same cannot be said for the closest canine phenotype, PCAG. In the WSS, PCAG is associated with PLD but characterisation of the deeper outflow pathways has not been performed.

This study showed significant associations between PCAG and PLD and microsatellites flanking *ADAMTS17*. *ADAMTS17* mutations have previously been reported to be associated with the canine ocular phenotypes POAG and PLL, as well as multiple ocular phenotypes in humans, suggesting the gene to be very important in microfibril function and maintenance[107,122,125]. Unfortunately, *ADAMTS17* exon resequencing of PCAG cases, PLD cases and control dogs failed to reveal any variants which fully segregated with disease. This was not surprising, however, as both PCAG and PLD are now, and

contrary to the early suggestion of autosomal dominant inheritance, considered to be complex diseases likely involving multiple genetic risk factors that are unlikely to segregate well. Furthermore, these diseases might results from intronic (including splice-site), intergenic and structural variants which were not investigated in this study. However, at this point it was decided not to pursue the candidate gene approach for PCAG and PLD in the WSS. Instead, a GWAS (which does not suffer from *a priori* bias) was undertaken with the aim of identifying PCAG and PLD susceptibility loci (**section 4.2**).

4.1.5 Conclusion

A microsatellite-based candidate gene linkage analysis study was performed to investigate associations between PCAG and PLD and 11 candidate genes which had previously been associated with primary glaucoma in the human and/or dog. Significant association was found for *ADAMTS17,* however, *ADAMTS17* exon resequencing failed to reveal variants which fully segregated with disease.

4.2 Pectinate ligament dysplasia and primary closed angle glaucoma in the Basset Hound, Flatcoated Retriever, Dandie Dinmont Terrier and Welsh Springer Spaniel: genome-wide association and next-generation sequencing strategies

4.2.1 Introduction

GWAS have become popular in the investigation of inherited canine traits and, recently, attention has turned towards PCAG. In the BH, a GWAS of 37 PCAG cases and 41 controls revealed significant associations at two novel loci which contain the candidate genes *COL1A2* and *RAB22A* but no candidate variants were reported[170]. In a subsequent paper, the same group reported a non-synonymous variant in *NEB* to segregate with PCAG in BH (CanFam2 chr19:55885214 A>G)[171]. In the DDT, a GWAS has been performed in a cohort of 23 PCAG cases and 23 controls, revealing an association with a novel 9.5 Mb locus on canine chromosome 8[106]. To date, however, no variants causative of canine PCAG have been reported. Here, a combination of GWAS and NGS was used to investigate the genetic mechanisms underlying PCAG and PLD in four breeds: BH, FCR, DDT and WSS. Results of the BH studies have been published[205].

4.2.2 Results

GWAS were first conducted for each individual breed using five case-control set definitions (**2.2.9**). **Table 4.4** summarises the results of the filtering steps undertaken for quality control of data and correction of population stratification using GEMMA for the four individual breeds. MDS and Q-Q plots were performed for each analysis and can be found in **Appendix VI** and haplotype and haplotype permutation analysis plots can be found in **Appendix VII**. The analytical descriptions and analysis plots below are all following analysis with GEMMA.

Table 4.4. Summary of number of samples, results of application of quality control filtering steps and correction of population stratification for the individual breed GWAS performed.

Breed	Phenotype of cases	Phenotype of controls	No. cases	No. controls	SNPs with MAF <0.05	SNPs with <0.97 call rate	SNPs remaining for analysis	λ before correction	λ after correction
BH	PCAG	Controls	24	37	71,687	11,749	96,259	1.96	1.04
	PCAG + PLD	Controls	81	37	71,633	10,166	97,282	1.34	1.00
	PLD	Controls	57	37	73,253	11,935	94,781	1.28	1.01
	PCAG	PLD	24	57	72,150	9,858	96,868	2.23	1.01
	PCAG	Controls + PLD	24	94	71,633	10,166	97,282	2.25	0.96
FCR	PCAG	Controls	19	89	78,384	6,519	92,489	1.12	1.06
	PCAG + PLD	Controls	78	89	78,333	5,664	92,970	1.21	1.03
	PLD	Controls	59	89	78,243	5,806	92,995	1.14	1.05
	PCAG	PLD	19	59	78,507	5,362	93,002	0.93	0.90
	PCAG	Controls + PLD	19	148	78,333	5,664	92,970	1.07	1.02
DDT	PCAG	Controls	32	51	85,752	5,300	85,854	1.70	1.01
	PCAG + PLD	Controls	53	51	85,824	5,013	85,945	1.70	1.04
	PLD	Controls	21	51	86,766	5,688	84,718	1.24	1.06

Breed	Phenotype of cases	Phenotype of controls	No. cases	No. controls	SNPs with MAF <0.05	SNPs with <0.97 call rate	SNPs remaining for analysis	λ before correction	λ after correction
	PCAG	PLD	32	21	86,580	5,502	84,950	1.26	1.06
	PCAG	Controls + PLD	32	72	85,824	5,502	84,950	1.66	1.01
WSS	PCAG	Controls	36	33	74,860	4,363	97,176	2.06	1.04
	PCAG + PLD	Controls	90	33	76,116	4,480	95,830	1.72	1.03
	PLD	Controls	54	33	76,330	4,622	95,582	1.54	0.99
	PCAG	PLD	36	54	75,018	4,295	97,028	1.86	1.04
	PCAG	Controls + PLD	36	87	76,116	4,363	97,176	2.00	1.02

No. = number, λ = lambda (genomic inflation factor)

4.2.2.1 BH

In this breed, the *NEB* variant reported by Ahram et al.[171] was first genotyped in a cohort of 158 BH by Sanger sequencing (10 PCAG cases, 52 PLD cases and 96 controls). One hundred and fifty-seven BH (10 PCAG cases, 52 PLD cases and 95 controls) were homozygous for the variant (G/G) and only one control was heterozygous (A/G). Eighty-three non-BH dogs were also genotyped for the variant. Fifty-nine of these were homozygous for the variant (G/G), 15 were heterozygous (A/G) and only 9 were homozygous for the reference allele (A/A). Thus, it appeared that the SNP at this location is a common polymorphism and may actually be more common in dogs than the reference allele.

For the GWAS, data derived from 153 dogs, comprising 59 PCAG cases, 57 PLD cases and 37 controls, were available for analysis. Thirty-five of the PCAG cases were derived from dogs bred in the USA, all other samples were from European bred dogs. An MDS plot of USA and European dogs revealed a heterogeneous distribution with USA dogs clustering separately (**Figure 4.1**). USA dogs were therefore excluded from the initial GWAS but were used to follow-up signals of interest and any identified candidate variants. Thus, GWAS were performed using 118 dogs, comprising 24 PCAG cases, 57 PLD cases and 37 controls.

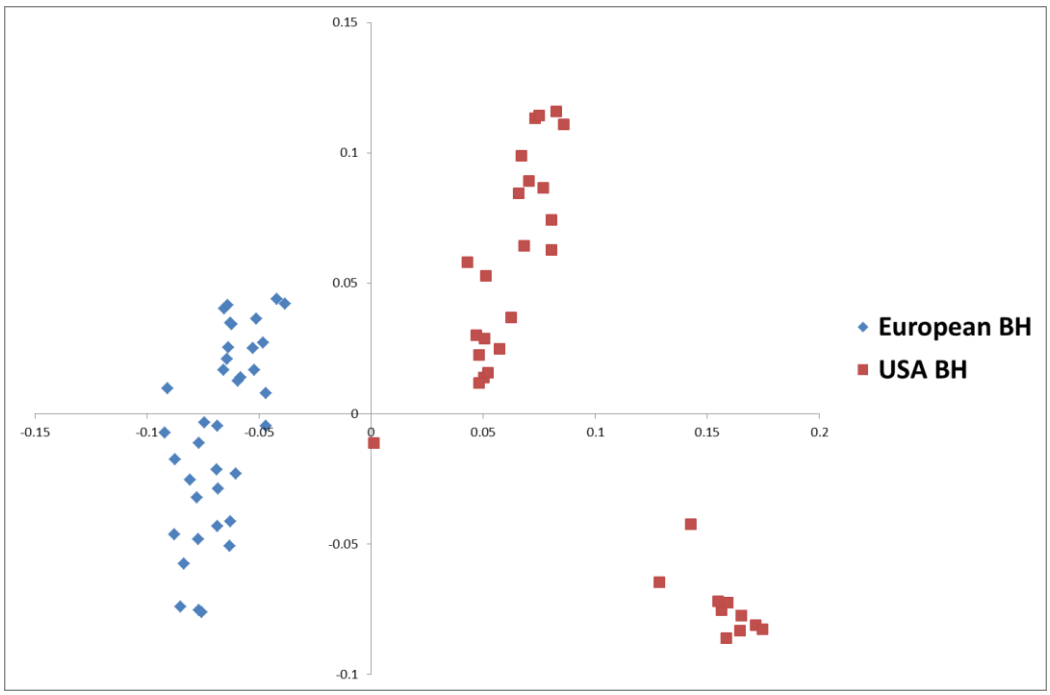

Figure 4.1. MDS plot of European and USA BH.

4.2.2.1.1 PCAG cases and controls

After filtering, 24 PCAG cases and 37 controls and 96,259 SNPs remained for analysis.

No SNPs reached the threshold suggestive of genome-wide significance (**Figure 4.2**).

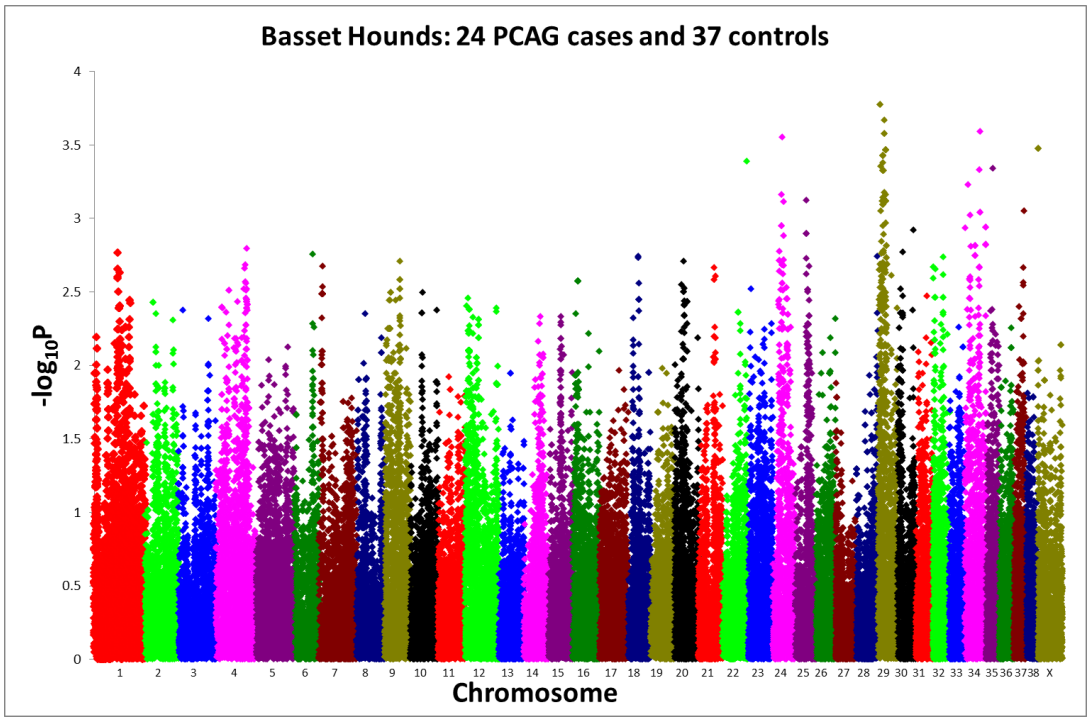

Figure 4.2. Manhattan plot demonstrating association of SNP markers with PCAG in BH.

4.2.2.1.2 PCAG and PLD cases and controls

After filtering, 81 PCAG and PLD cases and 37 controls and 97,282 SNPs remained for analysis. No SNPs reached the threshold suggestive of genome-wide significance (**Figure 4.3**).

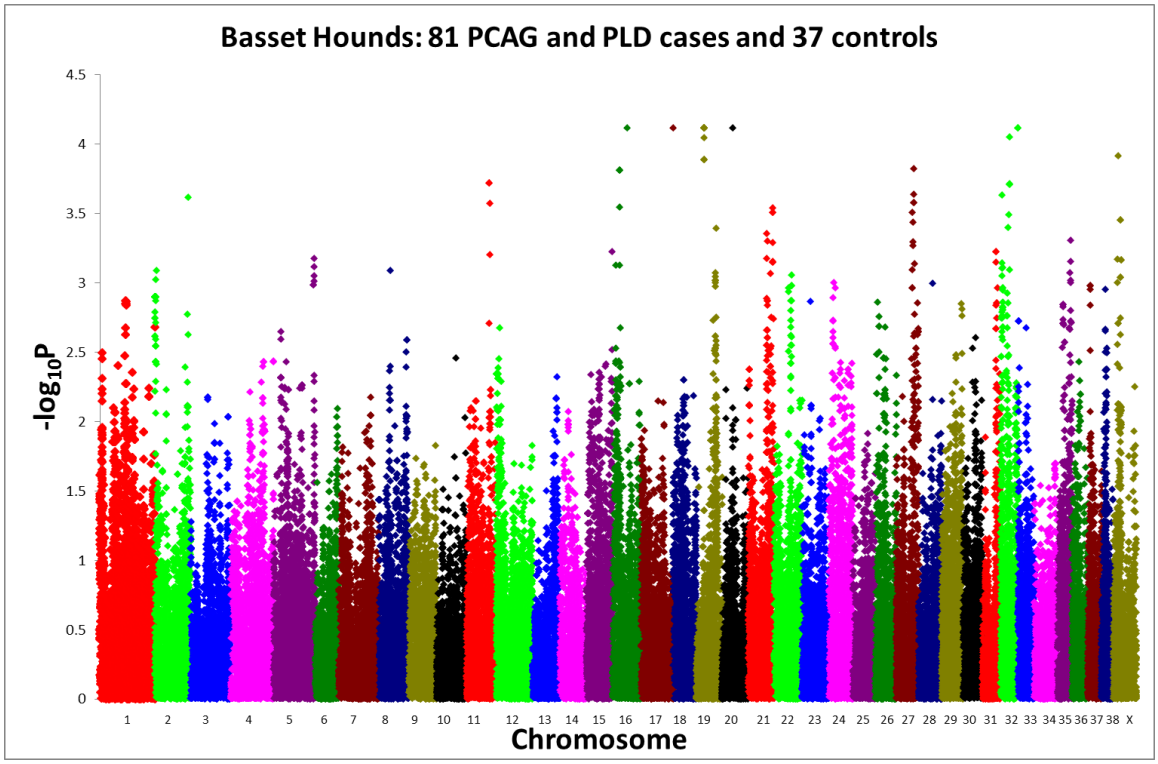

Figure 4.3. Manhattan plot demonstrating association of SNP markers with PCAG and PLD cases in BH.

4.2.2.1.3 PLD cases and controls

After filtering, 57 PLD cases and 37 controls and 94,781 SNPs remained for analysis. No SNPs reached the threshold suggestive of genome-wide significance (**Figure 4.4**).

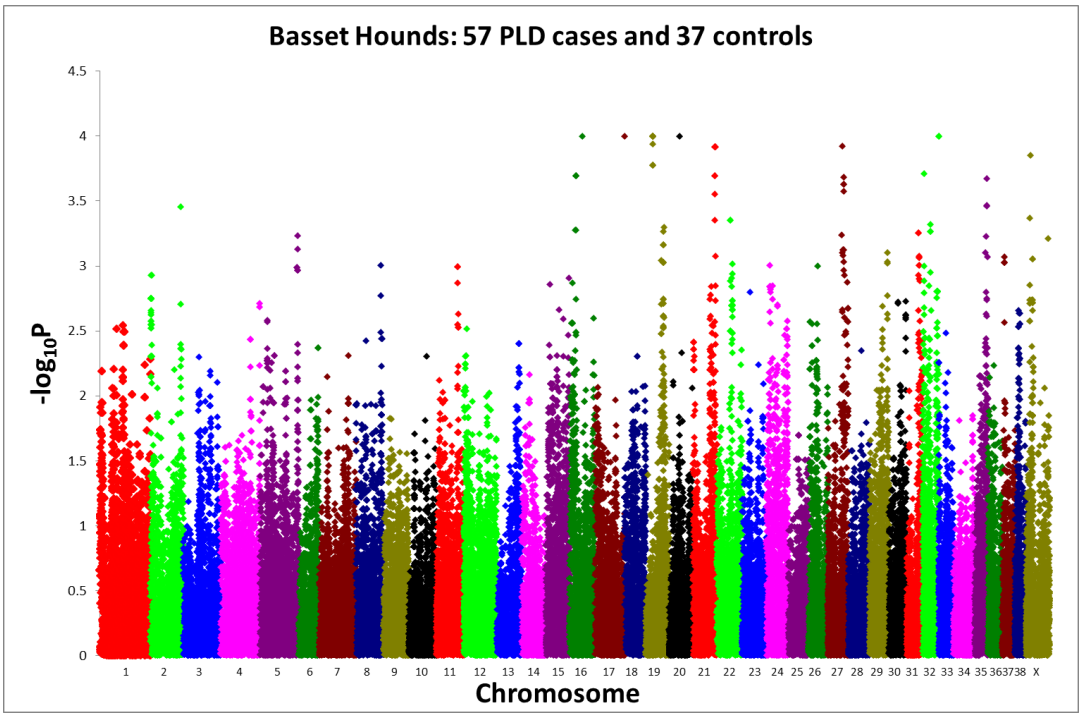

Figure 4.4. Manhattan plot demonstrating association of SNP markers with PLD in BH.

4.2.2.1.4 PCAG cases and PLD cases

For this analysis, 24 PCAG cases and 57 PLD cases and 96,868 SNPs remained after filtering. One SNP (BICF2G630505097; CanFam3.1 chr24:17381226; $-\log_{10}P = 6.42$) reached the threshold suggestive of genome-wide significance (**Figure 4.5**).

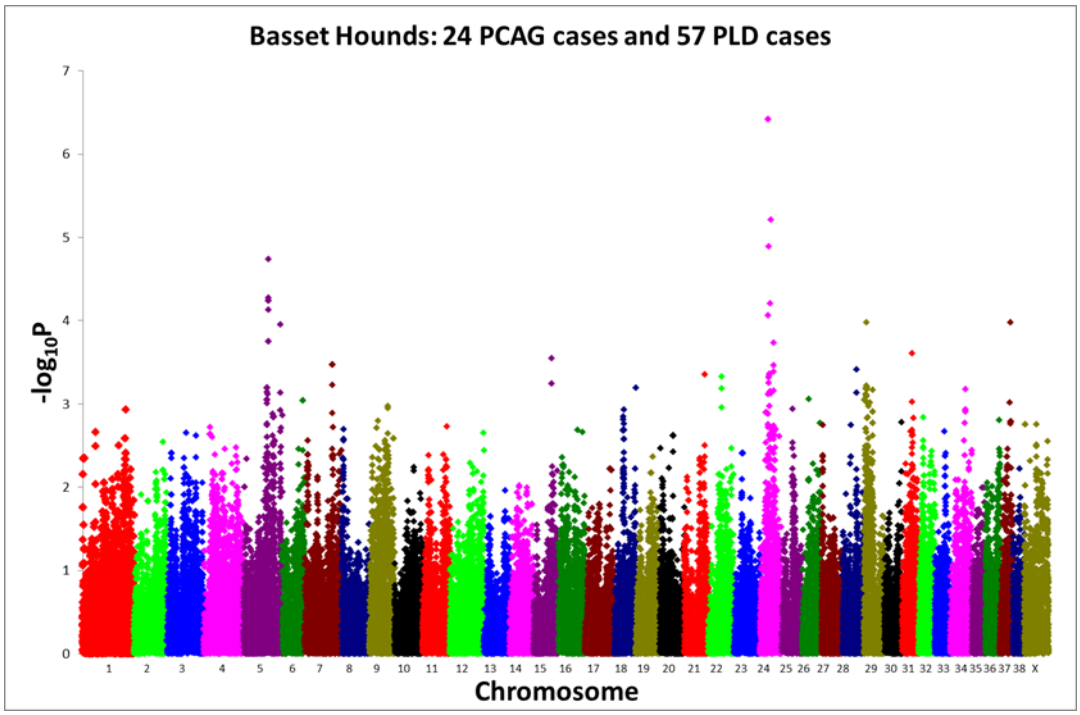

Figure 4.5. Manhattan plot demonstrating association of SNP markers with PCAG relative to PLD in BH.

4.2.2.1.5 PCAG cases and PLD cases and controls

After filtering, 24 PCAG cases and 94 PLD cases and controls and 97,282 SNPs remained. One SNP reached a stronger level of genome-wide statistical association in this analysis than in **4.2.2.1.4** (BICF2P544799; CanFam3.1 chr24:18739902; $-\log_{10}P = 6.84$) (**Figure 4.6**). Conditional analysis was used to assess whether additional loci were associated with PCAG in this breed. To achieve this, the top SNP was introduced as a covariate in the mixed model which revealed an additional SNP at a distinct chromosomal location that reached genome-wide significance (BICF2P928441; CanFam3.1 chr37: 24747131; $-\log_{10}P = 6.73$) **(Figure 4.7**). Conditional analysis using

both associated SNPs as covariates in the model revealed no further SNPs to reach genome-wide significance (**Figure 4.8**).

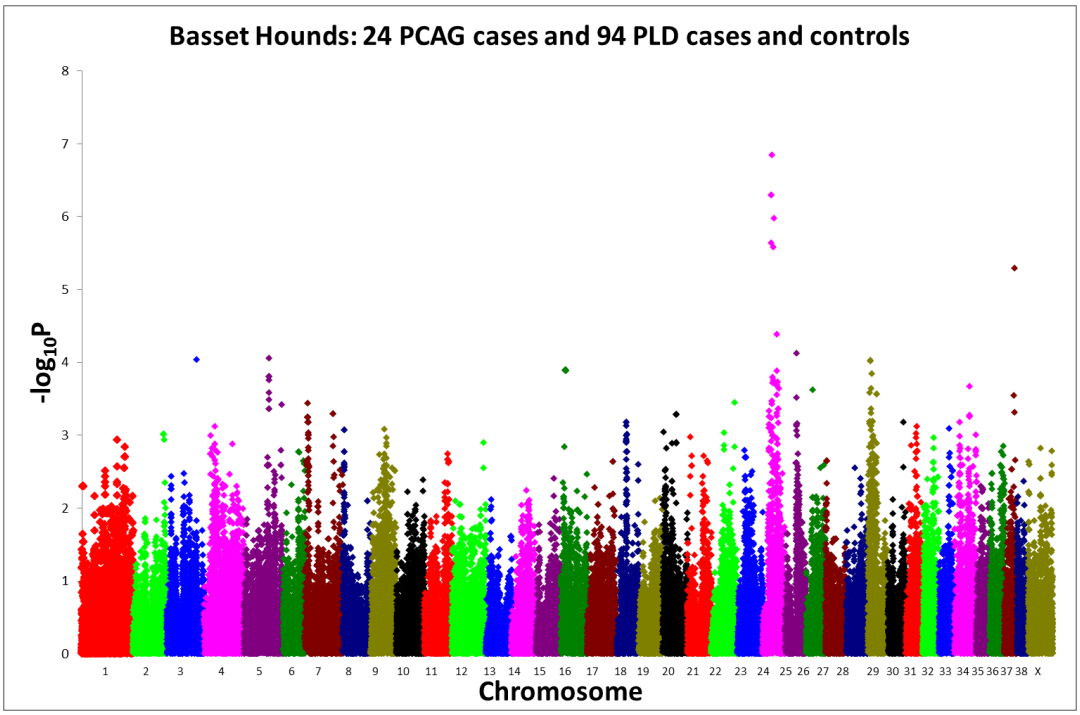

Figure 4.6. Manhattan plot demonstrating association of SNP markers with PCAG cases relative to PLD cases and controls in BH.

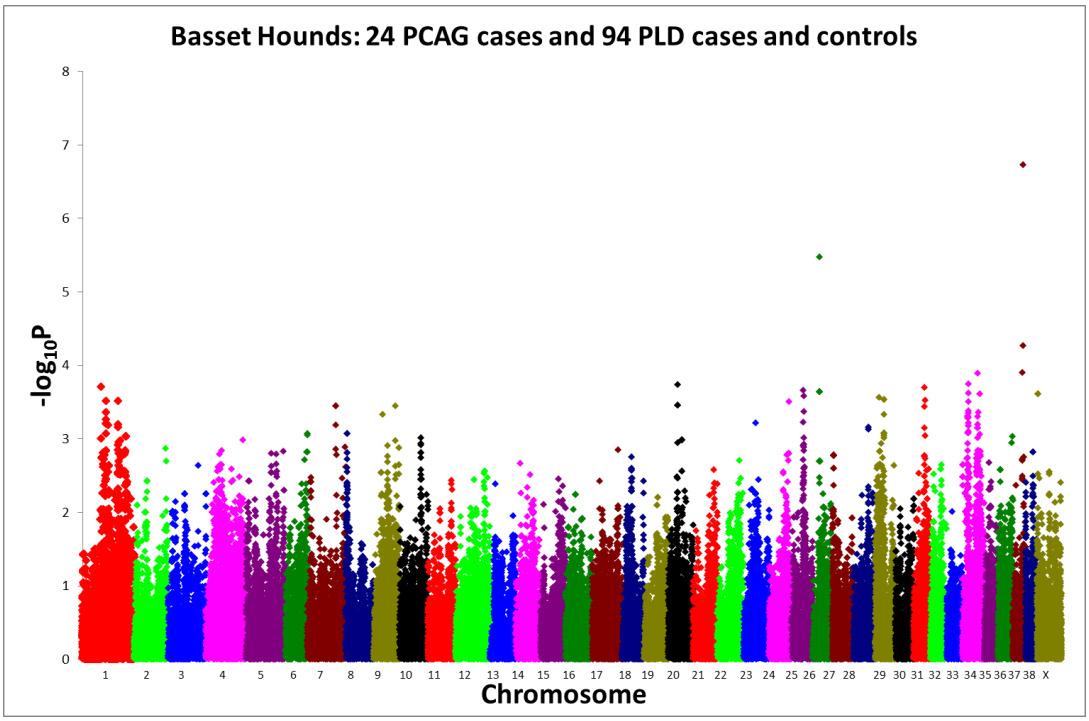

Figure 4.7. Manhattan plot demonstrating association of SNP markers with PCAG relative to PLD cases and controls in BH using BICF2P544799 as a covariate.

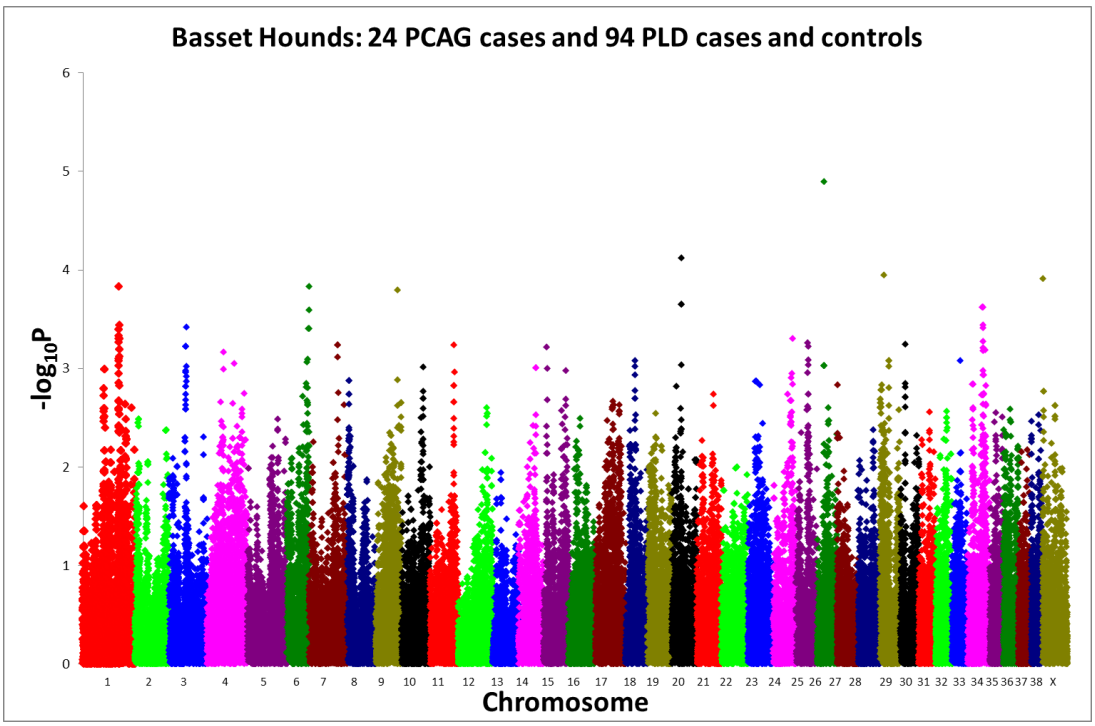

Figure 4.8 Manhattan plot demonstrating association of SNP markers with PCAG relative to PLD cases and controls in BH using BICF2P544799 and BICF2P928441 as covariates.

The strength of association of these three SNPs with PCAG was further assessed in the individual SNP dataset using logistic regression with assistance from Dr Sally Ricketts. This was done for both the original GWAS cohort and also with the addition of the USA PCAG samples. All three SNPs were strongly associated with PCAG and the strength of association increased following addition of USA PCAG samples to the analysis (**Table 4.5**). As an exploratory analysis, a non-weighted risk score was constructed using counts of risk alleles BICF2G630505097 and BICF2P928441 (the most strongly associated SNPs on chromosome 24 and 37 SNPs following addition of USA PCAG samples). The risk score explained 54 % of the phenotype variation.

4.2.2.1.6 Definition of associated loci

Associated loci were defined based on pair wise linkage disequilibrium estimates of these top three SNPs. The results of the strongest associated SNPs on chromosome 24 were combined to give a single locus by loading SNP data into Haploview and

assessing LD amongst SNPs. The following chromosomal loci were defined: CanFam3.1 chr24:17,381,226-18,739,902 and chr37:24,747,131-24,958,250.

4.2.2.1.6.1 Identification and genotyping of candidate variants

WGS data were available from three BH with PCAG (**Table 2.4**). However, only data from one BH PCAG case were used to interrogate the two loci identified from GWAS on the basis of genotypes of the top GWAS SNPs (BICF2P544799 and BICF2P928441). The case chosen (BaH_28502) was heterozygous for the alternative alleles (other BH PCAG cases for which WGS were held were homozygous for the reference alleles). Firstly, the identified associated loci were visually screened for structural variants using the WGS sequences from the BH PCAG case and those from six control dogs in IGV. Then the BH PCAG case was compared with WGS data from 97 dogs of other breeds (controls) as described in section **2.2.12**. The controls were dogs without PCAG and were of breeds not known to be predisposed to PLD or PCAG. The identified associated loci above were screened to identify variants for which the alternative allele segregated in the case but not in the controls. Identified variants were further screened in a consortium of 465 canid WGS (DBVD). Only variants that were private to the BH were further investigated. Three candidate variants were identified with this approach. Initial genotyping of one of these (chr37:24,861,167 A>G SNP) by Sanger sequencing in 126 BH (48 PCAG cases (European and USA), 49 PLD cases and 29 controls) revealed that 125 BH were homozygous for the reference allele (A/A) and only one (the PCAG cases WGS sample) was a heterozygote (A/G). This variant was not further investigated. The remaining two variants (**Table 4.6**) were genotyped in the GWAS cohort to test level of association with PCAG. For both variants, association with PCAG was weaker than that of the top three SNPs (**Table 4.6**), and they were therefore not investigated any further.

Table 4.5 Association of GWAS top SNPs with PCAG in the BH relative to controls and PLD cases.

Top SNP from GWAS	USA PCAG cases included?	No. PCAG cases	No. PLD cases and controls	OR	Lower 95% CI	Upper 95% CI	P-value (log likelihood ratio test)	Fisher's exact P-value
chr24:17381226 BICF2G630505097	No	24	94	13.73	5.06	37.26	4.2×10^{-11}	1.4×10^{-11}
	Yes	59	94	18.84	7.97	44.51	1.6×10^{-21}	1.2×10^{-21}
chr24:18739902 BICF2P544799	No	24	94	28.35	8.50	94.58	1.6×10^{-11}	1.1×10^{-10}
	Yes	59	94	15.81	6.03	41.45	1.4×10^{-12}	7.1×10^{-12}
chr37: 24747131 BICF2P928441	No	24	94	18.03	4.44	73.28	1.1×10^{-6}	3.9×10^{-6}
	Yes	59	94	14.76	4.19	51.96	3.6×10^{-8}	1.7×10^{-7}

No. = number, OR = odds ratio, CI = confidence interval

Table 4.6. Association of candidate variants with PCAG in the BH relative to PLD cases and controls

CanFam3.1 coordinate and associated gene	Nature of variant and genotyping method	USA PCAG cases included?	No. PCAG cases	No. PLD cases and controls	OR	Lower 95% CI	Upper 95% CI	P-value (log likelihood ratio test)	Fisher's exact P-value
chr24:17727188 *ATRN*	A>G intronic SNP Sanger sequencing	No	23	93	15.28	5.14	45.48	3.6×10^{-10}	4.6×10^{-10}
		Yes	57	93	11.77	4.90	28.26	6.5×10^{-14}	1.9×10^{-13}
chr24:18222425 *PTPRA*	2bp intergenic insertion AFLP	No	24	93	3.95	2.01	7.77	1.7×10^{-5}	6.4×10^{-5}
		Yes	59	93	3.24	2.01	5.21	1.9×10^{-7}	1.2×10^{-6}

No. = number, OR = odds ratio, CI = confidence interval

4.2.2.1.6.2 Identification of candidate genes from RNA-Seq

Whole transcriptome data derived from ICA tissues were used to compare differential gene expression between five BH PCAG cases and four non-BH controls in the loci determined from GWAS (**Table 4.7**). In the chromosome 24 locus, differential gene expression was present for five genes: *SIGLEC1*, C24H20orf194, *SLC4A11*, *PROSAPIP1* and *OXT*. In the chromosome 37 locus, differential expression was present for three genes: *CXCR2*, *CXCR1* and *ARPC2*. A survey of the functions and associated phenotypes of these genes revealed no evidence of reported association with glaucoma. All genes, however, appeared to be involved in inflammation and immunity (**Table 4.8**).

Table 4.7. Differential gene expression results for the BH PCAG loci.

Gene	CanFam3.1 coordinate	Test success	FPKM Controls	FPKM PCAG cases	log_2(fold change)	Test statistic	P-value	Q-value	Significant?
Locus chr24:17,381,226-18,739,902									
LOC100855425	24:17377802-17459234	OK	3.66177	4.27275	0.222624	0.105002	0.90045	0.972499	no
RNF24	24:17377802-17459234	OK	13.5062	15.8018	0.226461	0.549112	0.2461	0.564651	no
PAX1	24:1743907-1752578	NO TEST	0.751058	0.206085	-1.86569	0	1	1	no
PANK2	24:17463086-17489560	OK	19.9698	18.2754	-0.127921	-0.289163	0.55265	0.833548	no
MAVS	24:17511842-17529197	OK	29.2054	32.6664	0.161573	0.390852	0.42265	0.743935	no
AP5S1	24:17539786-17543605	OK	8.54101	8.52501	-0.00270593	-0.00393991	0.99425	0.998863	no
CDC25B	24:17552205-17561823	OK	12.1744	14.8	0.28175	0.556191	0.2447	0.563837	no
CENPB	24:17569396-17572311	OK	31.9742	38.916	0.283456	0.799702	0.1328	0.393219	no
SPEF1	24:17572374-17578571	OK	1.5338	1.92433	0.327243	0.400218	0.3999	0.724145	no
C24H20orf27	24:17586019-17600147	OK	22.4481	29.0792	0.373394	0.779776	0.1107	0.352522	no
HSPA12B	24:17600534-17619889	OK	6.57984	9.70452	0.560605	1.14769	0.0296	0.142427	no
SIGLEC1	**24:17636164-17667080**	**OK**	**2.18752**	**12.5593**	**2.52139**	**4.87528**	**5.00E-05**	**0.0008345**	**yes**
ADAM33	24:17668462-17682217	OK	10.7869	8.23265	-0.389845	-0.829875	0.0807	0.285699	no

Gene	CanFam3.1 coordinate	Test success	FPKM Controls	FPKM PCAG cases	log_2(fold change)	Test statistic	P-value	Q-value	Significant?
GFRA4	24:17686816-17690747	OK	3.16594	2.14218	-0.563553	-0.711984	0.2384	0.555935	no
ATRN	24:17698237-17859816	OK	18.7085	14.7908	-0.338994	-0.812765	0.08165	0.288073	no
C24H20orf194	**24:17908366-18050002**	**OK**	**14.0202**	**9.25396**	**-0.599364**	**-1.46229**	**0.00165**	**0.0153647**	**yes**
SLC4A11	24:18057411-18068425	OK	28.8724	6.6876	-2.11013	-4.36281	5.00E-05	0.0008345	yes
ITPA	24:18070979-18082187	OK	11.9247	16.3186	0.452557	0.814939	0.0945	0.316902	no
DDRGK1	24:18085722-18098868	OK	17.4284	15.1717	-0.200057	-0.450069	0.33115	0.659854	no
LOC102157332	24:18111855-18122295	NOTEST	0.531426	0.412288	-0.366218	0	1	1	no
PROSAPIP1	**24:18111855-18122295**	**OK**	**20.0459**	**12.6993**	**-0.658565**	**-1.63743**	**0.00105**	**0.0107012**	**yes**
FASTKD5	24:18124262-18166506	OK	13.9635	14.315	0.0358696	0.0772293	0.86905	0.965583	no
CST11	24:181590-184213	NOTEST	0	0	0	0	1	1	no
AVP	24:18183056-18184827	NOTEST	0.182349	0.0787568	-1.21123	0	1	1	no
OXT	**24:18193380-18194236**	**OK**	**18.6151**	**5.43912**	**-1.77503**	**-2.94744**	**0.0006**	**0.0068551**	**yes**
MRPS26	24:18215054-18217105	OK	24.9994	26.2617	0.0710653	0.176449	0.7648	0.934576	no
LOC102151131	24:18217903-18222755	NOTEST	0.0563875	0.0232463	-1.27838	0	1	1	no
LOC102154818	24:18224354-18395654	NOTEST	0.867838	0.884208	0.0269605	0	1	1	no
PTPRA	24:18224354-18395654	OK	30.9735	28.6433	-0.112839	-0.288467	0.5554	0.835146	no

Gene	CanFam3.1 coordinate	Test success	FPKM Controls	FPKM PCAG cases	log_2(fold change)	Test statistic	P-value	Q-value	Significant?
VPS16	24:18401450-18424606	OK	11.5555	11.6659	0.0137143	0.0286225	0.95285	0.989023	no
PCED1A	24:18424775-18429698	OK	18.7163	16.9792	-0.140525	-0.340822	0.5442	0.828421	no
LOC102155387	24:18442763-18443512	NOTEST	0.12029	0.206892	0.782359	0	1	1	no
TMEM239	24:18443575-18445637	NOTEST	0.308423	0.133061	-1.21283	0	1	1	no
C24H20orf141	24:18445693-18446873	NOTEST	0.202272	0.317907	0.652307	0	1	1	no
CPXM1	24:18453867-18460350	OK	8.40695	13.7502	0.7098	1.29913	0.0077	0.0506978	no
EBF4	24:18470596-18528305	OK	1.69066	1.6627	-0.0240522	-0.0278686	0.96215	0.991001	no
IDH3B	24:18556489-18561401	OK	46.7683	38.3285	-0.287114	-0.659815	0.1486	0.420704	no
NOP56	24:18561409-18566780	OK	28.0915	30.953	0.139945	0.325807	0.48615	0.78904	no
TMC2	24:18577342-18642204	NOTEST	0.308586	0.147869	-1.06136	0	1	1	no
ZNF343	24:18661008-18665685	NOTEST	0.245175	0.133892	-0.872746	0	1	1	no
SNRPB	24:18674022-18683315	OK	62.0096	61.9386	-0.00165212	-0.004023	0.99365	0.998542	no
TGM6	24:18700241-18721827	NOTEST	0.0171946	0	-	0	1	1	no
TGM3	24:18753637-18793790	NOTEST	0.0342808	0.138228	2.01158	0	1	1	no
Locus chr37:24,747,131-24,958,250									
RUFY4	37:24809358-24830254	OK	1.71109	1.18547	-0.52945	-0.51443	0.27475	0.599772	no

Gene	CanFam3.1 coordinate	Test success	FPKM Controls	FPKM PCAG cases	log_2(fold change)	Test statistic	P-value	Q-value	Significant?
CXCR2	**37:24831509-24846517**	**OK**	**3.35508**	**1.02764**	**-1.70702**	**-1.59836**	**0.00145**	**0.013826**	**yes**
CXCR1	**37:24861913-24866062**	**OK**	**1.82409**	**0.616257**	**-1.56557**	**-1.58159**	**0.0041**	**0.030963**	**yes**
ARPC2	**37:24914388-24936198**	**OK**	**84.4912**	**137.67**	**0.704343**	**1.97128**	**0.00035**	**0.004435**	**yes**
GPBAR1	37:24940929-24943399	OK	1.26415	2.05007	0.697505	0.919835	0.14675	0.417894	no
AAMP	37:24943657-24948585	OK	40.9075	43.1513	0.077039	0.181187	0.70665	0.913414	no
PNKD	37:24948682-25008542	OK	6.30845	7.78033	0.302547	0.202254	0.70135	0.911242	no

OK = test successful, NOTEST = not enough alignments for testing

Table 4.8. Details of differentially expressed genes, their functions and associated disorders and phenotypes.

Gene	Gene full name	Function	Associated disorders/phenotypes
SIGLEC1	Sialoadhesin	Endocytic receptor mediating clathrin dependent endocytosis	Glomerulonephritis Sclerosis X-linked intellectual disability
C20orf194	Chromosome 20 open reading frame 194	May act as an effector for ARL3	HIV-1 Hepatitis
SLC4A11	Solute Carrier Family 4 Member 11	Transporter which plays an important role in sodium-mediated fluid transport in different organs	Corneal dystrophy HIV-1 Hepatitis
PROSAPIP1	Proline Rich Synapse Associated Protein Interacting Protein 1	May be involved in promoting the maturation of dendritic spines	Hepatitis

Gene	Gene full name	Function	Associated disorders/phenotypes
OXT	Oxytocin	Contraction of smooth muscle of uterus and mammary gland	Persistent genital arousal Endometritis Inhibited male orgasm Epignathus Chorioamnionitis Parturition Lactation
CXCR1	Chemokine (CXC) Receptor 1	Neutrophil activation, neutrophil count	HIV-1 Pyelonephritis & urinary tract infections Idiopathic anterior uveitis

Gene	Gene full name	Function	Associated disorders/phenotypes
CXCR2	Chemokine (CXC) Receptor 2	Neutrophil activation, neutrophil count	Congenital neutropenia Neutrophil migration Pyelonephritis Septicaemia Granulocytic anaplasmosis
ARPC2	Actin Related Protein 2/3 Complex Subunit 2	Actin filament assembly. Platelet, reticulocyte and neutrophil count	Platelet, reticulocyte and neutrophil count

4.2.2.2 FCR

Genotyping data derived from 166 dogs, comprising 19 PCAG cases, 59 PLD cases and 89 controls, were analysed.

4.2.2.2.1 PCAG cases and controls

After filtering, 19 cases and 89 controls and 92,489 SNPs remained for analysis. No SNP markers reached the threshold suggestive of genome-wide significance (**Figure 4.9**).

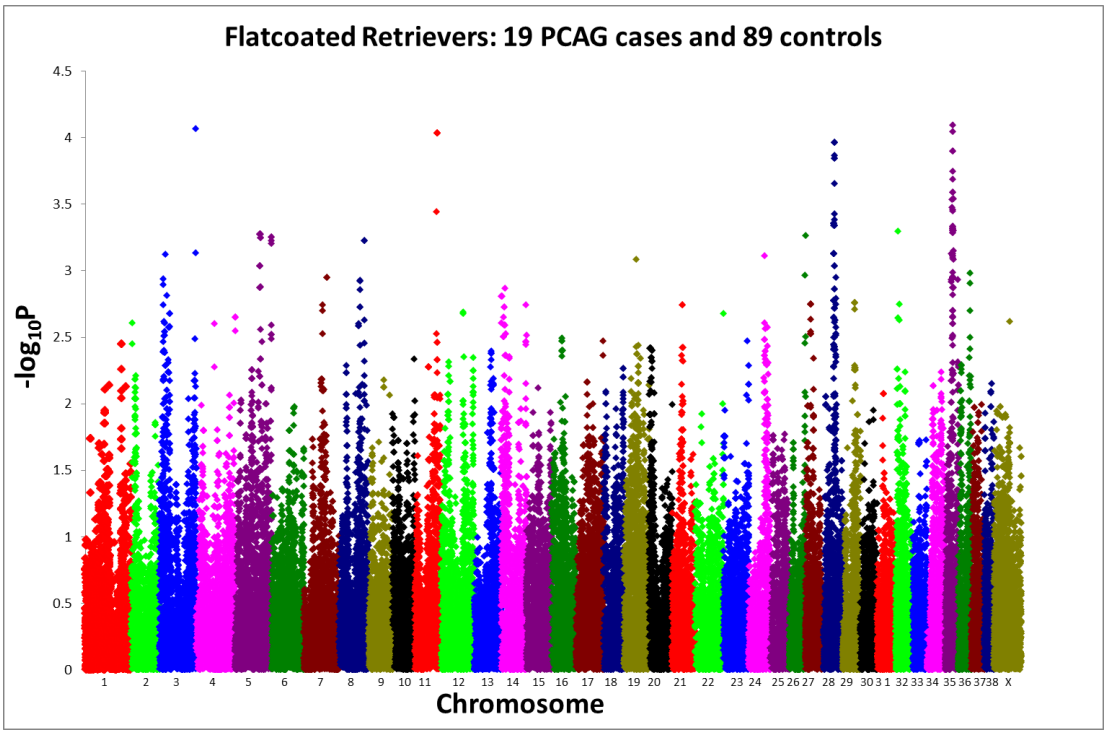

Figure 4.9. Manhattan plot demonstrating association of SNP markers with PCAG in FCR.

4.2.2.2.2 PCAG and PLD cases and controls

After frequency and genotype pruning of individuals and SNPs, 78 cases and 89 controls, and 92,970 SNPs remained for analysis. No SNPs reached the threshold suggestive of genome-wide significance (**Figure 4.10**).

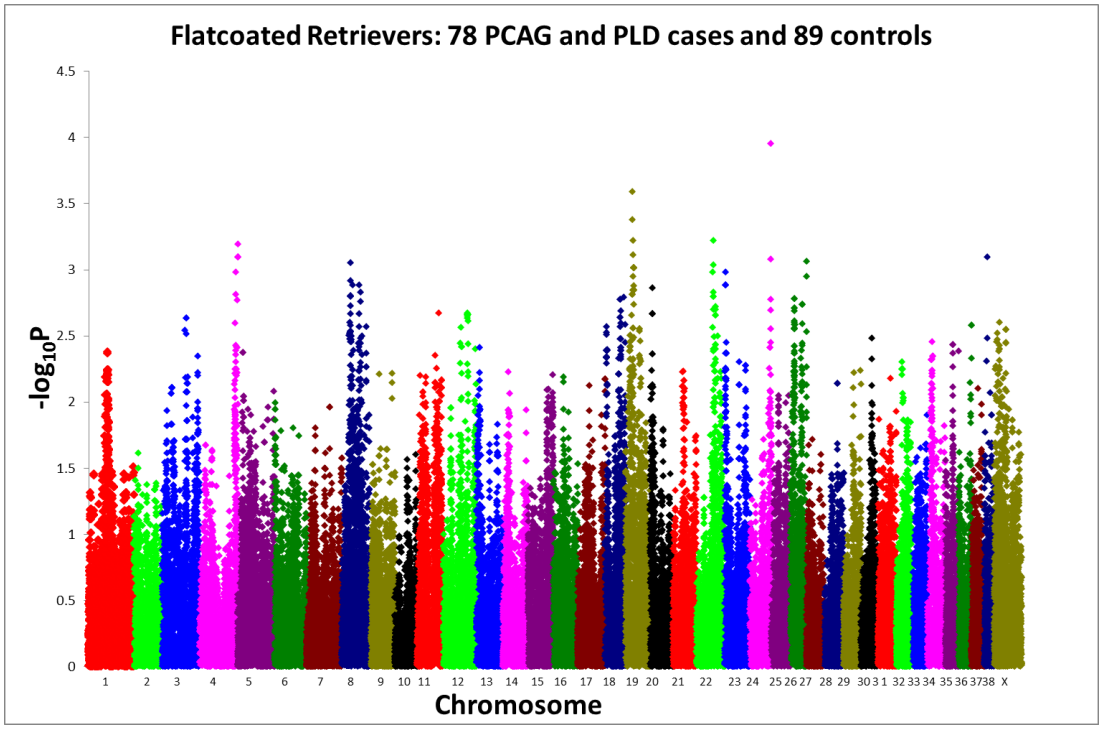

Figure 4.10. Manhattan plot demonstrating association of SNP markers with PCAG and PLD in FCR.

4.2.2.2.3 PLD cases and controls

After filtering, 59 cases and 89 controls and 92,995 SNPs remained for analysis. No SNPs reached the threshold of suggestive genome-wide significance (**Figure 4.11**).

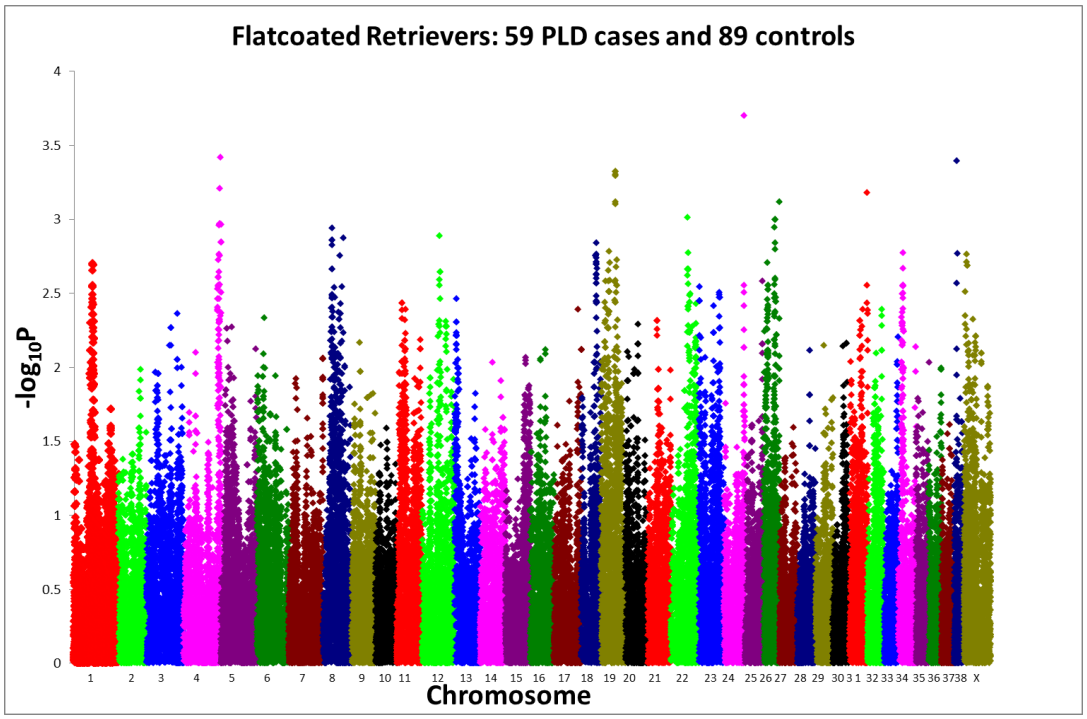

Figure 4.11. Manhattan plot demonstrating association of SNP markers with PLD in FCR.

4.2.2.2.4 PCAG cases and PLD cases

After filtering, 19 PCAG cases and 59 PLD cases and 93,002 SNPs remained for analysis. No SNPs reached the threshold suggestive of genome-wide significance (**Figure 4.12**).

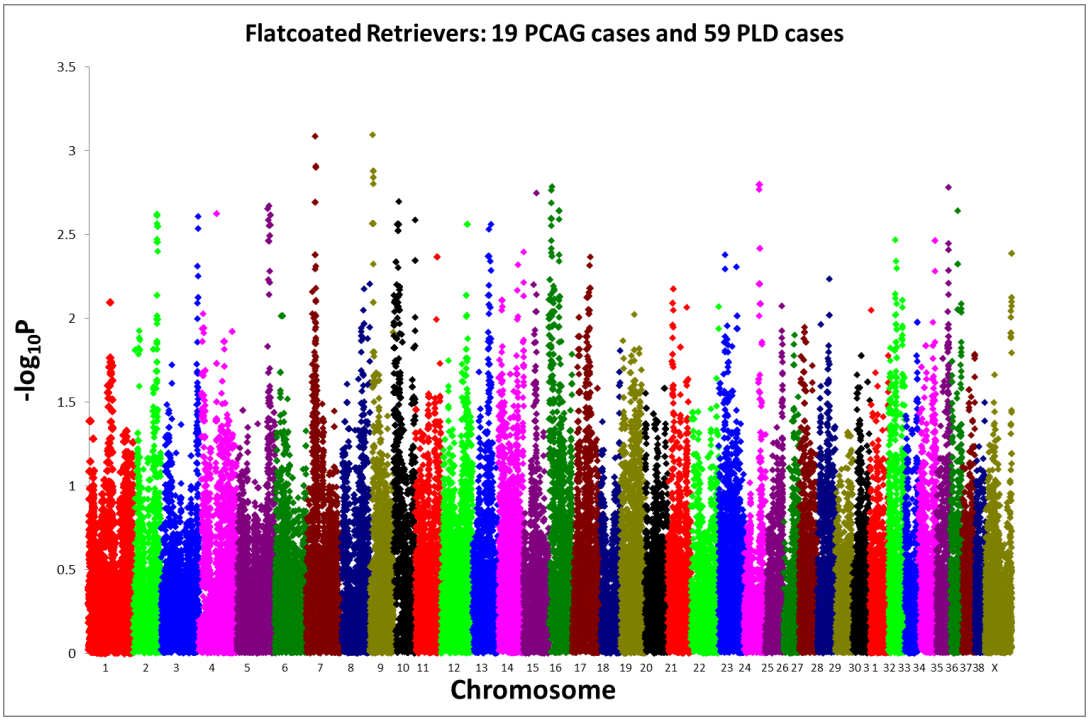

Figure 4.12. Manhattan plot demonstrating association of SNP markers with PCAG relative to PLD in FCR.

4.2.2.2.5 PCAG cases and PLD cases and controls

After filtering, 19 PCAG cases and 148 PLD cases and controls and 92,970 SNPs remained for analysis. No SNPs reached the threshold suggestive of genome-wide significance (**Figure 4.13**).

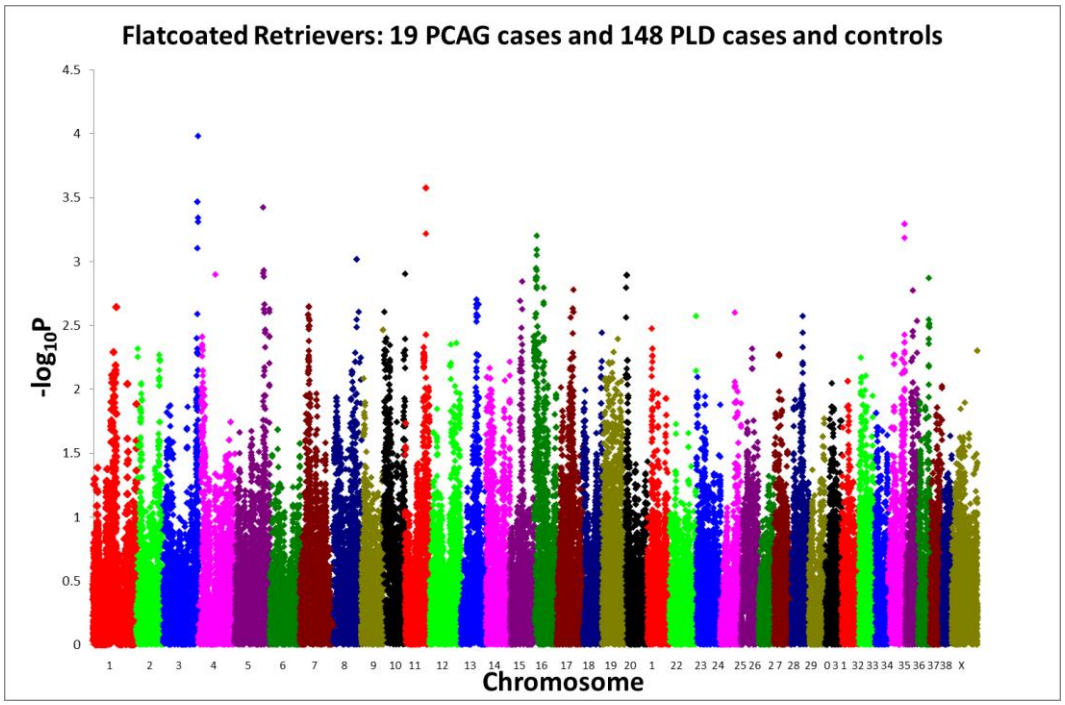

Figure 4.13. Manhattan plot demonstrating association of SNP markers with PCAG relative to PLD cases and controls in FCR.

4.2.2.3 DDT

Genotyping data derived from 104 dogs comprising 32 PCAG cases, 21 PLD cases and 51 controls, were analysed.

4.2.2.3.1 PCAG cases and controls

After filtering, 32 PCAG cases and 51 controls and 85,854 SNPs remained for analysis. No SNPs reached the threshold suggestive of genome-wide significance (**Figure 4.14**).

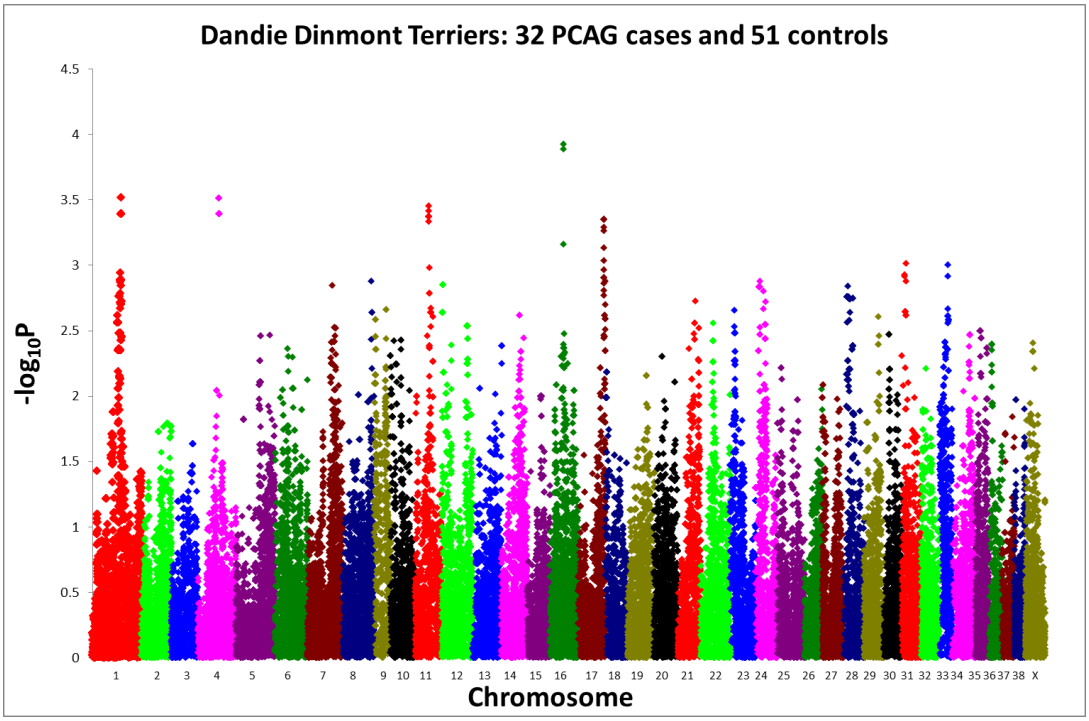

Figure 4.14. Manhattan plot demonstrating association of SNP markers with PCAG in DDT.

4.2.2.3.2 PCAG and PLD cases and controls

After filtering, 53 PCAG and PLD cases and 51 controls and 85,945 SNPs remained for analysis. No SNPs reached the threshold suggestive of genome-wide significance (**Figure 4.15**).

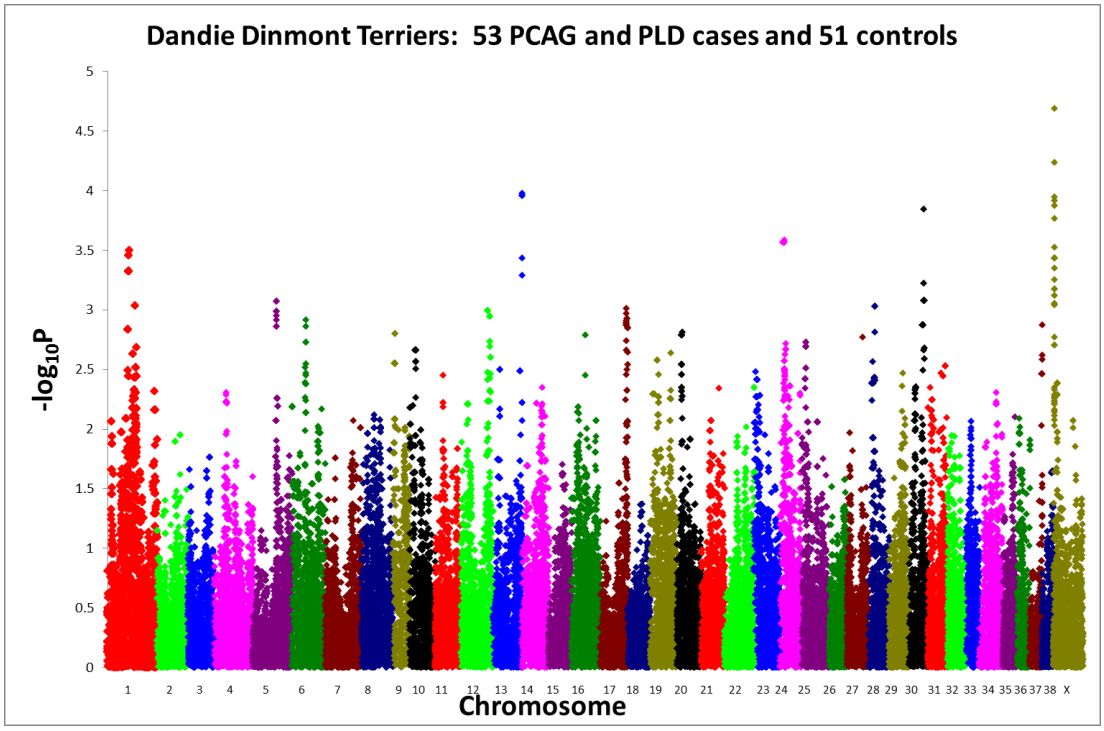

Figure 4.15. Manhattan plot demonstrating association of SNP markers with PCAG and PLD in DDT.

4.2.2.3.3 PLD cases and controls

After filtering, 21 PLD cases and 51 controls and 84,718 SNPs remained for analysis. No SNPs reached the threshold suggestive of genome-wide significance (**Figure 4.16**).

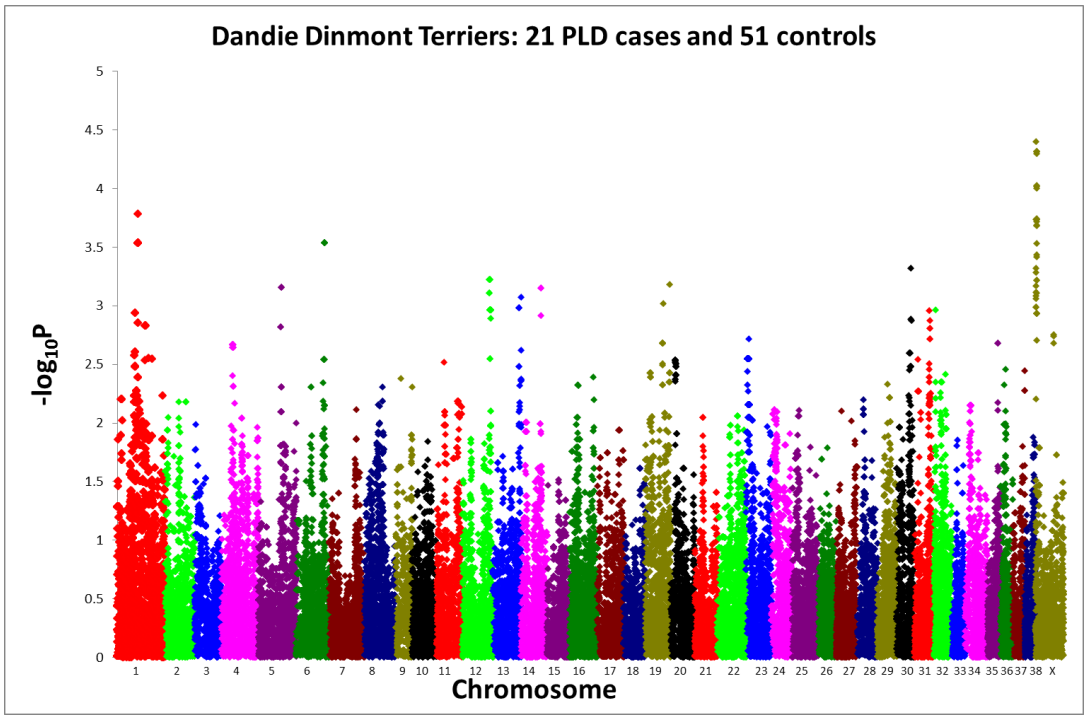

Figure 4.16. Manhattan plot demonstrating association of SNP markers with PLD in DDT.

4.2.2.3.4 PCAG cases and PLD cases

After filtering, 32 PCAG cases and 21 PLD cases and 84,950 SNPs remained for analysis. No SNPs reached the threshold suggestive of genome-wide significance (**Figure 4.17**).

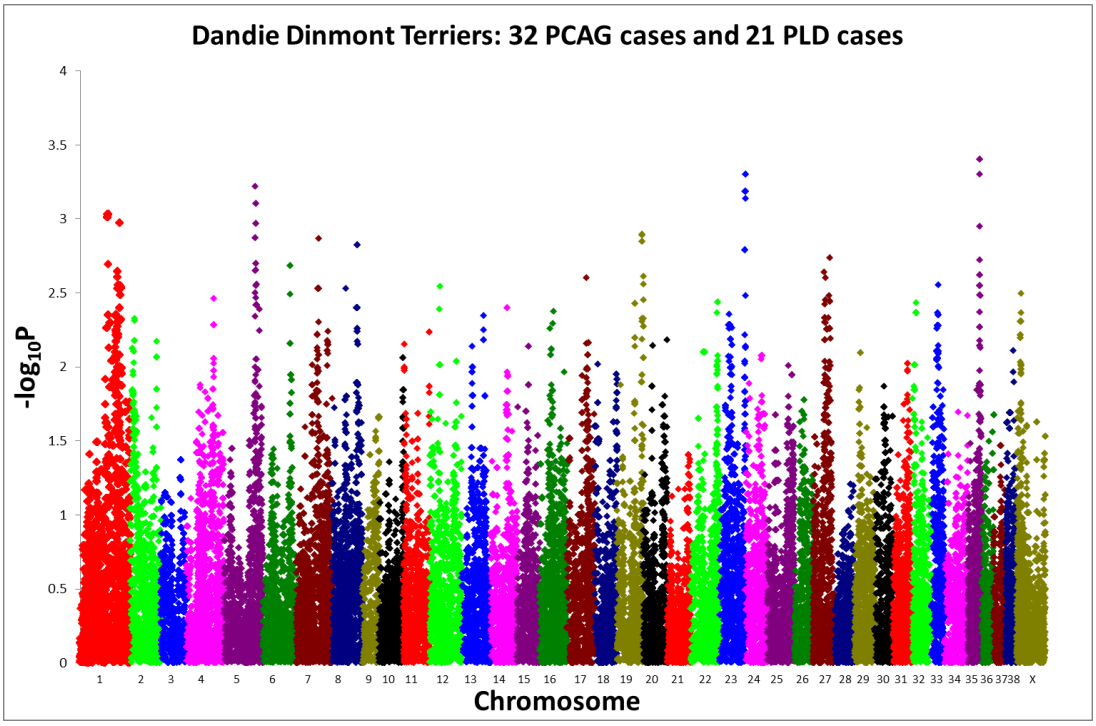

Figure 4.17. Manhattan plot demonstrating association of SNP markers with PCAG relative to PLD cases in DDT.

4.2.2.3.5 PCAG cases and PLD cases and controls

After filtering, 32 PCAG cases and 72 PLD cases and controls 85,824 SNPs remained for analysis. No SNPs reached the threshold suggestive of genome-wide significance (**Figure 4.18**).

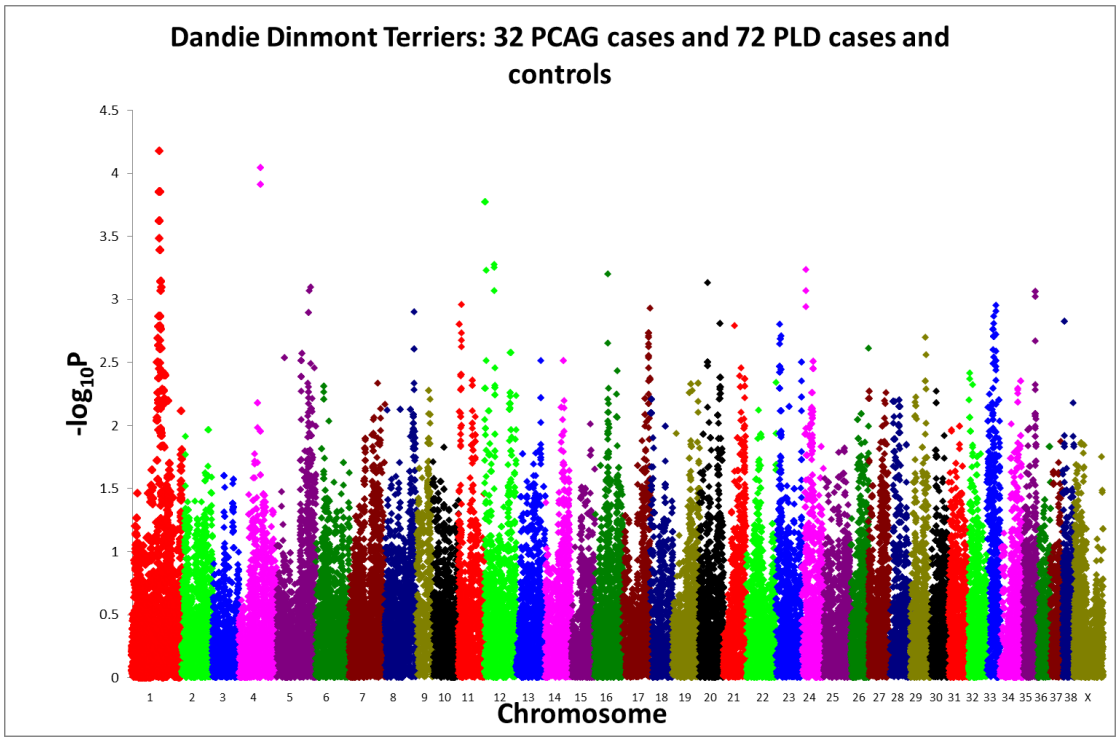

Figure 4.18. Manhattan plot demonstrating association of SNP markers with PCAG relative to PLD cases and controls in DDT.

4.2.2.4 WSS

Genotyping data derived from 123 dogs, comprising 36 PCAG cases, 54 PLD cases and 33 controls, were analysed.

4.2.2.4.1 PCAG cases and controls

After filtering, 36 PCAG cases and 33 controls and 97,176 SNPs remained for analysis. No SNPs reached the threshold suggestive of genome-wide significance (**Figure 4.19**).

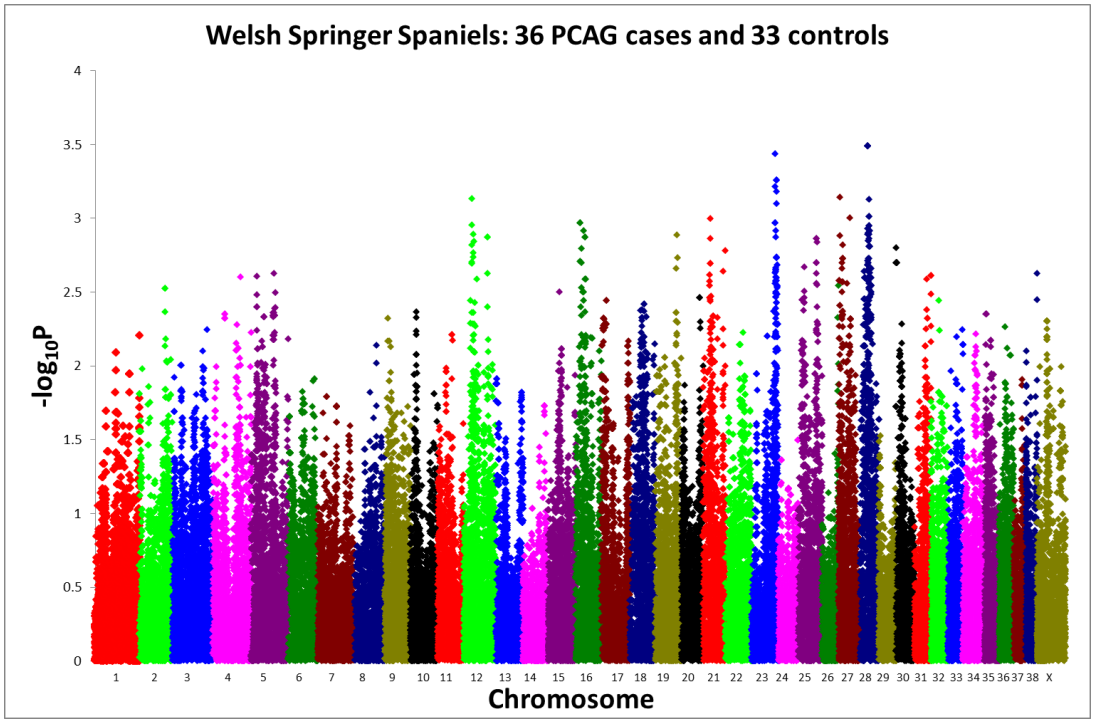

Figure 4.19. Manhattan plot demonstrating association of SNP markers with PCAG in WSS.

4.2.2.4.2 PCAG and PLD cases and controls

After filtering, 90 PCAG and PLD cases and 33 controls and 95,830 SNPs remained for analysis. No SNPs reached the threshold suggestive of genome-wide significance (**Figure 4.20**).

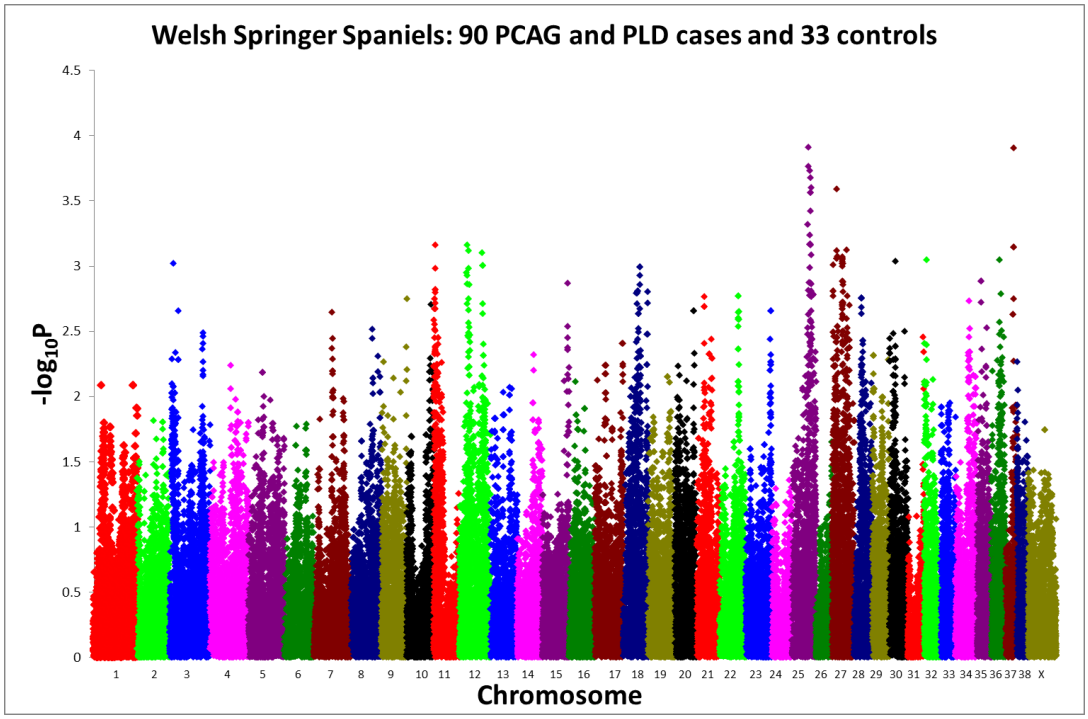

Figure 4.20. Manhattan plot demonstrating association of SNP markers with PCAG and PLD in WSS.

4.2.2.4.3 PLD cases and controls

After filtering, 54 PLD cases and 33 controls and 95,582 SNPs remained for analysis. No SNPs reached the threshold suggestive of genome-wide significance (**Figure 4.21**).

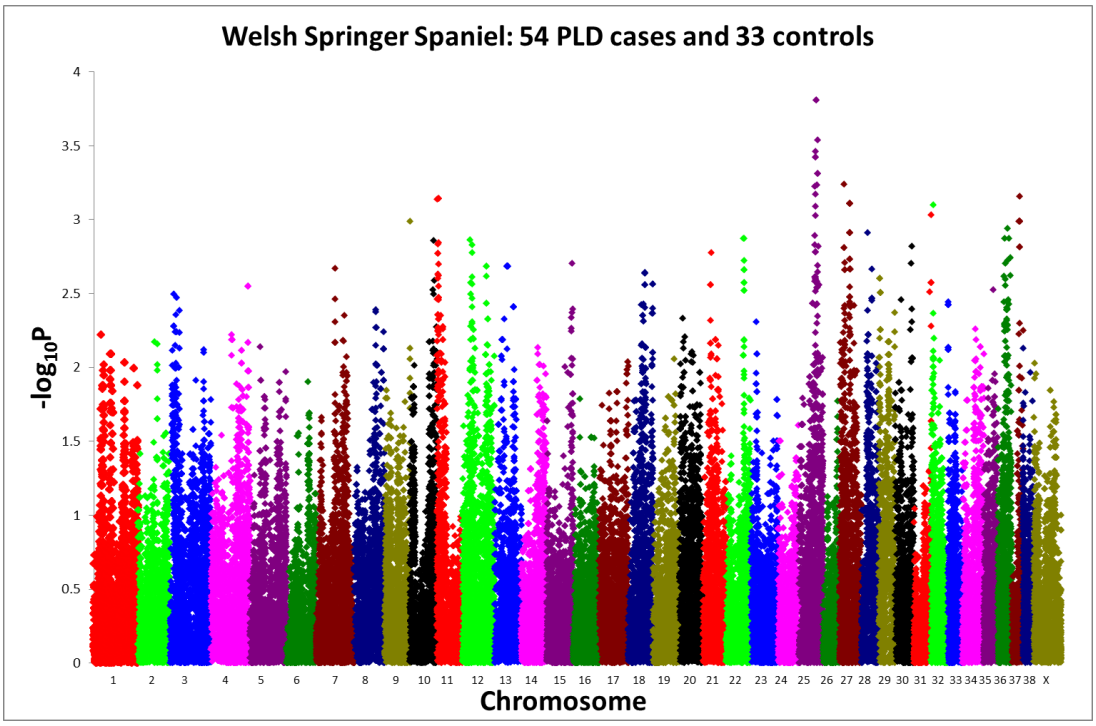

Figure 4.21. Manhattan plot demonstrating association of SNP markers with PLD in WSS.

4.2.2.4.4 PCAG cases and PLD cases

After filtering, 36 PCAG cases and 54 PLD cases and 97,028 SNPs remained for analysis. No SNPs reached the threshold suggestive of genome-wide significance (**Figure 4.22**).

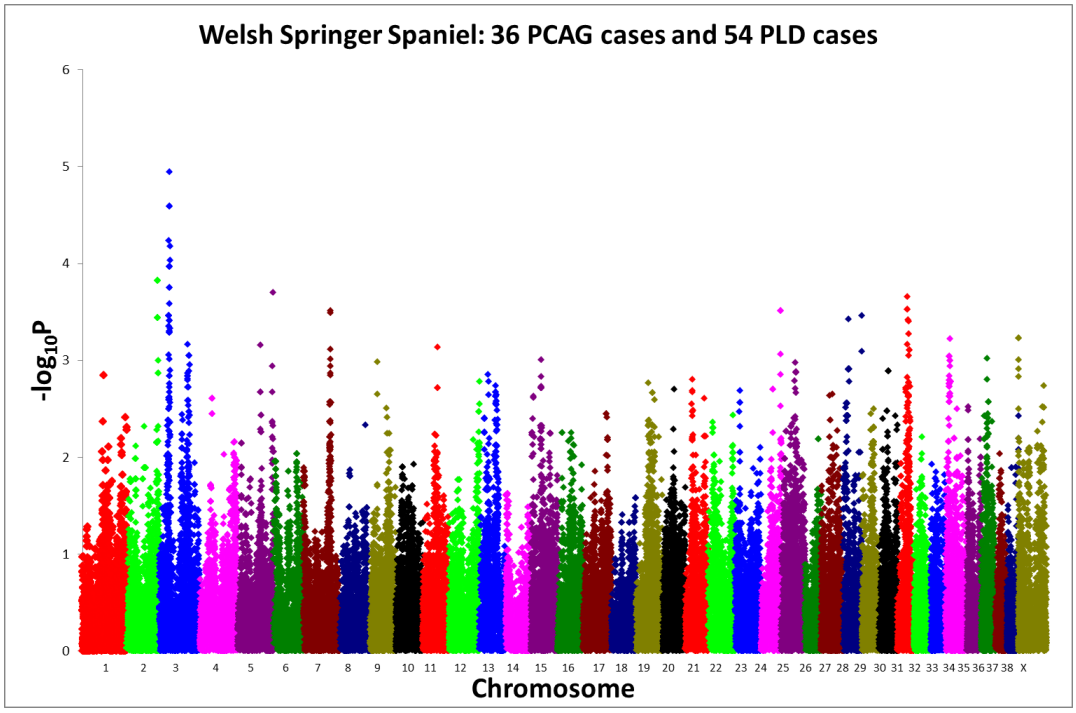

Figure 4.22. Manhattan plot demonstrating association of SNP markers with PCAG relative to PLD in WSS.

4.2.2.4.5 PCAG cases and PLD cases and controls

After filtering, 36 PCAG cases and 87 PLD cases and controls and 95,830 SNPs remained for analysis. No SNPs reached the threshold suggestive of genome-wide significance (**Figure 4.23**).

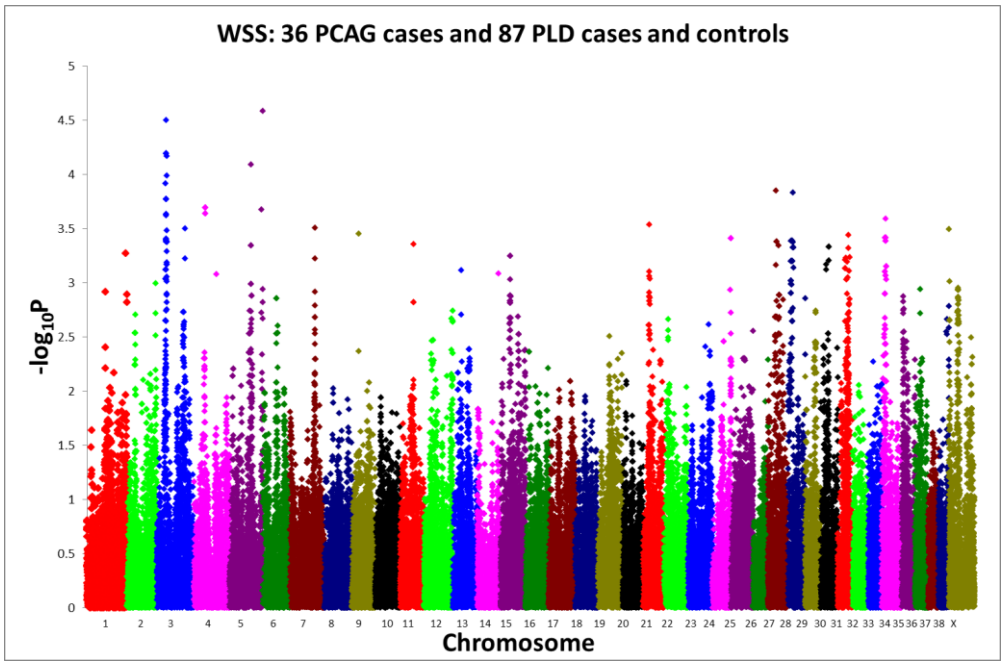

Figure 4.23. Manhattan plot demonstrating association of SNP markers with PCAG relative to PLD cases and controls in WSS.

4.2.2.5 BH, FCR, DDT and WSS Meta-analysis

Meta-analysis was performed across all four breeds to identify any shared regions of association with PCAG, PLD or both. This was done with assistance from Dr Sally Ricketts. Genotyping data derived from 111 PCAG cases, 191 PLD cases and 210 controls were analysed. Individual breed GWAS GEMMA analyses were utilised in these analyses. Q-Q plots were performed for all meta- analyses (**Appendix II**) but MDS plots were not generated as meta-analysis takes breed variation into account by combining the summary statistics from the single breed analyses. Meta-analysis was only performed for SNPs that were informative and passed quality control measures in all four breeds. A summary of meta-analysis GWAS and results is presented in **Table 4.9**.

Table 4.9. Summary of meta-analysis GWAS results.

Breeds	Phenotype		No. samples		No. SNPs analysed	λ	SNPs reaching Bonferroni significance	Pooled Values			P-value	P-value for heterogeneity (Q statistic)
	Cases	Controls	Cases	Controls				OR	Lower 95% CI	Upper 95% CI		
BH FCR DDT WSS	PCAG cases	Controls	111	210	37756	1.12	BICF2P161081 BICF2P242291 (R^2 = 1.0)	1.30	1.18	1.43	1.7 x 10^{-7}	0.81
	PCAG cases	PLD cases & controls	111	401	37726	1.07	None	NA	NA	NA	NA	NA
	PCAG & PLD cases	Controls	302	210	37726	1.05	None	NA	NA	NA	NA	NA
	PLD cases	Controls	191	210	36116	1.04	None	NA	NA	NA	NA	NA
	PCAG cases	PLD cases	111	191	37467	1.02	None	NA	NA	NA	NA	NA
DDT WSS	PCAG cases	Controls	68	84	62982	1.04	BICF2G630271568	0.76	0.69	0.85	2.1 x 10^{-7}	0.86

No. = number of dogs, OR = odds ratio, CI = confidence interval

4.2.2.5.1 PCAG cases and controls

After filtering, 111 PCAG cases and 210 controls and 37,756 SNPs remained (**Table 4.9**). In this analysis, two SNPs reached genome-wide significant association with PCAG (BICF2P242291; CanFam3.1 chr28:14711023 and BICF2P161081; CanFam3.1 chr28:14721865; both $-\log_{10}P = 6.77$) (**Figure 4.24)**. These two SNPs were in perfect correlation with each other ($R^2 = 1.0$) and the heterogeneity statistic (0.81) indicated low heterogeneity between breeds (i.e. there was no significant difference in heterogeneity effect of the risk alleles across breeds) (**Table 4.9**). The strength of association of these SNPs was strongest in the individual datasets for the DDT and WSS (**Table 4.10**). Conditional analysis on BICF2P242291 was performed to assess for the presence of additional associations. No further SNPs reached genome-wide significance.

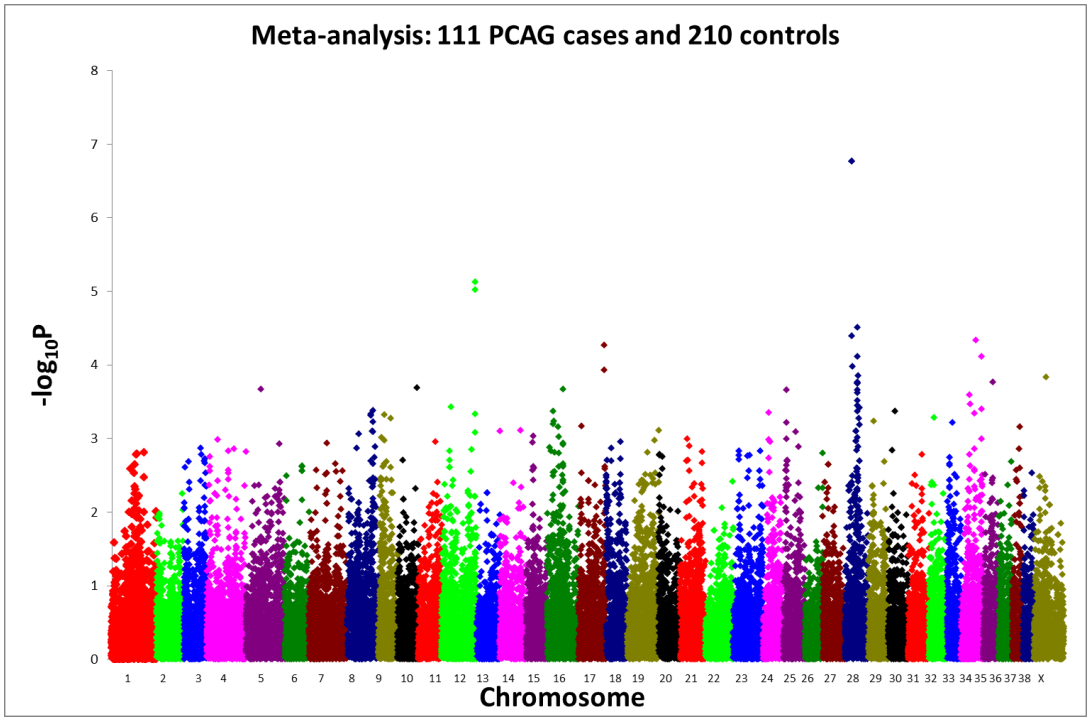

Figure 4.24. Manhattan plot of meta-analysis across all four breeds demonstrating association of SNP makers with PCAG.

Table 4.10. Association of meta-analysis top SNPs with PCAG by breed.

			Level of association following GEMMA			
			FCR	**DDT**	**WSS**	**BH**
SNP	**BICF2P242291**	**P-value**	0.015	0.006	0.006	0.166
		Beta coefficient	0.302	0.298	0.256	0.165
	BICF2P161081	**P-value**	0.015	0.006	0.006	0.166
		Beta coefficient	0.302	0.298	0.256	0.165

4.2.2.5.1.1 DDT and WSS PCAG cases and controls

Based on the finding of the strongest association of SNPs with PCAG from meta-analysis in the DDT and WSS, a pair wise meta-analysis of these two breeds was performed using 68 PCAG cases, 84 controls and 62,982 SNPs (**Table 4.9**). One SNP reached genome-wide significance (BICF2G630271568; CanFam3.1 chr28:18,871,699; $-\log_{10}P = 6.67$) (**Figure 4.5**). Following GEMMA correction of association data, association of this SNP with PCAG was stronger in both the DDT (P = 0.004) and WSS (P = 0.0003) than that of the top SNPs in the previous meta-analysis (P = 0.006 for both breeds). Introduction of this SNP as a covariate in the model did not reveal and further SNPs to be associated with PCAG.

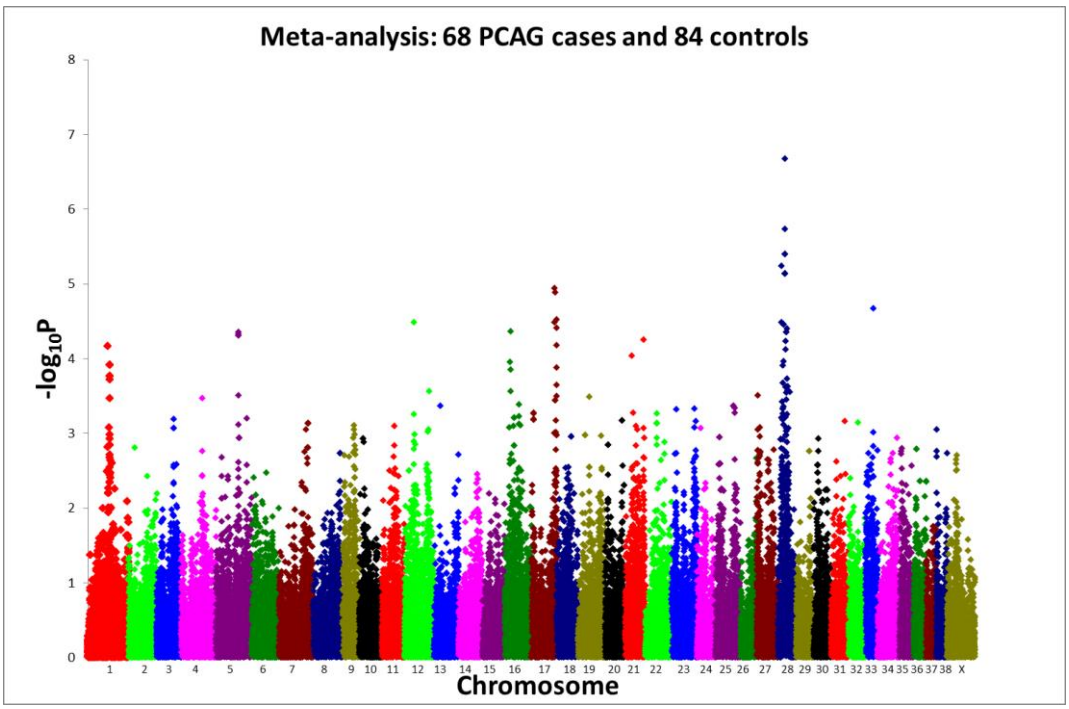

Figure 4.25. Manhattan plot of meta-analysis of DDT and WSS breeds demonstrating association of SNP markers with PCAG.

4.2.2.5.1.2 Identification of breed-specific associated loci

Breed-specific associated loci were defined based on pair wise linkage disequilibrium estimates ($R^2 \geq 0.5$) of the strongest associated SNP in each individual breed using Haploview (BICF2P242291 for the FCR and BICF2G630271568 for the WSS and DDT). The following chromosomal loci were defined (CanFam3.1): chr28:14,697,561-14,721,865 (FCR), chr28:18,835,904-19,259,305 (WSS) and chr28:18,871,699-19,358,417 (DDT).

4.2.2.5.1.3 Identification and genotyping of candidate variants

Firstly, the identified loci were visually screened for structural variants using the WGS data from one breed-specific PCAG case (selected on the basis that the alternative allele segregates in the case) and from six controls dogs in IGV. Identified loci were then screened for candidate variants using NGS approaches as for the BH (**section 4.2.2.1.6**). For each breed and locus, WGS data from PCAG-affected dogs (one FCR, one DDT and three WSS) of the breeds in question were compared with those from 97 control

dogs of other breeds. The control dogs were unaffected by PCAG and were from breeds not known to be predisposed to PCAG. Variants for which the alternative allele segregated in the cases, but not in the controls were identified. These were then further assessed in a consortium of 465 canid whole genome sequences (DBVD). Only variants which segregated in the PCAG case and were absent in all other sequences were further investigated. Candidate variants were then genotyped in the relevant breed specific GWAS cohorts. The following candidate variants were identified: a T>C intergenic SNP (chr28:14,624,548) in the FCR; a C>T intergenic SNP (chr28:19,274,452) in the DDT and; a 6 bp intergenic deletion (chr28:19,274,198-19,274,204) in the WSS. Only for the FCR candidate variant was association as strong as that of the top GWAS SNP (**Table 4.11**).

Table 4.11 Association of candidate variants with PCAG in the FCR, DDT and WSS.

Breed	Variant details (genomic coordinates are CanFam3.1)	Genotyping method	Correlation between GWAS top SNP and candidate variant	Cases	Controls	No. cases	No. controls	OR	Lower 95% CI	Upper 95% CI	P-value Log likelihood ratio test	Fisher's exact P-value
FCR	chr28:14,721,865 BICF2P161081 (GWAS top SNP)	GWAS data	1.0	PCAG cases	Controls	19	87	5.06	1.59	16.12	7.8×10^{-3}	8.4×10^{-3}
	chr28:14,624,548 T>C intergenic SNP (candidate variant)	Sanger sequencing		PCAG cases	Controls	19	87	5.06	1.59	16.12	7.8×10^{-3}	8.4×10^{-3}
DDT	chr28:18,871,699 BICF2G630271568 (GWAS top SNP)	GWAS data	0.46	PCAG cases	Controls	32	51	0.32	0.15	0.72	3.1×10^{-3}	5.1×10^{-3}

Breed	Variant details (genomic coordinates are CanFam3.1)	Genotyping method	Correlation between GWAS top SNP and candidate variant	Cases	Controls	No. cases	No. controls	OR	Lower 95% CI	Upper 95% CI	P-value Log likelihood ratio test	Fisher's exact P-value
	chr28:19,274,452 C>T intergenic SNP (candidate variant)	Sanger sequencing		PCAG cases	Controls	32	51	1.74	0.88	3.45	0.11	2.4×10^{-4}
WSS	chr28:18,871,699 BICF2G630271568 (GWAS top SNP)	GWAS data	0.76	PCAG cases	Controls	35	33	7.41	2.77	19.81	7.9×10^{-7}	4.8×10^{-6}
	chr28:19,274,198 intergenic 6bp deletion (candidate variant)	AFLP		PCAG cases	Controls	35	33	3.25	1.43	7.38	2.4×10^{-3}	2.9×10^{-3}

OR = odds ratio, CI = confidence interval

4.2.2.5.2 PCAG and PLD cases and controls

After filtering, 302 PCAG and PLD cases, 210 controls and 37,726 SNPs remained. No SNPs reached genome-wide significance (**Figure 4.26**).

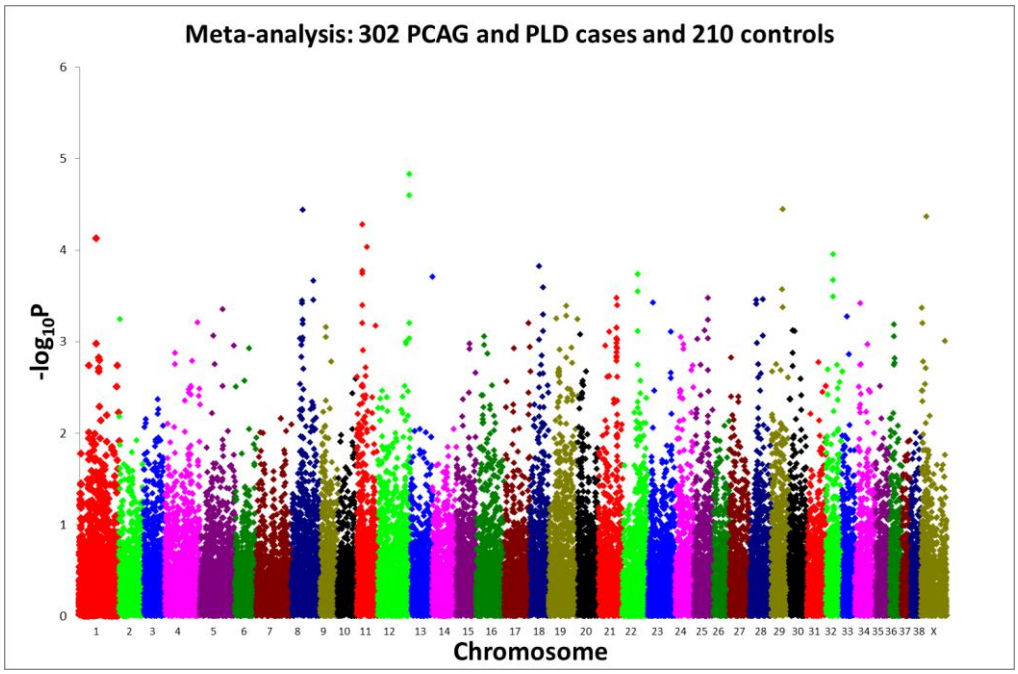

Figure 4.26. Manhattan plot of meta-analysis across all four breeds demonstrating association of SNP markers with PCAG cases and PLD cases.

4.2.2.5.3 PLD cases and controls

After filtering, 191 PLD cases, 210 controls and 36,116 SNPs remained for analysis. No SNPs reached genome-wide significance (**Figure 4.27**).

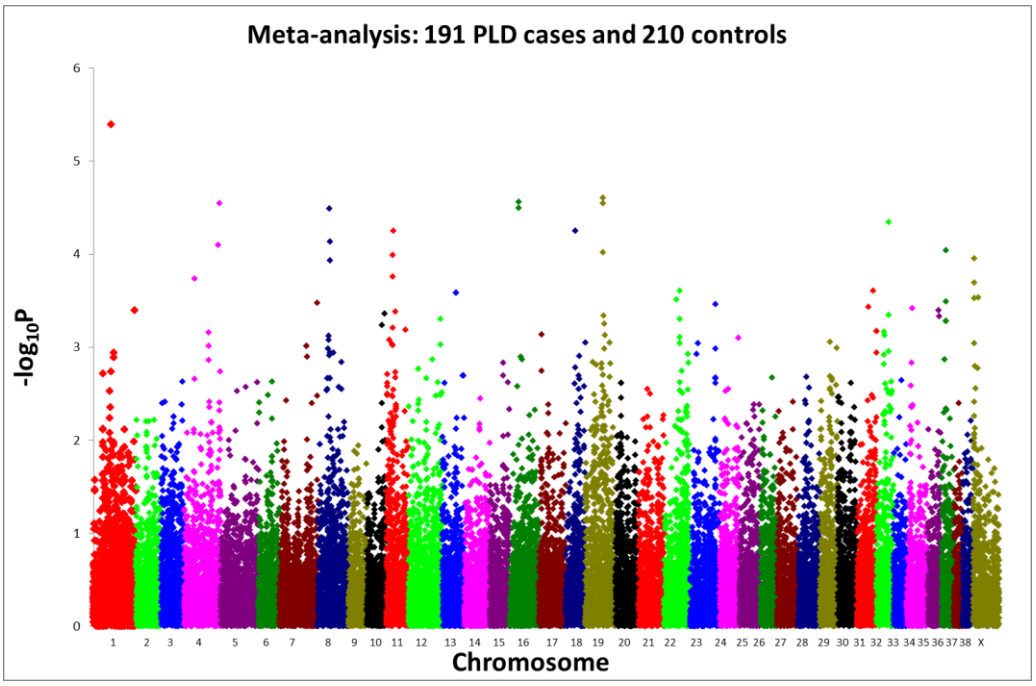

Figure 4.27. Manhattan plot meta-analysis across all four breeds demonstrating association of SNP markers with PLD.

4.2.2.5.4 PCAG cases and PLD cases

After filtering, 111 PCAG cases, 191 PLD cases and 37,467 SNPs remained. No SNPs reached genome-wide significance (**Figure 4.28**).

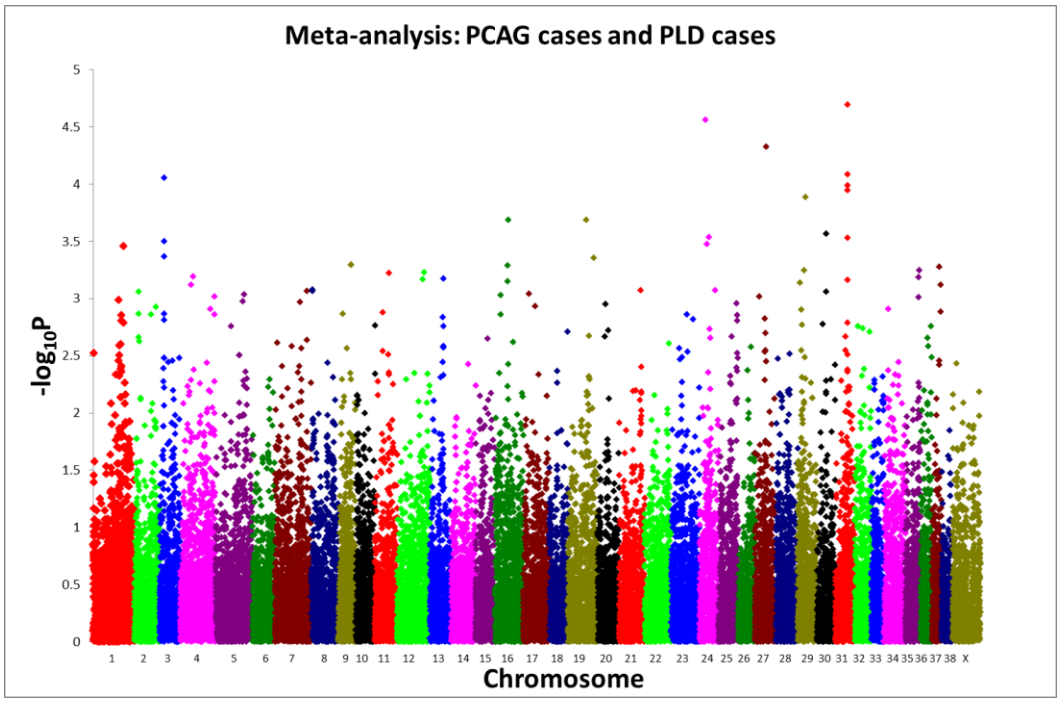

Figure 4.28. Manhattan plot of meta-analysis across all four breeds demonstrating association of SNP markers with PCAG relative to PLD.

4.2.2.5.5 PCAG cases and PLD cases and controls

After filtering, 111 PCAG cases, 401 PLD cases and controls and 37,726 SNPs remained for analysis. No SNPs reached genome-wide significance (**Figure 4.29**).

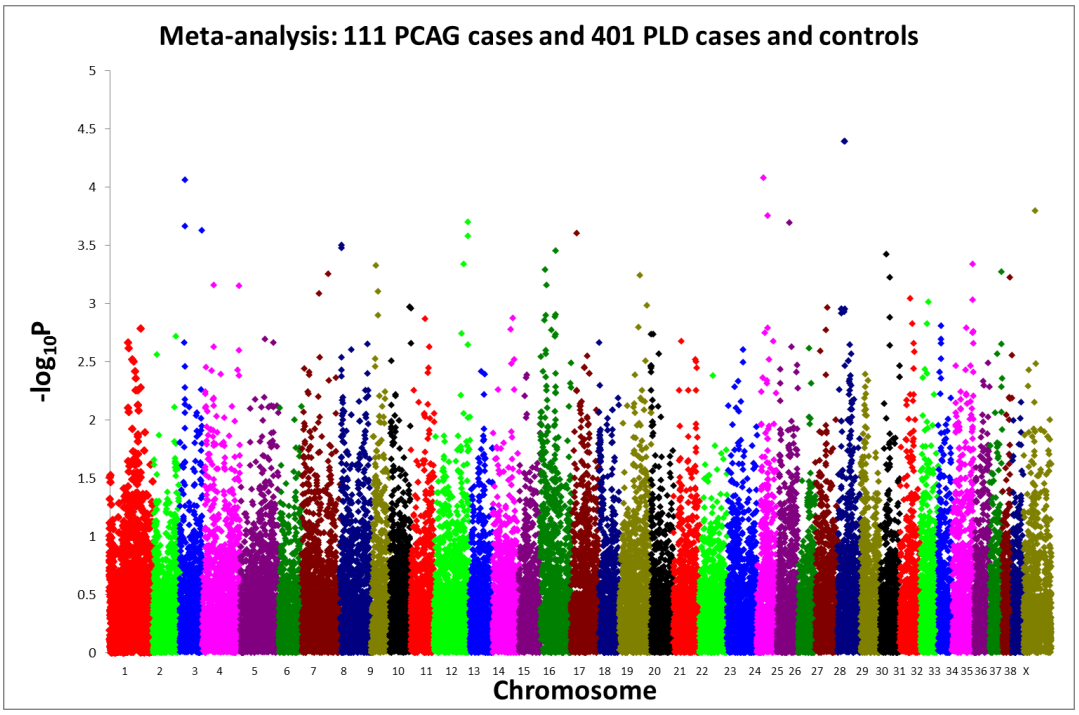

Figure 4.29. Manhattan plot of meta-analysis across all four breeds demonstrating association of SNP markers with PCAG relative to PLD cases and controls.

4.2.3 Discussion

In this series of studies, GWAS were performed in dogs of four different breeds with normal eyes, with PLD or with PCAG. In the BH, initial GWAS revealed two SNP markers on CFA24 to be significantly associated with PCAG. Analysis of sliding window haplotypes and permutations of these haplotypes corroborated these findings (**Figure A2** and **Figure A**). Conditional analysis using one of these SNP markers as a covariate revealed an additional SNP marker on CFA37 to be associated with PCAG in this breed. The GWAS findings were also supported by the fact that the strength of association of PCAG with these SNP markers increased when analysis was repeated with the addition SNP data from USA BH PCAG samples particularly for

BICF2G630505097 which was also the most strongly associated SNP in the original analysis. This SNP is located in an intergenic region (chr24:17,381,226) with *RNF24* (chr24:17,423,245-17,454,478) and *PANK2* (chr24:17,463,603-17,489,677) being the nearest upstream genes. These are potentially interesting candidate genes for PCAG as a previous study of a glaucoma-related trait in humans, optic nerve head morphology, revealed a significant linkage signal at the RNF24/PANK2 locus[206]. Further studies comparing optic nerve head morphology in dogs with normal eyes and those with PLD and/or PCAG are required however.

It was interesting that significant association of SNP makers with PCAG was found in the PCAG cases and PLD cases analysis and not in the PCAG cases and controls analysis. PLD is considered a consistent risk factor for, and therefore likely to be on the causal pathway to, canine PCAG[29,31-33]. Therefore, it is considered there are shared genetic factors between PCAG and PLD cases and significant association with disease (PCAG and/or PLD) would more likely be discovered when analysing PCAG and PLD cases combined with controls owing to the greater number of cases, and thus power, of such analysis. Instead, these studies revealed two loci which are significantly more common in PCAG cases than in both PLD cases and controls. This is not a completely unexpected finding, however, as, although PLD is a risk factor for PCAG, only a minority of dogs with PLD are thought to develop PCAG. It is thus likely that the two chromosomal loci identified are involved in the 'trigger' of progression from PLD to PCAG. It is considered that PLD is required for but not sufficient for PCAG, thus whether a dog develops PCAG will depend on its genotype at both the PLD locus and PCAG locus (or loci). It is possible that a similar (although admittedly likely more complex) scenario of genotypes illustrated in **Table 4.12** is present in the dog, where PCAG cases have both the PCAG and PLD risk alleles (homozygous or heterozygous depending on mode of inheritance), PLD cases have the PLD risk allele but not the

PCAG risk allele and controls may have a mixture of protective and risk alleles at both loci. In this situation, when SNP genotypes of PCAG cases and PLD cases are compared by GWAS, PCAG cases and PLD cases may be sufficiently different at the PCAG locus to detect a GWAS signal. When PCAG cases are compared with PLD cases and controls combined, there may only be a slight increase in GWAS signal intensity because controls have a mixture of risk and protective alleles at the PCAG locus. When PCAG cases or PLD cases and controls are compared, there may be insufficient power to detect a GWAS signal as the controls have a mixture of risk and protective alleles at both loci – presumably larger sample numbers would be required to detect a signal in this situation. This scenario may well explain the GWAS findings in the BH in which only PCAG loci, and not a PLD locus (or loci), were identified. The inability to detect GWAS signals in the other breeds could be explained by the presence of a greater number of PCAG loci in these breeds requiring greater sample numbers to provide sufficient power for locus detection.

Table 4.12. Simple model of genotypes at PLD and PCAG loci.

Phenotype	PLD locus genotype	PCAG locus genotype
PCAG cases	-	-
PLD cases	-	+
Controls	+ or -	+ or -

- denotes risk allele (homozygous or heterozygous depending on mode of inheritance), + denotes reference allele

The GWAS in the BH did not provide any evidence of association of PCAG with loci previously implicated in this phenotype in this breed. A previous study employing a GWAS of PCAG in USA BH reported two regions in association with PCAG following multiple hypothesis testing correction of raw P values by permutation[170]. These susceptibility loci were situated on CFA14 (chr14:19,911,001-20,161,358) and CFA24 (chr24:43,091,222-43,595,979) and contained the collagen gene *COL1A2* and oncogene *RAB22A* respectively. Five additional SNPs on five additional chromosomes were similarly associated with PCAG using the same permutation adjusted significance threshold but were not investigated because they were located in non-coding regions. The same investigators reported another study whereby they employed two-point and multipoint linkage analyses of genome-wide SNP data to identify a locus on CFA19 associated with PCAG in USA BH (including some dogs used in their previous GWAS). Using exome-sequencing analysis, a possibly damaging, non-synonymous variant in the Nebulin gene (*NEB*) was found to segregate with PCAG[171]. The data of this thesis do not corroborate the findings of these reports. The differences in susceptibility loci reported in USA BH may relate to their rarity in European BH. The difference in findings may also be partly explained by differing methodology employed. In the USA GWAS, population stratification was corrected using a MDS analysis and threshold for significance was set by permutation testing using 1,000 permutations. In the GWAS reported here, population stratification was corrected using the mixed model GEMMA and threshold for genome-wide significance was set using Bonferroni correction. Bonferroni is considered particularly stringent in the dog owing to the large LD in this species which provided reassurance of the reliability of the findings[207]. Finally, these data suggest that the reported *NEB* variant is a benign polymorphism.

Single breed GWAS in the other three breeds (FCR, DDT and WSS) did not reveal any significant association of SNP markers with either PCAG or PLD. The reason for this

likely relates to paucity of samples in light of the suspected complex nature of canine PCAG and PLD – PCAG in the BH may have a simpler genetic background than in the other three breeds. It is likely that multiple genetic, and possibly also environmental, factors are involved in canine PCAG and PLD[78]. The number of samples required for GWAS to be informative in locus identification depends on the inheritance pattern of the investigated trait. For complex traits in dogs, it has been predicted that a fivefold risk allele can be detected with 100 cases and 100 controls but a twofold risk allele would require approximately 500 cases and 500 controls to be identified[85]. Minimal numbers predicted to detect a fivefold disease risk allele were only achieved with meta-analysis of combined summarised GWAS data from the four breeds. In the meta-analysis, a significant association with PCAG was found on CFA28. The BH did not appear to contribute to the meta-analysis signal which complements the finding of the individual breed GWAS. It appears that BH PCAG associated loci are likely to be different to the other three breeds. The WSS and DDT breeds contributed the greatest to this signal with the top SNP in these two breeds being BICF2G630271568 (chr28:18,871,699) which maps to *SORCS1*. *SORCS1* is associated with amyloid deposition and has primarily been associated with Alzheimer's disease in humans[208-210]. Glaucoma in human has also been associated with amyloidosis and, thus, *SORCS1* may represent a promising candidate gene for canine PCAG[207,211,212].

A previous GWAS of PCAG in the DDT using 23 cases and 23 controls revealed a novel 9.5 Mb locus on CFA8 although level of association did not reach the Bonferroni threshold level of significance[106]. In this thesis, a larger sample cohort was used and no association of CFA8 SNP markers with PCAG in the DDT was found. Again, this could relate to the complex nature of PCAG and the presence of multiple causative genetic factors distributed at differing frequencies among populations. It is also interesting to note, that these GWAS did not support an association between PCAG or PLD with

ADAMTS17 in the WSS or any other breed. As it is known that this gene is well-captured by the CanineHD BeadChip, these results suggest that the association with *ADAMTS17* reported in **4.1.3.1** is unlikely to be true[107,122].

Following identification of susceptibility loci for PCAG, a NGS approach was used to identify variants associated with disease. The AHT has used this approach successfully before to identify variants responsible for single gene disorders[107,213,214]. WGS of PCAG-affected dogs (one from each of BH, FCR and DDT and three WSS) were used to perform breed-specific analyses using large numbers of WGS from control dogs to identify variants which segregated with disease in the loci defined by previous GWAS and subsequent analysis. All variants found using this approach were in non-coding regions and, as such, not immediately provocative as pathogenic. Having said this, intergenic and deep intronic variants are being increasingly recognised as having important gene regulatory functions in disease than previously thought[215,216]. Thus, perhaps the lack of discovery of an association of exonic variants with PCAG, which is thought to be complex, is unsurprising. However, all identified (non-coding) candidate variants, other than that identified in the FCR, were less strongly associated with PCAG than the relevant top SNP, making them unlikely to be pathogenic variants. Although it was disappointing not to find candidate variants for PCAG using this approach, it was not entirely unexpected. Similar to the dog, adult-onset forms of primary glaucoma in humans are inherited as complex traits[111]. Although GWAS have successfully identified genomic loci for PACG in humans using large case-control sets (thousands of individuals), as reported in this thesis in much smaller sets of canine samples, pathogenic variants remain elusive[169,217].

In parallel to the WGS-based PCAG approach, RNA-Seq data were used to attempt to elucidate candidate genes involved in PCAG in the BH. Similar to the candidate variant analysis, a targeted approach based on the loci identified as a result of GWAS was used.

Eight genes were found to be differentially expressed although, on the face of it, none of these appear to be obvious candidates for canine PCAG. Instead, all genes identified have functions related to inflammation and immunity. This finding was not completely unexpected. Jian et al. identified over 500 genes with statistically significant changes in expression level in the glaucomatous canine retina[218]. Genes with elevated expression were found to be largely associated with inflammation, such as antigen presentation, protein degradation, and innate immunity. Thus, it appears that the results reported here corroborate these findings and may contribute to an enhanced understanding of the molecular events that occur in canine eye with advanced primary closed angle glaucoma. Unfortunately, however, because intraocular inflammation is such a common finding in any canine eye with end-stage glaucoma (be it primary or secondary), traditional gene expression studies may be less helpful in helping understand the primary genetic aetiology of the disease having more power to detect 'effect' rather than 'cause'.

5 Primary open angle glaucoma: molecular investigation using a candidate gene approach in three dog breeds

5.1 Introduction

POAG is characterised by the presence of typical clinical signs of glaucoma, such as elevated IOP in the presence of an open ICA during the early stages of disease[72]. The only dog breed in which POAG has been extensively clinically characterised is the Beagle in which a laboratory colony was established and studied. In this breed, elevation of IOP is apparent before 12 months of age with other signs of glaucoma becoming apparent before 36 months of age[72]. In the clinical setting, however, dogs with POAG present much later than this and usually demonstrate advanced chronic clinical signs of glaucoma at the time of diagnosis. This late presentation is most likely explained by the chronic and insidious nature of the disease with affected dogs retaining some vision until very late in the disease process and without demonstrating signs of pain obvious to the owner.

During the course of gonioscopy screening sessions in BH (**Chapter 3**), two dogs with POAG were discovered – a form of glaucoma not previously reported in the breed. The AHT laboratory had also received DNA samples from a third BH and three BFdB dogs diagnosed with POAG and 21 SP dogs diagnosed with POAG and/or PLL, including 10 cases examined by myself. As discussed in **section 1.2**, differential diagnosis between PLL and POAG in the SP can be problematic and it is likely that there is only one breed-related condition in the SP, namely POAG which, in line with POAG in other breeds, leads to secondary buphthalmos and lens instability. To avoid confusion, and in line with the other two breeds, the phenotype in this breed will also be referred to as POAG hereafter, although it is acknowledged that a detailed clinical description of the phenotype in this breed is lacking.

In dogs, POAG is a relatively rare condition, although its high prevalence in specific breeds suggests an inherited aetiology. POAG has previously been reported in the Beagle and Norwegian Elkhound in which it is inherited as an autosomal recessive condition caused by two breed-specific mutations in *ADAMTS10*[68-70]. Further research in the Beagle has shown that the *ADAMTS10* mutation responsible for POAG is also associated with an inherently weaker and biochemically distinct posterior sclera before clinical evidence of optic nerve damage becomes apparent[124]. POAG in the Petit Basset Griffon Vendeen has recently been reported to be associated with a novel mutation in a closely related gene, *ADAMTS17,* and another mutation in this gene has been published as the cause of PLL in multiple breeds[74,122,123].

The specific objective of these studies was to interrogate *ADAMTS17* as a candidate gene for POAG in the BH, BFdB and SP. The ultimate aim of the studies was to develop and offer DNA tests for these breeds to reduce the prevalence of this painful and blinding disease. The data presented here have since been published[75,219] .

5.2 Materials and methods

5.2.1 Sample collection and DNA extraction

POAG was diagnosed by certified veterinary ophthalmologists in 3 BH (2 males, 1 female), 3 BFdB (1 male, 2 females) and 21 SP (11 females, 10 males) dogs. Thirteen of these dogs were examined by myself (2 BH and 10 SP). The mean age (± SD) of the POAG affected dogs was 49.3 ± 5.4 months (BH), 68.3 ± 12.7 months (BFdB) and 84.9 ± 8.9 months (SP). Inclusion criteria for dogs with POAG were; absence of an identifiable cause of secondary glaucoma, open ICA on gonioscopy in the clinically affected and/or contralateral eye (chronic corneal changes in the affected eye may preclude gonioscopy), elevated IOP (> 25 mmHg), buphthalmos and lens subluxation. A further 223 BH, 24 BFdB and 42 SP dogs underwent complete ophthalmic examination by myself and were all found to be free from all clinical signs of POAG as

described above. These dogs were at least 72 months of age at the time of examination and, in the absence of any signs of POAG, were considered suitable controls for subsequent genotyping experiments. The 223 clinically unaffected BH had a mean age of 52.0 ± 2.61 months, and 85 (38 %) were male and 138 (62 %) were female. The 24 clinically unaffected BFdB had a mean age of 124.38 ± 78.1 months, and 12 (50 %) were male and 12 (50 %) were female. The 42 clinically unaffected SP had a mean age of 93.5 ± 3.7 months, and 16 were male (38 %) and 26 (62 %) were female. DNA was extracted from buccal mucosal swabs from each dog as described in **section 2.2.1**.

5.2.2 *ADAMTS10* and *ADAMTS17* candidate variant genotyping

All POAG-affected BH, BFdB and SP dogs were genotyped for the two previously published *ADAMTS10* POAG-associated variants (Beagle and Norwegian Elkhound), the *ADAMTS17* POAG variant (Petit Basset Griffon Vendeen) and the *ADAMTS17* PLL variant (multiple terrier breeds) (details in **Table 5.1**) using primers and thermal cycling parameters as previously described[68,70,74]. Genotyping was performed in parallel for the BH and BFdB, but separately at a later date in the SP. As a result, in the SP, genotyping for the newly discovered BH and BFdB *ADAMTS17* POAG variants was also performed[75]. The SP project was initiated by colleagues, namely Sophie Rustidge and Louise Pettitt, who first identified the mutation in 10 affected dogs, after which the project was taken over by myself. Genotyping was performed using Sanger sequencing methodology as described in **section 2.2**.

5.2.3 *ADAMTS17* resequencing and sequencing data analysis

Primer pairs were designed to amplify the coding sequence and flanking splice sites for all 23 canine *ADAMTS17* exons using gene sequences derived from the Ensembl genome browser (ENSCAFG00000010709) (**Appendix IV**). This was performed in 3 affected and 3 unaffected BH, 3 affected and 3 unaffected BFdB and 10 affected and 5 unaffected SP. Genomic DNA was amplified using PCR with reaction components and

thermal cycling parameters as outlined in **Appendices II** and **III**. Illumina sequencing libraries were generated from the *ADAMTS17* exon as described in **section 2.2.10**. Read alignments (BAM files) were visualised and manually browsed for variants using IGV. The potential pathogenicity of non-synonymous variants was tested with the SIFT bioinformatics tool (http://sift.jcvi.org/)[220]. To demonstrate level of conservation relating to discovered variants, ADAMTS17 protein sequences were derived from the Ensembl genome browser (http://www.ensembl.org) and aligned using the Clustal Omega multiple sequence alignment tool (http://www.ebi.ac.uk/Tools/msa/clustalo/).

5.2.4 Genotyping of *ADAMTS17* candidate causal variants

Candidate causal variants were genotyped using one or more methods depending on the nature of the variant: AFLP, Sanger sequencing or allelic discrimination. Primers were designed to amplify the candidate causal variants using gene sequences derived from the UCSC genome browser (https://genome.ucsc.edu/)**.** PCR and thermal cycling reactions varied for each breed and are presented in **Appendix III**. The BH and SP deletion variants were genotyped by AFLP and the BFdB SNP variant by Sanger sequencing, as described in **section 2.2.12**. Additional genotyping of the BFdB SNP variant was performed by allelic discrimination, using primers and probes provided in **Appendix IV**, and as described in **section 2.2.12**[221]. Based on the entire genotyping data set for each breed, POAG association statistics for candidate variants were calculated using PLINK[178]. Mutant allele frequencies and the expected frequency of affected dogs (assuming the alleles were in Hardy-Weinberg equilibrium within the population) were determined for the BH and SP.

5.2.5 cDNA synthesis and sequencing

One POAG-affected BH and one POAG-affected SP underwent unilateral enucleation on welfare grounds. An additional dog (12 year old Golden Retriever) was euthanized for reasons unrelated to this study. Prior to euthanasia of this dog, a complete

ophthalmological examination (including gonioscopy and tonometry) was performed to rule out the presence of any clinical signs of POAG (or other inherited ocular disease), allowing the subsequently harvested ocular tissue to serve as (non-breed matched) control tissue. Ocular tissue was harvested and stored in RNA*later* (Ambion) at -80 ^{o}C. RNA was subsequently extracted from the tissues of the ICA and cDNA synthesised from the RNA as described in **section 2.3.2.2**. Primer pairs spanning each of the two breed-specific *ADAMTS17* mutations were designed using cDNA sequences derived from the Ensembl genome browser and Primer 3 (**Appendix IV**)[174,175,185,186]. Amplification of target regions of cDNA by PCR, PCR product purification and Sanger sequencing were performed as described in **section 2.2**. Sanger sequencing was performed for all four assays in the control dog's tissue (Golden Retriever) but only for the breed-relevant assays in the POAG-affected dogs' tissues. For the BH assays, Q solution was used in the PCR reaction (GC rich regions). This was replaced with MQ in the SP assays.

5.2.6 Quantitative reverse transcriptase PCR

cDNA synthesised in **5.2.5** was used for relative qRT-PCR to investigate *ADAMTS17* transcript expression in three technical replicates each of normal ocular tissue (Golden Retriever), POAG-affected SP ocular tissue and POAG-affected BH ocular tissue as described in **2.3.2.2**. *ADAMTS17* transcript expression was compared between normal tissue and affected tissue for the SP and BH separately. Assays were designed for the target *ADAMTS17* gene and for a ubiquitously expressed housekeeping gene (*TBP*) gene for comparison. Details of the designed assay are presented in **Appendix IV**.

5.3 Results

5.3.1 *ADAMTS10* and *ADAMTS17* variant genotyping

All POAG-affected BH, BFdB and SP dogs were homozygous for the wild type alleles at the chromosomal locations of all four previously published POAG/PLL-associated variants.

5.3.2 *ADAMTS17* resequencing

5.3.2.1 BH

Visual scanning of the sequence reads, aligned with CanFam3.1, from three clinically affected and three unaffected BH revealed only one variant that segregated with disease. This variant was a homozygous 19 bp deletion in exon 2 of *ADAMTS17* (CanFam3.1 chr3:40,614,853-40,614,872) and was confirmed by Sanger sequencing (**Figure 5.1**). This variant results in the loss of 19 coding nucleotides (c.193_211del), which in turn is predicted to shift the amino acid reading frame resulting in 87 aberrant amino acids before the introduction of a premature termination codon (p.Lys69GlyfsTer88).

Fifty clinically unaffected BH over the age of 72 months (controls) were genotyped for this allele by AFLP; all were homozygous for the wild type allele. Genotyping of 173 additional BH recruited for a different study and also known to be free of clinical signs of POAG, revealed 137 were homozygous for the wild type allele and 36 were heterozygous for the mutation. The frequency of the deletion in this subset of 223 BH was therefore 0.081 and the predicted frequency of affected dogs in the population estimated to be 0.007. One hundred and fifty-two dogs of unrelated breeds were all homozygous for the wild type allele. Following identification of this mutation, the owners of all affected dogs were contacted and pedigrees were obtained and reviewed. Analysis of these revealed two of the affected dogs to be full siblings although the third affected dog shared no common ancestors in its five generation pedigree. Taking into account the presence of the two full siblings, the association statistic between the deletion and POAG based on the entire genotyping dataset (two POAG affected and 220 unaffected) was $P = 1.26 \times 10^{-10}$.

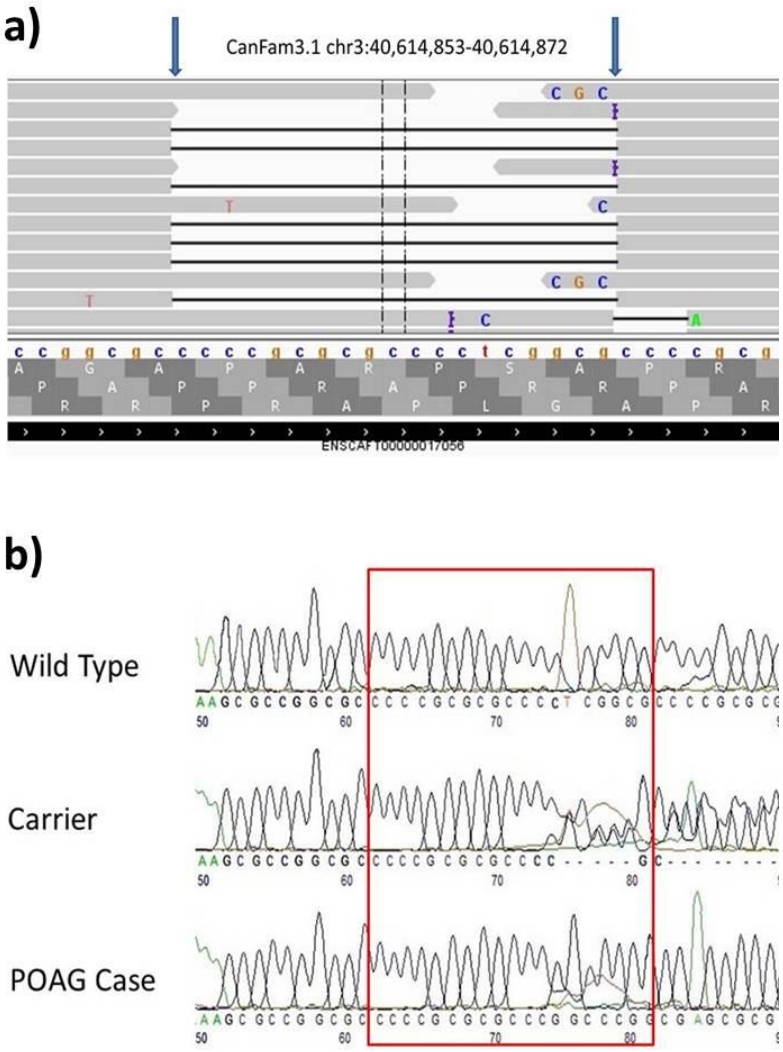

Figure 5.1. Next-generation and Sanger sequencing data depicting the site of 19bp deletion in a BH with POAG.

a) IGV view of the 19 bp deletion in a BH affected with POAG. The location of this homozygous deletion is chr3:40,614,853-40,614,872 (CanFam3.1). b) Electropherograms depicting the site of the deletion. The red box delineates the affected sequence in wild type, carrier and POAG-affected dogs.

5.3.2.2 BFdB

Visual scanning of the sequence reads, aligned with CanFam3.1, from three clinically affected and three clinically unaffected BFdB dogs revealed only one variant that segregated with disease - a homozygous G>A substitution in exon 11 of *ADAMTS17* (c.1552G>A; p.Gly519Ser) (CanFam3.1 chr3:40,808,345, **Figure 5.2**).

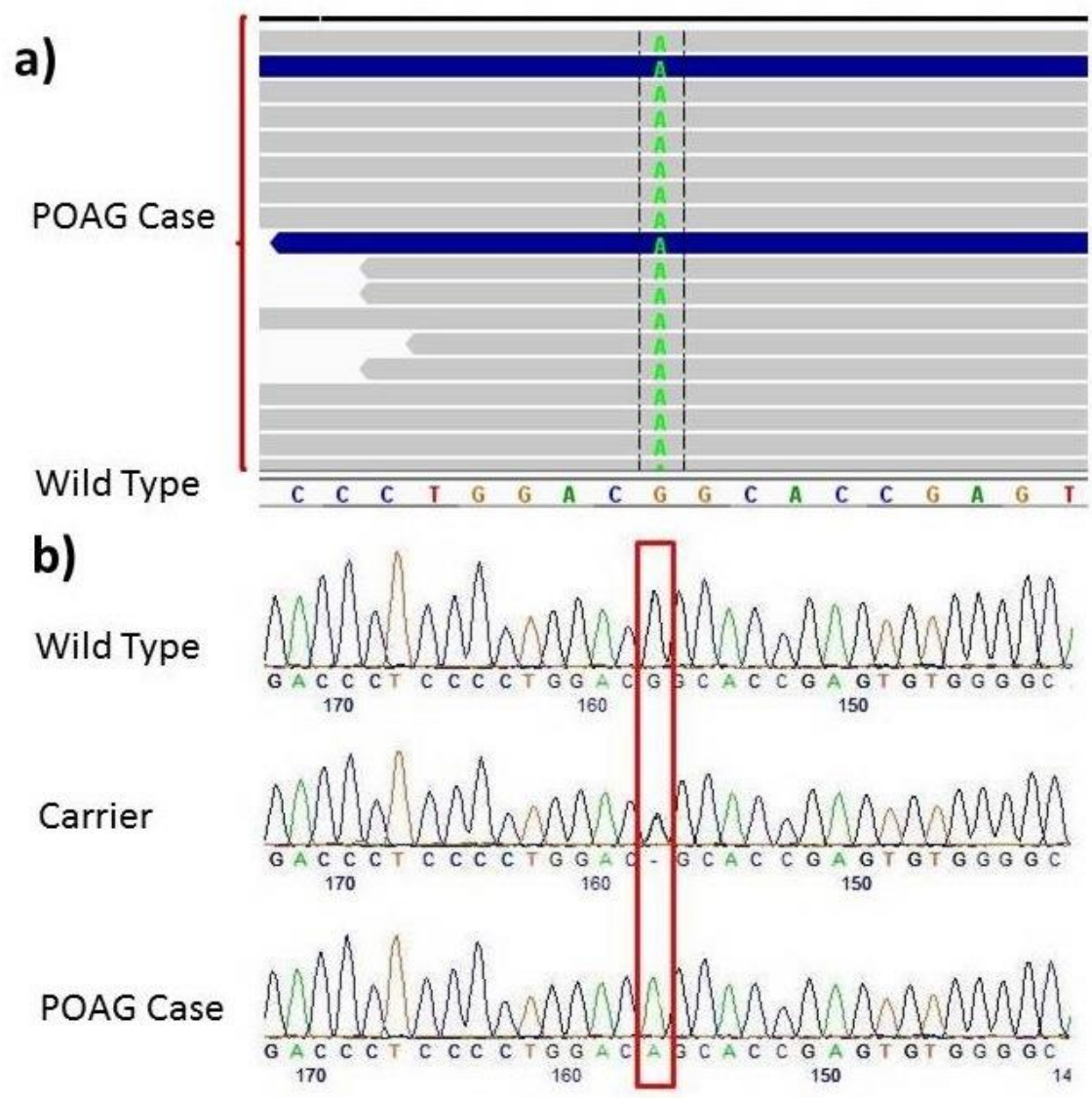

Figure 5.2. Next generation and Sanger sequencing results depicting the site of the SNP associated with POAG in BFdB.

a) Visualisation of the SNP in IGV. The localisation of this homozygous SNP is chr3:40,808,345 (CanFam 3.1). b) Electropherogram depicting the site of the SNP. The red box depicts the exact site of the mutation (CanFam3.1 chr3:40,808,345). At this location, the wild type is GG, the carrier is AG and the POAG case is AA.

All three affected BFdB dogs were homozygous for this non-synonymous SNP, which causes a glycine to serine (p.Gly519Ser) amino acid change in the disintegrin-like domain of ADAMTS17 and is predicted to be deleterious by SIFT[222]. Sequencing of 24 clinically unaffected BFdB dogs revealed five to be heterozygous for the mutation and

19 were homozygous for the wild type allele. The association statistic of the variant with POAG based on the entire genotyping dataset (three POAG affected and 24 unaffected) was $P = 2.80 \times 10^{-7}$. Genotyping of 85 dogs of unrelated breeds and 90 dogs of related breeds (BH, Standard Wire Haired Dachshund, Petit Basset Griffon Vendeen, Grande Basset Griffon Vendeen) for this variant with an allelic discrimination assay revealed them all to be homozygous for the wild type allele (**Figure 5.3** and **Figure 5.4**).

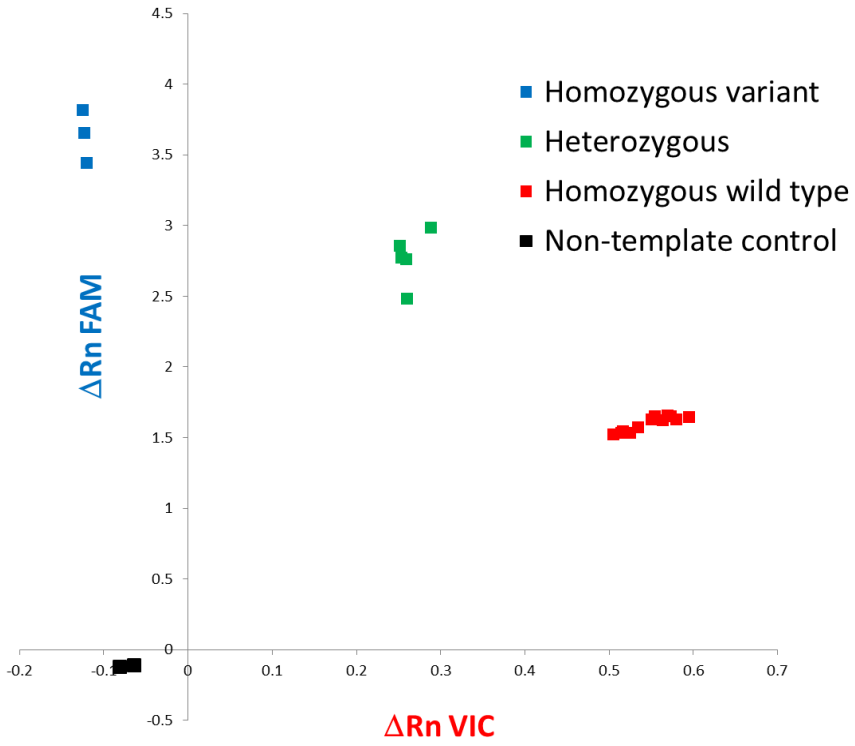

Figure 5.3. Allelic discrimination plot in BFdB dogs

Red squares indicate 10 BFdB dogs which are all homozygous for the wild type allele, blue squares indicate three BFdB dogs homozygous for the POAG variant and green squares indicate five heterozygous BFdB dogs. Black squares are non-template controls. The variant allele is detected by the relative intensity of VIC and the wildtype allele by the relative intensity of FAM. Rn = the normalised intensity of the reporter dye (FAM), ΔRn = Rn (post-PCR read) – Rn (pre-PCR read).

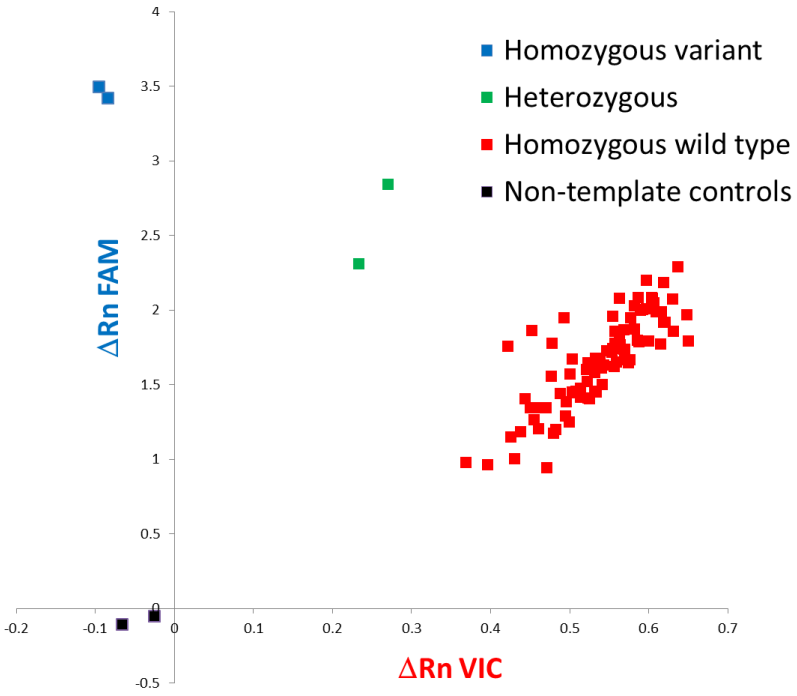

Figure 5.4. Allelic discrimination plot in affected, carriers and normal dogs

Red squares indicate dog of breeds related to BFdB which are all homozygous for the wild type allele, blue squares indicate two BFdB control dogs homozygous for the POAG mutation and green squares indicate two heterozygous BFdB control dogs. Black squares are non-template controls. The variant allele is detected by the relative intensity of VIC and the wildtype allele by the relative intensity of FAM. Rn = the normalised intensity of the reporter dye (FAM), ΔRn = Rn (post-PCR read) – Rn (pre-PCR read).

5.3.2.3 SP

Visual scanning of the sequence reads, aligned with CanFam3.1, revealed only one variant that segregated with disease in all 10 POAG-affected and 5 unaffected SP dogs. This variant was a homozygous 6 bp deletion in exon 22 of *ADAMTS17* (CanFam3.1 chr3:40,935,387-40,935,393) and was confirmed by Sanger sequencing (**Figure 5.5**).

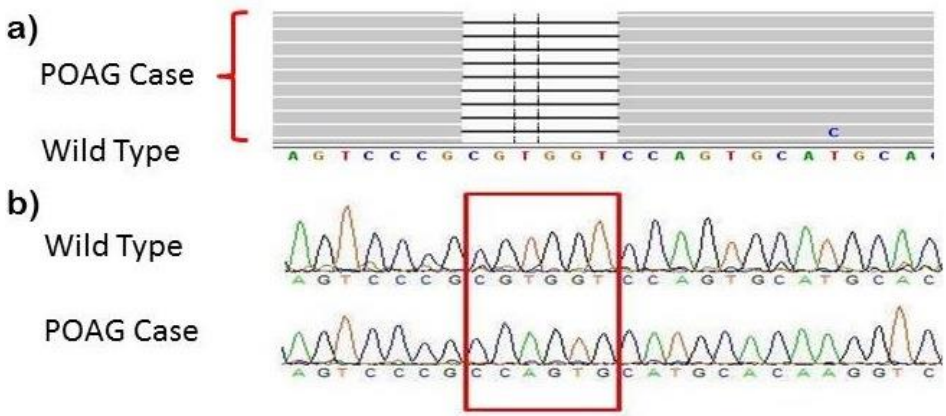

Figure 5.5. Next generation and Sanger sequencing results depicting the site of the 6bp deletion in the SP with POAG.

a) Visualisation of the 6 bp deletion in an affected dog in IGV. The location of this homozygous deletion is chr3:40,935,387-40,935,393 (CanFam3.1). b) Electropherograms depicting the site of the deletion. The red box delineates affected sequence in wild type and POAG-affected dogs.

The variant represents an inframe deletion (c.3070_3075del) and is predicted to result in the loss of two valine residues in the resultant polypetide, while the rest of the amino acid sequence remains unchanged (p.Val1024_Val1025del) (**Figure 5.6**).

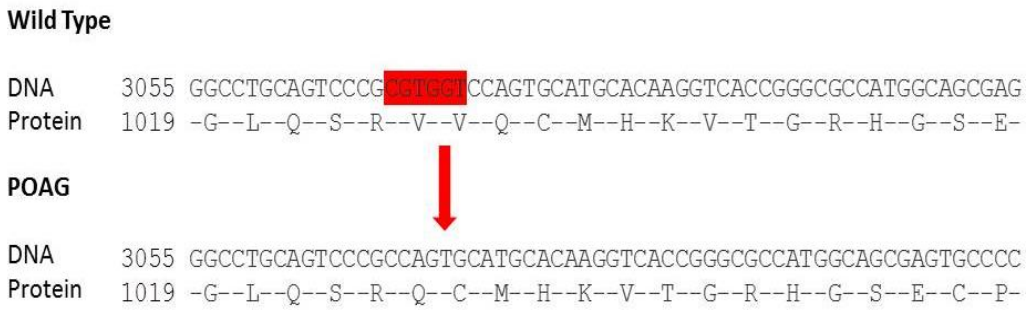

Figure 5.6. DNA and corresponding protein sequences in a normal SP (top) and one affected with POAG (bottom)

The 6 bases which are deleted are indicated by shading and the red arrow indicates the site of the deletion in the affected dog. The deletion is predicted to result in the loss of two valine residues in the resultant polypeptide.

A further 11 POAG-affected dogs were genotyped and were also found to be homozygous for the deletion. Forty-two clinically unaffected dogs over the age of 72 months (controls) were genotyped for this allele; all were either homozygous or heterozygous for the wild type. The association statistic between the deletion and POAG based on the entire genotyping data set was $P = 3.79 \times 10^{-14}$. Ninety five dogs of other breeds were all homozygous for the wild type allele. Since the discovery of this variant, genotyping of 100 further SP dogs without phenotype information has been performed which has enabled allele frequency within the breed to be calculated. Of these 100 dogs, 43 were homozygous for the wild type allele, 39 were heterozygous and 18 were homozygous for the mutant allele. This corresponds to a mutant allele frequency of 0.42.

5.3.3 cDNA sequencing results

cDNA sequencing was successfully achieved for all four primer pairs (two each for the 6 bp deletion in SP and the 19 bp deletion in BH) in the control dog's tissue and the relevant breed POAG-affected tissue. Visualisation of alignments in Staden confirmed the 6 bp deletion in the SP tissue, the 19 bp deletion in the BH and their absence in control tissue. This confirmed that both deletions were in coding genomic DNA and were transcribed into mRNA.

5.3.4 *ADAMTS17* expression analysis in the SP and BH

In the SP, mean ΔC_T was 3.76 for the case and 1.68 for the control providing a $\Delta\Delta C_T$ of 2.08. This corresponded to a 4.24 fold reduction in *ADAMTS17* expression in the case compared to the control ($P = 0.00063$) (**Figure 5.7**).

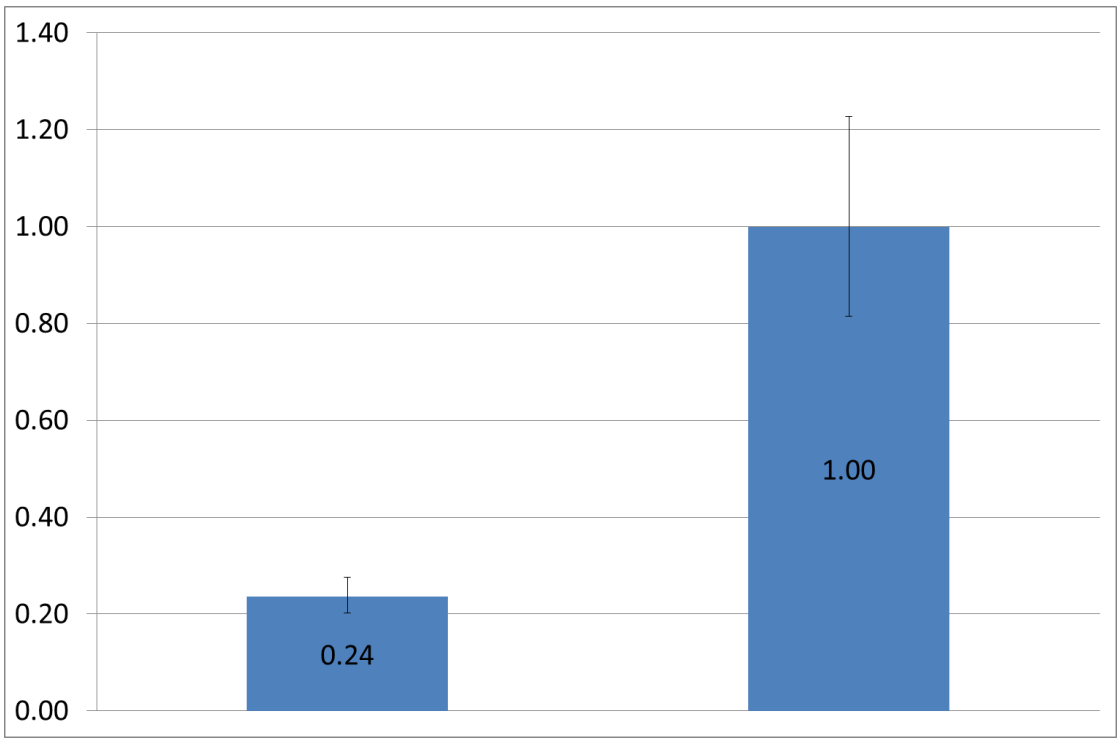

Figure 5.7. Histogram demonstrating a four-fold reduction in expression of ADAMTS17 transcript in ocular tissue from a SP POAG case compared to a Golden Retriever control. Error bars represent standard deviation.

In the BH, mean ΔC_T was 1.95 for the case and 1.68 for the control providing a $\Delta\Delta C_T$ of 2.08. This corresponded to a non-significant 1.21 fold reduction in *ADAMTS17* expression in the case compared to the control (P = 0.3).

5.4 Discussion

The objective of these studies was to investigate *ADAMTS17* as a candidate gene for POAG in three different dog breeds – the BH, BFdB and SP. *ADAMTS17* was considered a strong candidate gene for study for several reasons. Firstly, a different mutation in *ADAMTS17* has recently been reported to cause POAG in another dog breed by the AHT – the Petit Basset Griffon Vendeen[74]. Secondly, a different *ADAMTS17* mutation is known to cause another canine ocular phenotype, PLL, which is characterised by structural abnormalities and weakness of the lens zonular fibres with ultimate dislocation of the lens from the patellar fossa[122,123]. The ciliary body is not only

the site of origin of the lens zonular fibres and involved in their ongoing maintenance, but it also contributes to IOP. The ciliary body is both responsible for AH production and also forms the ciliary cleft via which AH is drained from the eye into the systemic circulation. It is also already known that *ADAMTS17* is expressed within the ciliary body[122]. Thus, with consideration, it would not be surprising for different mutations within this gene to be associated with multiple intraocular phenotypes relating to abnormal function of the same anatomical region of the eye[122]. Thirdly, *ADAMTS17* mutations cause Weill-Marchesani and Weill-Marchesani-like syndromes in humans[125,126]. These syndromes are rare connective tissue disorders which are characterised by various intraocular phenotypes including ectopia lentis, spherophakia, myopia and glaucoma along with joint stiffness and brachydactyly (**Table 5.1**). Clinical and genetic studies of these diseases suggest that *ADAMTS17* also plays a role in lens zonule and connective tissue formation in humans[125,126]. Finally, mutations in closely related genes, *ADAMTS10* and *ADAMTSL4*, are known to be involved in primary glaucoma and other ocular connective tissue disorders in both human and dog[68-70,124,125,132,144].

Table 5.1. Canine and human *ADAMTS17* mutations and their phenotypes

Species (breed or ethnicity)	Ocular phenotype	Systemic phenotype	Exon / intron	Mutation	Nature of mutation	State of zygosity	Reference
Previously identified							
Human (Saudi Arabian)	Lenticular myopia, ectopia lentis, spherophakia, glaucoma	Short stature	Exon 18	c.2458_2459insG p.Glu820GlyfsTer23	Frameshift	Homozygous	[125]
Human (Saudi Arabian)	Lenticular myopia, ectopia lentis, spherophakia	Short stature, brachydactyly, joint stiffness	Intron 12	c.1721+1G>A	Splice site	Homozygous	[125]
Human (Saudi Arabian)	Lenticular myopia, ectopia lentis, spherophakia,	Short stature	Exon 4	c.760C>T p.Gln254*	Nonsense	Homozygous	[125]
Human (Saudi Arabian)	Spherophakia	Short stature	Exon 4	c.652delG p.Asp218ThrfsTer41	Frameshift	Homozygous	[127]

Species (breed or ethnicity)	Ocular phenotype	Systemic phenotype	Exon / intron	Mutation	Nature of mutation	State of zygosity	Reference
Human (Tunisian)	Microspherophakia, myopia	Short stature, congenital ichthyosis	Exon 1-3	106.96 kb deletion	Deletion	Homozygous	[128]
Human (Indian)	Microspherophakia	Short stature, brachydactyly	Intron 5	c.873+1G>T	Splice site	Homozygous	[126]
Dog (multiple breeds)	PLL	None	Intron 10	c.1473G>A	Splice site	Homozygous	[122]
Dog (PBGV)	POAG	None	Intron 12	Large scale rearrangement	Inversion	Homozygous	[107]
Identified in present study							
Dog (BH)	POAG	None	Exon 2	c.193_211del p.Lys69GlyfsTer88	Deletion	Homozygous	[75]
Dog (BFdB)	POAG	None	Exon 11	c.1552G>A p.Gly519Ser	Missense	Homozygous	[75]
Dog (SP)	POAG	None	Exon 22	c.3070_3075del p.Val1024_Val1025del	Deletion	Homozygous	[219]

Although previous studies have implicated the importance of ADAMTS17 protein in mammalian intraocular physiology, its exact functions are unknown. ADAMTS17 (a disintegrin and metalloproteinase with thrombospondin type 1 motifs) is a member of a family of 19 known mammalian zinc-dependent metalloproteinases. Like other matrix metalloproteinases (MMPs), ADAMTSs have a role in ECM degradation and turnover as well as in proteolysis of cell surface and soluble proteins[223-225]. All ADAMTSs are secreted, extracellular enzymes that have a compound domain organisation comprising, from the amino terminus: a signal peptide followed by a pro-domain; a catalytic domain; and an ancillary domain that contains one or more thrombospondin type 1 repeats (**Figure 5.8**)[223,226]. The pro-domain, amongst other functions, maintains latency and directs proper folding of the enzyme. The catalytic domain is comprised of metalloproteinase and disintegrin-like modules and confers the protease activity of the protein. The ancillary domain determines substrate specificity, localisation of the protease and its interaction partners[126,223,226]. ADAMTS-like genes (*ADAMTSL*) encode proteins that resemble the ancillary domains of ADAMTS but lack their catalytic domains and it is thought that these proteins may modulate the activities of the ADAMTSs[225,226].

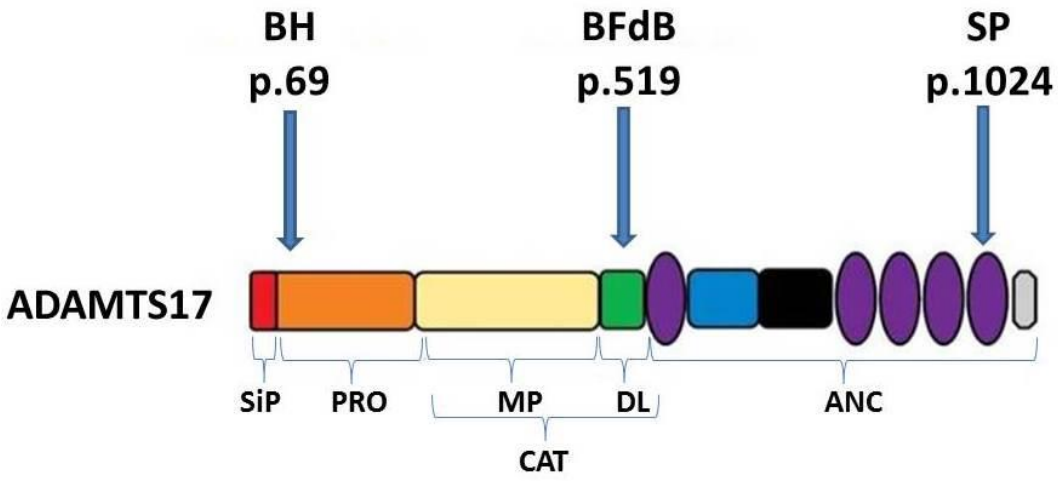

Figure 5.8. ADAMTS17 protein structure denoting amino acid positions of the BH, BFdB and SP POAG mutations

ADAMTS17 is composed of a signal peptide (SiP), prodomain (PRO), catalytic domain (CAT) (composed of the metalloproteinase (MP) and disintegrin-like domains (DL)) and an ancillary domain (ANC). The BH deletion corresponds to amino acid position (P) 65 which is located in PRO. The BFdB mutation corresponds to amino acid position 519 which is located in DL. The SP deletion corresponds to amino acid position 1024 which is located in ANC. Adapted from Kelwick et al.[223].

Although, the exact functions of ADAMTSs and ADAMTSLs are unknown, there is strong support of a functional association between ADAMTS proteins and fibrillin microfibrils. Mutations in *ADAMTS10*, *ADAMTS17* and *ADAMTSL4* result in phenotypes that resemble those caused by mutations in *fibrillin-1* (*FBN1*)[125,132,227-229]. It is thus suggested that ADAMTS and ADAMTSL proteins are involved either in microfibril assembly, stability and anchorage or the formation of function-specific supramolecular networks having microfibrils as their foundation[134]. How this functional relationship might be involved in POAG is unclear. The ECM of the trabecular meshwork is thought to be important in regulating IOP[21]. In response to elevated IOP, specific proteases including MMPs are thought to be released by trabecular meshwork cells and are activated to degrade selected ECM molecules, leading to decreased resistance to AH outflow[230,231]. Furthermore, ADAMTS4 mRNA levels increase in

response to increased IOP and recombinant ADAMTS4 increase outflow facility in human and porcine anterior segments[144]. Thus, loss of function mutations in genes which encode the proteins involved in ECM degradation are likely to be associated with elevated IOP and glaucoma.

Investigation of *ADAMTS17* as a candidate gene for POAG in the three breeds studied led to the discovery of three novel breed-specific POAG-associated mutations.

5.4.1 BH

In the BH, a homozygous 19 bp deletion in exon 2 was present in all POAG-affected dogs. The deletion is predicted to alter the reading frame of the gene, leading to 87 aberrant amino acids before introducing a premature stop codon at the 5' end of exon 3 (**Figure 5.9**), a predicted truncation of 86.1 % of the protein if the RNA is stable and not subjected to nonsense mediated decay. The observation from the ADAMTS17 transcript expression analysis that expression of the mutant transcript is not significantly different from the normal transcript suggests that nonsense-mediated decay does not occur. The truncated region of the protein includes the entire catalytic domain, which is expected to lead to complete loss of protein function. Unfortunately, it was not possible to directly demonstrate the presence of truncated protein (for example by Western blot) as sufficient ocular tissue was only available for RNA (and not protein) extraction.

Further supportive evidence for the deletion as the causative mutation of POAG in the BH was derived from genotyping. The genotyping cohort included 223 BH which had undergone complete ophthalmic examination and were found to be free from clinical signs of POAG at the time. Fifty of these were significantly older than the POAG cases and were thought to be at very low risk of developing POAG in the future. These dogs served as controls and none were found to be homozygous for the identified mutation. Genotyping of the entire cohort allowed calculation of carrier frequency within the

breed within the United Kingdom. These dogs were all resident in and distributed widely around the United Kingdom and DNA had been collected from them for a parallel study. They can therefore be considered a random cohort with respect to the current study and relatively representative of the BH population in the United Kingdom. The frequency of the mutant allele (0.081) and expected frequency of dogs affected with POAG (0.007) are fairly high.

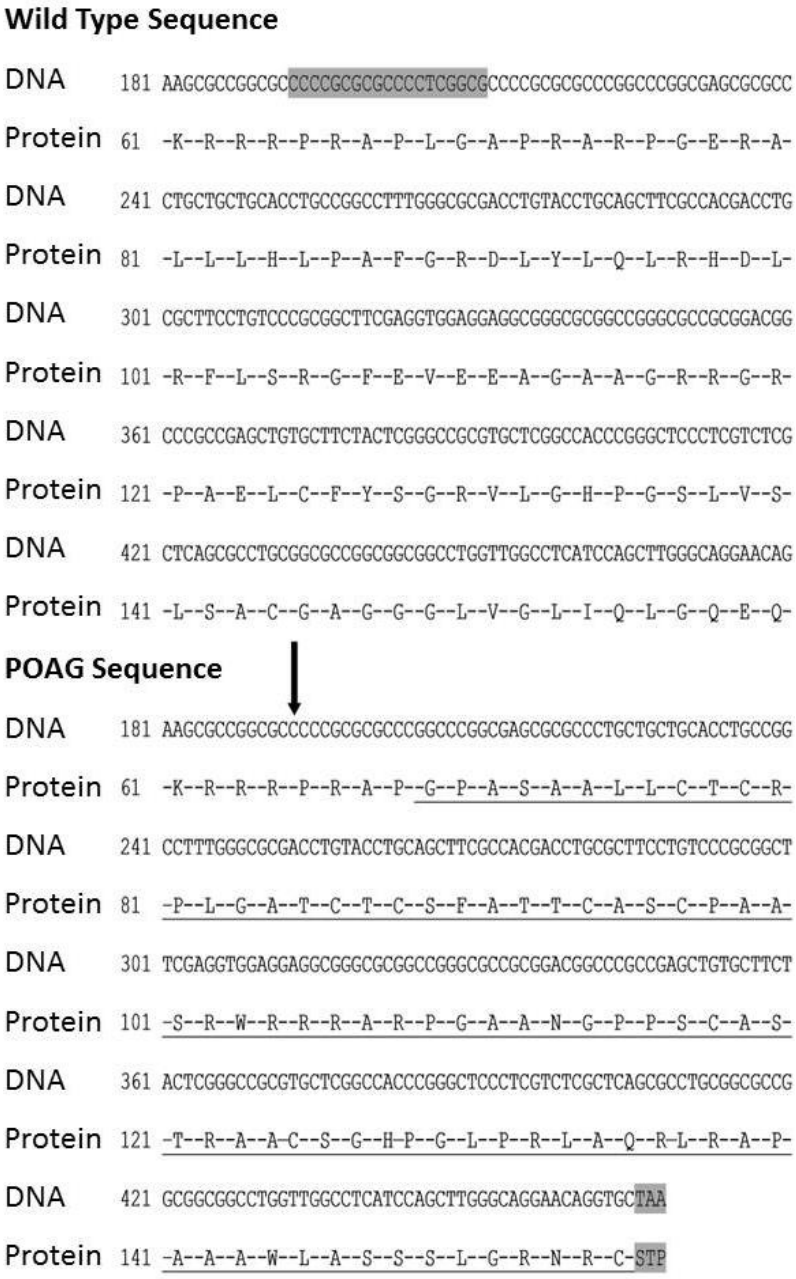

Figure 5.9. DNA and corresponding protein sequences in a normal BH and one with POAG.

The position of the deletion is indicated with a black arrow and the 19 deleted bases are indicated by shading in the DNA sequence of the normal (wild type) dog. The deletion generates a frame shift leading to 87 aberrant amino acids (underlined) before the introduction of a premature stop codon, indicated by shading in the POAG-affected dog.

5.4.2 BFdB

In the BFdB, the p.Gly519Ser variant identified to be associated with POAG corresponds to the disintegrin-like domain of ADAMTS17 which is essential for the catalytic function of the protein (**Figure 5.8**)[223]. This glycine is a highly conserved residue within the disintegrin-like domain across the entire ADAMTS family and also across species (**Figure 5.10** and **Figure 5.11**), providing strong evidence that this SNP is causal for POAG in this breed. Furthermore, 85 dogs of unrelated breeds and 90 dogs of related breeds were all homozygous for the wild type allele indicating that this variant is not a common polymorphism within the wider canine population. Owing to the lack of a sufficiently large cohort of randomly selected dogs, it was not possible to estimate the mutant allele frequency within the BFdB population.

ADAMTS1	Pro-Trp-Ala-Asp-Gly-Thr-Ser-Cys-Gly
ADAMTS2	Pro-Pro-Leu-Asp-Gly-Thr-Met-Cys-Ala
ADAMTS3	Pro-Pro-Leu-Asp-Gly-Thr-Met-Cys-Ala
ADAMTS4	Pro-Trp-Ala-Asp-Gly-Thr-Pro-Cys-Gly
ADAMTS5	Pro-Ala-Val-Glu-Gly-Thr-Pro-Cys-Gly
ADAMTS6	Pro-Ala-Ala-Glu-Gly-Thr-Leu-Cys-Gln
ADAMTS7	Ala-Ala-Val-Asp-Gly-Thr-Atg-Cys-Gly
ADAMTS8	Pro-Trp-Ala-Asp-Gly-Thr-Glu-Cys-Gly
ADAMTS9	Pro-Trp-Ala-Asp-Gly-Thr-Glu-Cys-Glu
ADAMTS10	Pro-Ala-Ala-Glu-Gly-Thr-Leu-Cys-Gln
ADAMTS12	Ala-Ala-Ala-Asp-Gly-Thr-Gln-Cys-Gly
ADAMTS13	Pro-Leu-Leu-Asp-Gly-Thr-Glu-Cys-Gly
ADAMTS14	Pro-Pro-Leu-Asp-Gly-Thr-Glu-Cys-Ala
ADAMTS15	Pro-Trp-Ala-Asp-Gly-Thr-Ser-Cys-Gly
ADAMTS16	Pro-Ala-Ala-Glu-Gly-Thr-Ile-Cys-Gly
ADAMTS17	Pro-Pro-Leu-Asp-Gly-Thr-Glu-Cys-Gly
ADAMTS18	Pro-Ala-Ala-Glu-Gly-Thr-Val-Cys-Gly
ADAMTS19	Pro-Pro-Met-Asp-Gly-Thr-Asp-Cys-Asp
ADAMTS20	Pro-Pro-Ala-Asp-Gly-Thr-Asp-Cys-Gly

Figure 5.10. A selected region of the amino acid sequence of the disintegrin-like domain in the entire ADAMTS family in dogs

The region is centred on the glycine residue (in red) which is highly conserved and is the site of the missense mutation in the BFdB.

Dog	Asp-Pro-Pro-Leu-Asp-Gly-Thr-Glu-Cys-Gly-Ala
Panda	Asp-Pro-Pro-Leu-Asp-Gly-Thr-Glu-Cys-Gly-Ala
Ferret	Asp-Pro-Pro-Leu-Asp-Gly-Thr-Glu-Cys-Gly-Ala
Cat	Asp-Pro-Pro-Leu-Asp-Gly-Thr-Glu-Cys-Gly-Ala
Horse	Asp-Pro-Pro-Leu-Asp-Gly-Thr-Glu-Cys-Gly-Ala
Microbat	Asp-Pro-Pro-Leu-Asp-Gly-Thr-Glu-Cys-Gly-Ala
Megabat	Asp-Pro-Pro-Leu-Asp-Gly-Thr-Glu-Cys-Gly-Ala
Cow	Asp-Pro-Pro-Leu-Asp-Gly-Thr-Glu-Cys-Gly-Ala
Sheep	Asp-Pro-Pro-Leu-Asp-Gly-Thr-Glu-Cys-Gly-Ala
Dolphin	Asp-Pro-Pro-Leu-Asp-Gly-Thr-Glu-Cys-Gly-Ala
Alpaca	Asp-Pro-Pro-Leu-Asp-Gly-Thr-Glu-Cys-Gly-Ala
Guinea Pig	Asp-Pro-Pro-Leu-Asp-Gly-Thr-Glu-Cys-Gly-Ala
Kangaroo Rat	Asp-Pro-Pro-Leu-Asp-Gly-Thr-Glu-Cys-Gly-Ala
Mouse	Asp-Pro-Pro-Leu-Asp-Gly-Thr-Glu-Cys-Gly-Ala
Rat	Asp-Pro-Pro-Leu-Asp-Gly-Thr-Glu-Cys-Gly-Ala
Squirrel	Asp-Pro-Pro-Leu-Asp-Gly-Thr-Glu-Cys-Gly-Ala
Rabbit	Asp-Pro-Pro-Leu-Asp-Gly-Thr-Glu-Cys-Gly-Ala
Vervet-AGM	Asp-Pro-Pro-Leu-Asp-Gly-Thr-Glu-Cys-Gly-Ala
Macaque	Asp-Pro-Pro-Leu-Asp-Gly-Thr-Glu-Cys-Gly-Ala
Gorilla	Asp-Pro-Pro-Leu-Asp-Gly-Thr-Glu-Cys-Gly-Ala
Human	Asp-Pro-Pro-Leu-Asp-Gly-Thr-Glu-Cys-Gly-Ala
Chimpanzee	Asp-Pro-Pro-Leu-Asp-Gly-Thr-Glu-Cys-Gly-Ala
Gibbon	Asp-Pro-Pro-Leu-Asp-Gly-Thr-Glu-Cys-Gly-Ala
Tarsier	Asp-Pro-Pro-Leu-Asp-Gly-Thr-Glu-Cys-Gly-Ala
Mouse Lemur	Asp-Pro-Pro-Leu-Asp-Gly-Thr-Glu-Cys-Gly-Ala
Bushbaby	Asp-Pro-Pro-Leu-Asp-Gly-Thr-Glu-Cys-Gly-Ala
Sloth	Asp-Pro-Pro-Leu-Asp-Gly-Thr-Glu-Cys-Gly-Ala
Armadillo	Asp-Pro-Pro-Leu-Asp-Gly-Thr-Glu-Cys-Gly-Ala
Lesser Hedgehog Tenrec	Asp-Pro-Pro-Leu-Asp-Gly-Thr-Glu-Cys-Gly-Ala
Hyrax	Asp-Pro-Pro-Leu-Asp-Gly-Thr-Glu-Cys-Gly-Ala

Figure 5.11. A selected region of the amino acid sequence of the disintegrin-like domain of ADAMTS17 in 31 species

The region is centred on the glycine residue (in red) which is highly conserved and is the site of the missense mutation in the BFdB.

5.4.3 SP

In the SP, a 6 bp deletion in exon 22 of *ADAMTS17* was significantly associated with POAG. This represents an inframe deletion and is predicted to result in the loss of two valine residues in the ancillary domain of the resultant protein. These two valine residues are highly conserved across species (**Figure 5.12**) and mutations affecting this domain have already been shown to be strongly associated with ectopia lentis and other ocular phenotypes in humans[125,223,232]. Further evidence in support of this mutation as causative of POAG in the SP is derived from the significant four-fold reduction in

ADAMTS17 mRNA expression in affected ocular tissue and from the fact that the mutation was not found in 95 dogs of other breeds.

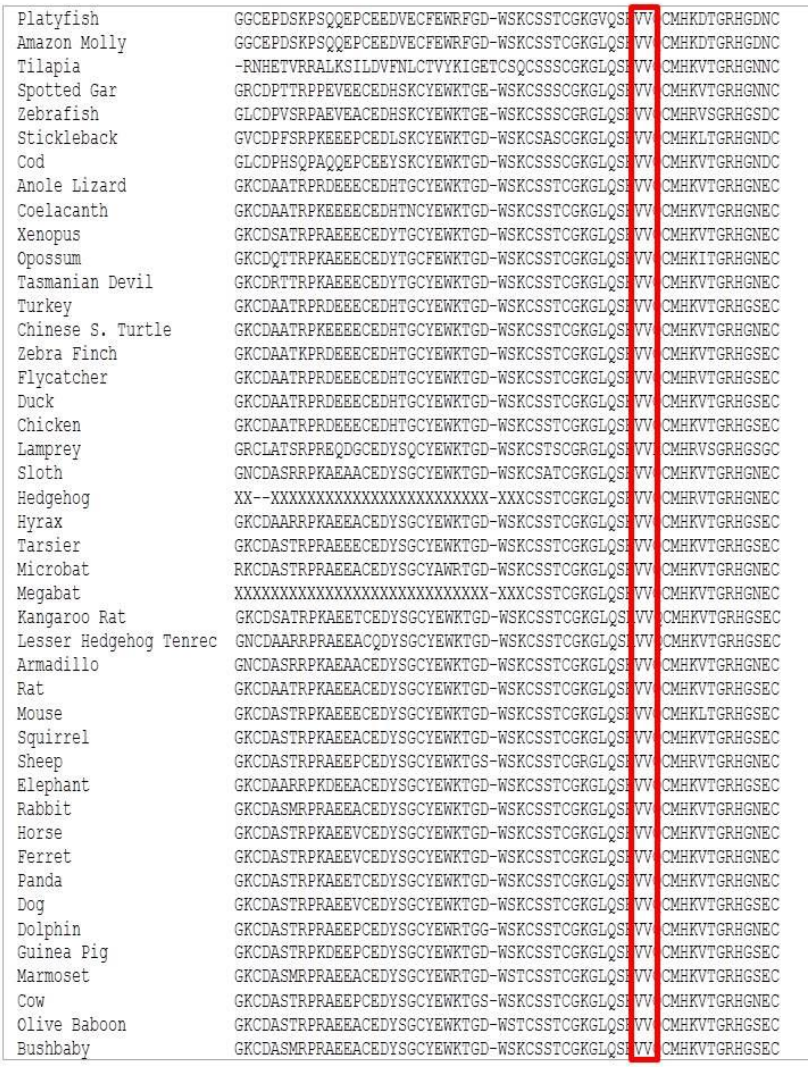

Figure 5.12. A selected region of the amino acid sequence of the ancillary domain of ADAMTS17 in 44 species.

The two valine residues (delineated in red) predicted to be removed by the 6 bp deletion in the POAG-affected SP are highly conserved.

5.4.4 DNA Testing for POAG

The ultimate aim of these studies was to develop DNA tests for POAG for those breeds in which disease-associated variants were discovered, and make these tests available to breeders. Level of interest in DNA testing varied between breeds but was sufficient for

the BH and SP to justify development and provision of these diagnostic tools. The DNA tests should have multiple benefits:

- DNA tests will allow for identification of genetically affected young dogs which have not yet developed POAG. This will allow for longitudinal clinical monitoring of these dogs for early signs of clinical disease which will allow improved phenotypic characterisation of the disease and facilitate understanding of POAG pathogenesis.
- Monitoring of genetically affected dogs for early signs of disease will also allow earlier medical and/or surgical intervention which may improve the prognosis for vision although, as yet, the most appropriate treatment remains unknown.
- DNA tests will also enable breeders to eliminate this painful and blinding disease from their breeds over time, whilst allowing them to judiciously breed with carriers which may have desirable inherited characteristics which it would be advantageous to retain.
- The ability to safely breed with carriers will also avoid the detrimental loss of genetic diversity in these breeds.

5.5 Conclusion

Three separate mutations in *ADAMTS17* are reported that are all strongly associated with the same ocular phenotype, POAG, in three different dog breeds. In all three breeds, and in line with all other previously reported canine *ADAMTS17* mutation-associated phenotypes, POAG appears to be an autosomal recessive condition. This study provides further evidence of the importance of ADAMTS17 in intraocular physiology and increases the total number of reported canine *ADAMTS17* mutations to five (**Table 5.1**). Further work, however, is required to understand how ADAMTS17 is involved in POAG pathogenesis.

6 General discussion and future perspectives

This study was conceived with three main aims:

1. To provide robust and current PLD prevalence data for seven dog breeds known to be affected by PLD and PCAG.

2. To investigate the genetic basis of PLD and PCAG in four dog breeds.

3. To investigate the genetic basis of POAG in three dog breeds.

Although the results of these studies have already been discussed in the relevant chapters, some further discussion of the most significant findings and future possibilities for research is warranted.

6.1 Prevalence of PLD

The prevalence of PLD in seven breeds known to be affected by PLD and PCAG has been published in three separate publications[45,46,192]. These data will aid breed clubs and veterinary health schemes in future surveillance of this abnormality and be informative of the benefit of screening for PLD prior to breeding. Previous PLD prevalence data had only been published for the FCR some 20 years ago and the current data suggest that the widespread use of gonioscopy testing in this breed has been very successful in reducing PLD (and possibly PCAG) prevalence in this breed[32]. The PLD data have also influenced the stance of the BVA/KC/ISDS Eye Scheme, with regard to recommendations regarding the necessity to perform gonioscopy in certain breeds, the frequency of gonioscopy eye testing and how PLD could be better graded than the existing system.

Perhaps, the most interesting finding of the investigations into PLD prevalence relates to evidence for PLD progression. In six of the seven breeds studied, there was significant association of PLD with age and it was also possible to show that PLD is progressive in > 50 % of individual dogs of a single breed. These findings corroborated those of Pearl et al. who reported PLD progression in 40 % of individual FCR[35]. The mechanisms by which an abnormality, previously considered to be congenital and static, can undergo significant progressive change in certain dogs are unknown but will be of important research interest for the future and will likely explain why only a minority of dogs with PLD go on to develop PCAG. If the underlying genetic variants which differentiate dogs with static PLD from those which develop PCAG can be determined, this would allow for accurate identification of at risk individuals and their elimination from the breeding population whilst, at the same time, allowing dogs with PLD but without the genetic risk factors for PCAG, to be used for breeding and therefore maintain genetic diversity. The genetic investigations of PCAG and PLD in the BH revealed two loci to be associated with PCAG but not PLD. These loci may harbour the genetic factors that separate static and progressive PLD although a separate GWAS to compare these two phenotypes (static and progressive PLD) would be required to demonstrate this.

To further understand the mechanisms underlying PLD progression, a better characterisation of the phenotype of PLD and the deeper changes that occur within the ciliary cleft is needed. Gonioscopy only permits visual evaluation of the ICA and, if PLD is extensive, not even the anterior ciliary cleft can be examined. Although PLD is considered a risk factor for PCAG, it is likely that other anatomical and physiological components of the AH outflow pathways are at least involved or may be causative of PCAG itself. Serial characterisation of the AH outflow pathways of large numbers of individual dogs by digital photography, high resolution ultrasound biomicroscopy

and/or ocular computed tomography should shed light on the chronological changes in those eyes which demonstrate PLD progression and develop PCAG. Furthermore, it is not yet known if congenital PLD differs from adult progressive PLD. To investigate this, histological studies of numerous dogs of different ages would need to be performed, however, such studies are unlikely to be performed as they would be impractical, expensive and unethical.

A possible mechanism which may explain progressive changes in the AH outflow pathways may relate to abnormalities in maintenance and turnover of the ECM. As discussed in **1.1.2.1**, the ECM is critical in providing resistance to AH outflow and IOP regulation and, thus, any changes in its formation, processing or molecular interactions may play important roles in the pathogenesis of glaucoma. The research presented in this thesis, and the work of others, have shown highly significant associations of *ADAMTS10* and *ADAMTS17* with canine POAG. These genes encode enzymes involved in ECM degradation and turnover and loss of function mutations in these genes is thought to play a role in IOP elevation and glaucoma development. These canine POAG genes, and related genes, would make logical candidates for canine PCAG and, indeed, the microsatellite-association work provided some limited evidence of association of *ADAMTS17* with this phenotype.

6.2 Genetic investigations of PLD and PCAG

6.2.1 Limitations of GWAS

PCAG is considered complex, likely involving multiple genetic, and possibly environmental, factors. GWAS were used to identify chromosomal loci associated with PCAG and PLD and the findings are likely to prove to be significant breakthroughs for PCAG, paving the way for other techniques to explore these regions for candidate causal variants and genes. GWAS have been used extensively over the last decade to

improve the understanding of the genetic basis of many complex traits by revealing associated susceptibility loci. This has provided invaluable insights into the allelic architecture of many multifactorial traits. In humans, GWAS typically involves thousands of subjects whereas, in the dog, much more modest samples numbers are used because many fewer canine samples are required to detect significant association compared to human studies, owing to the extensive LD, and also owing to financial constraints and difficulty in case and control collection[85]. A study by Bianchi et al. demonstrated how GWAS can be used with relatively modest sample numbers to detect associations with complex canine disease[207]. They investigated canine hypothyroidism – a complex clinical disease thought to be caused by a combination of genetic and environmental factors. They first performed GWAS in three individual breeds: Hungarian Vizslas (n = 74), Rhodesian Ridgebacks (n = 95) and Gordon Setters (n = 165). Association with disease was found within the same locus for each breed although, admittedly, Bonferroni significance was only reached for the largest (Gordon Setter) study. Subsequent meta-analysis of summary data from these three studies was used extremely effectively to increase the power of the individual GWAS and confirm the associated shared locus which reached Bonferroni significance. Some interesting comparisons can be made between this and the GWAS studies reported in this thesis. The GWAS reported herein also resulted in some significant and promising findings using very modest numbers. In the BH, two loci were found to be associated with PCAG relative to PLD using a total of only 81 samples (24 PCAG cases and 57 PLD cases) and level of association was increased when combining controls with the PLD cases (a total of 118 samples). It was not possible to show significant association with PCAG in the other individual breed analyses using similar sample numbers. This likely relates to an increased complexity of PCAG in these breeds with the small sample sizes used being too modest to provide sufficient statistical power for detecting small genetic

effects. This is particularly true if the risk variant is a rare allele with a small OR[233]. In human studies, when the causal SNP is rare (MAF < 10 %), a sample size of 3,000 may still be underpowered to detect small genetic effects[234]. For complex traits in canine GWAS, approximately 100 cases and 100 controls are required to detect a five-fold risk allele and 300 cases and 300 controls to detect a two-fold risk allele[85,103]. Although these studies suggest that the GWAS reported here were underpowered for the most part, sample numbers compare favourably to other canine GWAS for complex disease (including those for PCAG) that have also used modest sample numbers and have reported significant findings[106,170,235,236]. Evidence for the negative impact small sample size had on the GWAS reported here, comes from the meta-analysis in the DDT and WSS. No association with PCAG was found in the GWAS of PCAG cases and controls in either breed in the individual breed analyses using 83 DDT and 69 WSS. However, when summary data from these analyses were meta-analysed (152 samples), significant association with disease was discovered revealing a shared locus for PCAG in the DDT and WSS. Thus, similar to that of Bianchi et al., the meta-analysis approach reported here improved power to detect association of disease risk. Further samples will be genotyped in the future, in the hope that significant associations can also be shown for individual breed GWAS in the FCR, WSS and DDT.

Current GWAS may also have insufficient power to detect true association of SNP variants with disease by virtue of design. In humans, because > 10 million common genetic variants are likely to exist in the human genome, and only around 500,000 variants are genotyped in individuals in GWAS, only a fraction of all genetic variants is being studied[237]. In the GWAS presented, the SNP array used contained 172,115 SNPs which have a mean spacing of 13 kb which, although would be sufficient for studies in single gene diseases, would have much less power to detect associations with diseases caused by multiple genetic variants in particular where sample sizes are small and there

is variable or poor tagging of causal variants[85,103]. Hayward et al. showed, by using simulation studies, that reducing the mean SNP marker spacing in canine GWAS to 2 kb resulted in a significant increase in power for detecting moderate effect loci and, thus, the availability of denser canine arrays will improve the power of GWAS to detect associations with complex disease[238]. The most recent Illumina CanineHD BeadChip contains over 220,000 SNP markers to improve density across breeds, fill in gaps and replace poorly tagged coding variants. Furthermore, ThermoFisher Scientific has recently launched a canine genotyping array containing over 670,000 variants equally distributed across the chromosomes. Future work is needed, however, to assess what level of increased power is actually afforded with the use of these new arrays.

Another important potential limitation of GWAS is the possibility of false positive associations of tested SNPs with disease. In human GWAS, nearly 500,000 SNPs are commonly scored and, even if there is no true association of any of these SNPs with disease, it is still common for some of the statistical tests performed to offer P-values of the order of 10^{-6}, and the inference of false positive association with disease. False positive calls may be less of a problem in canine GWAS, in which many fewer SNPs tend to be studied (in the region of 90,000 SNPs were used in the GWAS reported in this thesis). Also, to reduce the possibility of false positives in the GWAS, Bonferroni correction was used which is considered a particularly stringent means of correction for canine GWAS and perhaps, if anything, is more likely to result in false negative calls[207,239]. Confirmation of true association of SNPs with disease risk, however, is best achieved by replication studies but this is often not possible, particularly in dogs, owing to the lack of adequate numbers of samples in a given population.

6.2.2 Imputation

Given the modest sample numbers combined with the stringent method of correction used in the reported GWAS, false negative calls are very likely to have been

experienced. Imputation has been used in human studies to reduce the possibility of false negative calls. Imputation has now become an essential tool in the analysis of human GWAS and allows geneticists to accurately evaluate the evidence for association at genetic markers that are not directly genotyped[237]. Genotype imputation has been used widely in the analysis of GWAS to boost power, fine-map associations and facilitate the combination of results across studies using meta-analysis[240]. Imputation exploits the correlated structure of genomic variation to impute (predict) genotypes at missing sites and to then test for association with both observed and unobserved imputed SNPs[241]. Imputation may, therefore, allow GWAS to reveal associations with disease at loci which would otherwise go undetected. This is because, in GWAS, the association of SNPs with disease risk will be weakened by any departure from perfect LD between the observed (tested) SNP and the unobserved risk-enhancing SNP. Imputation can 'close the gap' between observed unassociated SNPs and unobserved associated SNPs by incorporating haplotype information of observed SNPs along with LD structure of the full HapMap[242]. In humans, imputation can be highly accurate (> 98 %) in regions of the genome but reduces particularly in 'recombination hotspots'[241]. Imputation can also be used to generate SNP data for GWAS from low-coverage WGS. Cai et al. reported how they imputed genotypes across 11,670 human samples, using 1.7 X WGS data, allowing them to perform a successful GWAS of major depressive disorder as part of the CONVERGE project[243]. To the author's knowledge, imputation has not yet been used in the genetic investigation of canine complex disease. This most likely relates to the lack of availability of a canine haplotype map. The situation may change in the future, however, as more and more dogs are genotyped and these data are subsequently shared. The accuracy of imputation, however, may be variable as it will depend on the availability of sufficient genotyping data for the specific population of interest (e.g. a particular breed).

6.2.3 Copy number variant screening

Genome-wide copy number variant (CNV) screening presents another method to investigate the genetic basis of complex disease and, thus far, has only experienced limited use in the dog. CNV is a type of genomic structural variation in which sections of the genome are repeated or deleted and the number of repeats/deletes in the genome varies between individuals. CNVs may represent up to 10 % of the human genome and their effects range from benign to directly pathogenic. Pathogenic consequences of CNVs include altered gene regulation and structure and unmasking of recessive alleles, and their importance has been shown in several human complex diseases such as Crohn's disease, rheumatoid arthritis and psoriasis[244-246]. The importance of CNVs in canine phenotypes has also been demonstrated with a duplication event encompassing three genes causing the dorsal hair ridge in Ridgeback dogs and an upstream gene duplication causing skin wrinkling in Chinese Shar-Pei[247,248]. Genome-wide CNV scans can be performed by various methods but one is whole-genome SNP-genotyping arrays which potentially allow CNV detection in conjunction with GWAS making it an attractive tool. Molin et al. presented the first CNV investigation based on the CanineHD 170 K genotyping array used in this thesis and identified 29 novel CNV regions[249]. The development of a growing catalogue of canine CNV regions will act as a rich resource for future investigation of canine complex disease.

6.2.4 Identification of candidate genes and causal variants

A main challenge of GWAS in investigating complex disease is to pinpoint causative genes as the majority of GWAS hits are in non-coding or intergenic regions because complex disease is often caused by disturbance to biological networks, not by isolated genes or proteins. Regulatory SNPs can influence gene expression through a number of mechanisms that include the three dimensional organisation of the genome, RNA splicing, transcription factor binding, DNA methylation, and long non-coding

RNAs[250,251]. Investigation of SNPs with complex trait disease in dogs with potential regulatory function through expressed quantitative trait loci (eQTL) studies or other methods is currently lacking. Recently, attention has turned towards use of genome-wide gene association analyses (GWGAS) to help detect the most relevant, likely causal genes. MAGMA is a tool for gene analysis and generalised gene-set analysis of GWAS data and can be used to analyse both raw genotype data as well as summary SNP P-values from a previous GWAS or meta-analysis[252]. Along with performing imputation methods in their GWAS, Hammerschlag et al. also performed a GWGAS using MAGMA in their investigations of persistent insomnia[253]. They used 19,427 protein coding genes and annotated all the SNPs of the association analysis to these genes resulting in 18,355 genes being covered by at least one SNP. The advantage of GWGAS is that it has the potential to identify genes in which multiple genetic variants may mask effects that are not significantly strong enough to be picked up by GWAS. Conversely, however, and because GWGAS takes all SNPs within the gene into account, it is possible that a gene that is truly associated with disease is not identified by GWGAS because the genes may harbour many more tested SNPs that do not show an association.

To investigate causal variants for PCAG in the loci determined by the GWAS reported in this thesis, a NGS WGS approach using one or three cases (depending on the breed) and > 500 controls was employed. Such an approach has previously proven successful in identifying causal variants in single gene canine disorders[254-256]. It is perhaps not surprising, that a similar approach to investigate complex disease using so few cases was unsuccessful. Future studies using WGS approaches to elucidate candidate PCAG causal variants should take several factors into account. Firstly, a much larger sample cohort is likely to be needed to detect causal variants for PCAG than for single gene disorders. Secondly, efficiency of a WGS approach will be improved by selecting samples on the basis of a homozygous genotype for the GWAS top SNP. Unfortunately,

owing to timing logistics, GWAS were performed following the acquisition of WGS data which reduced the number of useful WGS for analysis and these were all heterozygotes. Since the completion of the PhD, however, our GWAS findings in the BH have been published which has aided in application for further funding[205]. WGS will now be performed in 15 BH comprising 9 with PCAG which are homozygous for one or both of the two top GWAS SNPs and 6 with PLD which are homozygous for the alternative alleles. Finally, because the use of a large number of WGS is likely to be cost prohibitive for most modestly sized canine research laboratories, future availability of imputation could potentially be used to reduce costs.

Further investigation of canine PCAG should probably integrate several of the above discussed methodologies. Integrative approaches that combine multiple forms of data can more accurately capture pathway associations and so provide a comprehensive understanding of the molecular mechanisms that cause complex diseases[257].

6.3 Genetic investigation of POAG

In this thesis, highly significant associations of three different *ADAMTS17* mutations with canine POAG are reported. *ADAMTS17* is a strong candidate gene for POAG as the role of metalloproteinases in AH outflow resistance and IOP has long been suggested, being hypothesised to relate to changes in the amount or composition of the ECM of the outflow pathways[21,144,258]. Furthermore, several studies have identified the matrix metalloproteinase gene *MMP-9* as a candidate gene for POAG and PACG in humans[259-262].

Functional evidence for the causality of the *ADAMTS17* mutations reported in this thesis, however, was lacking mainly due to lack of tissue availability. Although, it was possible to demonstrate reduced *ADAMTS17* expression for one of the POAG mutations (the 6 bp deletion in the SP), this was only performed using technical replicates of a single case and control. Additional experiments could be undertaken to assess the

effects the three different mutations have on ADAMTS17 protein, including whether or not the protein is expressed in truncated forms or whether they are differentially expressed in the AH outflow pathways of biological replicates of each breed. Furthermore, immunohistochemistry could be used to pinpoint the precise cellular location of protein expression and whether the mutation causes mislocalisation.

RNA and protein experiments could also be expanded to include genes and proteins known to be involved in the same biological pathways or, indeed, to identify novel genes/proteins in the same pathways.

To further help understand possible effects of the mutations on protein function, it would be interesting to understand what effect the different mutations have on ADAMTS17 structure. Structural modelling can be used to predict possible disruption caused by different variants and different programs are available to facilitate this[263]. Kuchtey et al. reported a Gly661Arg variant to be associated with POAG in the Beagle and used homology modelling to locate the position of the residue[68]. This was suggestive that the Gly661 residue was located within a tight turn, buried within the interface between the cysteine rich and thrombospondin repeat domains. The long polar side chain of arginine substituted at this position was predicted to disrupt the normal protein fold.

Disruption of folding may reduce the stability of the protein which, in turn, is likely to have important functional consequences. Protein half-life measurement can be used to demonstrate, in vitro, the effect variants have on protein stability. Kuchtey et al. used commercially available mutagenesis and transcription/translation kits to demonstrate that the Gly661Arg form of ADAMTS10 is less stable, with a protein half-life of approximately 40 % of normal ADAMTS10. It would be interesting to perform similar experiments with the ADAMTS17 variants reported in this thesis.

In both humans and dogs, the TM undergoes ultrastructural changes with advancing age which are more pronounced in POAG patients[142,264]. These changes include thickening of the sheaths that surround elastin fibres and are composed of ECM, including fibrillin. How the canine *ADAMTS10* and *ADAMTS17* mutations might be involved in these ultrastructural changes is entirely speculative but it is interesting to note that, for both enzymes, fibrillin 1, has been proposed as a substrate[122,136].

6.4 Thesis conclusion

To conclude, this thesis project has led to the provision of robust and current PLD prevalence data for seven dog breeds along with evidence of PLD progression which have formed the basis of three separate publications. Investigations of the genetic basis of PLD and PCAG led to the discovery of two novel PCAG loci in the BH and a shared PCAG locus in the DDT and WSS. These loci will be the focus of deeper investigation for causal variants in the future. The discovery and publication of three breed-specific POAG-associated mutations has not only further highlighted the importance of ADAMTS17 in intraocular physiology and AH outflow, but, through the provision of commercially available DNA test, has also had a significant and beneficial impact on canine welfare.

List of references

1. Gelatt KN, MacKay EO. Distribution of intraocular pressure in dogs. *Vet Ophthalmol* 1998;1:109-114.
2. Giannetto C, Piccione G, Giudice E. Daytime profile of the intraocular pressure and tear production in normal dog. *Vet Ophthalmol* 2009;12:302-305.
3. Martin-Suarez E, Molleda C, Tardon R, et al. Diurnal variations of central corneal thickness and intraocular pressure in dogs from 8:00 am to 8:00 pm. *Can Vet J* 2014;55:361-365.
4. Pizzirani S, Gong H. Functional Anatomy of the Outflow Facilities. *Vet Clin North Am Small Anim Pract* 2015;45:1101-1126.
5. Van Buskirk EM, Brett J. The canine eye: in vitro studies of the intraocular pressure and facility of aqueous outflow. *Invest Ophthalmol Vis Sci* 1978;17:373-377.
6. Barrie KP, Gum GG, Samuelson DA, et al. Quantitation of uveoscleral outflow in normotensive and glaucomatous Beagles by 3H-labeled dextran. *Am J Vet Res* 1985;46:84-88.
7. Alm A, Nilsson SF. Uveoscleral outflow--a review. *Exp Eye Res* 2009;88:760-768.
8. Danford ID, Verkuil LD, Choi DJ, et al. Characterizing the "POAGome": A bioinformatics-driven approach to primary open-angle glaucoma. *Prog Retin Eye Res* 2017;58:89-114.
9. Samuelson D, Streit A. Microanatomy of the anterior uveoscleral outflow pathway in normal and primary open-angle glaucomatous dogs. *Vet Ophthalmol* 2012;15 Suppl 1:47-53.
10. Hann CR, Springett MJ, Wang X, et al. Ultrastructural localization of collagen IV, fibronectin, and laminin in the trabecular meshwork of normal and glaucomatous eyes. *Ophthalmic Res* 2001;33:314-324.
11. WuDunn D. Mechanobiology of trabecular meshwork cells. *Exp Eye Res* 2009;88:718-723.
12. Haddadin RI, Oh DJ, Kang MH, et al. SPARC-null mice exhibit lower intraocular pressures. *Invest Ophthalmol Vis Sci* 2009;50:3771-3777.
13. Haddadin RI, Oh DJ, Kang MH, et al. Thrombospondin-1 (TSP1)-null and TSP2-null mice exhibit lower intraocular pressures. *Invest Ophthalmol Vis Sci* 2012;53:6708-6717.
14. Keller KE, Vranka JA, Haddadin RI, et al. The effects of tenascin C knockdown on trabecular meshwork outflow resistance. *Invest Ophthalmol Vis Sci* 2013;54:5613-5623.
15. Rhee DJ, Haddadin RI, Kang MH, et al. Matricellular proteins in the trabecular meshwork. *Exp Eye Res* 2009;88:694-703.
16. Tripathi RC, Chan WF, Li J, et al. Trabecular cells express the TGF-beta 2 gene and secrete the cytokine. *Exp Eye Res* 1994;58:523-528.
17. Fuchshofer R, Yu AH, Welge-Lussen U, et al. Bone morphogenetic protein-7 is an antagonist of transforming growth factor-beta2 in human trabecular meshwork cells. *Invest Ophthalmol Vis Sci* 2007;48:715-726.
18. Flugel-Koch C, Ohlmann A, Fuchshofer R, et al. Thrombospondin-1 in the trabecular meshwork: localization in normal and glaucomatous eyes, and induction by TGF-beta1 and dexamethasone in vitro. *Exp Eye Res* 2004;79:649-663.
19. Ueda J, Yue BY. Distribution of myocilin and extracellular matrix components in the corneoscleral meshwork of human eyes. *Invest Ophthalmol Vis Sci* 2003;44:4772-4779.
20. Ueda J, Wentz-Hunter K, Yue BY. Distribution of myocilin and extracellular matrix components in the juxtacanalicular tissue of human eyes. *Invest Ophthalmol Vis Sci* 2002;43:1068-1076.

21. Acott TS, Kelley MJ. Extracellular matrix in the trabecular meshwork. *Exp Eye Res* 2008;86:543-561.

22. Gum GG, Samuelson DA, Gelatt KN. Effect of hyaluronidase on aqueous outflow resistance in normotensive and glaucomatous eyes of dogs. *Am J Vet Res* 1992;53:767-770.

23. Ryland TR, Lewis PA, Chisholm M, et al. Localization of smooth muscle actin in the iridocorneal angle of normal and spontaneous glaucomatous beagle dogs. *Vet Ophthalmol* 2003;6:205-209.

24. Goel M, Picciani RG, Lee RK, et al. Aqueous humor dynamics: a review. *Open Ophthalmol J* 2010;4:52-59.

25. Anderson DR. The development of the trabecular meshwork and its abnormality in primary infantile glaucoma. *Trans Am Ophthalmol Soc* 1981;79:458-485.

26. Martin CL. Development of pectinate ligament structure of the dog: study by scanning electron microscopy. *Am J Vet Res* 1974;35:1433-1439.

27. Samuelson DA, Gelatt KN. Aqueous outflow in the beagle. I. Postnatal morphologic development of the iridocorneal angle: pectinate ligament and uveal trabecular meshwork. *Curr Eye Res* 1984;3:783-794.

28. Gelatt KN, Brooks DE, Kallberg ME. Chapter 16. The Canine Glaucomas. *In Veterinary Ophthalmology* 2007;2:768-769.

29. Bjerkås E, Ekesten B, Farstad W. Pectinate ligament dysplasia and narrowing of the iridocorneal angle associated with glaucoma in the English Springer Spaniel. *Vet Ophthalmol* 2002;5:49-54.

30. Ekesten B, Narfstrom K. Correlation of morphologic features of the iridocorneal angle to intraocular pressure in Samoyeds. *Am J Vet Res* 1991;52:1875-1878.

31. Read RA, Wood JL, Lakhani KH. Pectinate ligament dysplasia (PLD) and glaucoma in Flat Coated Retrievers. I. Objectives, technique and results of a PLD survey. *Vet Ophthalmol* 1998;1:85-90.

32. Wood JL, Lakhani KH, Read RA. Pectinate ligament dysplasia and glaucoma in Flat Coated Retrievers. II. Assessment of prevalence and heritability. *Vet Ophthalmol* 1998;1:91-99.

33. van der Linde-Sipman JS. Dysplasia of the pectinate ligament and primary glaucoma in the Bouvier des Flandres dog. *Vet Pathol* 1987;24:201-206.

34. Ekesten B, Narfstrom K. Age-related changes in intraocular pressure and iridocorneal angle in Samoyeds. *Progress in Veterinary and Comparative Ophthalmology* 1992;2:37-40.

35. Pearl R, Gould D, Spiess B. Progression of pectinate ligament dysplasia over time in two populations of Flat-Coated Retrievers. *Vet Ophthalmol* 2015;18:6-12.

36. Samuelson DA, Gelatt KN. Aqueous outflow in the beagle. II. Postnatal morphologic development of the iridocorneal angle: corneoscleral trabecular meshwork and angular aqueous plexus. *Curr Eye Res* 1984;3:795-807.

37. Grierson I, Howes RC. Age-related depletion of the cell population in the human trabecular meshwork. *Eye (Lond)* 1987;1 (Pt 2):204-210.

38. Alvarado J, Murphy C, Juster R. Trabecular meshwork cellularity in primary open-angle glaucoma and nonglaucomatous normals. *Ophthalmology* 1984;91:564-579.

39. Babizhayev MA, Brodskaya MW. Fibronectin detection in drainage outflow system of human eyes in ageing and progression of open-angle glaucoma. *Mech Ageing Dev* 1989;47:145-157.

40. Gabelt BT, Kaufman PL. Changes in aqueous humor dynamics with age and glaucoma. *Prog Retin Eye Res* 2005;24:612-637.

41. Pizzirani S. Definition, Classification, and Pathophysiology of Canine Glaucoma. *Vet Clin North Am Small Anim Pract* 2015;45:1127-1157, v.

42. Bedford PG. Gonioscopy in the dog. *J Small Anim Pract* 1977;18:615-629.
43. Crispin S. Hereditary Eye Disease in Dogs In: Association BV, ed. *https://wwwbvacouk/uploadedFiles/Content/Canine_Health_Schemes/20160321%20CHS%20Eye%20leaflet%202016%20v8Apdf*, 2016.
44. Martin CL. Gonioscopy and anatomical correlations of the drainage angle of the dog. *J Small Anim Pract* 1969;10:171-184.
45. Oliver JA, Ekiri A, Mellersh CS. Prevalence and progression of pectinate ligament dysplasia in the Welsh springer spaniel. *J Small Anim Pract* 2016;57:416-421.
46. Oliver JA, Ekiri A, Mellersh CS. Prevalence of pectinate ligament dysplasia and associations with age, sex and intraocular pressure in the Basset hound, Flatcoated retriever and Dandie Dinmont terrier. *Canine Genet Epidemiol* 2016;3:1.
47. Ekesten B, Narfström K. Age-related changes in intraocular pressure and iridocorneal angle in Samoyeds. *Progress in Veterinary and Comparative Ophthalmology* 1992;2:37-40.
48. Fricker GV, Smith K, Gould DJ. Survey of the incidence of pectinate ligament dysplasia and glaucoma in the UK Leonberger population. *Vet Ophthalmol* 2015.
49. Ekesten B, K. N. Age-related changes in intraocular pressure and iridocorneal angle in Samoyeds. *Progress in Veterinary and Comparative Ophthalmology* 1992;2:37-40.
50. Gibson TE, Roberts SM, Severin GA, et al. Comparison of gonioscopy and ultrasound biomicroscopy for evaluating the iridocorneal angle in dogs. *J Am Vet Med Assoc* 1998;213:635-638.
51. Hann CR, Vercnocke AJ, Bentley MD, et al. Anatomic changes in Schlemm's canal and collector channels in normal and primary open-angle glaucoma eyes using low and high perfusion pressures. *Invest Ophthalmol Vis Sci* 2014;55:5834-5841.
52. Bentley E, Miller PE, Diehl KA. Evaluation of intra- and interobserver reliability and image reproducibility to assess usefulness of high-resolution ultrasonography for measurement of anterior segment structures of canine eyes. *Am J Vet Res* 2005;66:1775-1779.
53. Gelatt KN, MacKay EO. Prevalence of the breed-related glaucomas in pure-bred dogs in North America. *Vet Ophthalmol* 2004;7:97-111.
54. Teikari J, Raivio I, Nurminen M. Incidence of acute glaucoma in Finland from 1973 to 1982. *Graefes Arch Clin Exp Ophthalmol* 1987;225:357-360.
55. David R, Tessler Z, Yassur Y. Epidemiology of acute angle-closure glaucoma: incidence and seasonal variations. *Ophthalmologica* 1985;191:4-7.
56. Wong TY, Foster PJ, Seah SK, et al. Rates of hospital admissions for primary angle closure glaucoma among Chinese, Malays, and Indians in Singapore. *Br J Ophthalmol* 2000;84:990-992.
57. Strom AR, Hassig M, Iburg TM, et al. Epidemiology of canine glaucoma presented to University of Zurich from 1995 to 2009. Part 1: Congenital and primary glaucoma (4 and 123 cases). *Vet Ophthalmol* 2011;14:121-126.
58. Foster PJ. The epidemiology of primary angle closure and associated glaucomatous optic neuropathy. *Semin Ophthalmol* 2002;17:50-58.
59. Quigley HA, Broman AT. The number of people with glaucoma worldwide in 2010 and 2020. *Br J Ophthalmol* 2006;90:262-267.
60. Cottrell B, Barnett K. Primary glaucoma in the Welsh springer spaniel. *Journal of Small Animal Practice* 1988;29:185-189.
61. Lovekin L. Primary glaucoma in dogs. *Journal of the American Veterinary Medical Association* 1964;145:1081-1091.

62. Boillot T, Rosolen SG, Dulaurent T, et al. Determination of morphological, biometric and biochemical susceptibilities in healthy eurasier dogs with suspected inherited glaucoma. *PLoS One* 2014;9:e111873.

63. Tsai S, Bentley E, Miller PE, et al. Gender differences in iridocorneal angle morphology: a potential explanation for the female predisposition to primary angle closure glaucoma in dogs. *Vet Ophthalmol* 2012;15 Suppl 1:60-63.

64. Kato K, Sasaki N, Matsunaga S, et al. Incidence of canine glaucoma with goniodysplasia in Japan : a retrospective study. *J Vet Med Sci* 2006;68:853-858.

65. Wood JL, Lakhani KH, Mason IK, et al. Relationship of the degree of goniodysgenesis and other ocular measurements to glaucoma in Great Danes. *Am J Vet Res* 2001;62:1493-1499.

66. Miller PE, Bentley E. Clinical Signs and Diagnosis of the Canine Primary Glaucomas. *Vet Clin North Am Small Anim Pract* 2015;45:1183-1212, vi.

67. Bauer BS, Sandmeyer LS, Philibert H, et al. Chronic Glaucoma in Dogs: Relationships Between Histologic Lesions and the Gonioscopic Diagnosis of Pectinate Ligament Dysplasia. *Vet Pathol* 2016.

68. Kuchtey J, Kunkel J, Esson D, et al. Screening ADAMTS10 in dog populations supports Gly661Arg as the glaucoma-causing variant in beagles. *Invest Ophthalmol Vis Sci* 2013;54:1881-1886.

69. Kuchtey J, Olson LM, Rinkoski T, et al. Mapping of the disease locus and identification of ADAMTS10 as a candidate gene in a canine model of primary open angle glaucoma. *PLoS Genet* 2011;7:e1001306.

70. Ahonen SJ, Kaukonen M, Nussdorfer FD, et al. A Novel Missense Mutation in ADAMTS10 in Norwegian Elkhound Primary Glaucoma. *PLoS One* 2014;9:e111941.

71. Oshima Y, Bjerkas E, Peiffer RL, Jr. Ocular histopathologic observations in Norwegian Elkhounds with primary open-angle, closed-cleft glaucoma. *Vet Ophthalmol* 2004;7:185-188.

72. Gelatt KN, Peiffer RL, Jr., Gwin RM, et al. Clinical manifestations of inherited glaucoma in the beagle. *Invest Ophthalmol Vis Sci* 1977;16:1135-1142.

73. Gelatt KN, Peiffer RL, Jr., Gwin RM, et al. Glaucoma in the beagle. *Trans Sect Ophthalmol Am Acad Ophthalmol Otolaryngol* 1976;81:Op636-644.

74. Forman OP, Pettitt L, Komaromy AM, et al. A Novel Genome-Wide Association Study Approach Using Genotyping by Exome Sequencing Leads to the Identification of a Primary Open Angle Glaucoma Associated Inversion Disrupting ADAMTS17. *PLoS One* 2015;10:e0143546.

75. Oliver JA, Forman OP, Pettitt L, et al. Two Independent Mutations in ADAMTS17 Are Associated with Primary Open Angle Glaucoma in the Basset Hound and Basset Fauve de Bretagne Breeds of Dog. *PLoS One* 2015;10:e0140436.

76. Lazarus JA, Pickett JP, Champagne ES. Primary lens luxation in the Chinese Shar Pei: clinical and hereditary characteristics. *Vet Ophthalmol* 1998;1:101-107.

77. Davidson MG, Nelms SR. Diseases of the lens and cataract formation In: Gelatt KN, ed. *Veterinary Ophthalmology*. Iowa: Blackwell Publishing, 2013;1199-1233.

78. Komaromy AM, Petersen-Jones SM. Genetics of Canine Primary Glaucomas. *Vet Clin North Am Small Anim Pract* 2015;45:1159-1182, v.

79. Gelatt KN, Gum GG. Inheritance of primary glaucoma in the beagle. *Am J Vet Res* 1981;42:1691-1693.

80. Kato K, Sasaki N, Matsunaga S, et al. Possible association of glaucoma with pectinate ligament dysplasia and narrowing of the iridocorneal angle in Shiba Inu dogs in Japan. *Vet Ophthalmol* 2006;9:71-75.

81. Martin CL, Wyman M. Glaucoma in the Basset Hound. *J Am Vet Med Assoc* 1968;153:1320-1327.

82. Mellersh C. Microsatellite-based candidate gene linkage analysis studies. *Methods Mol Biol* 2008;439:75-86.

83. Sutter NB, Eberle MA, Parker HG, et al. Extensive and breed-specific linkage disequilibrium in Canis familiaris. *Genome Res* 2004;14:2388-2396.

84. Gray MM, Granka JM, Bustamante CD, et al. Linkage disequilibrium and demographic history of wild and domestic canids. *Genetics* 2009;181:1493-1505.

85. Lindblad-Toh K, Wade CM, Mikkelsen TS, et al. Genome sequence, comparative analysis and haplotype structure of the domestic dog. *Nature* 2005;438:803-819.

86. Mellersh CS, Pettitt L, Forman OP, et al. Identification of mutations in HSF4 in dogs of three different breeds with hereditary cataracts. *Vet Ophthalmol* 2006;9:369-378.

87. Itakura T, Peters DM, Fini ME. Glaucomatous MYOC mutations activate the IL-1/NF-kappaB inflammatory stress response and the glaucoma marker SELE in trabecular meshwork cells. *Mol Vis* 2015;21:1071-1084.

88. Janssen SF, Gorgels TG, Ramdas WD, et al. The vast complexity of primary open angle glaucoma: disease genes, risks, molecular mechanisms and pathobiology. *Prog Retin Eye Res* 2013;37:31-67.

89. Takamoto M, Araie M. Genetics of primary open angle glaucoma. *Jpn J Ophthalmol* 2014;58:1-15.

90. Williams SE, Carmichael TR, Wainstein T, et al. MYOC mutations in black south african patients with primary open-angle glaucoma: genetic testing and cascade screening. *Ophthalmic Genet* 2015;36:31-38.

91. Yang Y, Shi Y, Huang X, et al. Identification of a novel MYOC mutation in a Chinese family with primary open-angle glaucoma. *Gene* 2015;571:188-193.

92. Kato K, Sasaki N, Gelatt KN, et al. Autosomal recessive primary open angle glaucoma (POAG) in beagles is not associated with mutations in the myocilin (MYOC) gene. *Graefes Arch Clin Exp Ophthalmol* 2009;247:1435-1436.

93. Kato K, Sasaki N, Matsunaga S, et al. Cloning of canine myocilin cDNA and molecular analysis of the myocilin gene in Shiba Inu dogs. *Vet Ophthalmol* 2007;10 Suppl 1:53-62.

94. Kanemaki N, Tchedre KT, Imayasu M, et al. Dogs and humans share a common susceptibility gene SRBD1 for glaucoma risk. *PLoS One* 2013;8:e74372.

95. Ott J. Methods of analysis and resources available for genetic trait mapping. *J Hered* 1999;90:68-70.

96. Sheffield VC, Stone EM, Alward WL, et al. Genetic linkage of familial open angle glaucoma to chromosome 1q21-q31. *Nat Genet* 1993;4:47-50.

97. Sarfarazi M, Child A, Stoilova D, et al. Localization of the fourth locus (GLC1E) for adult-onset primary open-angle glaucoma to the 10p15-p14 region. *Am J Hum Genet* 1998;62:641-652.

98. McCarthy MI, Abecasis GR, Cardon LR, et al. Genome-wide association studies for complex traits: consensus, uncertainty and challenges. *Nat Rev Genet* 2008;9:356-369.

99. Power RA, Parkhill J, de Oliveira T. Microbial genome-wide association studies: lessons from human GWAS. *Nat Rev Genet* 2017;18:41-50.

100. Schaid DJ, Chen W, Larson NB. From genome-wide associations to candidate causal variants by statistical fine-mapping. *Nat Rev Genet* 2018.

101. Vaysse A, Ratnakumar A, Derrien T, et al. Identification of genomic regions associated with phenotypic variation between dog breeds using selection mapping. *PLoS Genet* 2011;7:e1002316.

102. Lequarre AS, Andersson L, Andre C, et al. LUPA: a European initiative taking advantage of the canine genome architecture for unravelling complex disorders in both human and dogs. *Vet J* 2011;189:155-159.

103. Karlsson EK, Lindblad-Toh K. Leader of the pack: gene mapping in dogs and other model organisms. *Nat Rev Genet* 2008;9:713-725.

104. Altshuler D, Daly MJ, Lander ES. Genetic mapping in human disease. *Science* 2008;322:881-888.

105. Ostrander EA, Wayne RK. The canine genome. *Genome Res* 2005;15:1706-1716.

106. Ahonen SJ, Pietila E, Mellersh CS, et al. Genome-wide association study identifies a novel canine glaucoma locus. *PLoS One* 2013;8:e70903.

107. Forman O, Mellersh C. Use of novel GWAS approaches and genome sequencing facilitates identification of large scale rearrangements assocaited with two inherited diseases. *Abstract The 8th International Conference of Advances in Canine and Feline Genomics and Inherited Disease, Cambridge, UK* 2015.

108. Allingham RR, Liu Y, Rhee DJ. The genetics of primary open-angle glaucoma: a review. *Exp Eye Res* 2009;88:837-844.

109. Liu Y, Allingham RR. Molecular genetics in glaucoma. *Exp Eye Res* 2011;93:331-339.

110. Gauthier AC, Liu J. Epigenetics and Signaling Pathways in Glaucoma. *Biomed Res Int* 2017;2017:5712341.

111. Wiggs JL, Pasquale LR. Genetics of glaucoma. *Hum Mol Genet* 2017;26:R21-r27.

112. Stone EM, Fingert JH, Alward WL, et al. Identification of a gene that causes primary open angle glaucoma. *Science* 1997;275:668-670.

113. Rezaie T, Child A, Hitchings R, et al. Adult-onset primary open-angle glaucoma caused by mutations in optineurin. *Science* 2002;295:1077-1079.

114. Monemi S, Spaeth G, DaSilva A, et al. Identification of a novel adult-onset primary open-angle glaucoma (POAG) gene on 5q22.1. *Hum Mol Genet* 2005;14:725-733.

115. Awadalla MS, Fingert JH, Roos BE, et al. Copy number variations of TBK1 in Australian patients with primary open-angle glaucoma. *Am J Ophthalmol* 2015;159:124-130.e121.

116. MacKay EO, Kallberg ME, Barrie KP, et al. Myocilin protein levels in the aqueous humor of the glaucomas in selected canine breeds. *Vet Ophthalmol* 2008;11:234-241.

117. Mackay EO, Kallberg ME, Gelatt KN. Aqueous humor myocilin protein levels in normal, genetic carriers, and glaucoma Beagles. *Vet Ophthalmol* 2008;11:177-185.

118. Bailey JN, Loomis SJ, Kang JH, et al. Genome-wide association analysis identifies TXNRD2, ATXN2 and FOXC1 as susceptibility loci for primary open-angle glaucoma. *Nat Genet* 2016;48:189-194.

119. Khawaja AP, Cooke Bailey JN, Wareham NJ, et al. Genome-wide analyses identify 68 new loci associated with intraocular pressure and improve risk prediction for primary open-angle glaucoma. *Nat Genet* 2018;50:778-782.

120. Shiga Y, Akiyama M, Nishiguchi KM, et al. Genome-wide association study identifies seven novel susceptibility loci for primary open-angle glaucoma. *Hum Mol Genet* 2018;27:1486-1496.

121. Gao XR, Huang H, Nannini DR, et al. Genome-wide association analyses identify new loci influencing intraocular pressure. *Hum Mol Genet* 2018;27:2205-2213.

122. Farias FH, Johnson GS, Taylor JF, et al. An ADAMTS17 splice donor site mutation in dogs with primary lens luxation. *Invest Ophthalmol Vis Sci* 2010;51:4716-4721.

123. Gould D, Pettitt L, McLaughlin B, et al. ADAMTS17 mutation associated with primary lens luxation is widespread among breeds. *Vet Ophthalmol* 2011;14:378-384.

124. Palko JR, Iwabe S, Pan X, et al. Biomechanical properties and correlation with collagen solubility profile in the posterior sclera of canine eyes with an ADAMTS10 mutation. *Invest Ophthalmol Vis Sci* 2013;54:2685-2695.

125. Morales J, Al-Sharif L, Khalil DS, et al. Homozygous mutations in ADAMTS10 and ADAMTS17 cause lenticular myopia, ectopia lentis, glaucoma, spherophakia, and short stature. *Am J Hum Genet* 2009;85:558-568.

126. Shah MH, Bhat V, Shetty JS, et al. Whole exome sequencing identifies a novel splice-site mutation in ADAMTS17 in an Indian family with Weill-Marchesani syndrome. *Mol Vis* 2014;20:790-796.

127. Khan AO, Aldahmesh MA, Al-Ghadeer H, et al. Familial spherophakia with short stature caused by a novel homozygous ADAMTS17 mutation. *Ophthalmic Genet* 2012;33:235-239.

128. Radner FP, Marrakchi S, Kirchmeier P, et al. Mutations in CERS3 cause autosomal recessive congenital ichthyosis in humans. *PLoS Genet* 2013;9:e1003536.

129. Zhai Y, Wang W, Zhu YN, et al. A novel FBN1 missense mutation (p.C102Y) associated with ectopia lentis syndrome in a Chinese family. *Int J Ophthalmol* 2015;8:855-859.

130. Liu DL, Cao JH, Yang J, et al. A novel mutation in fibrillin-1 gene identified in a Chinese family with marfan syndrome. *Int J Clin Exp Med* 2015;8:7419-7424.

131. Yin Y, Liu XH, Li XH, et al. A novel FBN1 heterozygous mutation identified in a Chinese family with autosomal dominant Marfan syndrome. *Genet Mol Res* 2015;14:4125-4132.

132. Ahram D, Sato TS, Kohilan A, et al. A homozygous mutation in ADAMTSL4 causes autosomal-recessive isolated ectopia lentis. *Am J Hum Genet* 2009;84:274-278.

133. Hubmacher D, Apte SS. Genetic and functional linkage between ADAMTS superfamily proteins and fibrillin-1: a novel mechanism influencing microfibril assembly and function. *Cell Mol Life Sci* 2011;68:3137-3148.

134. Hubmacher D, Apte SS. ADAMTS proteins as modulators of microfibril formation and function. *Matrix Biol* 2015.

135. Hubmacher D, Schneider M, Berardinelli SJ, et al. Unusual life cycle and impact on microfibril assembly of ADAMTS17, a secreted metalloprotease mutated in genetic eye disease. *Sci Rep* 2017;7:41871.

136. Dagoneau N, Benoist-Lasselin C, Huber C, et al. ADAMTS10 mutations in autosomal recessive Weill-Marchesani syndrome. *Am J Hum Genet* 2004;75:801-806.

137. Kuchtey J, Kuchtey RW. The microfibril hypothesis of glaucoma: implications for treatment of elevated intraocular pressure. *J Ocul Pharmacol Ther* 2014;30:170-180.

138. Kutz WE, Wang LW, Bader HL, et al. ADAMTS10 protein interacts with fibrillin-1 and promotes its deposition in extracellular matrix of cultured fibroblasts. *J Biol Chem* 2011;286:17156-17167.

139. Kutz WE, Wang LW, Dagoneau N, et al. Functional analysis of an ADAMTS10 signal peptide mutation in Weill-Marchesani syndrome demonstrates a long-range effect on secretion of the full-length enzyme. *Hum Mutat* 2008;29:1425-1434.

140. Ono RN, Sengle G, Charbonneau NL, et al. Latent transforming growth factor beta-binding proteins and fibulins compete for fibrillin-1 and exhibit exquisite specificities in binding sites. *J Biol Chem* 2009;284:16872-16881.

141. Ramirez F, Rifkin DB. Extracellular microfibrils: contextual platforms for TGFbeta and BMP signaling. *Curr Opin Cell Biol* 2009;21:616-622.

142. Samuelson DA, Gum GG, Gelatt KN. Ultrastructural changes in the aqueous outflow apparatus of beagles with inherited glaucoma. *Invest Ophthalmol Vis Sci* 1989;30:550-561.

143. Lutjen-Drecoll E, Shimizu T, Rohrbach M, et al. Quantitative analysis of 'plaque material' in the inner- and outer wall of Schlemm's canal in normal- and glaucomatous eyes. *Exp Eye Res* 1986;42:443-455.

144. Keller KE, Bradley JM, Acott TS. Differential effects of ADAMTS-1, -4, and -5 in the trabecular meshwork. *Invest Ophthalmol Vis Sci* 2009;50:5769-5777.

145. Sihota R, Ghate D, Mohan S, et al. Study of biometric parameters in family members of primary angle closure glaucoma patients. *Eye (Lond)* 2008;22:521-527.

146. Bonomi L, Marchini G, Marraffa M, et al. Epidemiology of angle-closure glaucoma: prevalence, clinical types, and association with peripheral anterior chamber depth in the Egna-Neumarket Glaucoma Study. *Ophthalmology* 2000;107:998-1003.

147. Foster PJ, Alsbirk PH, Baasanhu J, et al. Anterior chamber depth in Mongolians: variation with age, sex, and method of measurement. *Am J Ophthalmol* 1997;124:53-60.

148. Alsbirk PH. Anterior chamber depth in Greenland Eskimos. I. A population study of variation with age and sex. *Acta Ophthalmol (Copenh)* 1974;52:551-564.

149. Liza-Sharmini AT, Ng GF, Nor-Sharina Y, et al. Clinical presentation, severity and progression of primary angle closure in Malay and Chinese patients. *Med J Malaysia* 2014;69:245-251.

150. Coleman AL. Glaucoma. *Lancet* 1999;354:1803-1810.

151. Foster PJ, Johnson GJ. Glaucoma in China: how big is the problem? *Br J Ophthalmol* 2001;85:1277-1282.

152. Hu CN. [An epidemiologic study of glaucoma in Shunyi County, Beijing]. *Zhonghua Yan Ke Za Zhi* 1989;25:115-119.

153. Day AC, Luben R, Khawaja AP, et al. Genotype-phenotype analysis of SNPs associated with primary angle closure glaucoma (rs1015213, rs3753841 and rs11024102) and ocular biometry in the EPIC-Norfolk Eye Study. *Br J Ophthalmol* 2013;97:704-707.

154. Vithana EN, Khor CC, Qiao C, et al. Genome-wide association analyses identify three new susceptibility loci for primary angle closure glaucoma. *Nat Genet* 2012;44:1142-1146.

155. Shuai P, Yu M, Li X, et al. Genetic associations in PLEKHA7 and COL11A1 with primary angle closure glaucoma: a meta-analysis. *Clin Exp Ophthalmol* 2015;43:523-530.

156. Cong Y, Guo X, Liu X, et al. Association of the single nucleotide polymorphisms in the extracellular matrix metalloprotease-9 gene with PACG in southern China. *Mol Vis* 2009;15:1412-1417.

157. Awadalla MS, Burdon KP, Kuot A, et al. Matrix metalloproteinase-9 genetic variation and primary angle closure glaucoma in a Caucasian population. *Mol Vis* 2011;17:1420-1424.

158. Shi H, Zhu R, Hu N, et al. Association of frizzled-related protein (MFRP) and heat shock protein 70 (HSP70) single nucleotide polymorphisms with primary angle closure in a Han Chinese population: Jiangsu Eye Study. *Mol Vis* 2013;19:128-134.

159. Awadalla MS, Burdon KP, Thapa SS, et al. A cross-ethnicity investigation of genes previously implicated in primary angle closure glaucoma. *Mol Vis* 2012;18:2247-2254.

160. Michael S, Qamar R, Akhtar F, et al. C677T polymorphism in the methylenetetrahydrofolate reductase gene is associated with primary closed angle glaucoma. *Mol Vis* 2008;14:661-665.

161. Cao D, Liu X, Guo X, et al. Investigation of the association between CALCRL polymorphisms and primary angle closure glaucoma. *Mol Vis* 2009;15:2202-2208.

162. Chua J, Seet LF, Jiang Y, et al. Increased SPARC expression in primary angle closure glaucoma iris. *Mol Vis* 2008;14:1886-1892.

163. Abu-Amero KK, Morales J, Mohamed GH, et al. Glutathione S-transferase M1 and T1 polymorphisms in Arab glaucoma patients. *Mol Vis* 2008;14:425-430.

164. Awadalla MS, Thapa SS, Hewitt AW, et al. Association of eNOS polymorphisms with primary angle-closure glaucoma. *Invest Ophthalmol Vis Sci* 2013;54:2108-2114.

165. Al-Dabbagh NM, Al-Dohayan N, Arfin M, et al. Apolipoprotein E polymorphisms and primary glaucoma in Saudis. *Mol Vis* 2009;15:912-919.

166. Razeghinejad MR, Rahat F, Kamali-Sarvestani E. Association of TNFA -308 G/A and TNFRI +36 A/G gene polymorphisms with glaucoma. *Ophthalmic Res* 2009;42:118-124.

167. Jiang Z, Liang K, Ding B, et al. Hepatocyte growth factor genetic variations and primary angle-closure glaucoma in the Han Chinese population. *PLoS One* 2013;8:e60950.

168. Awadalla MS, Thapa SS, Burdon KP, et al. The association of hepatocyte growth factor (HGF) gene with primary angle closure glaucoma in the Nepalese population. *Mol Vis* 2011;17:2248-2254.

169. Khor CC, Do T, Jia H, et al. Genome-wide association study identifies five new susceptibility loci for primary angle closure glaucoma. *Nat Genet* 2016;48:556-562.

170. Ahram DF, Cook AC, Kecova H, et al. Identification of genetic loci associated with primary angle-closure glaucoma in the basset hound. *Mol Vis* 2014;20:497-510.

171. Ahram DF, Grozdanic SD, Kecova H, et al. Variants in Nebulin (NEB) Are Linked to the Development of Familial Primary Angle Closure Glaucoma in Basset Hounds. *PLoS One* 2015;10:e0126660.

172. Altman D. *Practical statistics for medical research*. London: Chapman and Hall, 1991.

173. Rozen S, Skaletsky H. Primer3 on the WWW for general users and for biologist programmers. *Methods Mol Biol* 2000;132:365-386.

174. Untergasser A, Cutcutache I, Koressaar T, et al. Primer3--new capabilities and interfaces. *Nucleic Acids Res* 2012;40:e115.

175. Koressaar T, Remm M. Enhancements and modifications of primer design program Primer3. *Bioinformatics* 2007;23:1289-1291.

176. Tozaki T, Mashima S, Hirota K, et al. Characterization of equine microsatellites and microsatellite-linked repetitive elements (eMLREs) by efficient cloning and genotyping methods. *DNA Res* 2001;8:33-45.

177. Bonfield JK, Smith K, Staden R. A new DNA sequence assembly program. *Nucleic Acids Res* 1995;23:4992-4999.

178. Purcell S, Neale B, Todd-Brown K, et al. PLINK: a tool set for whole-genome association and population-based linkage analyses. *Am J Hum Genet* 2007;81:559-575.

179. Zhou X, Stephens M. Genome-wide efficient mixed-model analysis for association studies. *Nat Genet* 2012;44:821-824.

180. Price AL, Zaitlen NA, Reich D, et al. New approaches to population stratification in genome-wide association studies. *Nat Rev Genet* 2010;11:459-463.

181. Li H, Durbin R. Fast and accurate short read alignment with Burrows-Wheeler transform. *Bioinformatics* 2009;25:1754-1760.

182. Robinson JT, Thorvaldsdottir H, Wenger AM, et al. Variant Review with the Integrative Genomics Viewer. *Cancer Res* 2017;77:e31-e34.

183. Thorvaldsdottir H, Robinson JT, Mesirov JP. Integrative Genomics Viewer (IGV): high-performance genomics data visualization and exploration. *Brief Bioinform* 2013;14:178-192.

184. McKenna A, Hanna M, Banks E, et al. The Genome Analysis Toolkit: a MapReduce framework for analyzing next-generation DNA sequencing data. *Genome Res* 2010;20:1297-1303.

185. Cunningham F, Amode MR, Barrell D, et al. Ensembl 2015. *Nucleic Acids Res* 2015;43:D662-669.

186. Yates A, Akanni W, Amode MR, et al. Ensembl 2016. *Nucleic Acids Res* 2016;44:D710-716.

187. Barrett JC, Fry B, Maller J, et al. Haploview: analysis and visualization of LD and haplotype maps. *Bioinformatics* 2005;21:263-265.

188. de Bakker PI, Yelensky R, Pe'er I, et al. Efficiency and power in genetic association studies. *Nat Genet* 2005;37:1217-1223.

189. Malik KJ, Chen CD, Olsen TW. Stability of RNA from the retina and retinal pigment epithelium in a porcine model simulating human eye bank conditions. *Invest Ophthalmol Vis Sci* 2003;44:2730-2735.

190. Wang WH, McNatt LG, Shepard AR, et al. Optimal procedure for extracting RNA from human ocular tissues and expression profiling of the congenital glaucoma gene FOXC1 using quantitative RT-PCR. *Mol Vis* 2001;7:89-94.

191. Livak KJ, Schmittgen TD. Analysis of relative gene expression data using real-time quantitative PCR and the 2(-Delta Delta C(T)) Method. *Methods* 2001;25:402-408.

192. Oliver JA, Ekiri AB, Mellersh CS. Pectinate ligament dysplasia in the Border Collie, Hungarian Vizsla and Golden Retriever. *Vet Rec* 2017;180:279.

193. Spiess, Bolliger, Borer G, et al. [Prevalence of pectinate ligament dysplasia in golden retrievers in Switzerland]. *Schweiz Arch Tierheilkd* 2014;156:279-284.

194. De Rousseau CJ, Bito LZ. Intraocular pressure of rhesus monkeys (Macaca mulatta). II.Juvenile ocular hypertension and its apparent relationship to ocular growth. *Exp Eye Res* 1981;32:407-417.

195. Shiose Y. The aging effect on intraocular pressure in an apparently normal population. *Arch Ophthalmol* 1984;102:883-887.

196. Armaly MF. ON THE DISTRIBUTION OF APPLANATION PRESSURE. I. STATISTICAL FEATURES AND THE EFFECT OF AGE, SEX, AND FAMILY HISTORY OF GLAUCOMA. *Arch Ophthalmol* 1965;73:11-18.

197. Goldberg I, Hollows FC, Kass MA, et al. Systemic factors in patients with low-tension glaucoma. *Br J Ophthalmol* 1981;65:56-62.

198. Oliver JAC, Cottrell BC, Newton JR, et al. Gonioscopy in the dog: inter-examiner variability and the search for a grading scheme. *J Small Anim Pract* 2017.

199. Aung T, Lim MC, Wong TT, et al. Molecular analysis of CHX10 and MFRP in Chinese subjects with primary angle closure glaucoma and short axial length eyes. *Mol Vis* 2008;14:1313-1318.

200. Chakrabarti S, Ghanekar Y, Kaur K, et al. A polymorphism in the CYP1B1 promoter is functionally associated with primary congenital glaucoma. *Hum Mol Genet* 2010;19:4083-4090.

201. Markiewicz L, Majsterek I, Przybylowska K, et al. Gene polymorphisms of the MMP1, MMP9, MMP12, IL-1beta and TIMP1 and the risk of primary open-angle glaucoma. *Acta Ophthalmol* 2013;91:e516-523.

202. Micheal S, Yousaf S, Khan MI, et al. Polymorphisms in matrix metalloproteinases MMP1 and MMP9 are associated with primary open-angle and angle closure glaucoma in a Pakistani population. *Mol Vis* 2013;19:441-447.

203. Mossbock G, Weger M, Faschinger C, et al. Role of functional single nucleotide polymorphisms of MMP1, MMP2, and MMP9 in open angle glaucomas. *Mol Vis* 2010;16:1764-1770.

204. Mabuchi F, Sakurada Y, Kashiwagi K, et al. Association between SRBD1 and ELOVL5 Gene Polymorphisms and Primary Open-Angle Glaucoma. *Investigative Ophthalmology & Visual Science* 2011;52:4626-4629.

205. Oliver JAC, Ricketts SL, Kuehn MH, et al. Primary closed angle glaucoma in the Basset Hound: Genetic investigations using genome-wide association and RNA sequencing strategies. *Molecular Vision* 2019;25:93-105.

206. Axenovich T, Zorkoltseva I, Belonogova N, et al. Linkage and association analyses of glaucoma related traits in a large pedigree from a Dutch genetically isolated population. *J Med Genet* 2011;48:802-809.

207. Bianchi M, Dahlgren S, Massey J, et al. A Multi-Breed Genome-Wide Association Analysis for Canine Hypothyroidism Identifies a Shared Major Risk Locus on CFA12. *PLoS One* 2015;10:e0134720.

208. Hanon O, Vidal JS, Lehmann S, et al. Plasma amyloid levels within the Alzheimer's process and correlations with central biomarkers. *Alzheimers Dement* 2018.

209. Ridler C. Alzheimer disease: Blood amyloid-beta successfully signals AD. *Nat Rev Neurol* 2018.

210. Villemagne VL, Dore V, Burnham SC, et al. Imaging tau and amyloid-beta proteinopathies in Alzheimer disease and other conditions. *Nat Rev Neurol* 2018.

211. Gama IF, Almeida LD. De novo intraocular amyloid deposition after hepatic transplantation in familial amyloidotic polyneuropathy. *World J Transplant* 2017;7:243-249.

212. Wostyn P, De Groot V, Van Dam D, et al. Age-related macular degeneration, glaucoma and Alzheimer's disease: amyloidogenic diseases with the same glymphatic background? *Cell Mol Life Sci* 2016;73:4299-4301.

213. Downs LM, Wallin-Hakansson B, Bergstrom T, et al. A novel mutation in TTC8 is associated with progressive retinal atrophy in the golden retriever. *Canine Genet Epidemiol* 2014;1:4.

214. Downs LM, Mellersh CS. An Intronic SINE insertion in FAM161A that causes exon-skipping is associated with progressive retinal atrophy in Tibetan Spaniels and Tibetan Terriers. *PLoS One* 2014;9:e93990.

215. Taft RJ, Pang KC, Mercer TR, et al. Non-coding RNAs: regulators of disease. *J Pathol* 2010;220:126-139.

216. Ying SY, Lin SL. Current perspectives in intronic micro RNAs (miRNAs). *J Biomed Sci* 2006;13:5-15.

217. Vithana EN, Khor CC, Qiao C, et al. Genome-wide association analyses identify three new susceptibility loci for primary angle closure glaucoma. *Nat Genet* 2012;44:1142-1146.

218. Jiang B, Harper MM, Kecova H, et al. Neuroinflammation in advanced canine glaucoma. *Mol Vis* 2010;16:2092-2108.

219. Oliver JAC, Rustidge S, Pettitt L, et al. Evaluation of ADAMTS17 in Chinese Shar-Pei with primary open-angle glaucoma, primary lens luxation, or both. *Am J Vet Res* 2018;79:98-106.

220. Grimm DG, Azencott CA, Aicheler F, et al. The evaluation of tools used to predict the impact of missense variants is hindered by two types of circularity. *Hum Mutat* 2015;36:513-523.

221. Livak KJ. Allelic discrimination using fluorogenic probes and the 5' nuclease assay. *Genet Anal* 1999;14:143-149.

222. Sim NL, Kumar P, Hu J, et al. SIFT web server: predicting effects of amino acid substitutions on proteins. *Nucleic Acids Res* 2012;40:W452-457.

223. Kelwick R, Desanlis I, Wheeler GN, et al. The ADAMTS (A Disintegrin and Metalloproteinase with Thrombospondin motifs) family. *Genome Biol* 2015;16:113.

224. Apte SS. A disintegrin-like and metalloprotease (reprolysin type) with thrombospondin type 1 motifs: the ADAMTS family. *Int J Biochem Cell Biol* 2004;36:981-985.

225. Apte SS. A disintegrin-like and metalloprotease (reprolysin-type) with thrombospondin type 1 motif (ADAMTS) superfamily: functions and mechanisms. *J Biol Chem* 2009;284:31493-31497.

226. Dubail J, Apte SS. Insights on ADAMTS proteases and ADAMTS-like proteins from mammalian genetics. *Matrix Biol* 2015.

227. Chandra A, Aragon-Martin JA, Hughes K, et al. A genotype-phenotype comparison of ADAMTSL4 and FBN1 in isolated ectopia lentis. *Invest Ophthalmol Vis Sci* 2012;53:4889-4896.

228. Greene VB, Stoetzel C, Pelletier V, et al. Confirmation of ADAMTSL4 mutations for autosomal recessive isolated bilateral ectopia lentis. *Ophthalmic Genet* 2010;31:47-51.

229. Li J, Jia X, Li S, et al. Mutation survey of candidate genes in 40 Chinese patients with congenital ectopia lentis. *Mol Vis* 2014;20:1017-1024.

230. Alexander JP, Samples JR, Van Buskirk EM, et al. Expression of matrix metalloproteinases and inhibitor by human trabecular meshwork. *Invest Ophthalmol Vis Sci* 1991;32:172-180.

231. Bradley JM, Vranka J, Colvis CM, et al. Effect of matrix metalloproteinases activity on outflow in perfused human organ culture. *Invest Ophthalmol Vis Sci* 1998;39:2649-2658.

232. Dubail J, Apte SS. Insights on ADAMTS proteases and ADAMTS-like proteins from mammalian genetics. *Matrix Biol* 2015;44-46c:24-37.

233. Marchini J, Howie B, Myers S, et al. A new multipoint method for genome-wide association studies by imputation of genotypes. *Nat Genet* 2007;39:906-913.

234. Spencer CC, Su Z, Donnelly P, et al. Designing genome-wide association studies: sample size, power, imputation, and the choice of genotyping chip. *PLoS Genet* 2009;5:e1000477.

235. Utsunomiya YT, Ribeiro ES, Quintal AP, et al. Genome-Wide Scan for Visceral Leishmaniasis in Mixed-Breed Dogs Identifies Candidate Genes Involved in T Helper Cells and Macrophage Signaling. *PLoS One* 2015;10:e0136749.

236. Vernau KM, Runstadler JA, Brown EA, et al. Genome-wide association analysis identifies a mutation in the thiamine transporter 2 (SLC19A3) gene associated with Alaskan Husky encephalopathy. *PLoS One* 2013;8:e57195.

237. Li Y, Willer C, Sanna S, et al. Genotype imputation. *Annu Rev Genomics Hum Genet* 2009;10:387-406.

238. Hayward JJ, Castelhano MG, Oliveira KC, et al. Complex disease and phenotype mapping in the domestic dog. *Nat Commun* 2016;7:10460.

239. Baker LA, Kirkpatrick B, Rosa GJ, et al. Genome-wide association analysis in dogs implicates 99 loci as risk variants for anterior cruciate ligament rupture. *PLoS One* 2017;12:e0173810.

240. Marchini J, Howie B. Genotype imputation for genome-wide association studies. *Nat Rev Genet* 2010;11:499-511.

241. Clark AG, Li J. Conjuring SNPs to detect associations. *Nat Genet* 2007;39:815-816.

242. Sabeti PC, Varilly P, Fry B, et al. Genome-wide detection and characterization of positive selection in human populations. *Nature* 2007;449:913-918.

243. Cai N, Bigdeli TB, Kretzschmar WW, et al. 11,670 whole-genome sequences representative of the Han Chinese population from the CONVERGE project. *Sci Data* 2017;4:170011.

244. Feuk L, Carson AR, Scherer SW. Structural variation in the human genome. *Nat Rev Genet* 2006;7:85-97.

245. Craddock N, Hurles ME, Cardin N, et al. Genome-wide association study of CNVs in 16,000 cases of eight common diseases and 3,000 shared controls. *Nature* 2010;464:713-720.

246. Hollox EJ, Huffmeier U, Zeeuwen PL, et al. Psoriasis is associated with increased beta-defensin genomic copy number. *Nat Genet* 2008;40:23-25.

247. Olsson M, Meadows JR, Truve K, et al. A novel unstable duplication upstream of HAS2 predisposes to a breed-defining skin phenotype and a periodic fever syndrome in Chinese Shar-Pei dogs. *PLoS Genet* 2011;7:e1001332.

248. Salmon Hillbertz NH, Isaksson M, Karlsson EK, et al. Duplication of FGF3, FGF4, FGF19 and ORAOV1 causes hair ridge and predisposition to dermoid sinus in Ridgeback dogs. *Nat Genet* 2007;39:1318-1320.

249. Molin AM, Berglund J, Webster MT, et al. Genome-wide copy number variant discovery in dogs using the CanineHD genotyping array. *BMC Genomics* 2014;15:210.

250. Schierding W, Cutfield WS, O'Sullivan JM. The missing story behind Genome Wide Association Studies: single nucleotide polymorphisms in gene deserts have a story to tell. *Front Genet* 2014;5:39.

251. Huang Q. Genetic study of complex diseases in the post-GWAS era. *J Genet Genomics* 2015;42:87-98.

252. de Leeuw CA, Mooij JM, Heskes T, et al. MAGMA: generalized gene-set analysis of GWAS data. *PLoS Comput Biol* 2015;11:e1004219.

253. Hammerschlag AR, Stringer S, de Leeuw CA, et al. Genome-wide association analysis of insomnia complaints identifies risk genes and genetic overlap with psychiatric and metabolic traits. *Nat Genet* 2017;49:1584-1592.

254. Karlskov-Mortensen P, Proschowsky HF, Gao F, et al. Identification of the mutation causing progressive retinal atrophy in Old Danish Pointing Dog. *Anim Genet* 2018.

255. Bauer A, Jagannathan V, Hogler S, et al. MKLN1 splicing defect in dogs with lethal acrodermatitis. *PLoS Genet* 2018;14:e1007264.

256. Bauer A, Waluk DP, Galichet A, et al. A de novo variant in the ASPRV1 gene in a dog with ichthyosis. *PLoS Genet* 2017;13:e1006651.

257. Momtaz R, Ghanem NM, El-Makky NM, et al. Integrated analysis of SNP, CNV and gene expression data in genetic association studies. *Clin Genet* 2018;93:557-566.

258. Maatta M, Tervahartiala T, Harju M, et al. Matrix metalloproteinases and their tissue inhibitors in aqueous humor of patients with primary open-angle glaucoma, exfoliation syndrome, and exfoliation glaucoma. *J Glaucoma* 2005;14:64-69.

259. Thakur N, Kupani M, Pandey RK, et al. Genetic association of -1562C>T polymorphism in the MMP9 gene with primary glaucoma in a north Indian population. *PLoS One* 2018;13:e0192636.

260. Wu MY, Wu Y, Zhang Y, et al. Associations between matrix metalloproteinase gene polymorphisms and glaucoma susceptibility: a meta-analysis. *BMC Ophthalmol* 2017;17:48.

261. Suh W, Won HH, Kee C. The Association of Single-Nucleotide Polymorphisms in the MMP-9 Gene with Normal Tension Glaucoma and Primary Open-Angle Glaucoma. *Curr Eye Res* 2018;43:534-538.

262. Chen X, Chen Y, Wiggs JL, et al. Association of Matrix Metalloproteinase-9 (MMP9) Variants with Primary Angle Closure and Primary Angle Closure Glaucoma. *PLoS One* 2016;11:e0157093.

263. Roy A, Kucukural A, Zhang Y. I-TASSER: a unified platform for automated protein structure and function prediction. *Nat Protoc* 2010;5:725-738.

264. Tektas OY, Lutjen-Drecoll E. Structural changes of the trabecular meshwork in different kinds of glaucoma. *Exp Eye Res* 2009;88:769-775.

Appendices

I. Buffers and solutions

- Nucleon Reagent A: 6.304 g Tris Hydrochloride, 438.12 g Sucrose, 4.066 g MgCl2, 40 mL Triton X-100, Make up to 4 L with MQ, Adjust to pH 8.0 with 40 % NaOH.
- Nucleon Reagent B: 63 g Tris Hydrochloride, 22.3 g EDTA, 8.8 g NaCl, 800 mL MQ, Adjust to pH 8.0 with 2M NaOH, Adjust to 1 litre with MQ and then add 10 g Sodium Dodecyl Sulphate (SDS).
- 1X TE Buffer (10mM Tris-HCL, 0.1mM EDTA): 10 mL 1 M Tris-hydrochloride, 2 mL 500 mM EDTA, Add MQ to 1 L, Adjust to pH 8.0.
- STOP: 10 mL Glycerol, 4 mL 500 mM EDTA, 1 mL 1M Tris, 1 mL Bromophenol blue. Diluted 1:5 with 1X TAE Buffer.
- 50X TAE Buffer: 242 g Tris base, 57.1 mL Glacial acetic acid, 37.2 g EDTA, Add double-distilled water to 1 L, Adjust to pH 8.0.
- 2-Log DNA ladder: 120 µL STOP, 240 µL 1X TAE Buffer, 40 µL 500 µg/mL 2-Log DNA ladder.
- SBDD Buffer: 160 mL 1M Tris base, 3 mL 1 M MgCl2, 50 mL Tetramethylenesulphone, 290 mL MQ.

II. PCR and sequencing reaction components

Table A1. Microsatellite genotyping by AFLP.

Component	Volume/reaction (µL)	Final concentration
Genomic DNA (20ng/µL)	2.00	
dNTPs (1.5mM)	1.60	200µM
Tailed Forward Primer (20µM)	0.10	0.17µM
Reverse Primer (20µM)	0.25	0.42µM
FAM-labelled tailed primer (10µM)	0.60	0.5µM
HotStartTaq (5U/µL)	0.25	0.10U/µL
Buffer (10X)	1.20	1X
MilliQ	6.00	
Total	12.00	

Table A2. ADAMTS17 exon resequencing.

Component	Volume/reaction (µL)	Final concentration
Genomic DNA (20ng/µL)	2.00	
dNTPs (1.5mM)	1.60	200µM
Forward Primer (20µM)	0.50	0.83µM
Reverse Primer (20µM)	0.50	0.83µM
HotStartTaq (5U/µL)	0.12	0.05U/µL
Buffer (10X)	1.20	1X
MilliQ	6.08	
Total	12.00	

*The Qiagen Q solution additive (1X) was used for GC rich amplicons (exons 1 & 2).

Table A3. BH POAG variant genotyping.

Component	Volume/reaction (µL)	Final concentration
Genomic DNA (20ng/µL)	2.00	
dNTPs (1.5mM)	1.60	200µM
Forward Primer (20µM)	0.24	0.4µM
Reverse Primer (20µM)	0.24	0.4µM
HotStartTaq (5U/µL)	0.48	0.04U/µL
Buffer (10X)	1.20	1X
MilliQ	6.24	
Total	12.00	

Table A4. BFdB and SP variant genotyping.

Component	Volume/reaction (µL)	Final concentration
Genomic DNA (20ng/µL)	2.00	
dNTPs (1.5mM)	1.60	200µM
Forward Primer (20µM)	0.5	0.83µM
Reverse Primer (20µM)	0.5	0.83µM
HotStartTaq (5U/µL)	0.12	0.05U/µL
Buffer (10X)	1.20	1X
MilliQ	6.08	
Total	12.00	

Table A5. BFdB POAG variant assay.

Component	Volume/reaction (µL)	Final concentration
Genomic DNA (20ng/µL)	2.00	
Kapa Probe Fast qPCR (2X)	4.00	200µM
Primer/probe assay (40X)	0.2	0.83µM
MilliQ	1.80	
Total	8.00	

III. Thermal cycling parameters

Table A6. Microsatellite genotyping.

Step	Temperature	Time
Initiation	94 ºC	4 m
Denaturation	94 ºC	30 s 30 s X 30 1 m
Annealing	55 ºC	
Elongation	72 ºC	
Denaturation	94 ºC	30 s 30 s X 8 1 m
Annealing	50 ºC	
Elongation	72 ºC	
Final elongation	72 ºC	30 m
Final hold	12 ºC	∞

Table A7. ADAMTS17 exon resequencing.

Step	Temperature	Time
Initiation	95 ºC	10 m
Denaturation	95 ºC	30 s 30 s X 35 1 m
Annealing	56 ºC	
Elongation	72 ºC	
Final elongation	72 ºC	10 m
Final hold	12 ºC	∞

Table A8. BH POAG candidate variant genotyping.

Step	Temperature	Time
Initiation	95 ºC	5 m
Denaturation	95 ºC	30 s 30 s X 35 30 s
Annealing	60 ºC	
Elongation	72 ºC	
Final elongation	72 ºC	30 m
Final hold	12 ºC	∞

Table A9. BFdB POAG candidate variant genotyping.

Step	Temperature	Time
Initiation	95 ºC	5 m
Denaturation	95 ºC	30 s 30 s X 35 30 s
Annealing	57 ºC	
Elongation	72 ºC	
Final elongation	72 ºC	5 m
Final hold	12 ºC	∞

Table A10. SP POAG candidate variant genotyping.

Step	Temperature	Time
Initiation	95 ºC	5 m
Denaturation	95 ºC	30 s

Annealing	60 ºC	30 s X 35 30 s
Elongation	72 ºC	
Final elongation	72 ºC	5 m
Final hold	12 ºC	∞

Table A11. Allelic discrimination assay.

Step	**Temperature**	**Time**	
Denaturation	95 ºC	3 s 15s	X 40
Annealing	60 ºC		
Final hold	12 ºC	∞	

IV. Primers

Table A12. Primers for microsatellites flanking candidate genes.

Candidate gene microsatellite name	Microsatellite*	Start genomic coordinate (CanFam3.1)	Tail-Forward primer sequence (5'-3')+	Reverse primer sequence (5'-3')	Product size (bp)	Tm (°C)
ADAMTS10_M1	(GT)22	Chr20:53,027,087	GGTGGTGTTTCAGACCAGTTG	GGGAGACACTAGAGAAAGAGGAAC	186	57
ADAMTS10_M2	(GA)14	Chr20:53,132,686	CAGATGAGCTGTCCTCCTTCC	GTGAAACCAGTCACCATCTCC	113	57
ADAMTS17_M1	(CA)19	Chr3:40,636,343	GGCTACCTTGCATCAGTAGCTT	GAGGTCAGTGAAAGATGCAGTG	136	57
ADAMTS17_M2	(GT)19	Chr3:40,920,305	TCCAGAGGACACAGTGGAACT	TAGCAATGGGAACGTCTGTTT	159	57
C1QTNF5_M1	(CA)15	Chr5:14,349,500	ACTCATCCATTCCCAGGTAGC	GTTAAGGATCCTGTGTGTCAAGG	100	57
C1QTNF5_M2	(CA)13	Chr5:14,630,315	ATGTGGCACCATTTGTGAGC	GGGCACTACTCTACCTGGTTCC	180	57
CHX10_M1	(GT)16	Chr8:46,605,605	ATGTCAGCAGAGCAGGTATGG	ATTCCTGAGCACTGCAAACC	169	57
CHX10_M2	(CA)16	Chr8:47,514,640	GAGGATATGAGGTCAAGGATGG	AGGTTCCCATCAACAATTTCC	144	57
COL1A2_M1	(CA)17	Chr14:19,849,088	TCTCTCCAACACCTGAACCAC	TAATTGTTGGTGGAACCGAGA	137	57
COL1A2_M2	(CA)19	Chr14:20,593,102	AACCACAGGTGTGCTTAAAGG	GTTCCCTGCCATGTTTATGC	134	57
CYP1B1_M1	(CA)20	Chr17:30,265,057	TAGGGTGGGAGGAAGAGGATA	GTAAGTGCCCTGGTGTGGTAA	179	57
CYP1B1_M2	(GT)19	Chr17:30,339,848	TGGACCATCTTGCTTTGTACC	GGTCATTTGCCTTGATGTGAC	186	57
HGF_M1	(GT)15	Chr18:21,311,362	GCGGTTTAGAGCCACCTTTAG	TCATTCTGGATGAATAGGCTTG	193	57
HGF_M2	(CA)19	Chr18:21,382,566	TGGTTGGTAAATTAATAGGCAACA	AAACCAACATGTTTCCCTTCC	176	57
MMP_M1	(CA)17	Chr24:33,120,996	CTGCACTTGCATTACCTCTGG	TTAAGAGCTCAGGCTTTGCTG	192	57
MMP_M2	(CA)18	Chr24:33,312,853	AGGGCACTCAGGAAGACAGG	CACAGGGAGTCTGCTTCTCC	174	57
NOS3_M1	(CA)18	Chr16:14,901,925	AAGCCTTGTGGCTTAGTGGAT	AACACCTCCTCCTTCCGTAGA	184	57
NOS3_M2	(CA)17	Chr16:15,224,341	TATGCATGTGTGCCCTCAGT	GGGCAAAGGCAAGGATATAAA	180	57
RAB22A_M1	(CA)16	Chr4:43,040,954	GTCTCCCTTCCCAATGAGG	GGACAAATGAGTAGCCCTTGG	177	57
RAB22A_M2	(CA)17	Chr4:43,173,556	AAGAAGAGAGCTGGGCAGATT	GAGGGAGCCTGGTCTTATTGT	153	57
SRBD1_M1	(GA)12	Chr10:47,753,474	GAGGCTGCTTGGAGTCTTAGG	TGATGGAAGTGACTTTGGTAGC	143	57
SRBD1_M2	(CA)20	Chr10:47,866,917	CTTAGGGATACAGAAACACATGG	TATTGGAAAGGAGGCATAAGG	173	57

M1 = microsatellite upstream of gene, M2 = microsatellite downstream of gene, *The number is the number of times the dinucleotide in brackets is repeated, +Tail= 5'-TGACCGGCAGCAAAATTG-3'

Table A13. PCR primers for PCAG candidate variant genotyping.

Target name/ genomic coordinate (CanFam3.1)	Forward primer sequence Reverse primer sequence	Amplicon size (bp)	Annealing temp (^{o}C)
NEB chr19:52,857,772	ACCAGTAAGGTGAGTGCTTTCC AGGCTATGATCTCAGAACTGATGC	103	57
CXCR chr37:24,861,167	TCCTTACCCTATCGAGTGGTTG GAGAGAGGCAGAGGAAGAAGG	278	57
ATRN chr24:17,727,188	TTTCTCTCCCTCCAAGACTGG TTCCCATAGTGAGCCATTAGGT	218	57
PTPRA chr24:18,222,425	TGGCTCAGTTGGTAAAGCATC GTCCTGGGTTGCCTCCTTAC	377	57
FCR chr:28:14,624,548	CTGCCCAAGAATCACAATTTC CCTATCCTCTTACTCATCTTTCTGAC	300	57
DDT chr28:19,274,452	GCCTGGAGAAACAGATTGCT TAAGGCCACATTGAGATTTGC	390	57
WSS Chr28:19,274,198	GTGGTTTACGTGGCAACATTT TTGGCCAAGAGATGAGCTG	291	57

Table A14. PCR Primers for *ADAMTS17* exon resequencing.

Target	Forward primer sequence Reverse primer sequence	Amplicon size (bp)	Annealing temp (°C)
Exon 1	TGATTTACCACGTTGGGTTTG AGCTGGAACTGGATCCGAAG	273	56
Exon 2 (5')	GCTGACGCGTCTCCTCTCTCCC CCGCCTCCTCCACCTCGAA	285	56
Exon 2 (3')	CCCCGGACCCCGAAAGC GCGACTAAGCGACGGGCAGA	334	56
Exon 3	ACATGAGGACCAGGCCAGA AGGGCTGCTACACATGAAATG	474	56
Exon 4	TTCGATGTGCCTCAGCTCTAC GACCCAGGCACTGAAACTACA	591	56
Exon 5	CCAACATCTTCCTCTGTTCCA GGAGAGCAGACAAGACTGACAA	300	56
Exon 6	CATGACCTGATCAACCACTGA TTACTGATGAGGATGCCAAGG	558	56
Exon 7	ATTGCTATGTGCAGGATGACC GCAACAGGAAAGGCAGAGTTT	293	56
Exon 8	GGTGAATCCCAAAGCATTACA GTAATCTCTCCCGTTCCCTGA	488	56
Exon 9	GTAGCCAAGTACAGGGCATCA CCTGGGAGAAATGAAGTAGGG	567	56
Exon 10	TCCAATGCCTGAGTCATCTTC AACTGCCTGTGAGGGTGTATG	434	56
Exon 11	TGAATTCCAAGTCCAAACCAG CCAGTGGAGCTTTAGGCACTAT	315	56
Exon 12	TGCAGTGATCTGGTGAGTGAG GCTTTGTTGAAGCTGAGATGC	426	56
Exon 13	GGAGGTTGCTTTGGAAACTCT ACTCTCCCAGAGTTGGGTCAT	490	56
Exon 14	GAACATGTGCTGGGTTTCTGT GTGGGCTTTATGCTCAGTCAC	490	56
Exon 15	CCTAGGCACCAACACTTGCT GCCTTTCAGCAAGCATAACAC	450	58
Exon 16	CTCAGAGTCAGACCAGCCTGT GCTTCCTTCCCTCTGTCATCT	468	56
Exon 17	CTGTGAGCCAGTCTTCCATTC ACCAGAACCCAGGTGATCTCT	432	56
Exon 18	TCTGAGGAACCCAAGAGTGAA GTTCCTGTGGAGAGACAGGTG	449	56
Exon 19	GCCATGTCTTACACACCCTCA GCAAGCAGAAGTCACTTAGCAA	468	56
Exon 20	TGAGTACATTTCCCTCCCTCA GGCAAGGACTGTGATACTTGG	458	56
Exon 21	TCAGACTCTAGATGCCCAGGA CTCTAGGGAGCATTGGGTTTC	490	56
Exon 22	AGCCTCCTTGTCCTGCATTAT AATCCCATCTCTGCAACCTCT	489	56
Exon 23	CGAGTGAGGGCAGCTTAGAGT TCAGGTTCACGCTCAAGTTCT	469	56

Table A15. Primers for amplification of POAG candidate causal variants in *ADAMTS17*.

Target	Forward primer sequence Reverse primer sequence	Amplicon size bp	Annealing temp (ºC)
Exon 2 19bp deletion (BH)	6FAM-ACGTGGAGGTGGTGGTGCTG CGAAGCTGCAGGTACAGGTC	190	60
Exon 11 SNP (BFdB)	ATCCAGATTCACAACCCTCCT GGAGATAGAAGTGTTCCTCTTGC	409	57
Exon 22 6bp deletion (SP)	AGCCTCCTTGTCCTGCATTAT TCTTGTCATTGCAGACCTCCT	287	60

Table A16. Allelic discrimination primers and probes used to genotype the BFdB POAG variant.

Assay name	Forward primer sequence Reverse primer sequence	Reporter 1 sequence (5'VIC)	Reporter 2 sequence (5'6-FAM)
BFdBPOAG	CTGCAAGACCAAGCTGGA ACTATTGAGTACAGTGCAGACCA	CCTGGACGGCACCGAGT	CCCTGGACAGCACCGAGT

Table A17. Primers for sequencing the SP and BH *ADAMTS17* mutations in cDNA. For each mutation, two pairs of primers were designed (SPPOAG 1 & 2 and BHPOAG 1 & 2).

Assay name	Target (exon / deletion)	Forward primer Reverse primer	Amplicon size bp	Annealing temp (ºC)
SPPOAG1	Exon 22 / 6bp deletion	CGAGGACTATTCAGGCTGCTA TCTTGTCATTGCAGACCTCCT	194	60
SPPOAG2	Exon 22 / 6bp deletion	GAGGTGTGCGAGGACTATTCA ATGTCCTGGCAGAGGTTCTTT	317	60
BHPOAG1	Exon 2 / 19bp deletion	GACGTGGAGGTGGTGCTG GCGAAGCTGCAGGTACAGG	192	61
BHPOAG2	Exon 2 / 19bp deletion	TGCTGCTGCTGCTGGTTT CCCGAGTAGAAGCACAGCTC	346	61

Table A18. *ADAMTS17* qRT-PCR assay.

Assay name	Forward primer sequence	Reverse primer sequence	Probe (5'FAM)
ADAMTS17	GGTCTCAATTTGGCCTTTACC	CTTTACCCACTCTCCTGACATG	ATCCTGTGCTGGC
TBP	AGCGAGGAAATATGCCAGAG	TTCAAGATTCAGAACATGGTGGG	TTCAAGATTCAGAA CATGGTGGG

V. Raw data collected for Chapter 4 (CD ROM)

Table A19. Data on breed, sex, age at examination, IOP (where taken), PLD percentage and equivalent ordinal grade.

VI. Genome-wide association Q-Q and MDS plots.

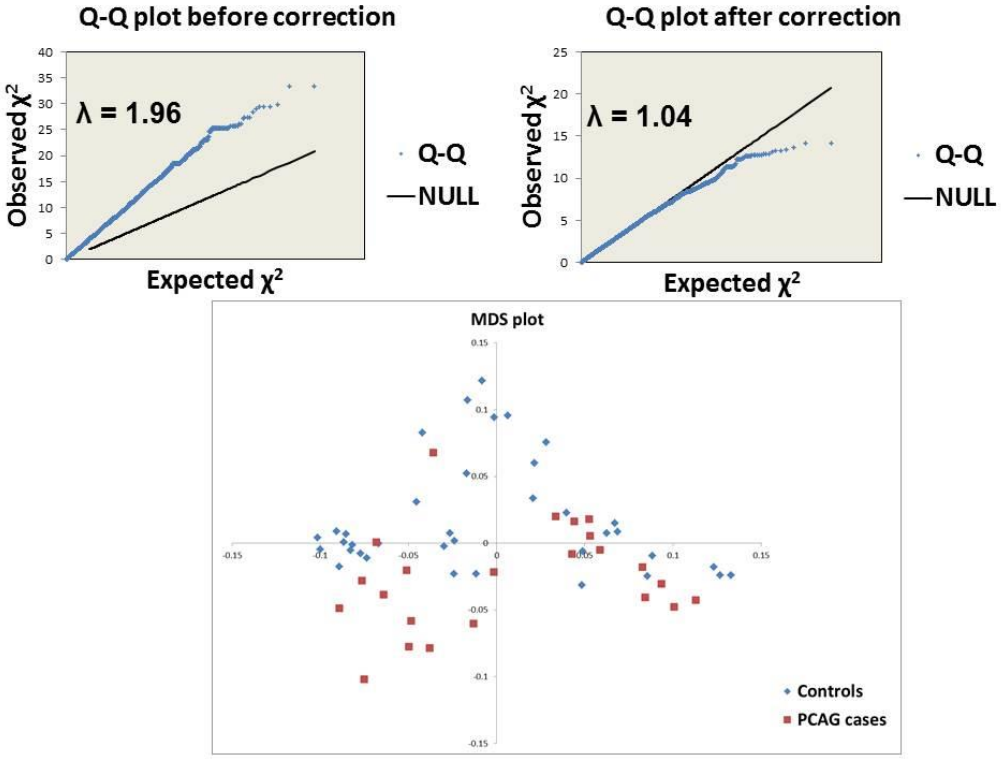

Figure A1. BH: PCAG cases and controls.

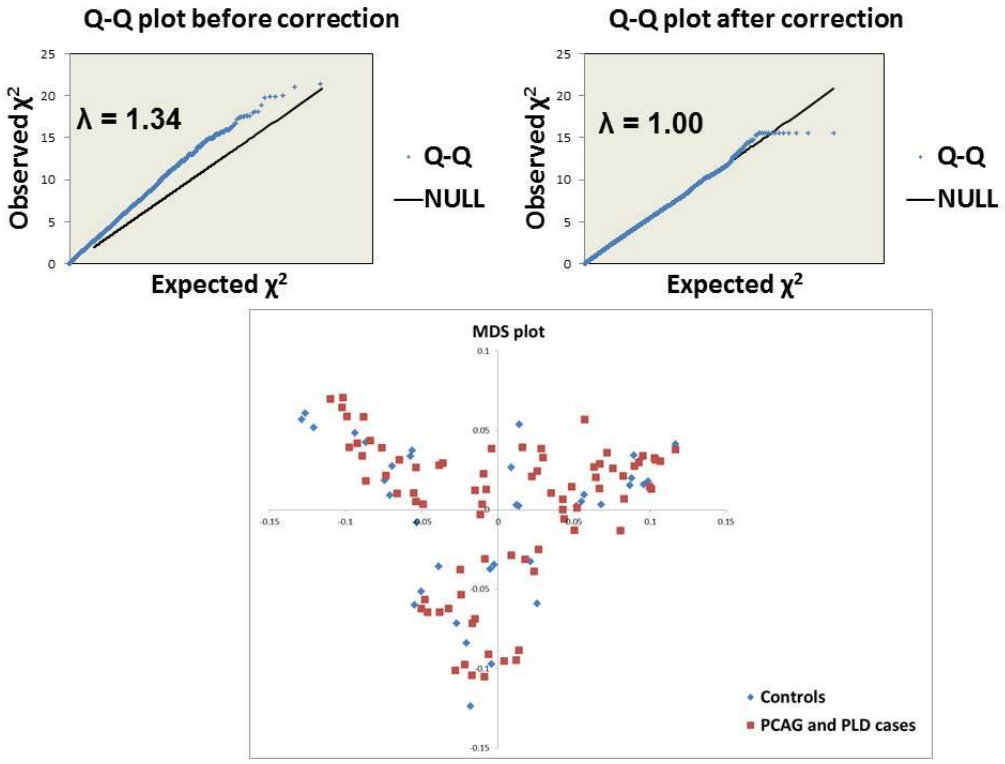

Figure A2. BH: PCAG and PLD cases and controls.

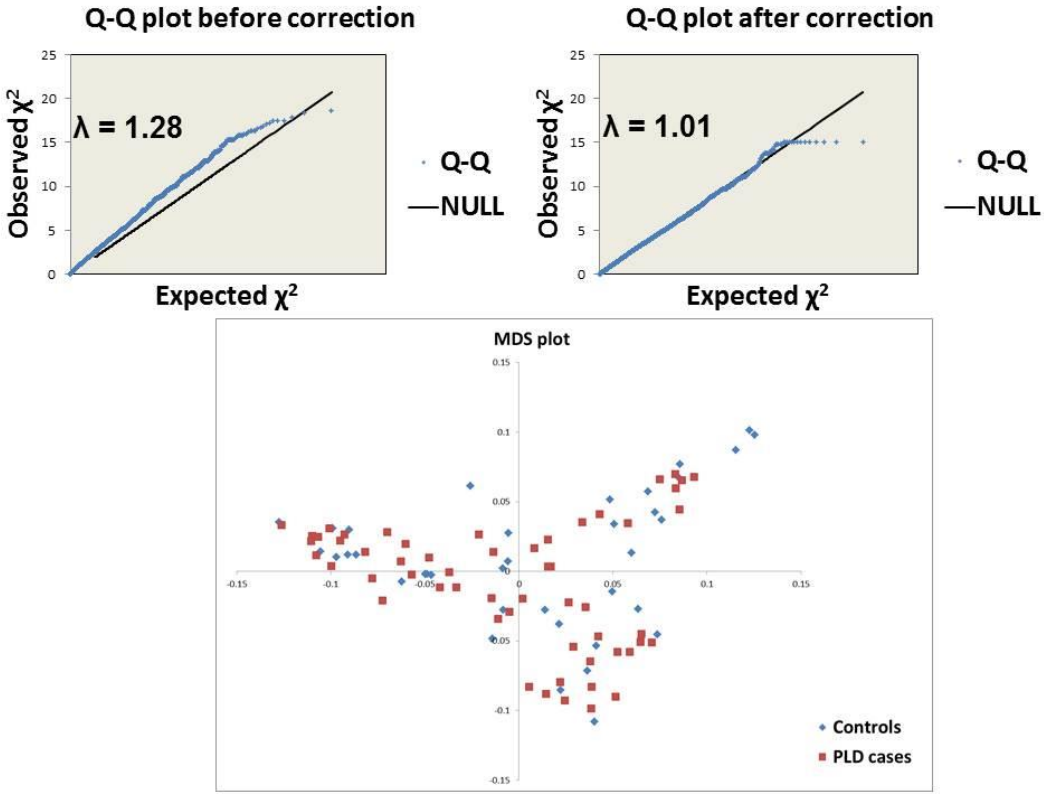

Figure A3. BH: PLD cases and controls.

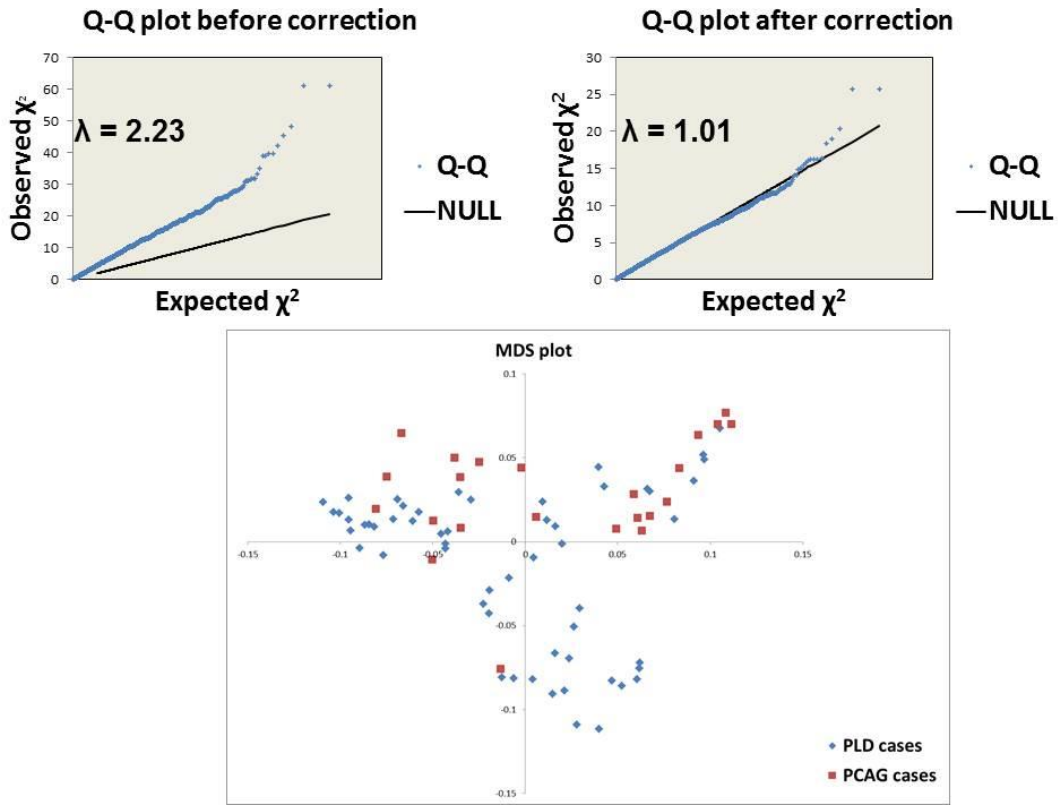

Figure A4. BH: PCAG cases and PLD cases.

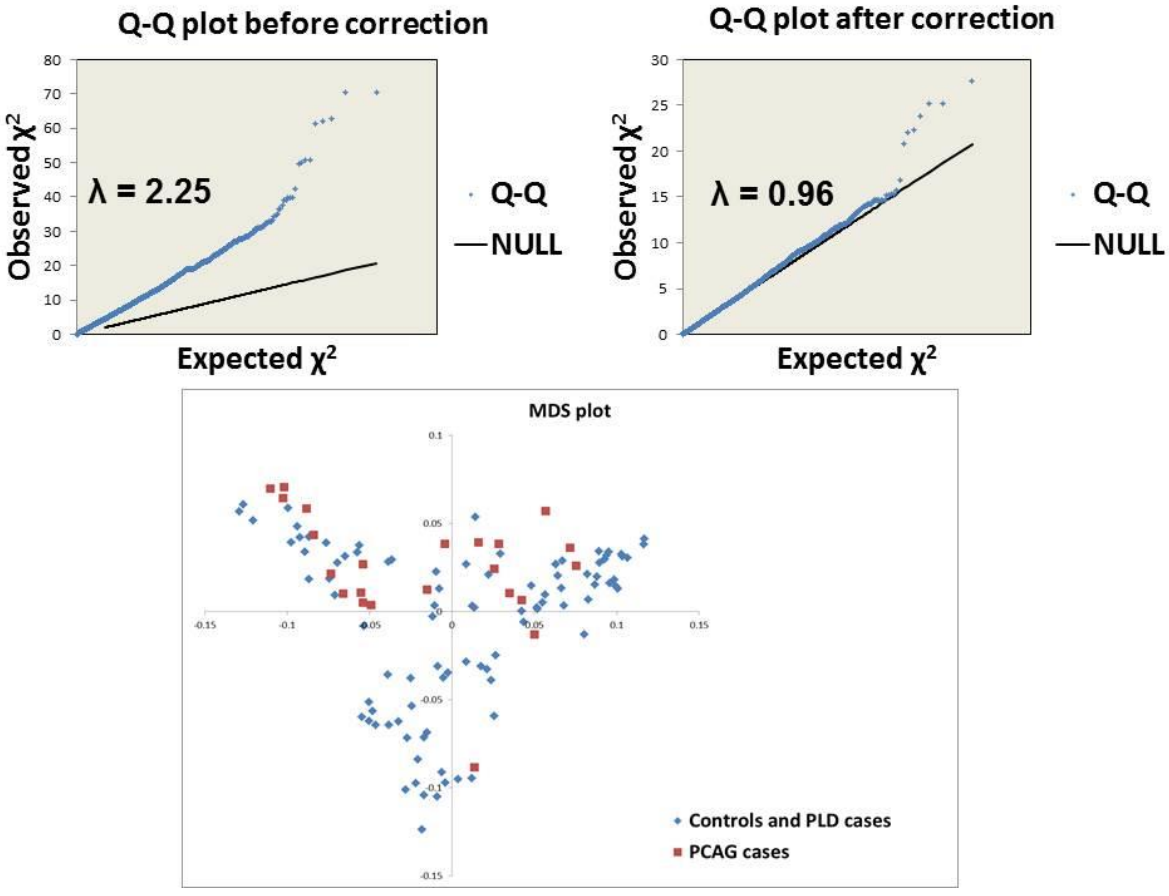

Figure A5. BH: PCAG cases and PLD cases and controls.

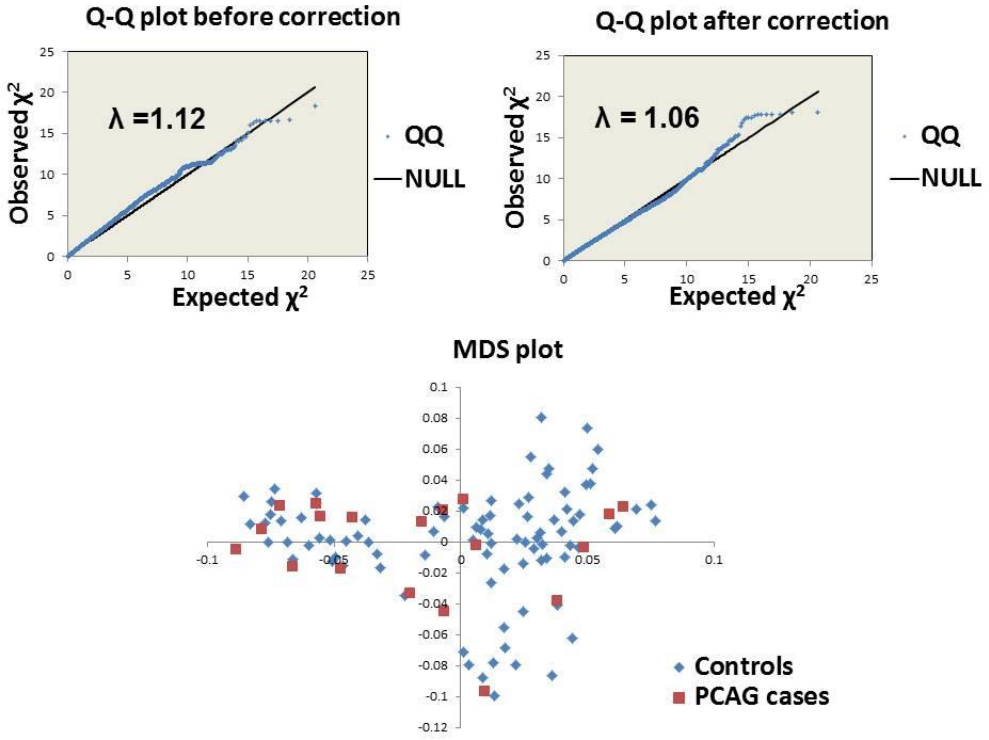

Figure A6. FCR: PCAG cases and controls.

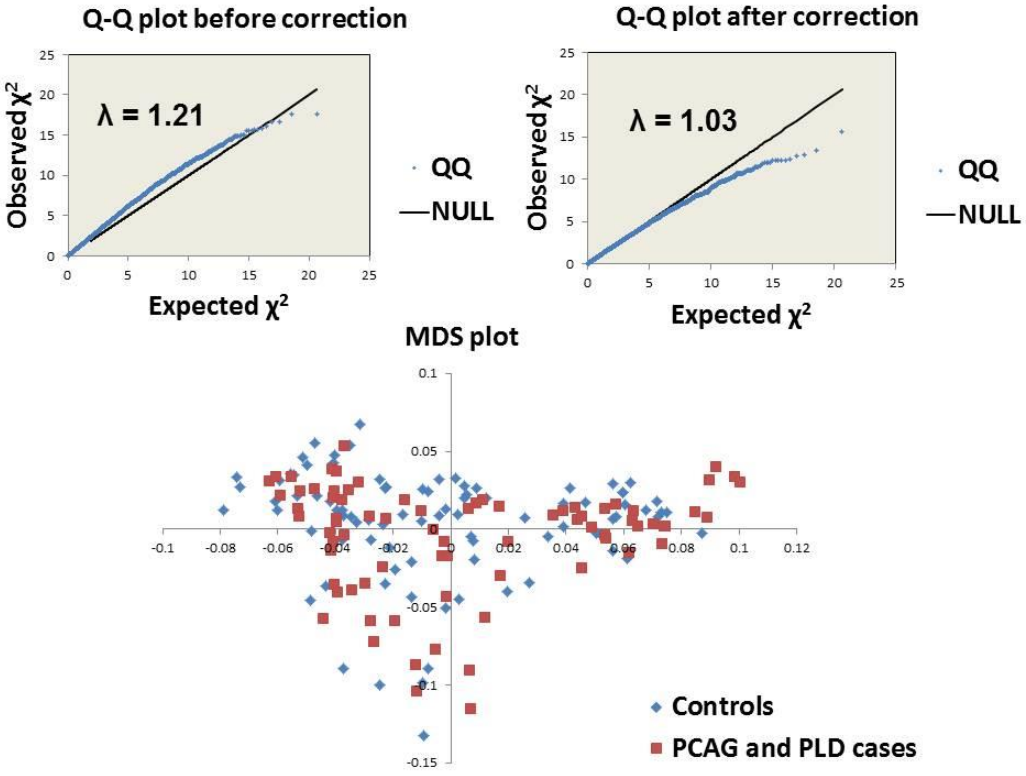

Figure A7. FCR: PCAG and PLD cases and controls.

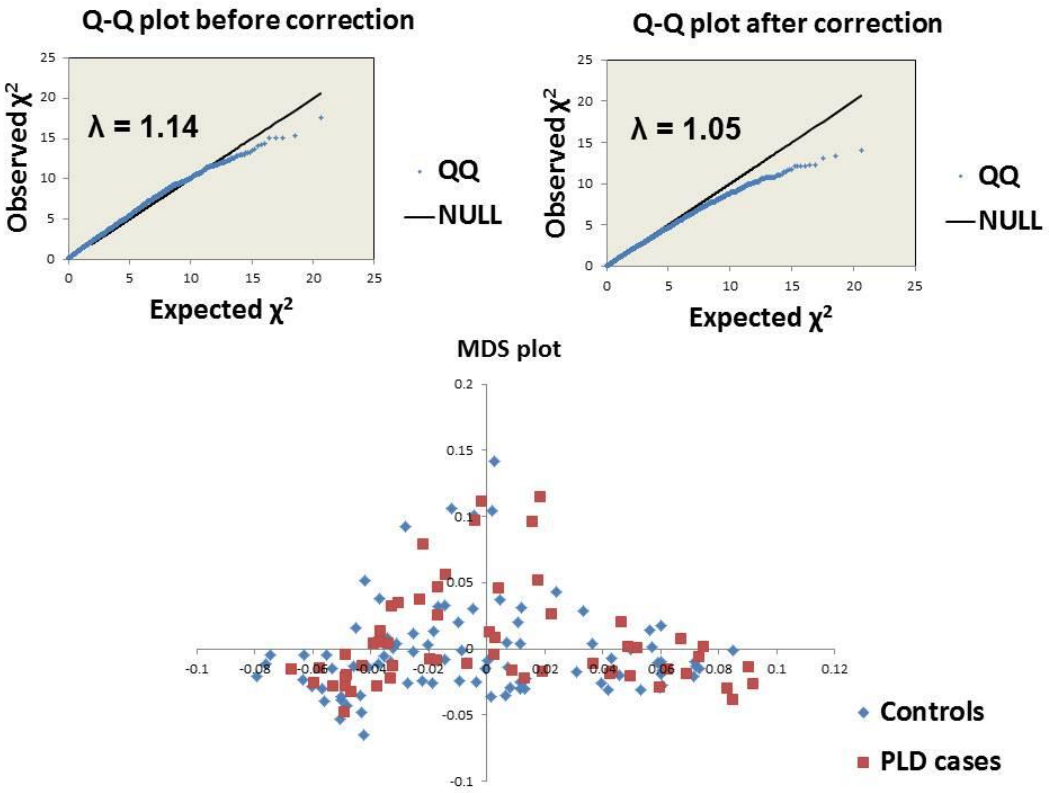

Figure A8. FCR: PLD cases and controls.

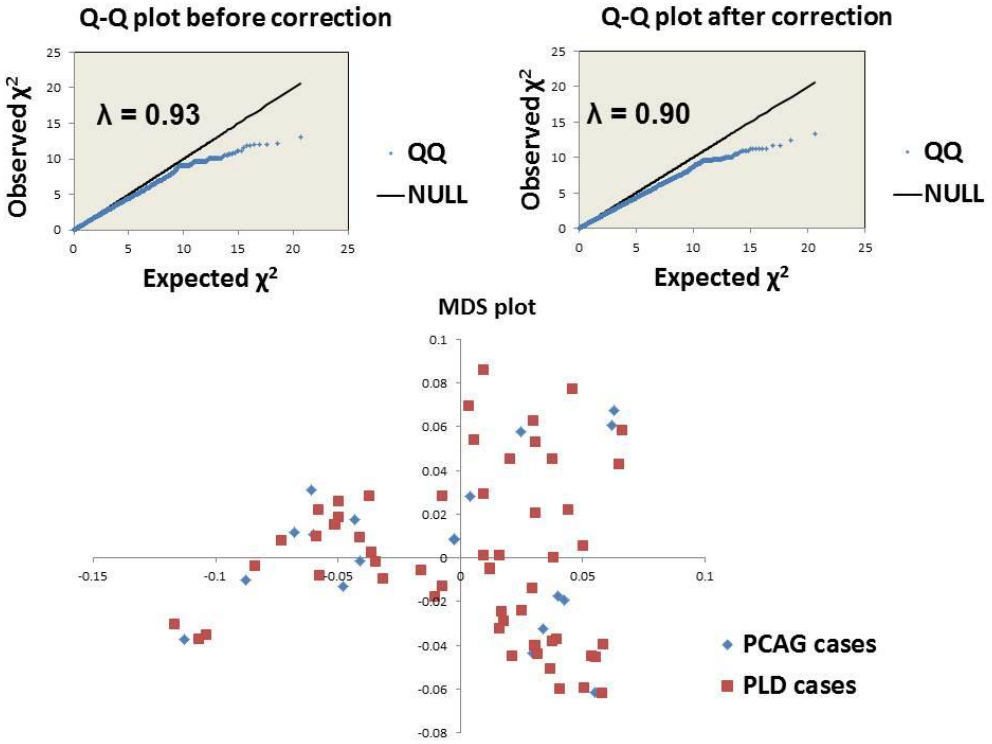

Figure A9. FCR: PCAG cases and PLD cases.

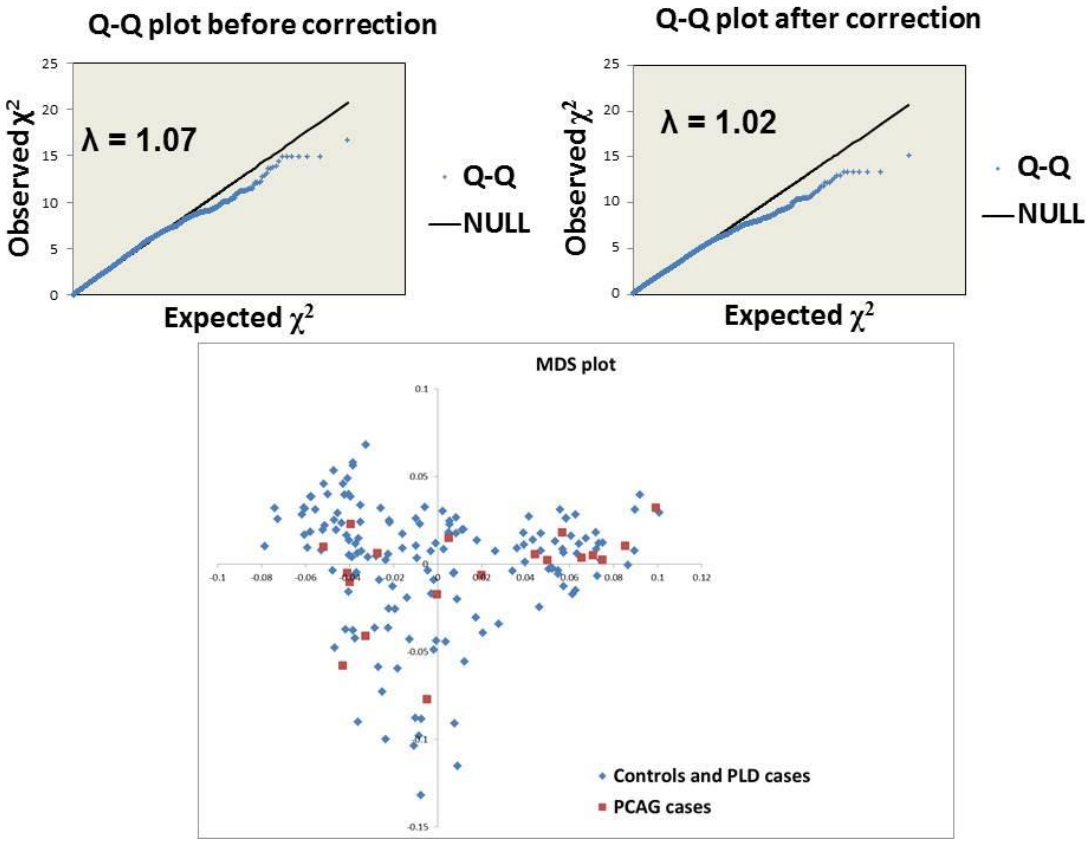

Figure A10. FCR: PCAG cases and PLD cases and controls.

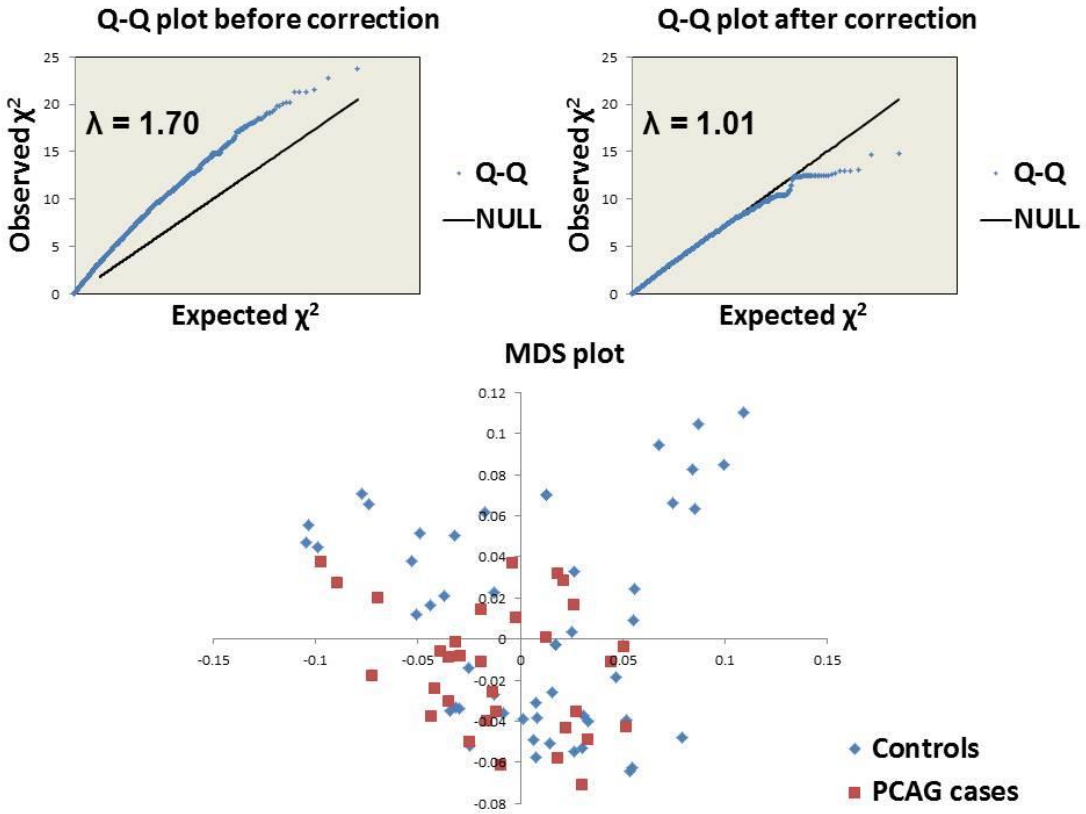

Figure A11. DDT: PCAG cases and controls.

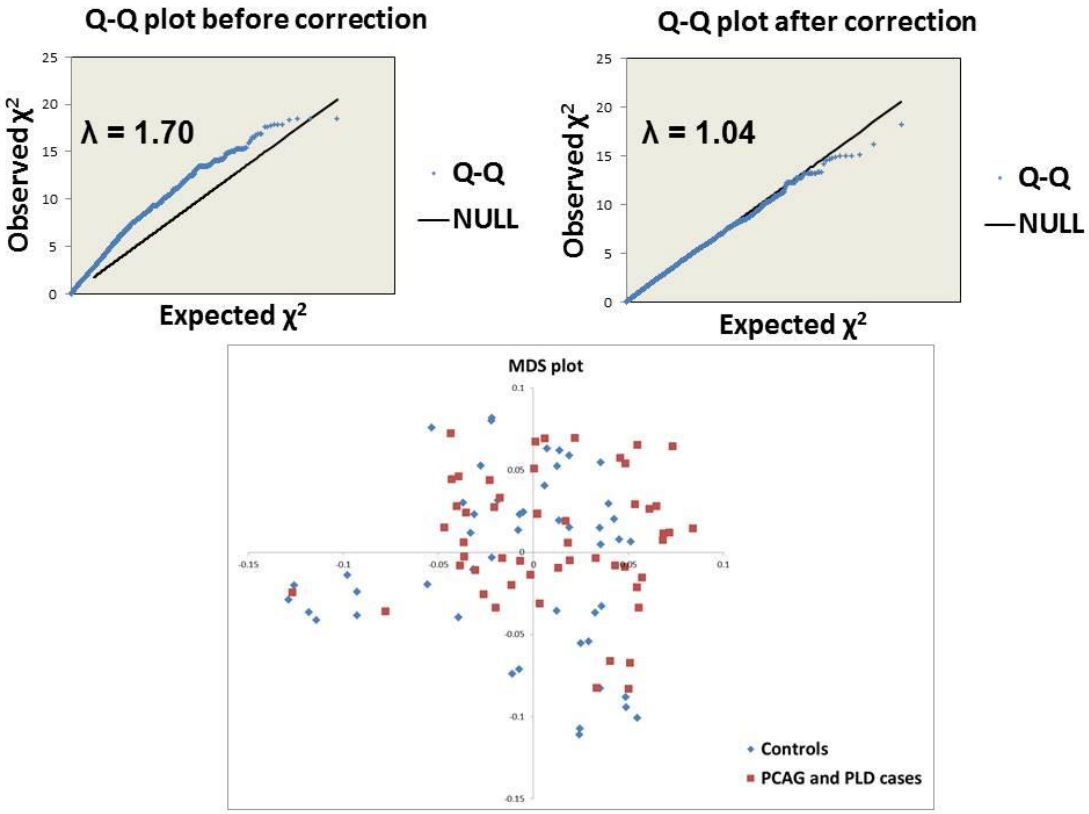

Figure A12. DDT: PCAG and PLD cases and controls.

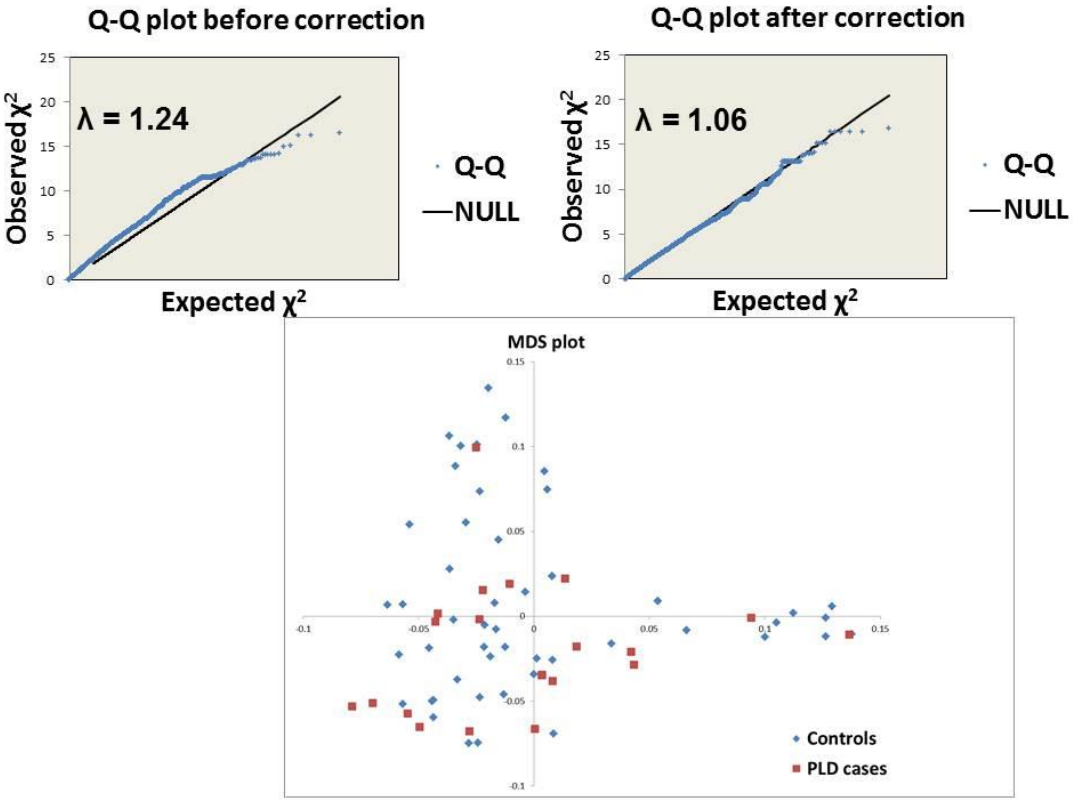

Figure A13. DDT: PLD cases and controls.

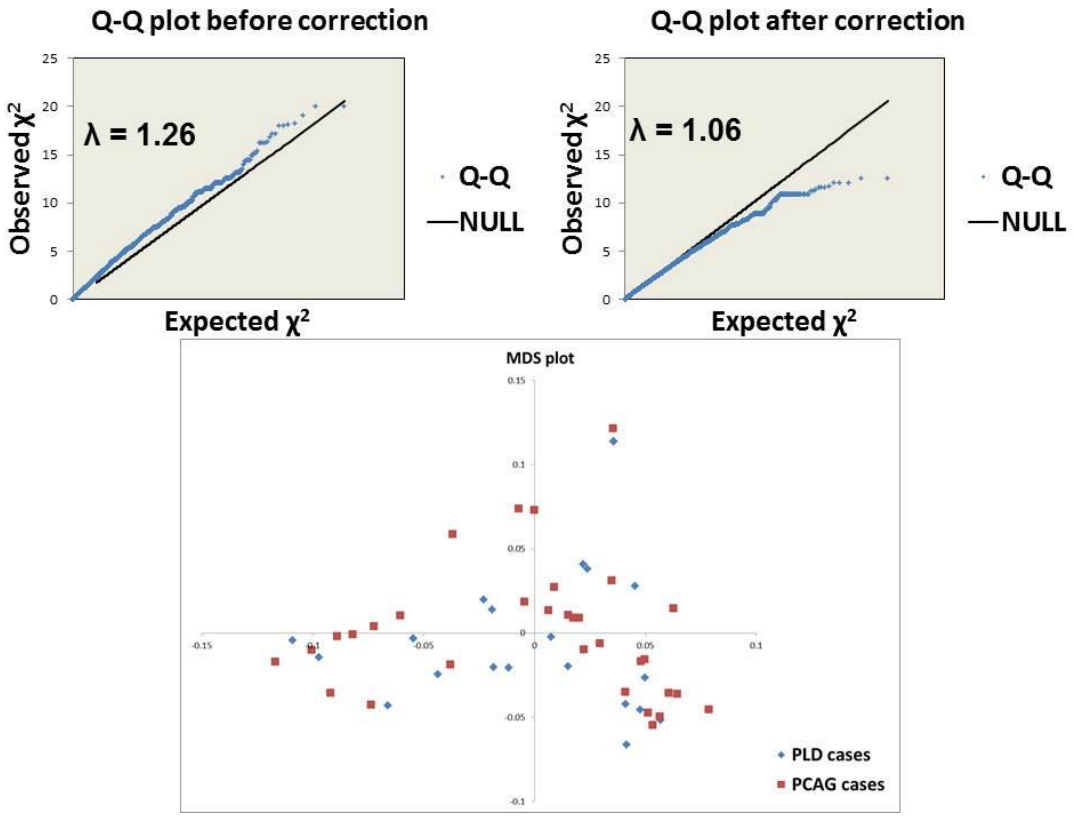

Figure A14. DDT: PCAG cases and PLD cases.

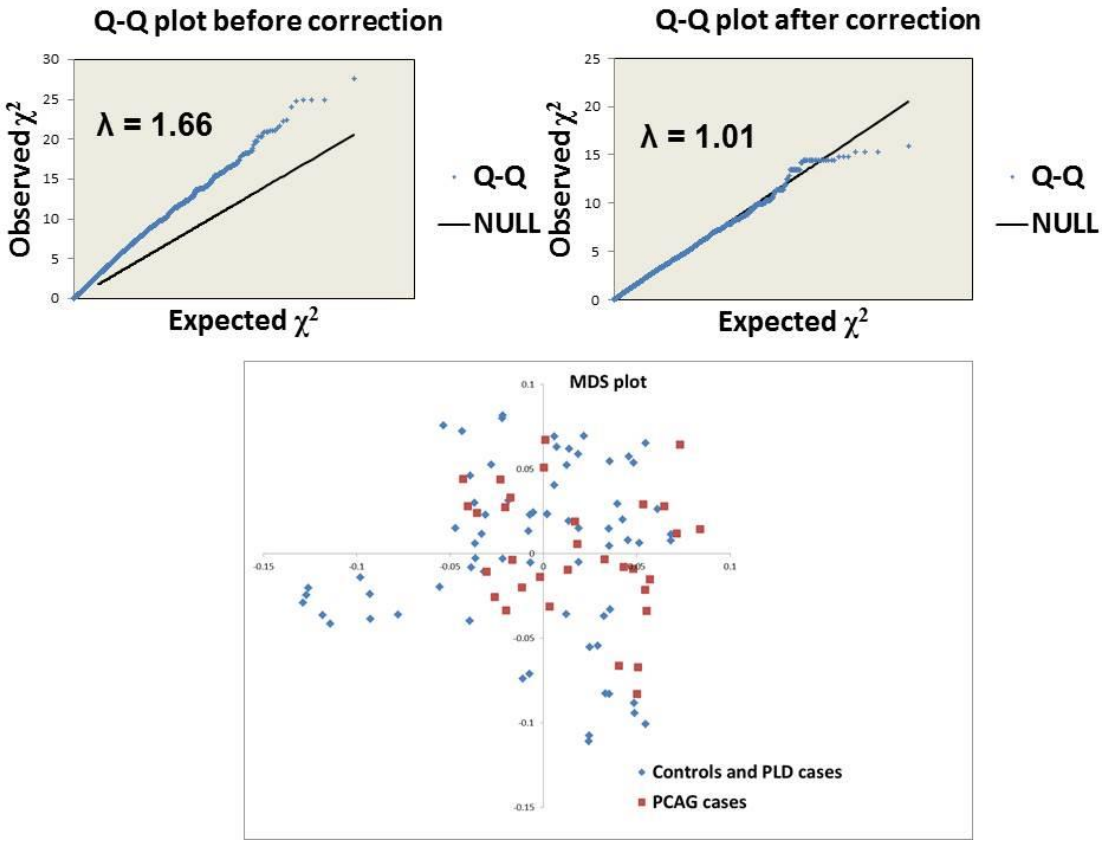

Figure A15. DDT: PCAG cases and PLD cases and controls.

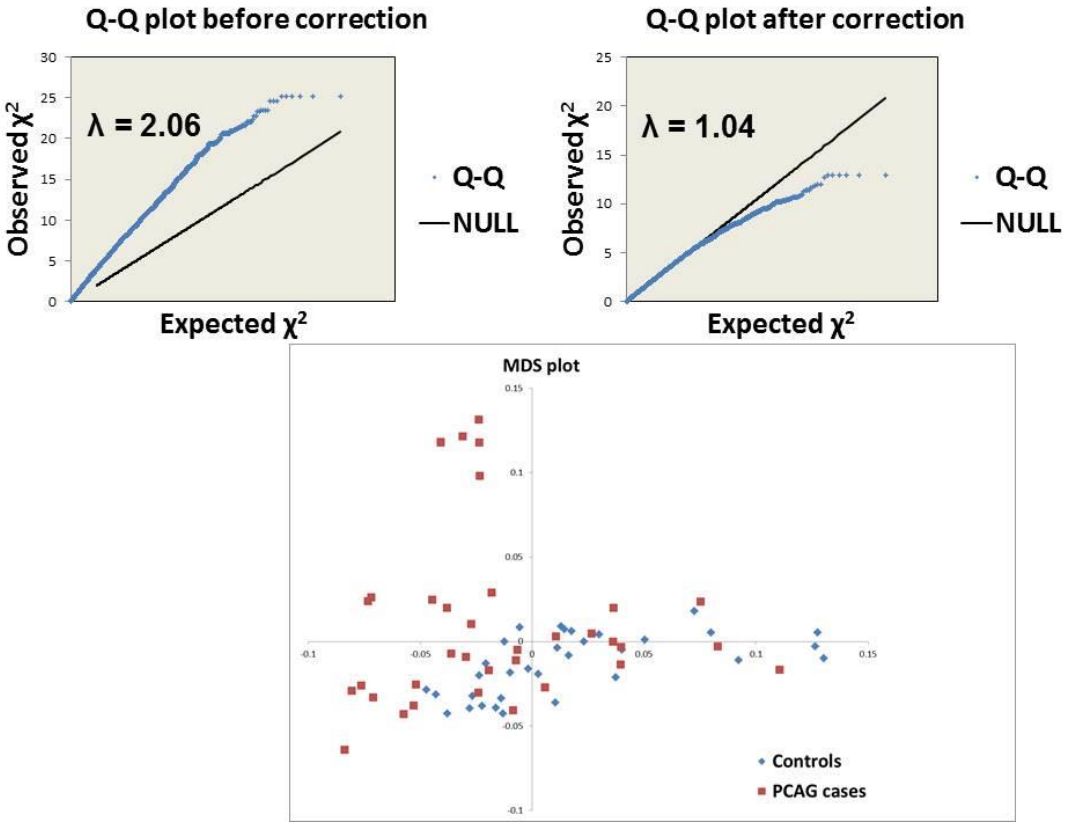

Figure A16. WSS: PCAG cases and controls.

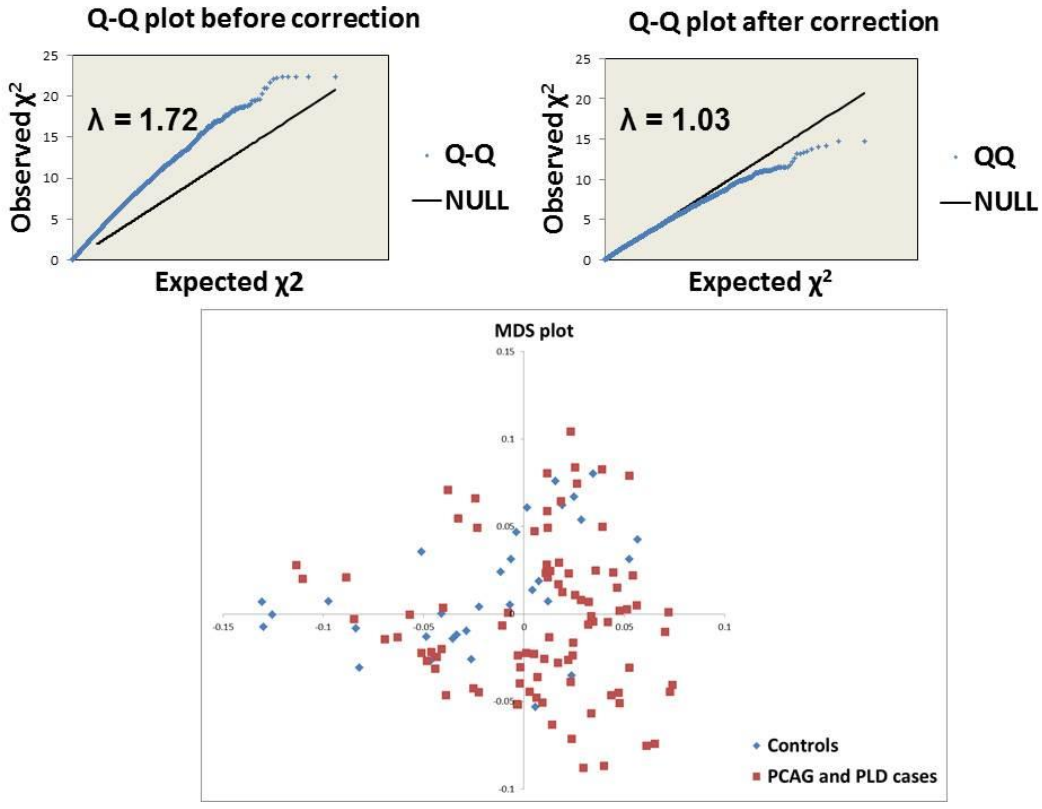

Figure A17. WSS: PCAG and PLD cases and controls.

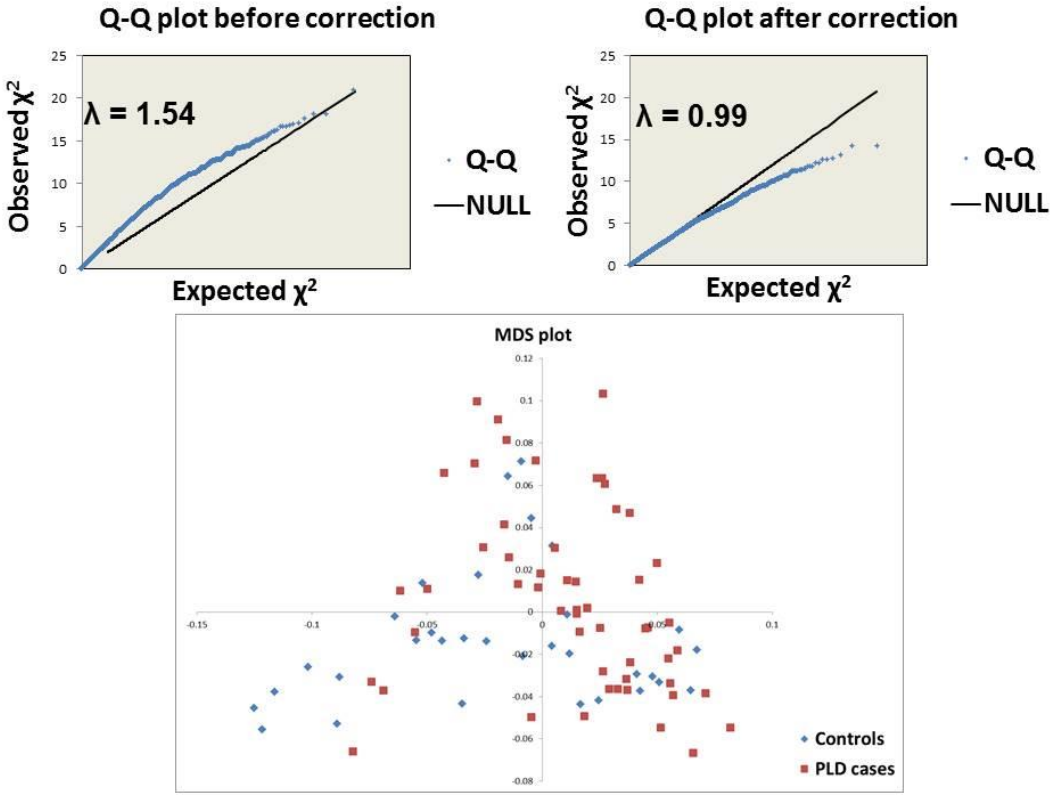

Figure A18. WSS: PLD cases and controls.

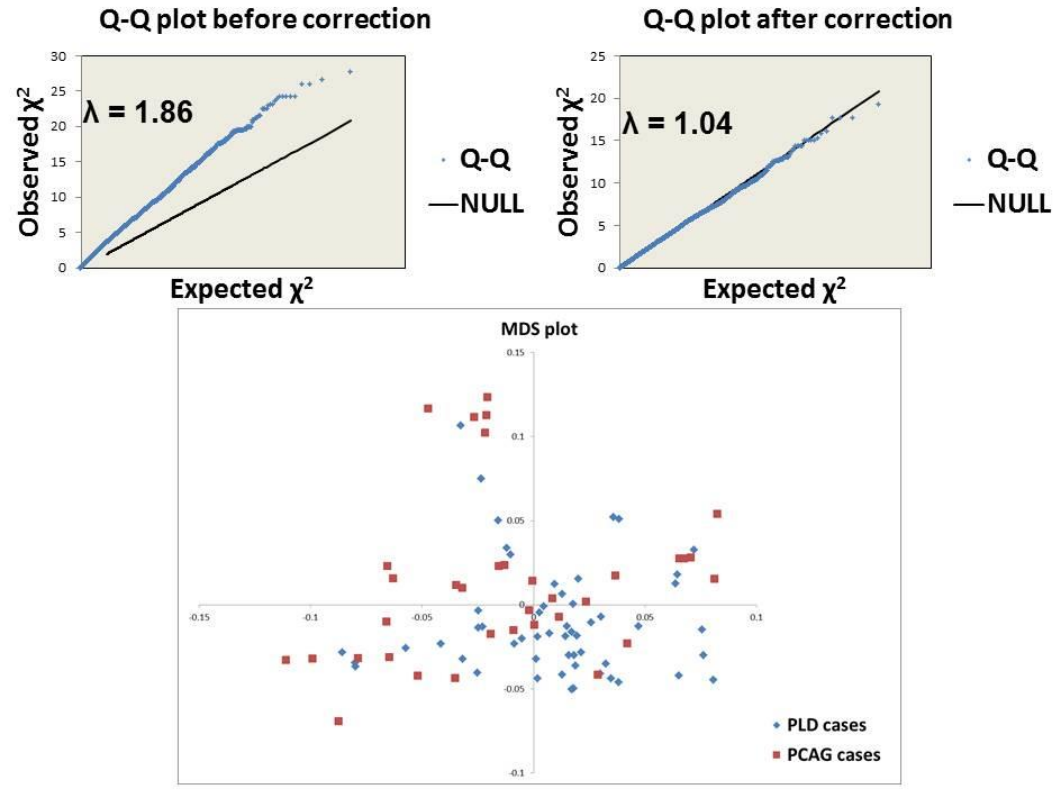

Figure A19. WSS: PCAG cases and PLD cases.

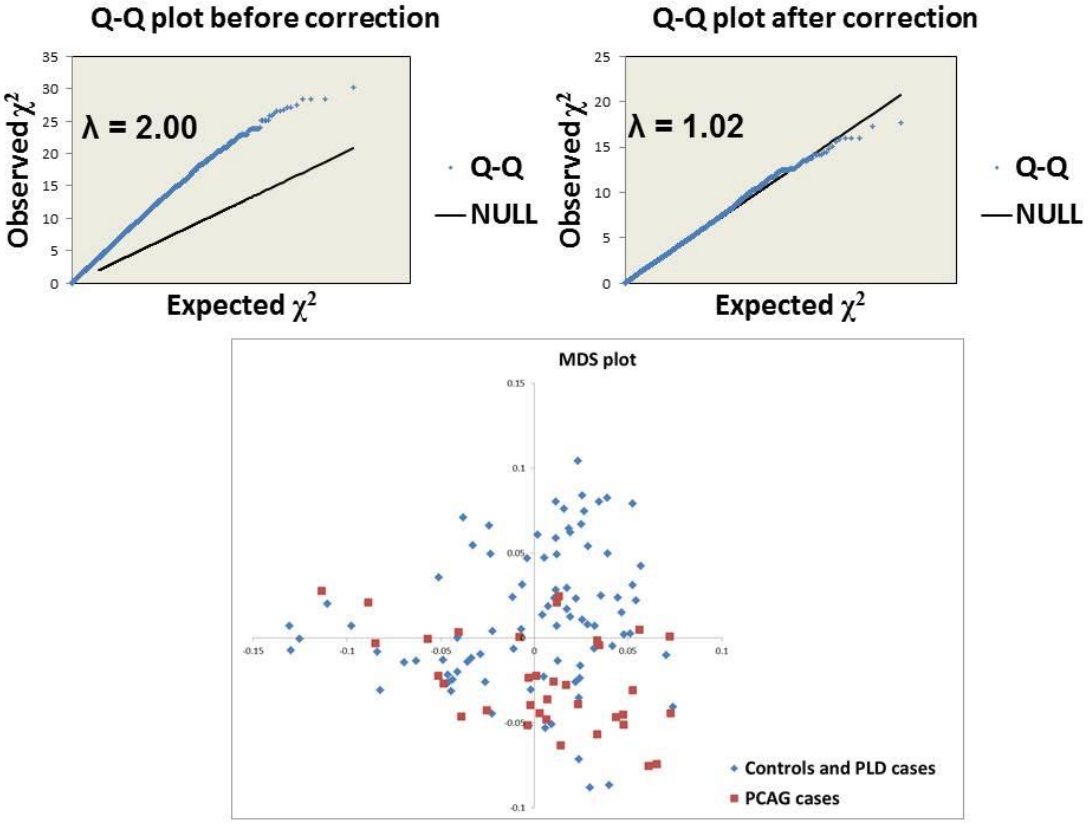

Figure A20. WSS: PCAG cases and PLD cases and controls.

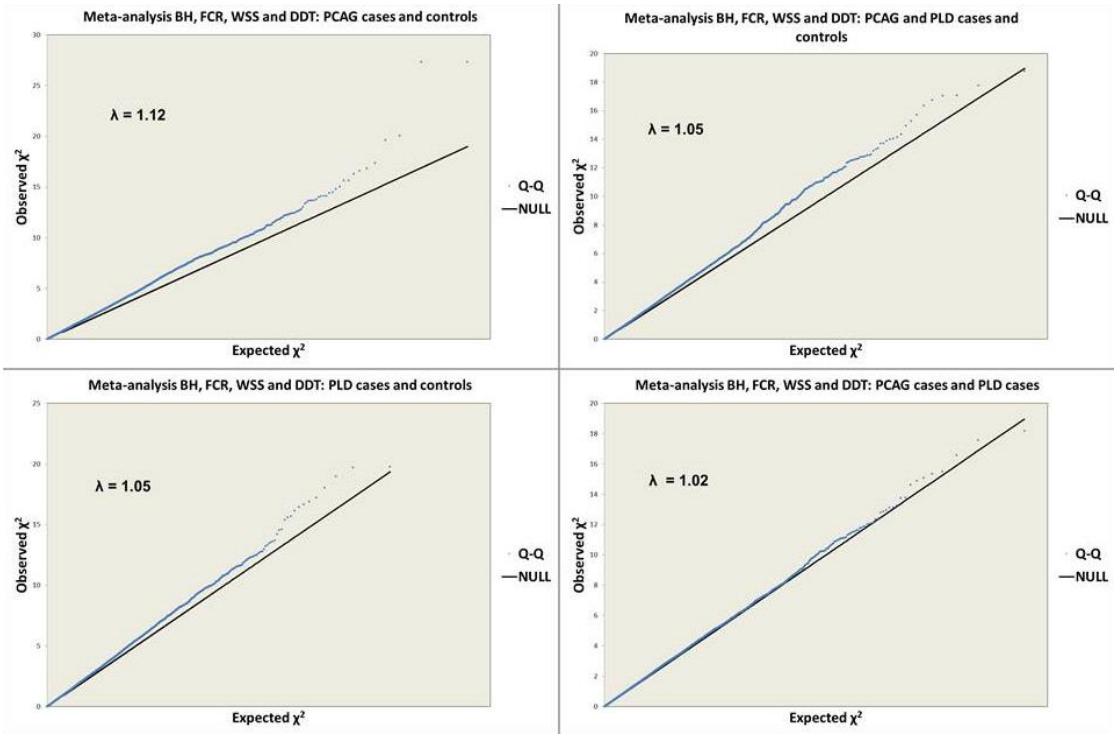

Figure A21. Q-Q plots of meta-analyses of BH, FCR, DDT & WSS.

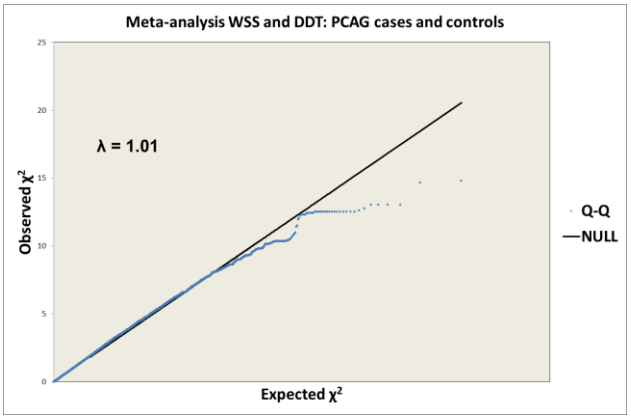

Figure A22. Q-Q plot of meta-analysis of DDT & WSS: PCAG cases and controls.

VII. GWAS haplotype and haplotype permutation association plots

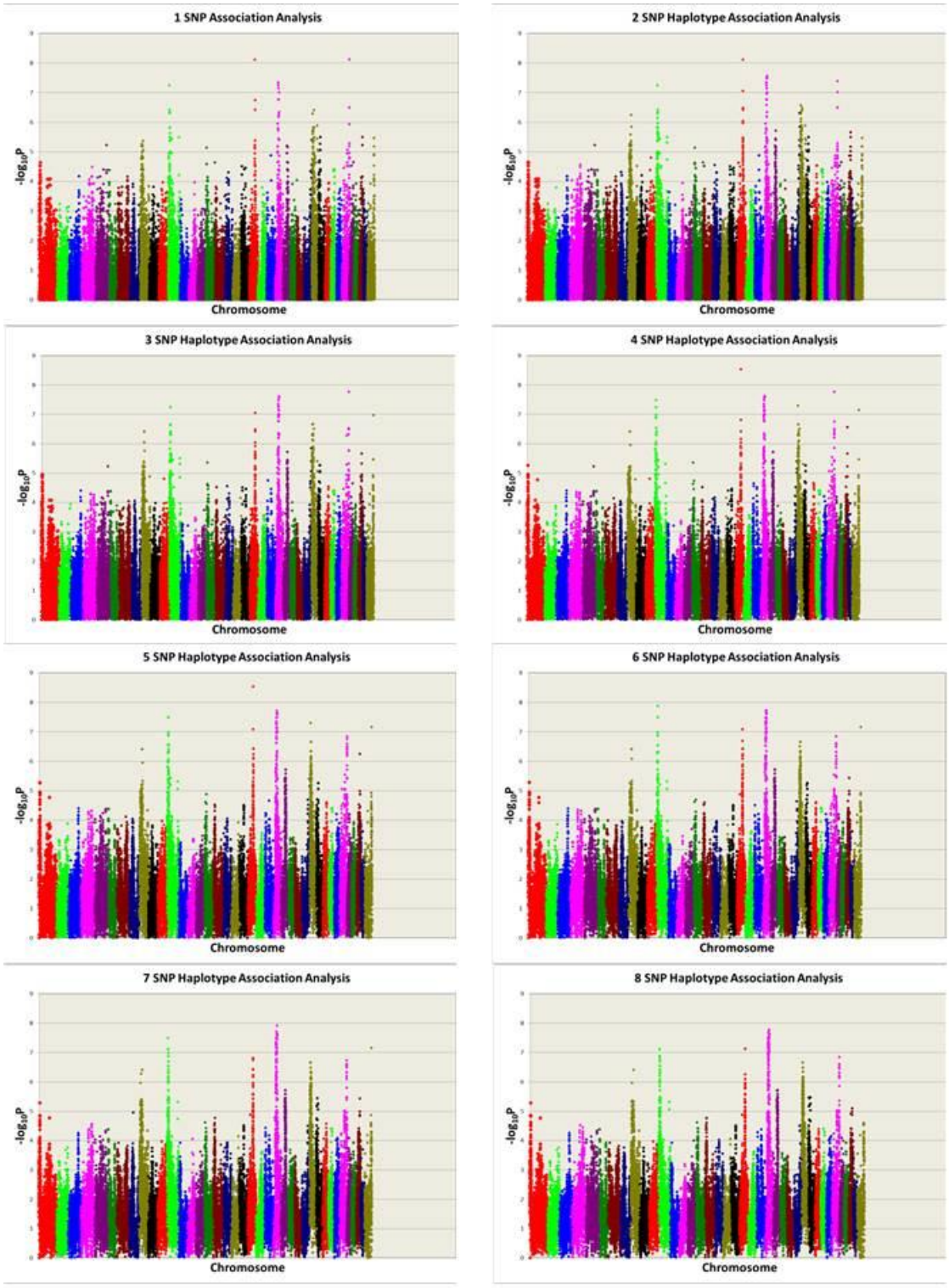

Figure A23. Haplotype association analysis. BH: PCAG cases and controls.

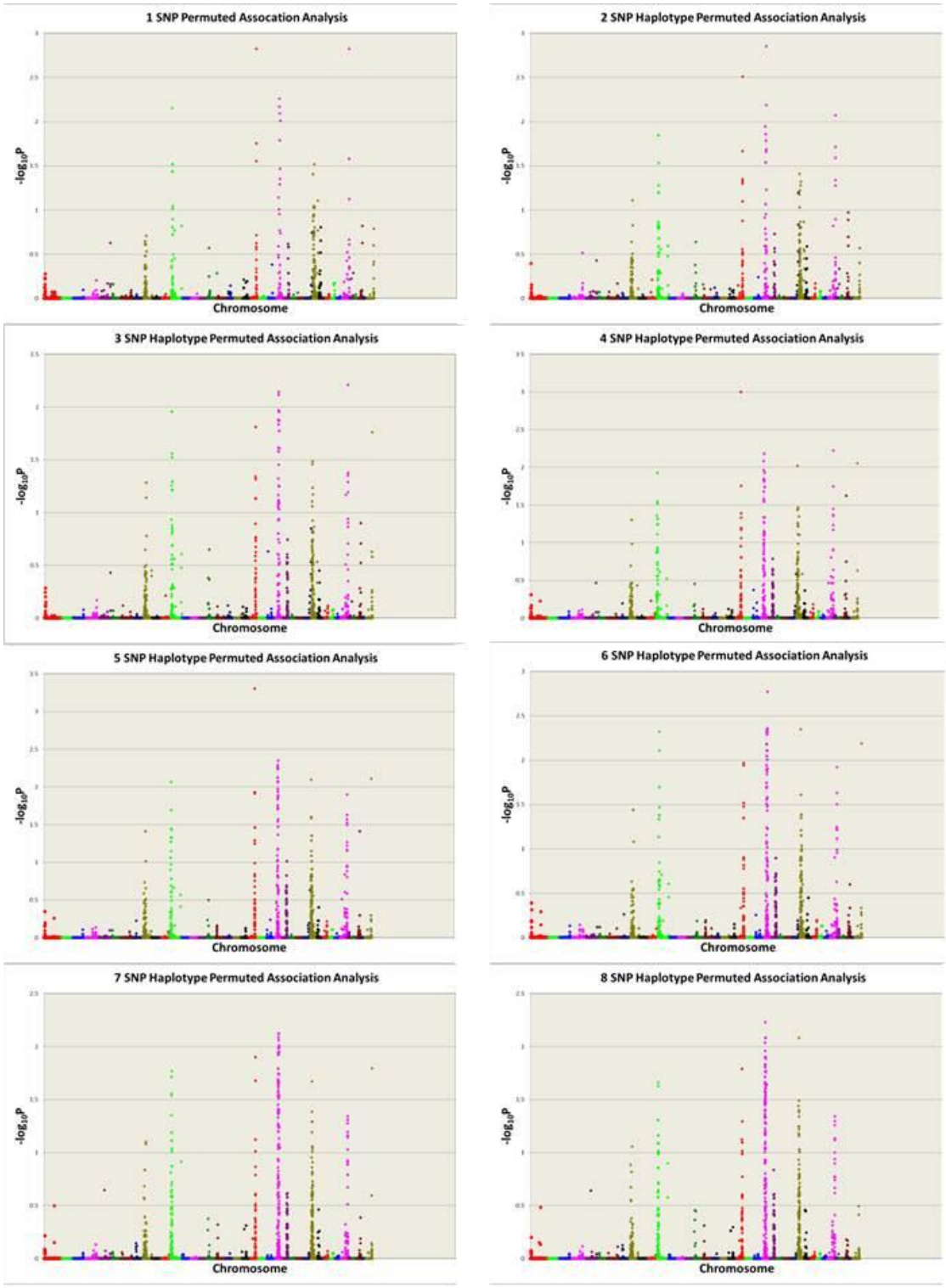

Figure A24. Haplotype permutation association analysis. BH: PCAG cases and controls.

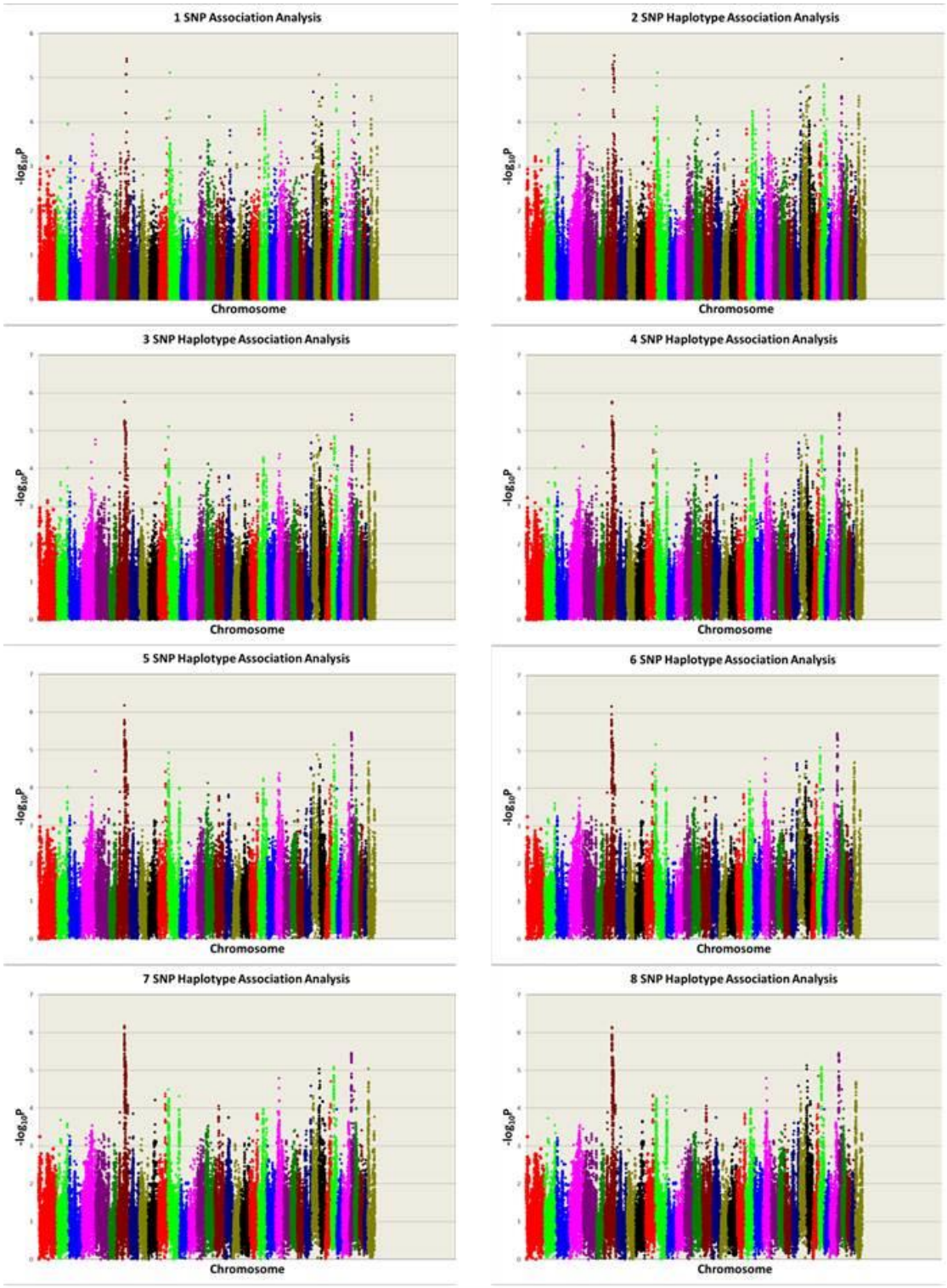

Figure A25. Haplotype association analysis. BH: PCAG and PLD cases and controls.

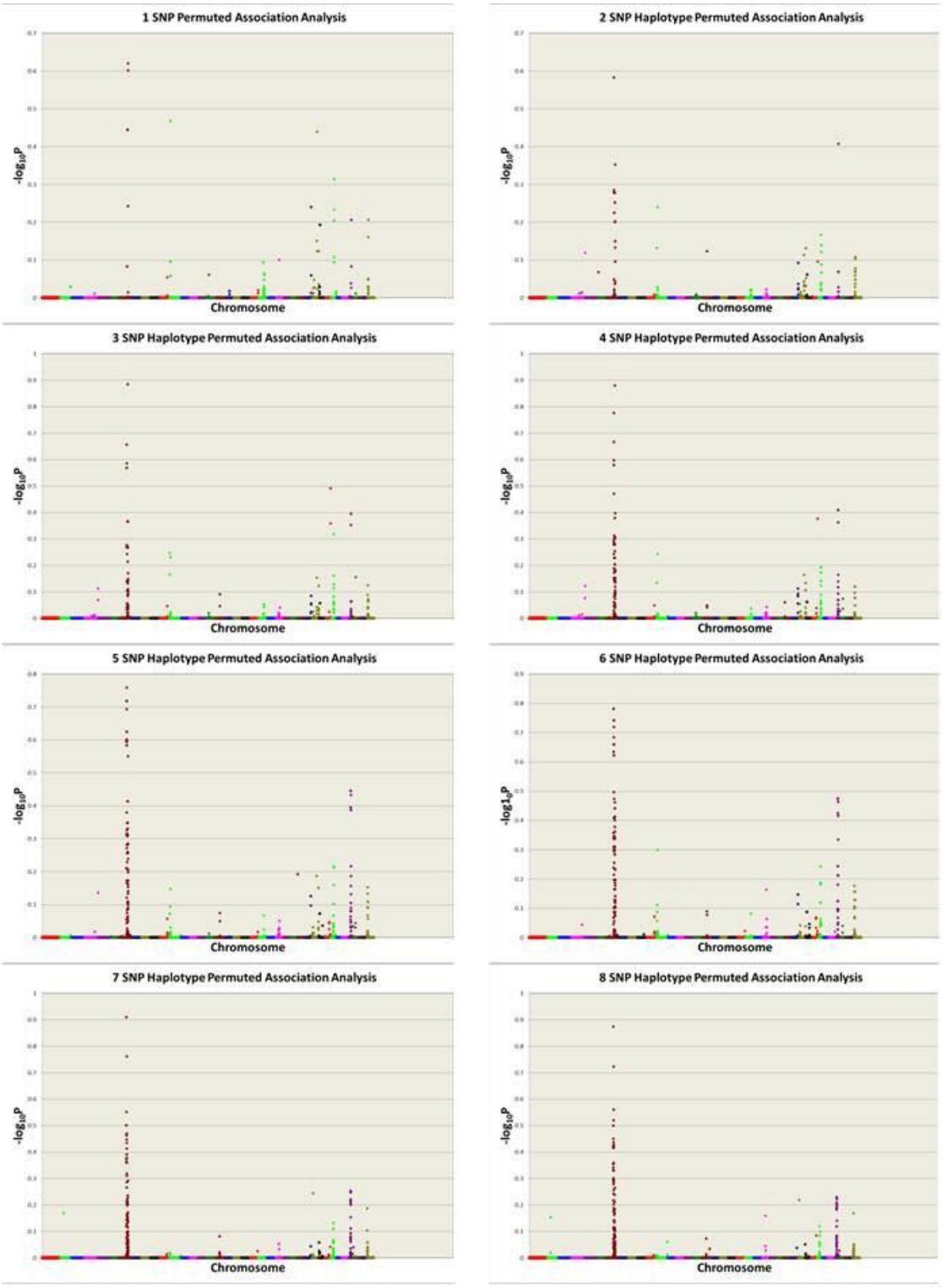

Figure A26. Haplotype permutation association analysis. BH: PCAG and PLD cases and controls.

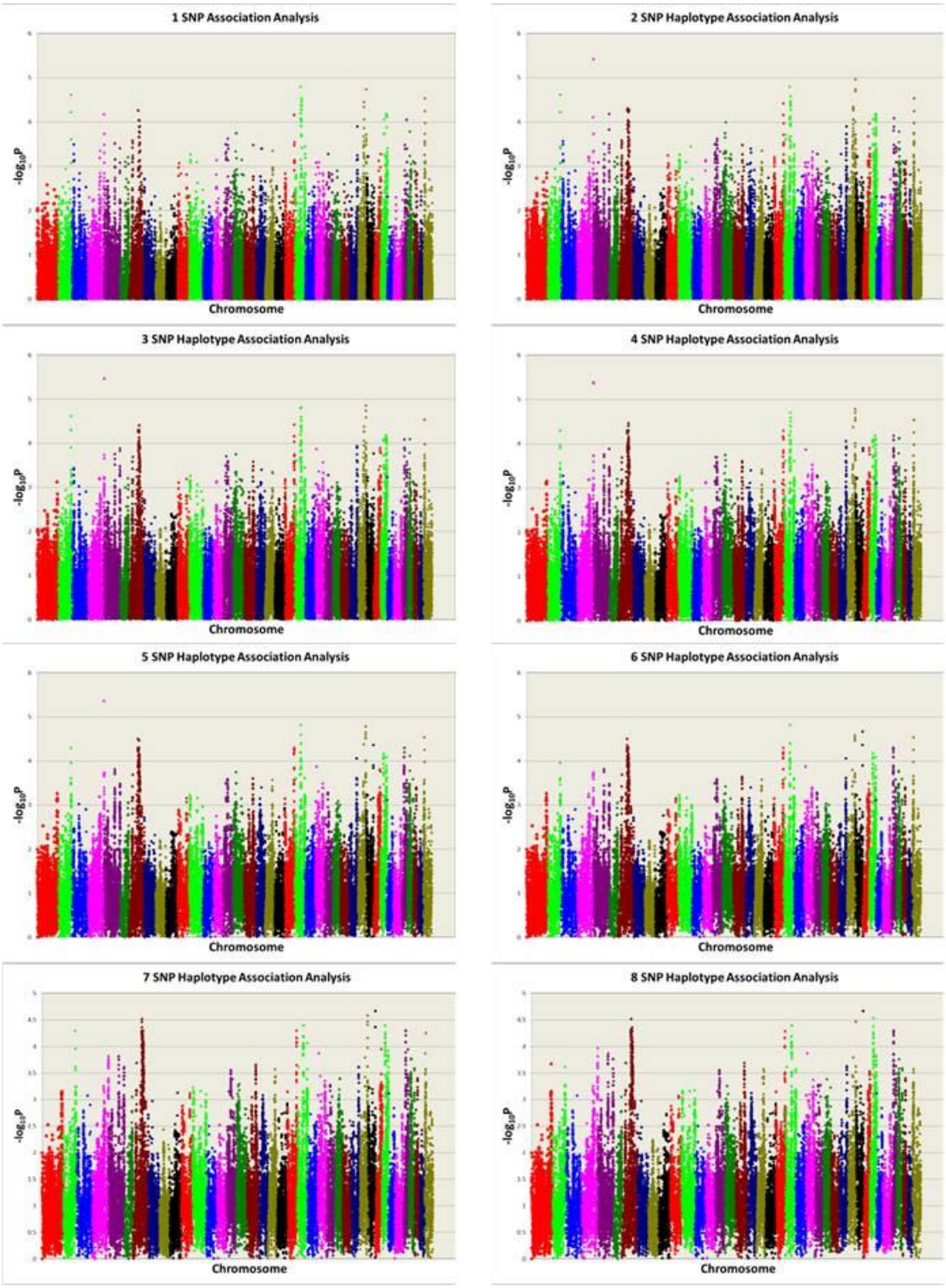

Figure A27. Haplotype association analysis. BH: PLD cases and controls.

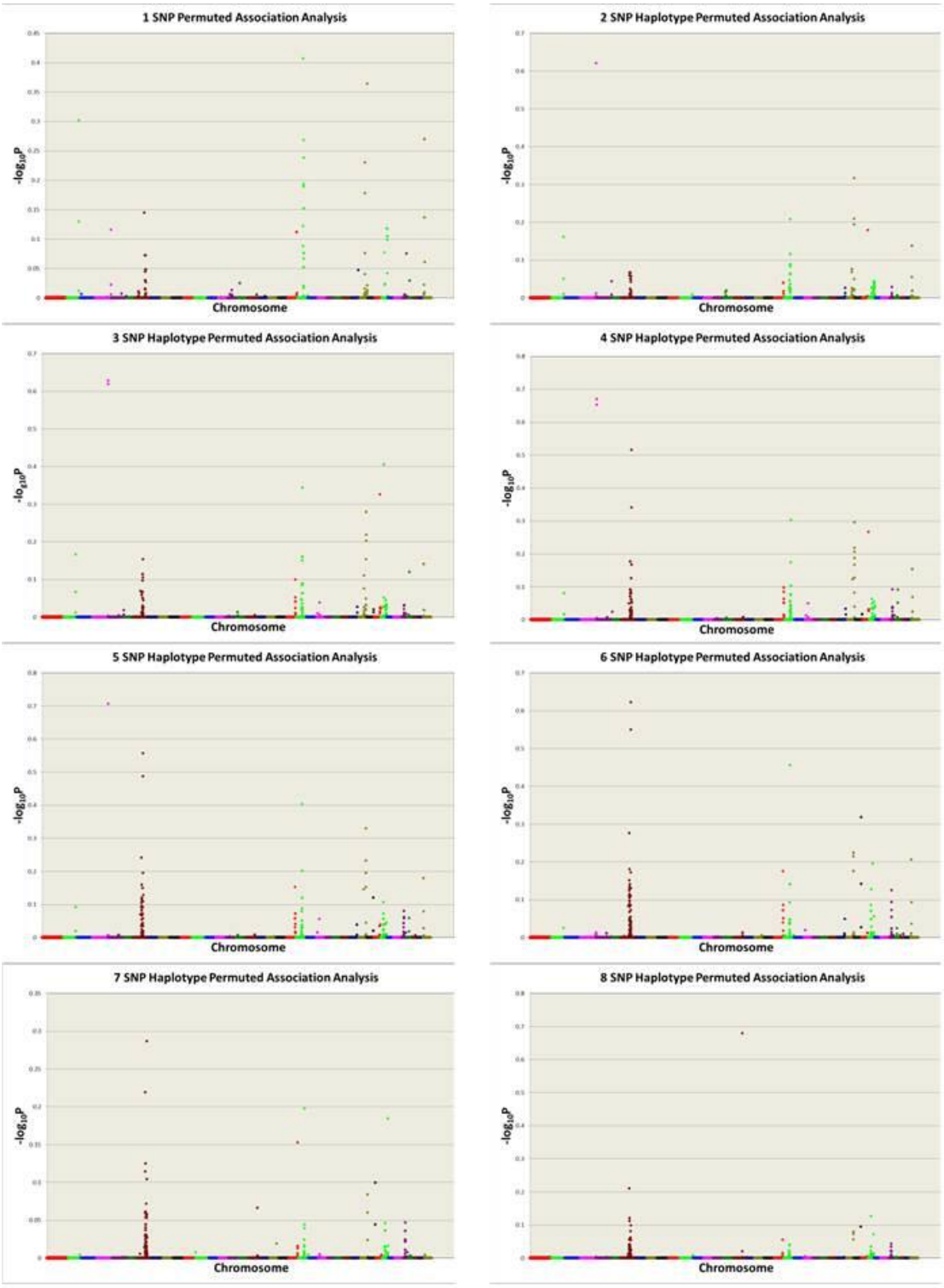

Figure A28. Haplotype permutation association analysis. BH: PLD cases and controls.

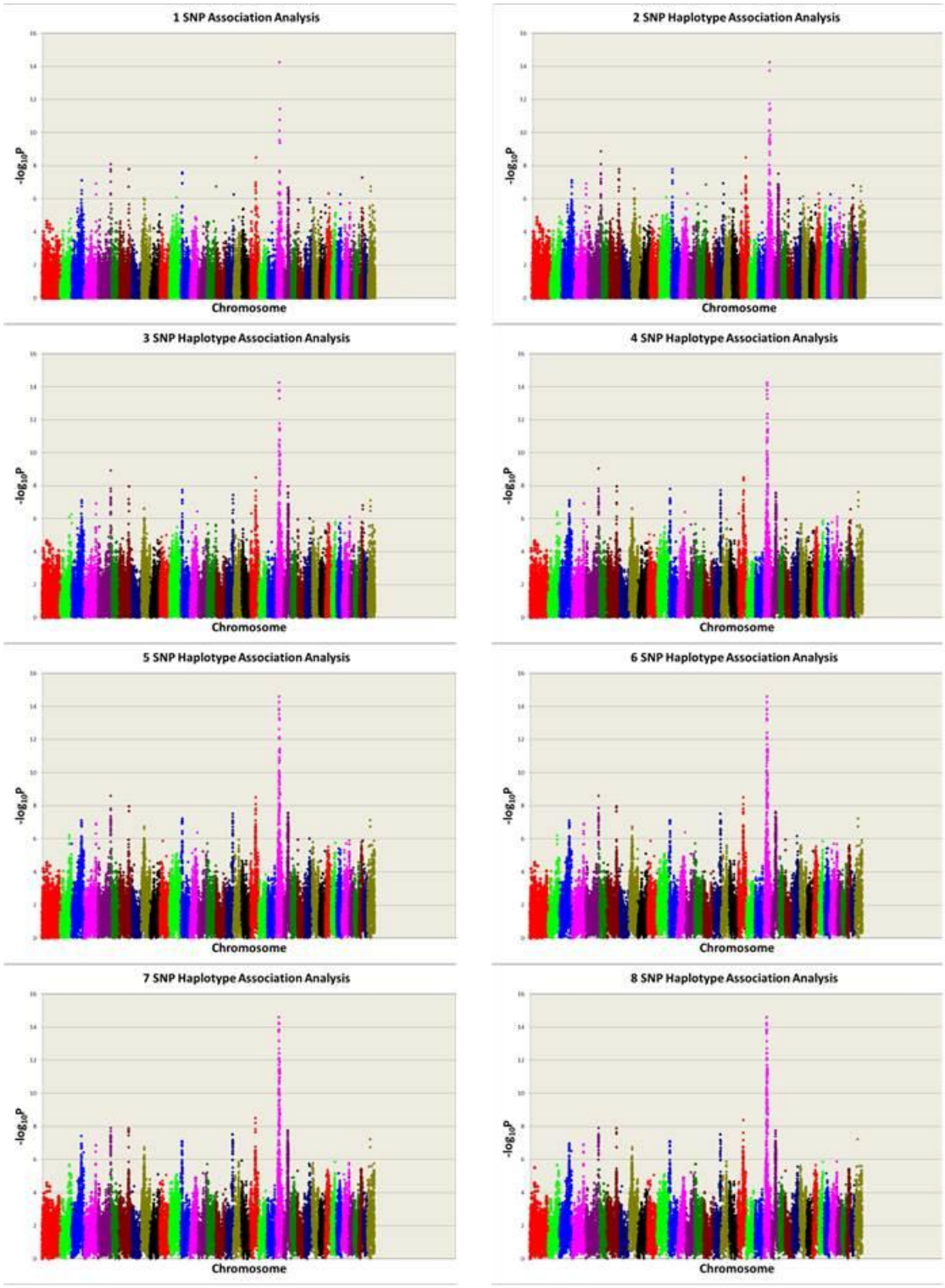

Figure A29. Haplotype association analysis. BH: PCAG cases and PLD cases.

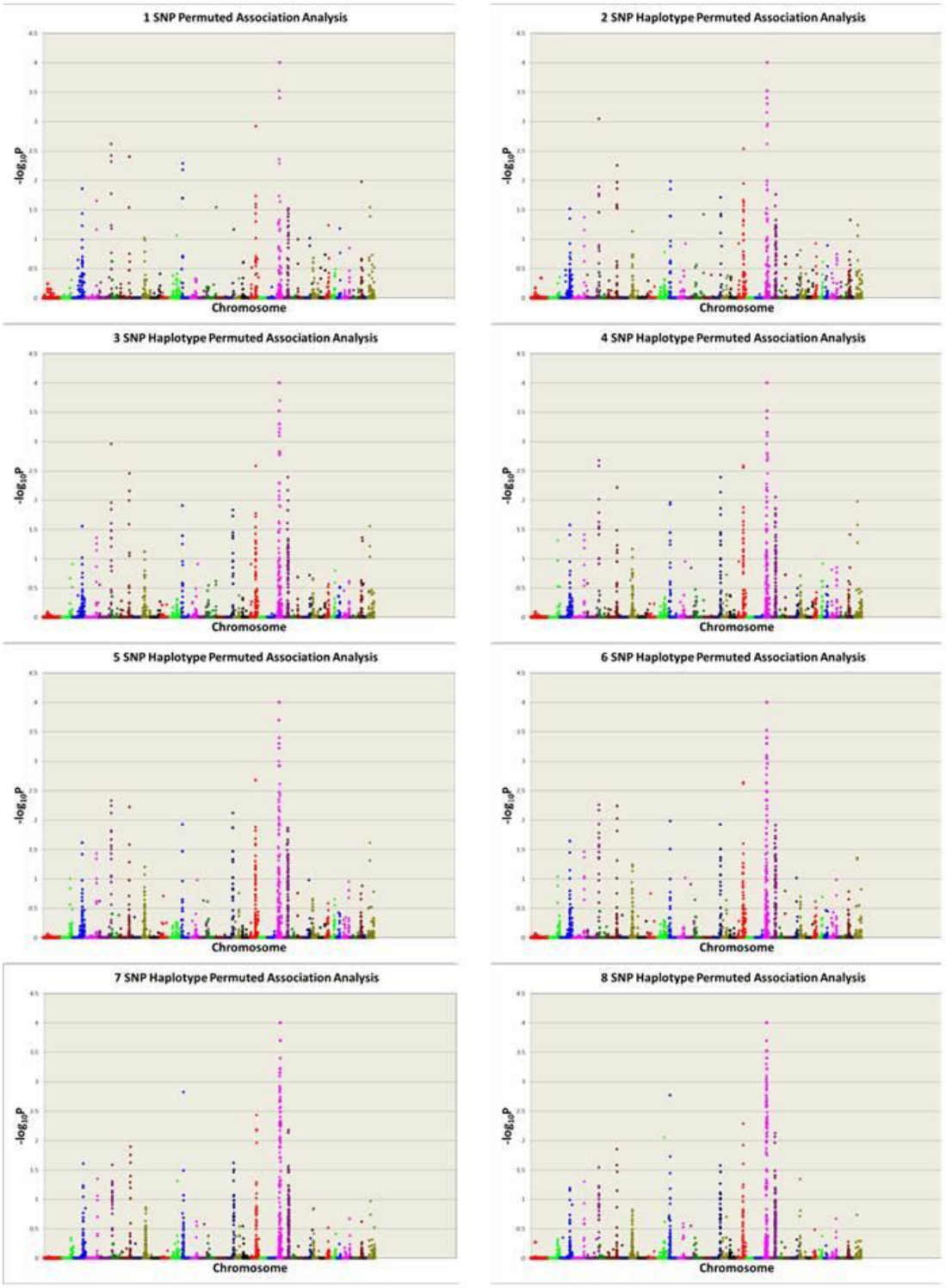

Figure A30. Haplotype permutation association analysis. BH: PCAG cases and PLD cases.

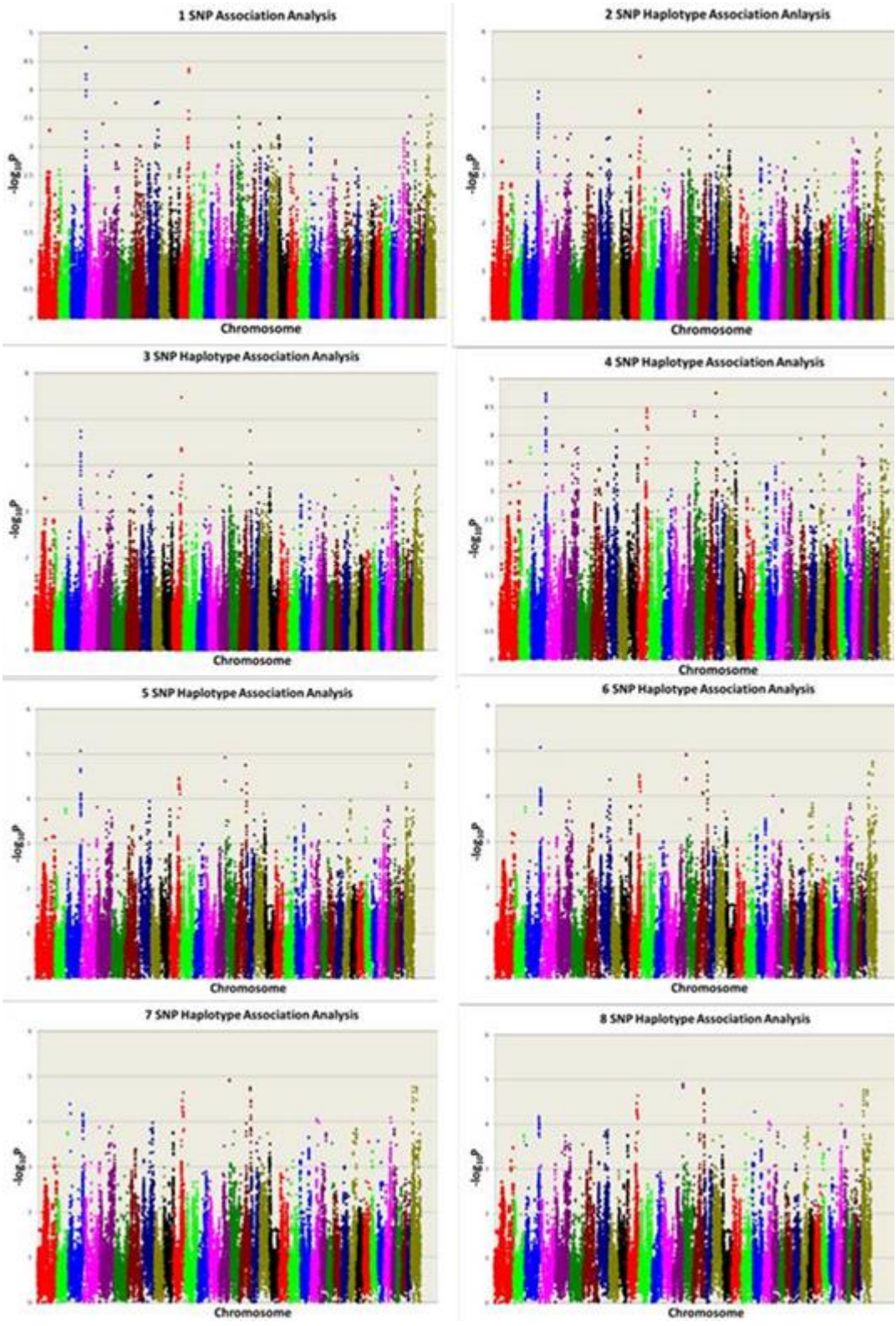

Figure A31. Haplotype association analysis. FCR: PCAG cases and controls.

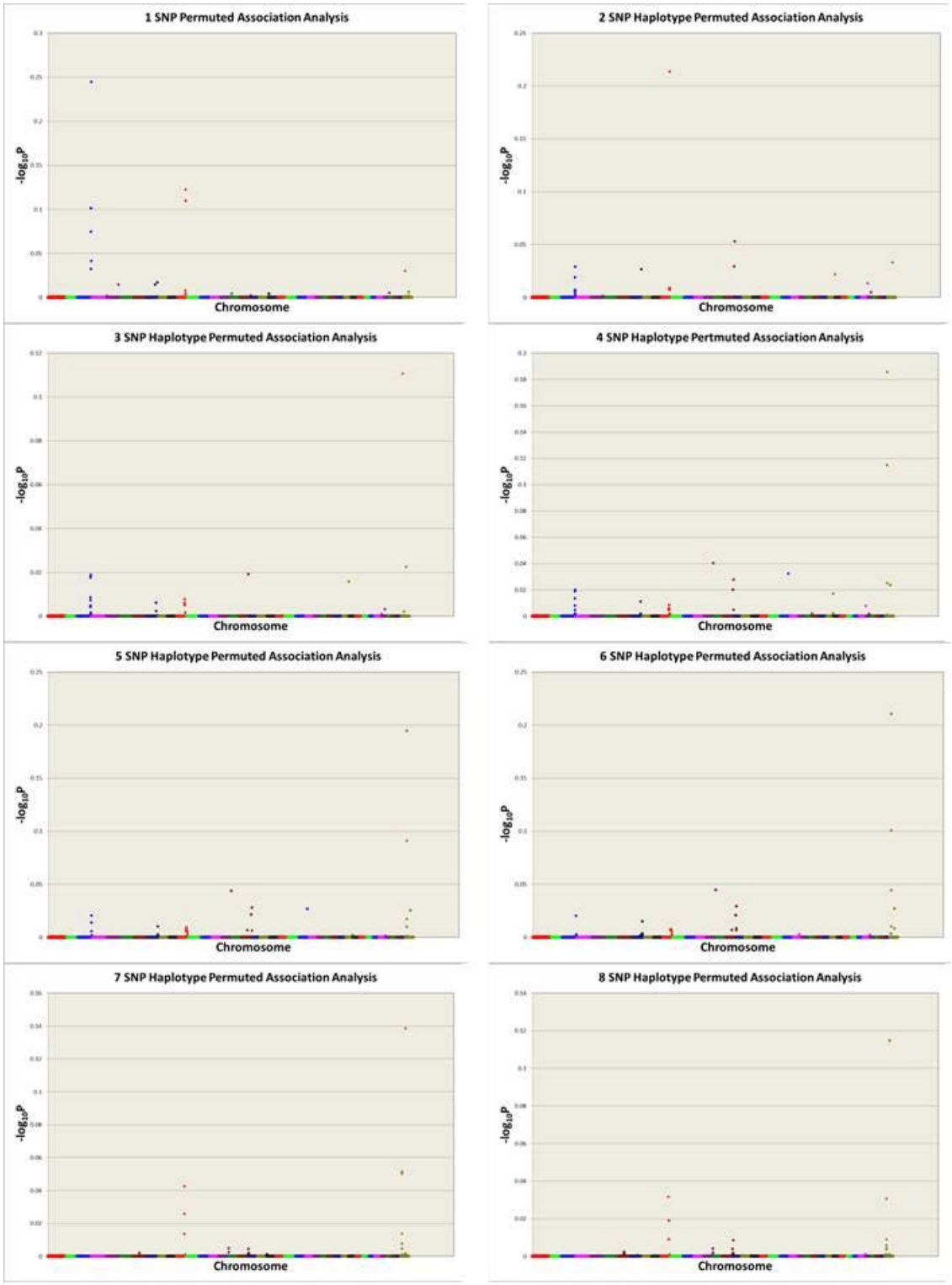

Figure A32. Haplotype permutation association analysis. FCR: PCAG cases and controls.

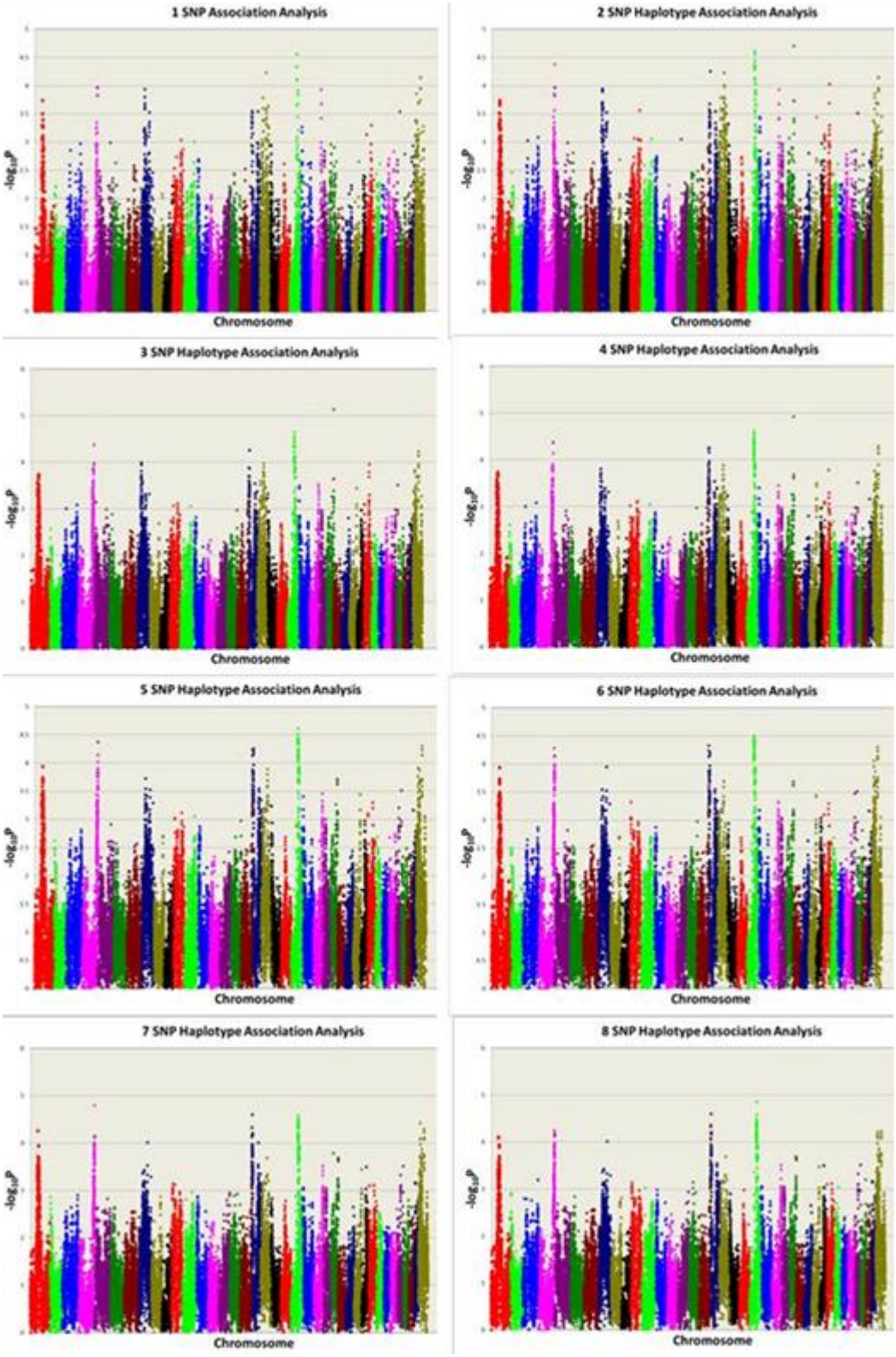

Figure A33. Haplotype association analysis. FCR: PCAG and PLD cases and controls.

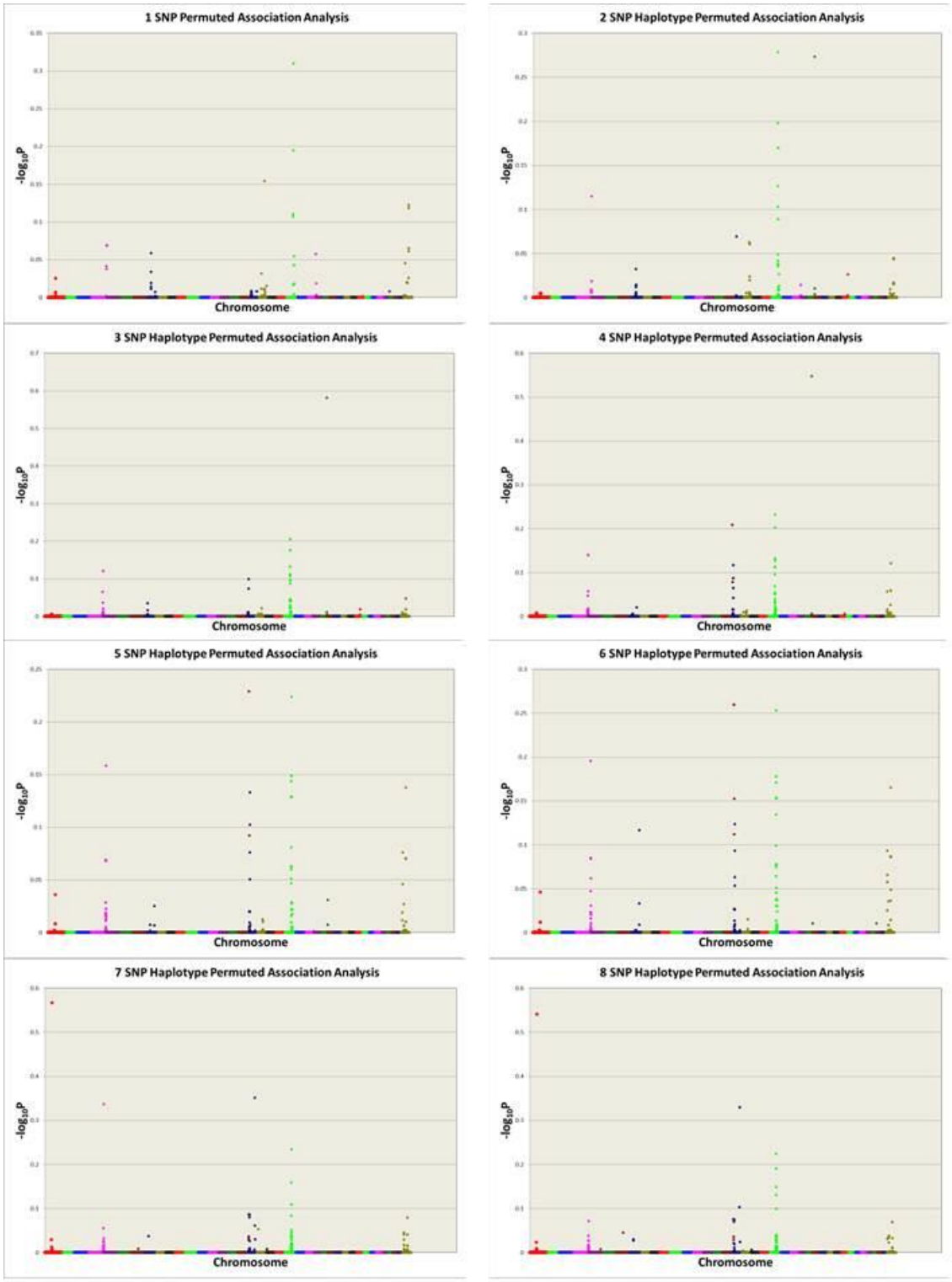

Figure A34. Haplotype permutation association analysis. FCR: PCAG cases and PLD cases vs controls.

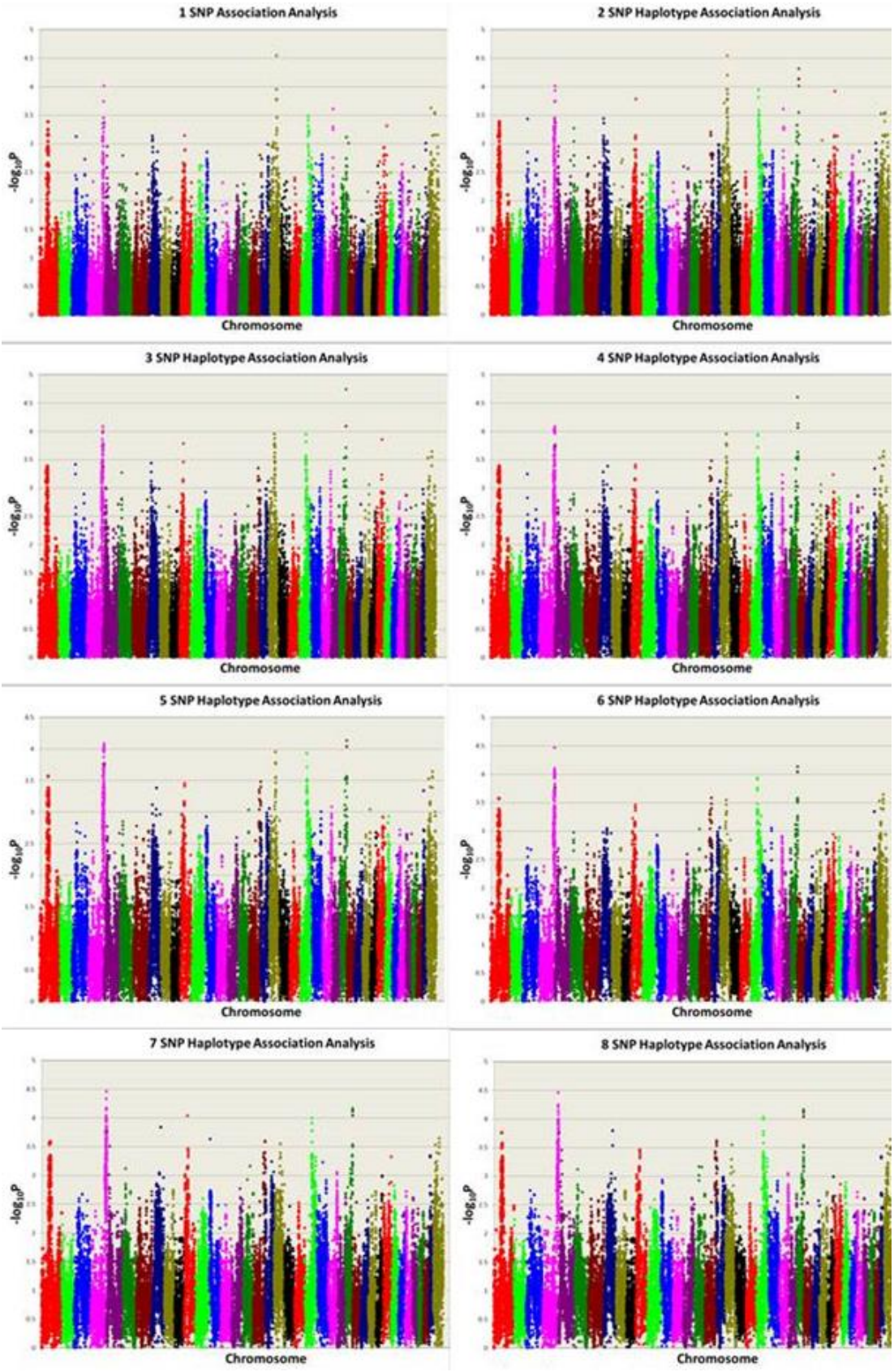

Figure A35. Haplotype association analysis. FCR: PLD cases and controls.

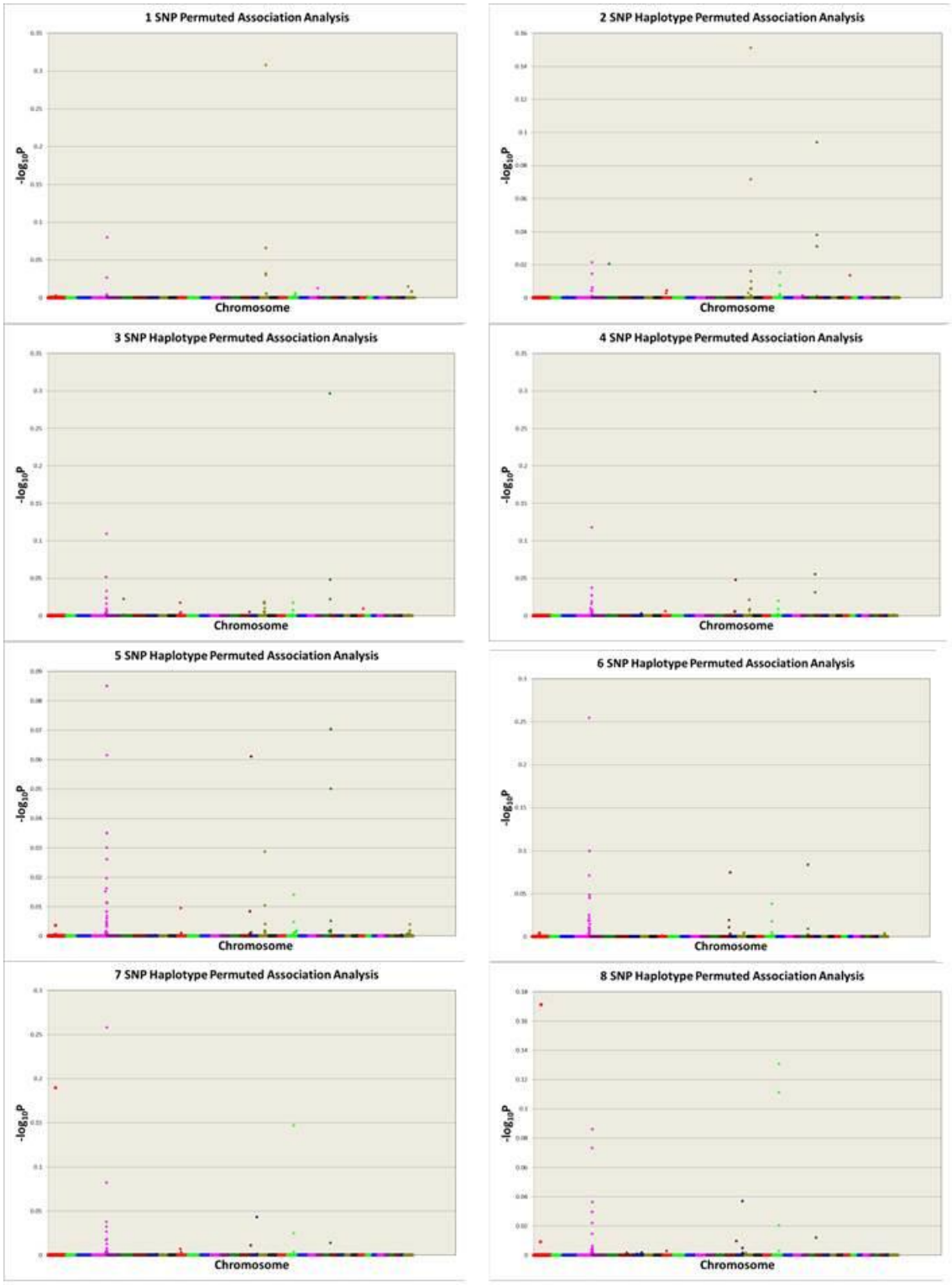

Figure A36. Haplotype permutation association analysis. FCR: PLD cases and controls.

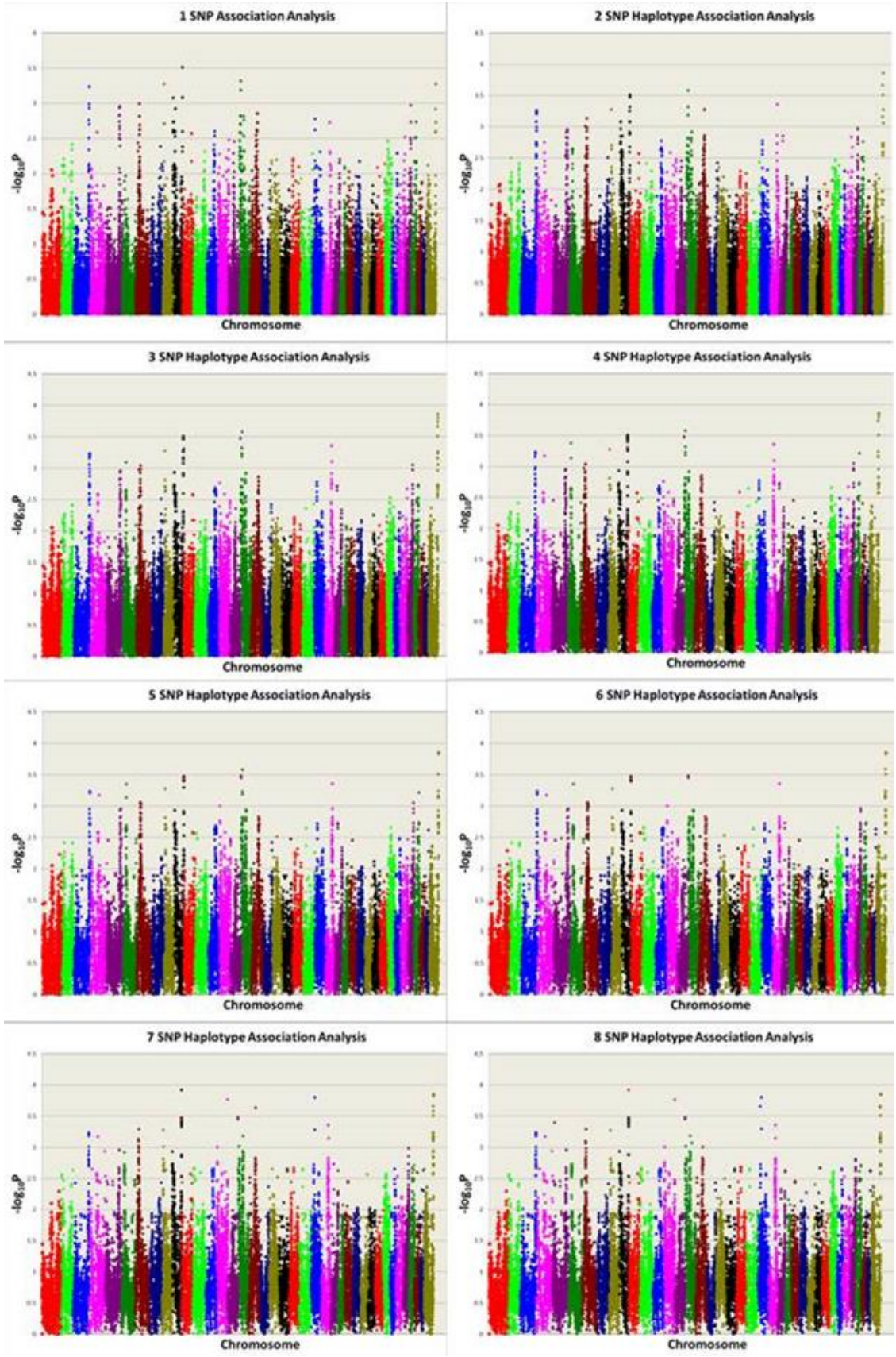

Figure A37. Haplotype association analysis. FCR: PCAG cases and PLD cases.

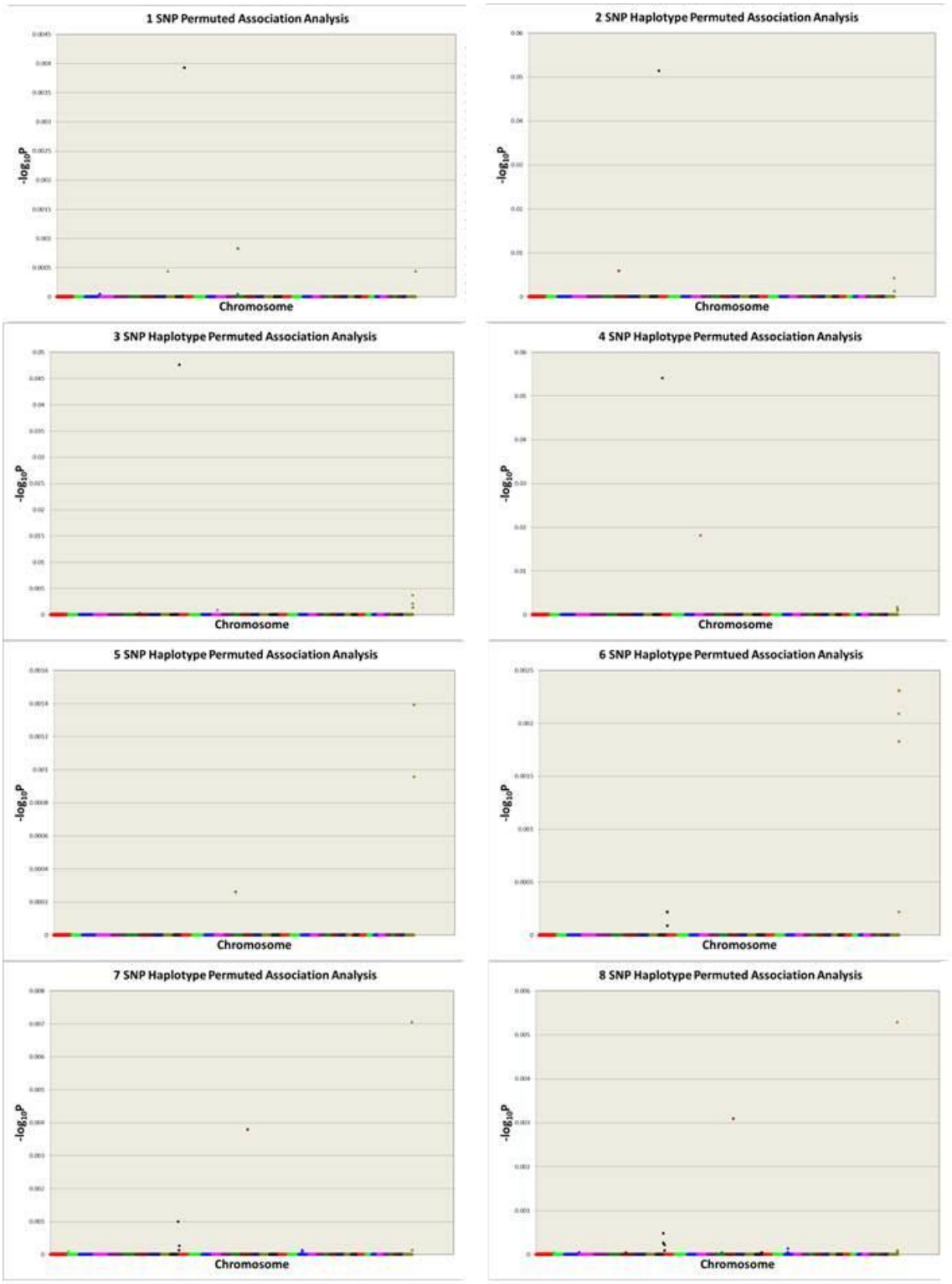

Figure A38. Haplotype permutation association analysis. FCR: PCAG cases and PLD cases.

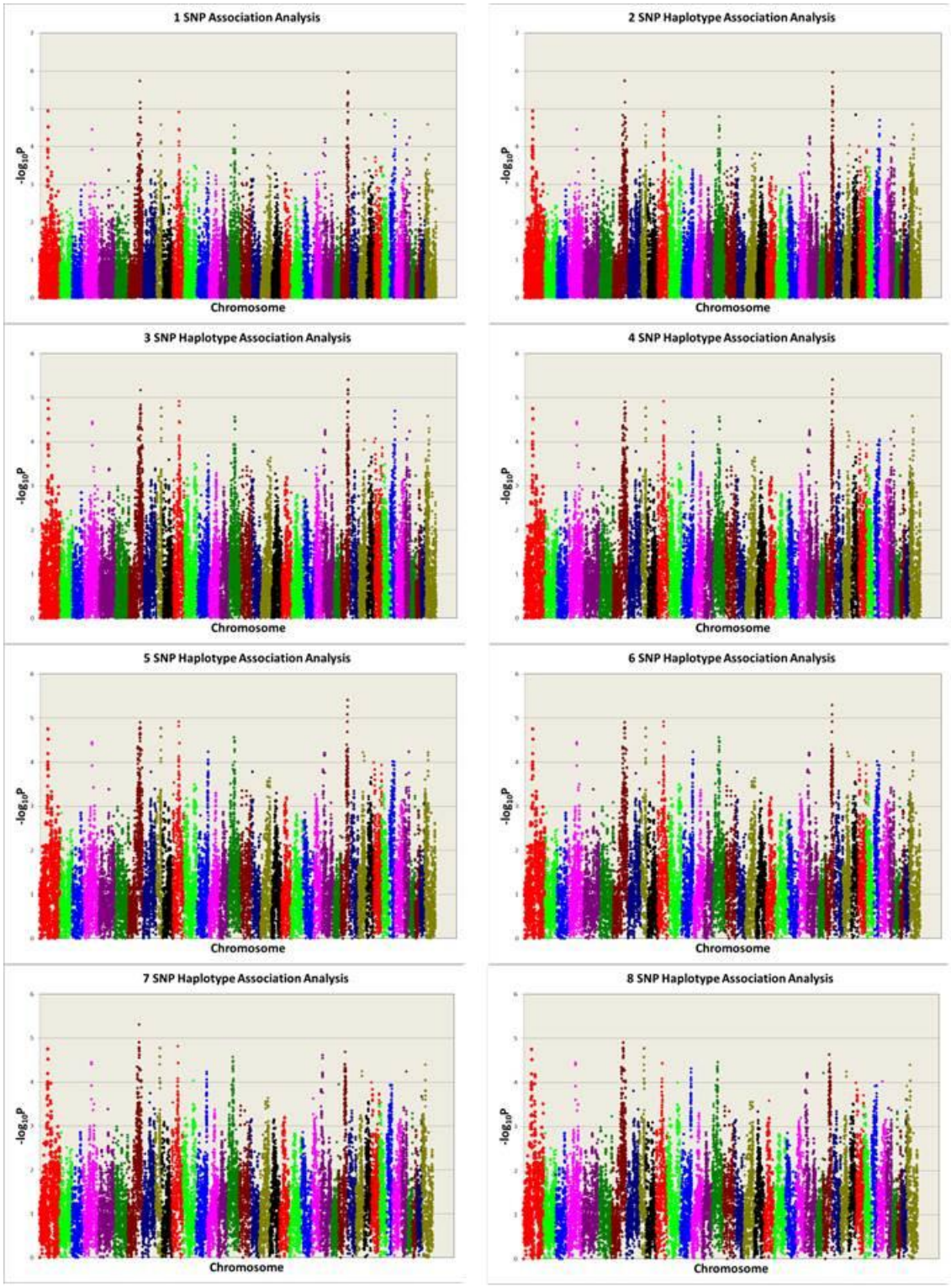

Figure A39. Haplotype association analysis. DDT: PCAG cases and controls.

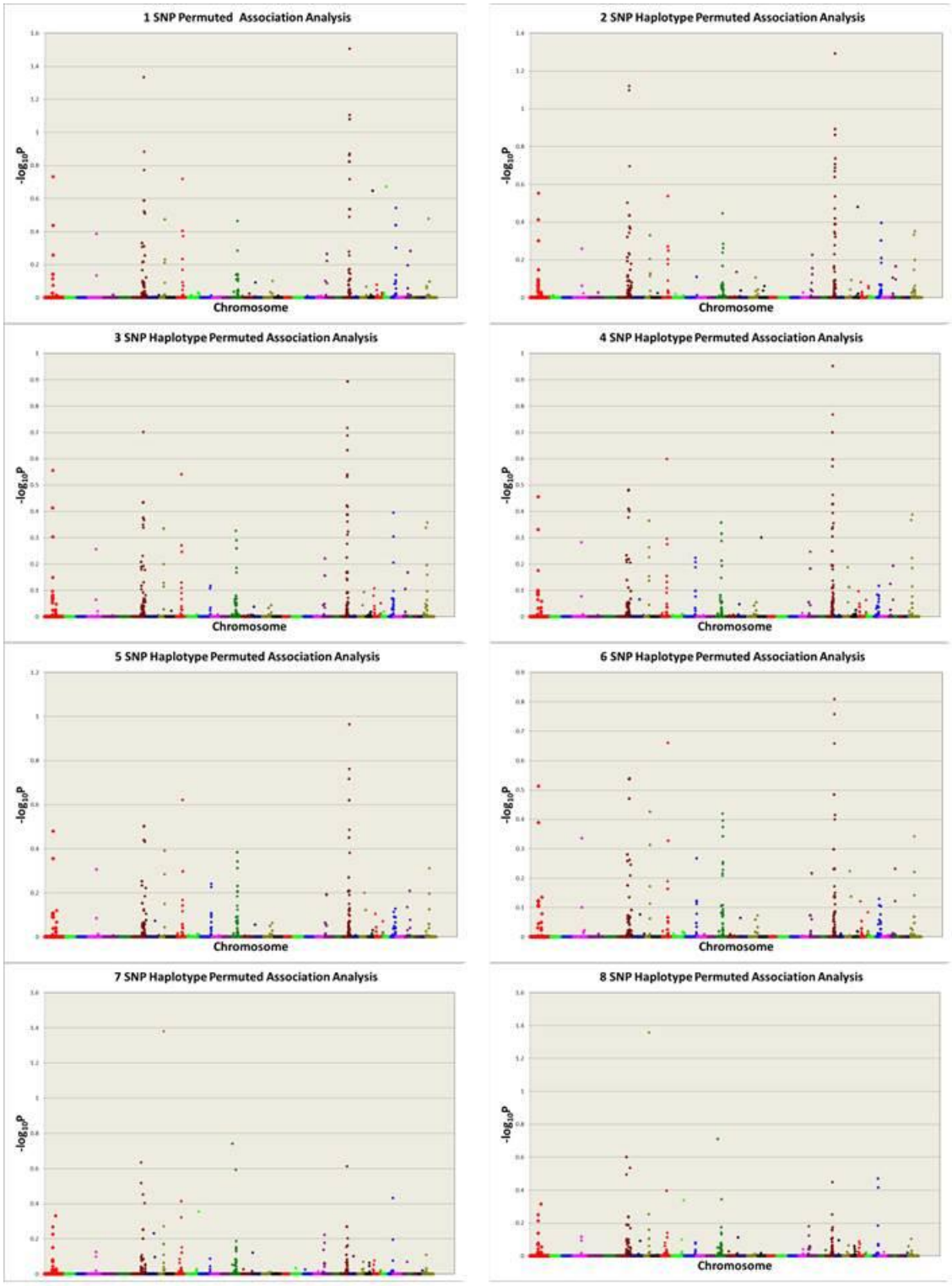

Figure A40. Haplotype permutation association analysis. DDT: PCAG cases and controls.

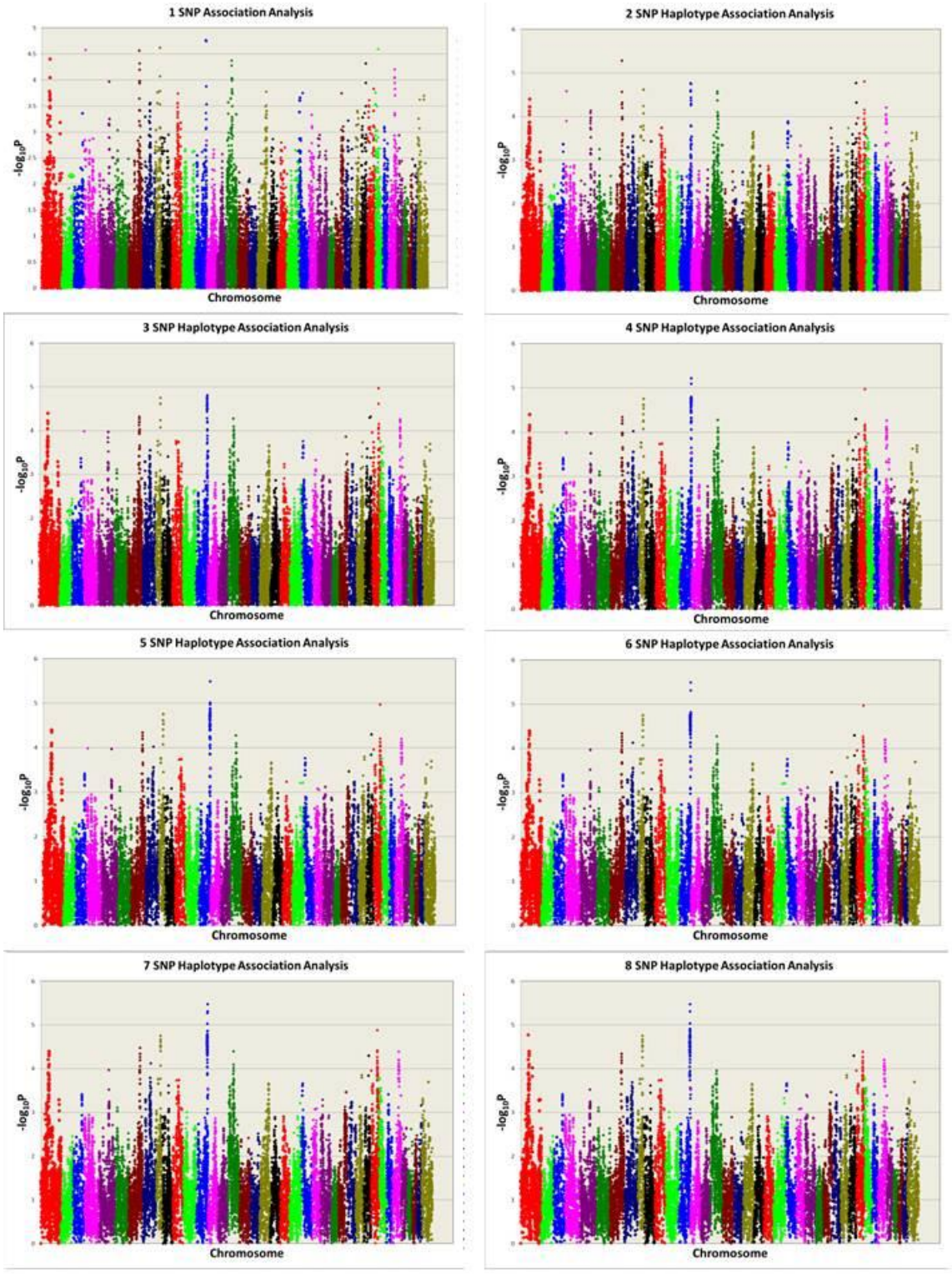

Figure A41. Haplotype association analysis. DDT: PCAG and PLD cases and controls.

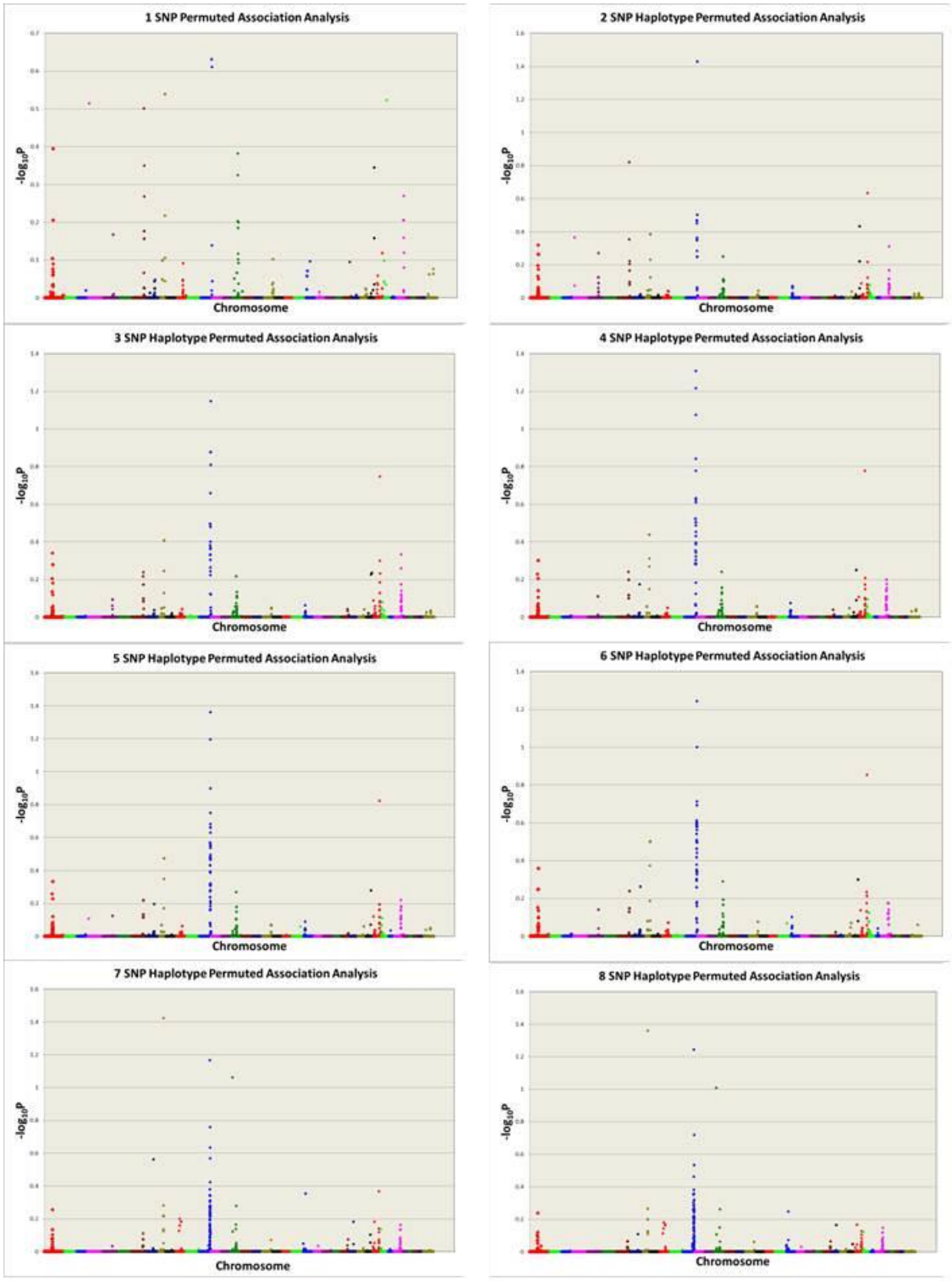

Figure A42. Haplotype permutation association analysis. DDT: PCAG and PLD cases and controls.

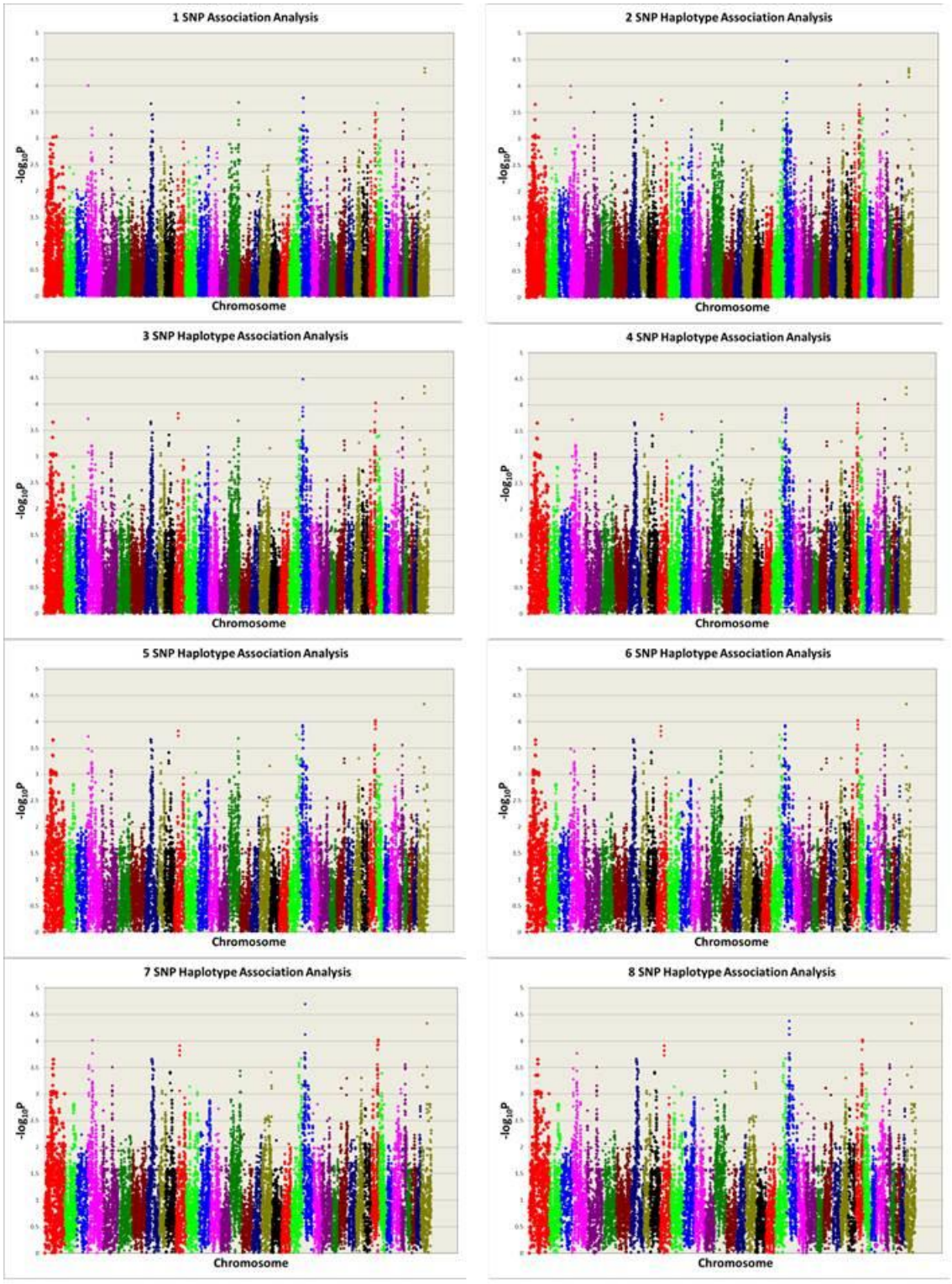

Figure A43. Haplotype association analysis. DDT: PLD cases and controls.

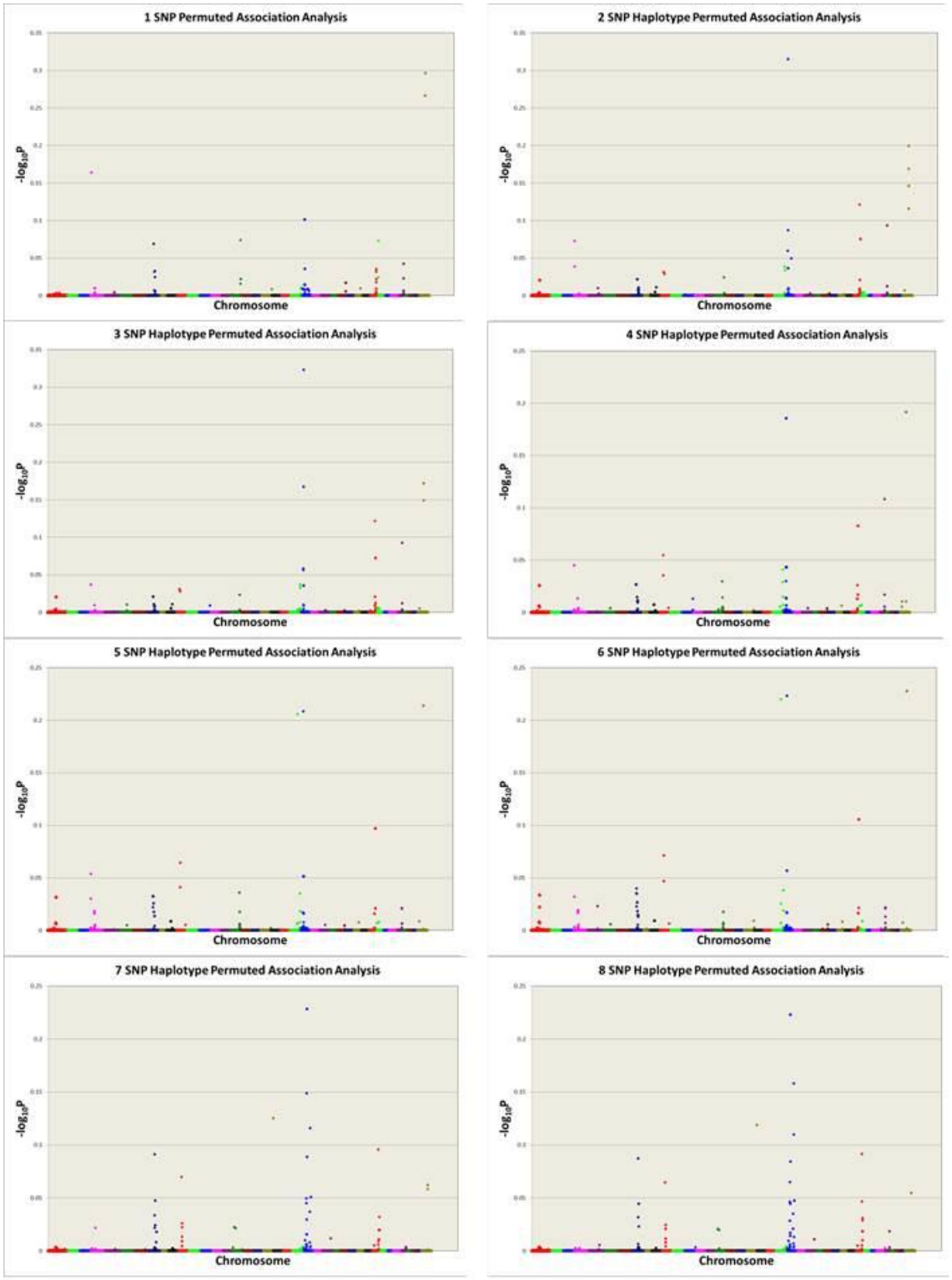

Figure A44. Haplotype permutation association analysis. DDT: PLD cases and controls.

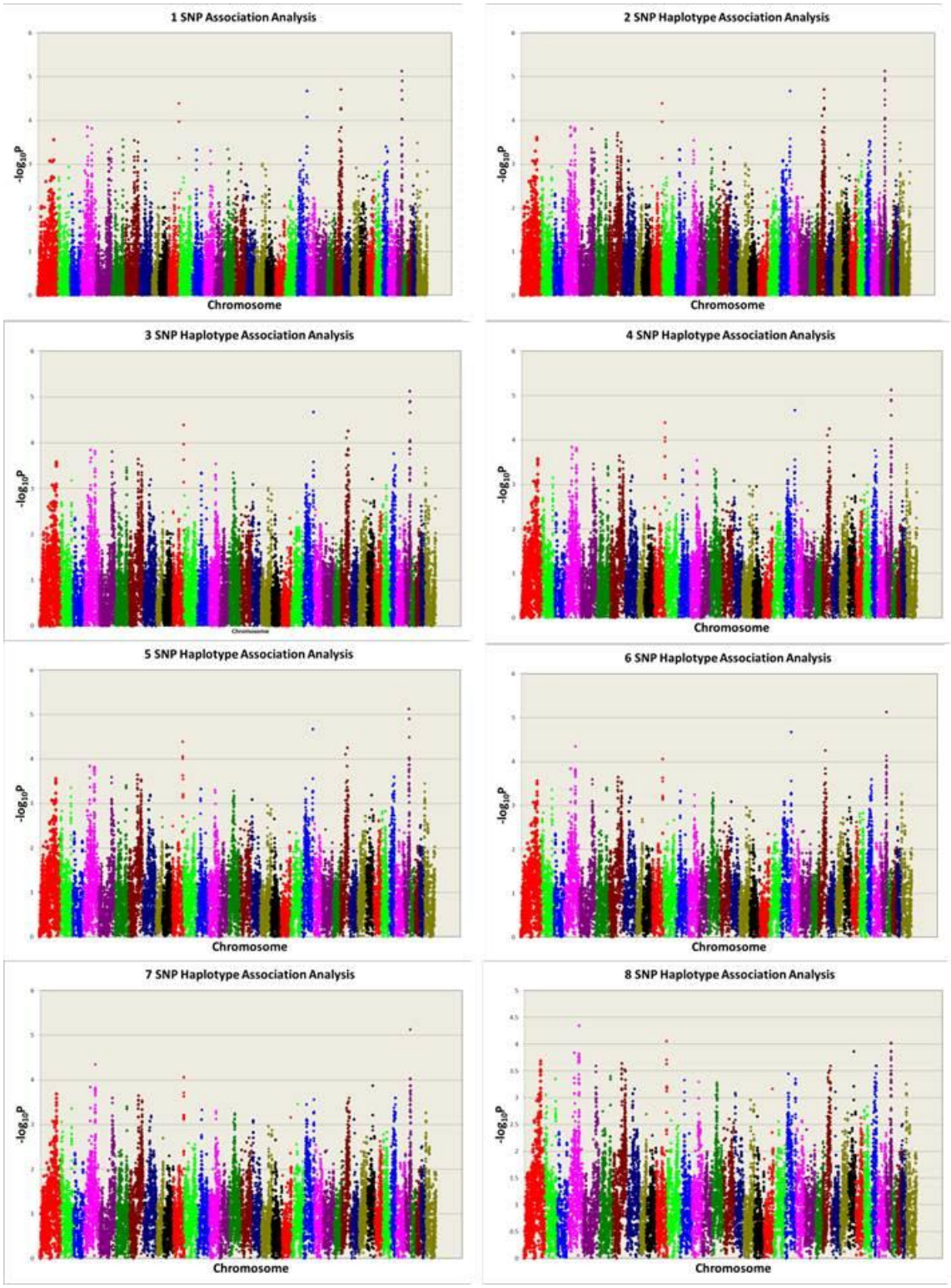

Figure A45. Haplotype association analysis. DDT: PCAG cases and PLD cases.

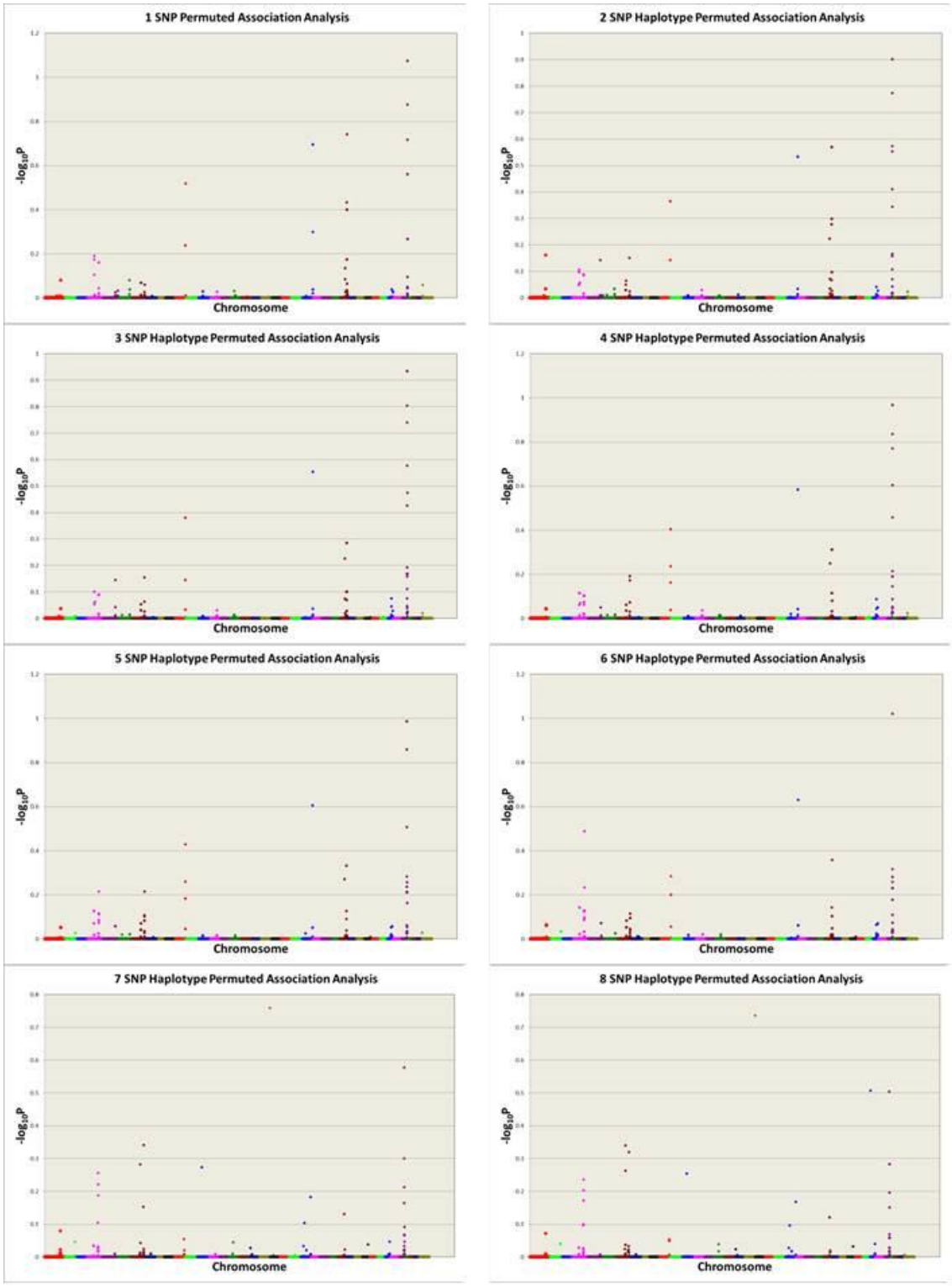

Figure A46. Haplotype permutation association analysis. DDT: PCAG cases and PLD cases.

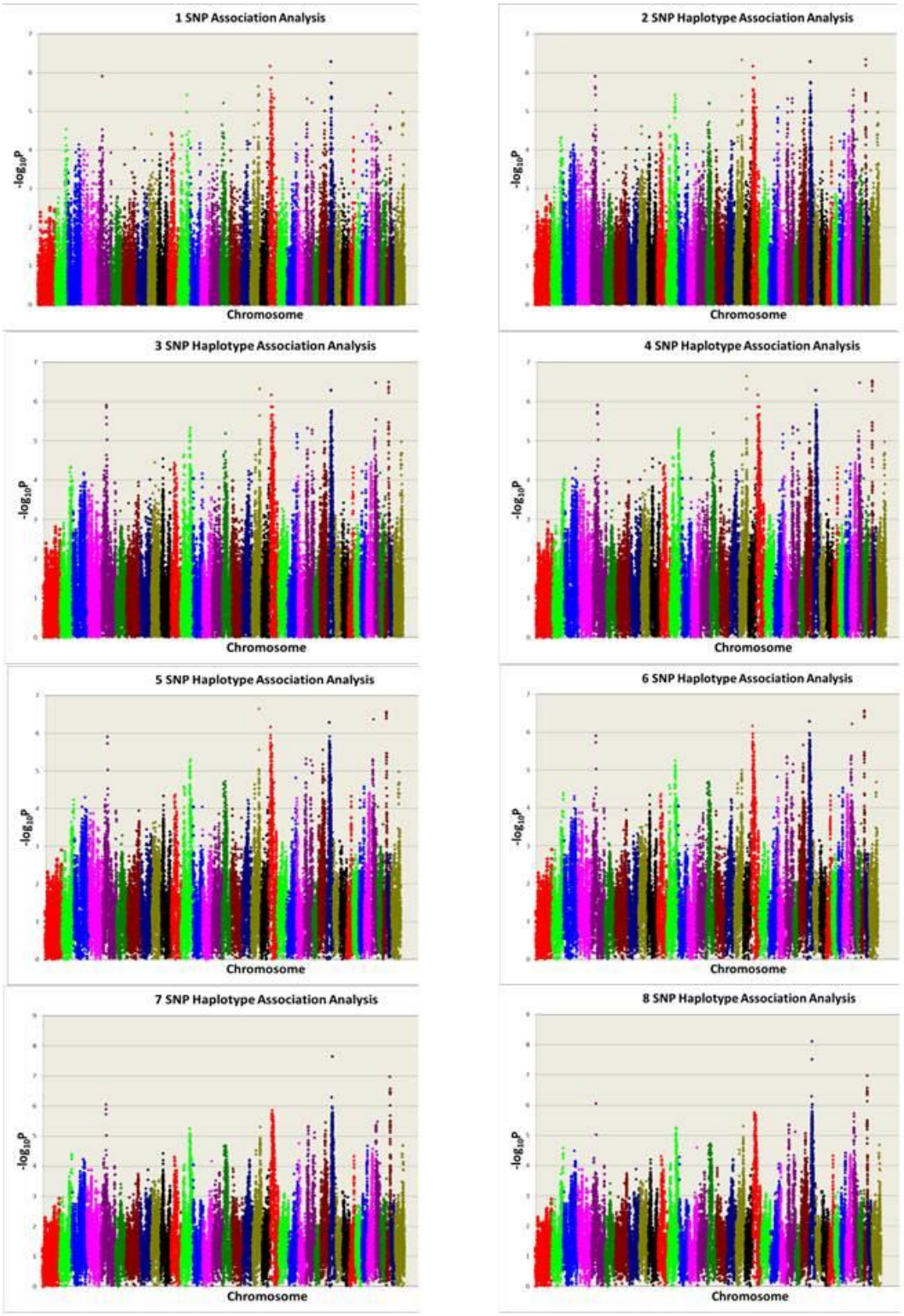

Figure A47. Haplotype association analysis. WSS: PCAG cases and controls.

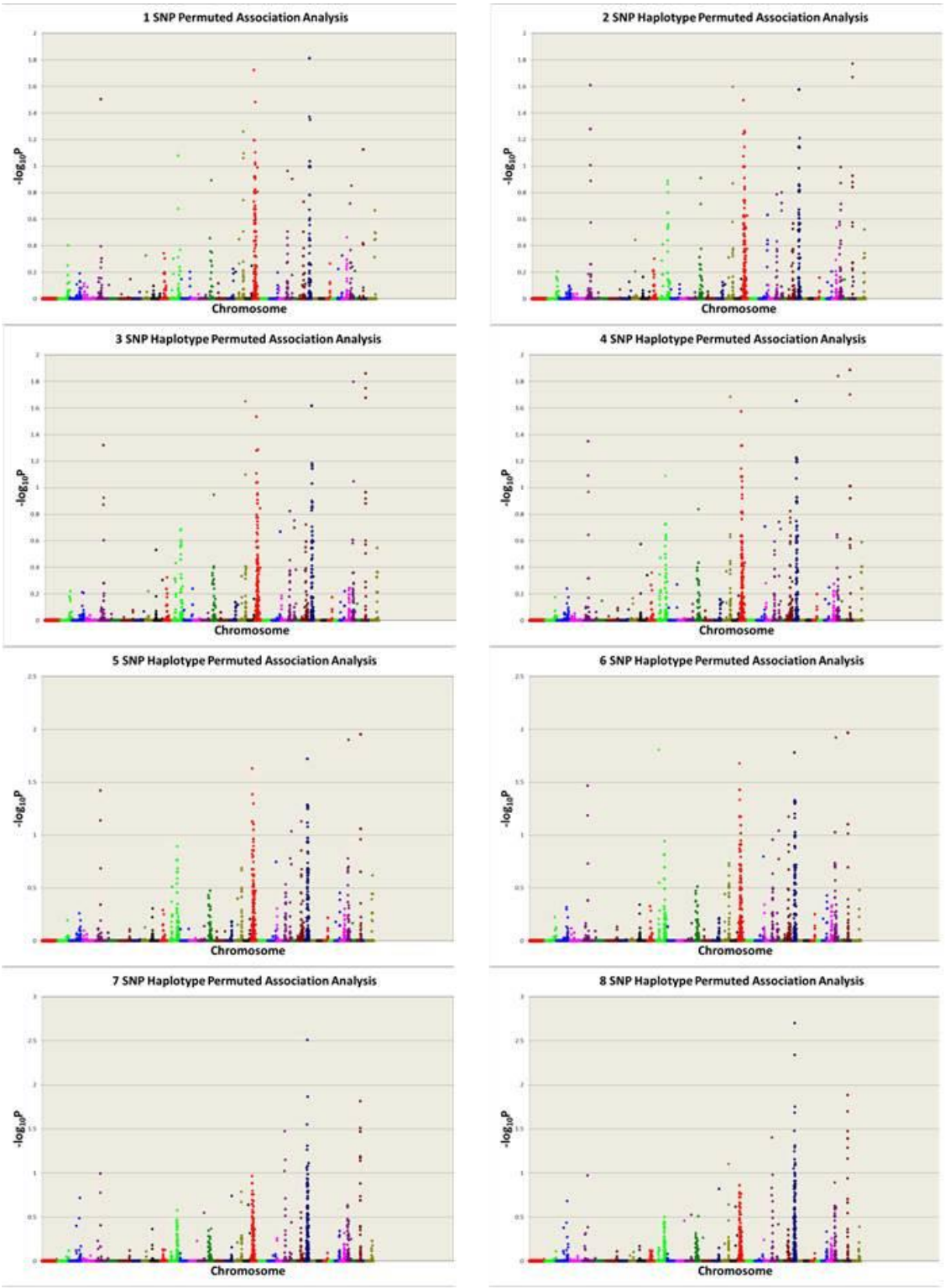

Figure A48. Haplotype permutation association analysis. WSS: PCAG cases and controls.

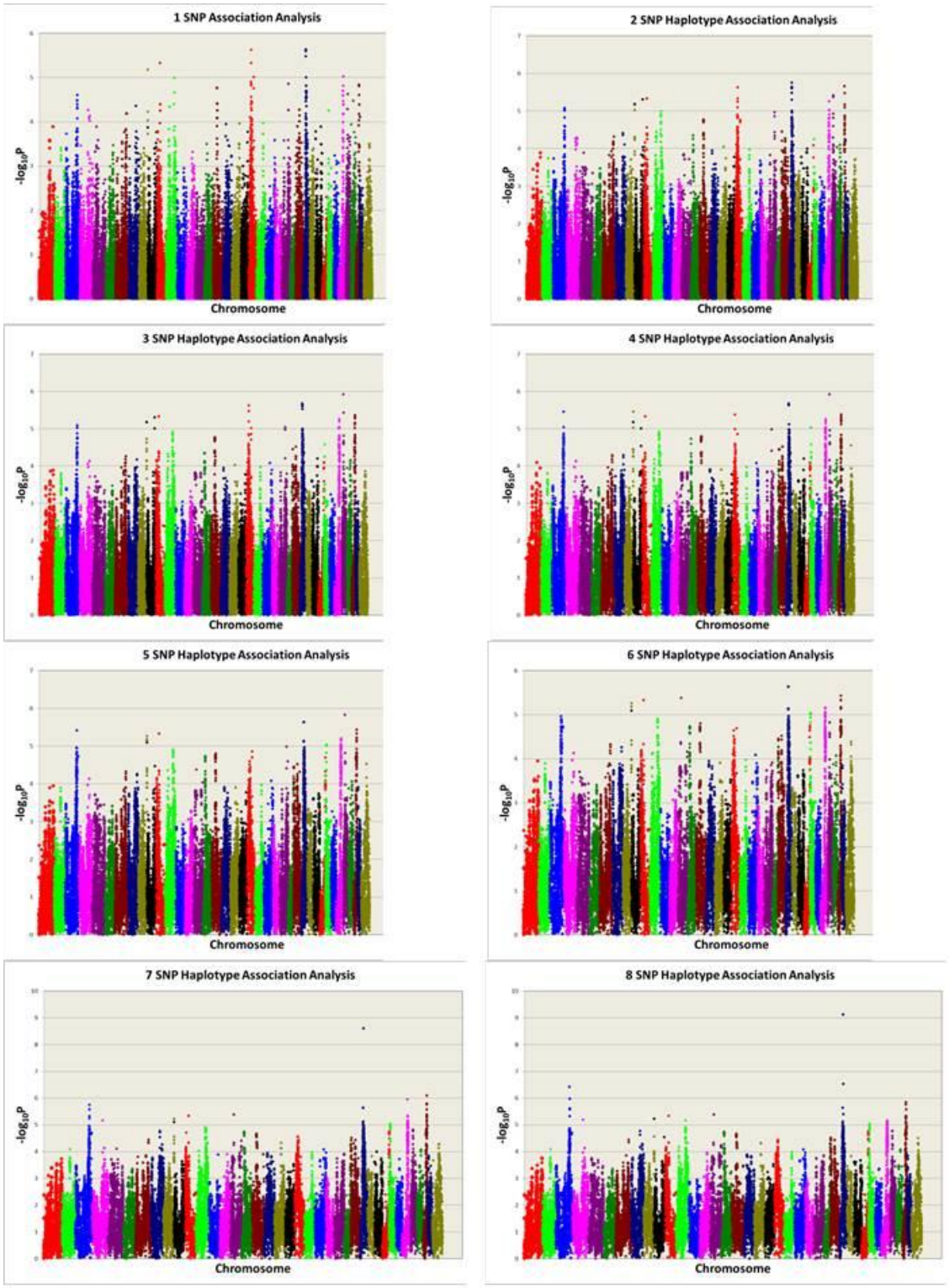

Figure A49. Haplotype association analysis. WSS: PCAG and PLD cases and controls.

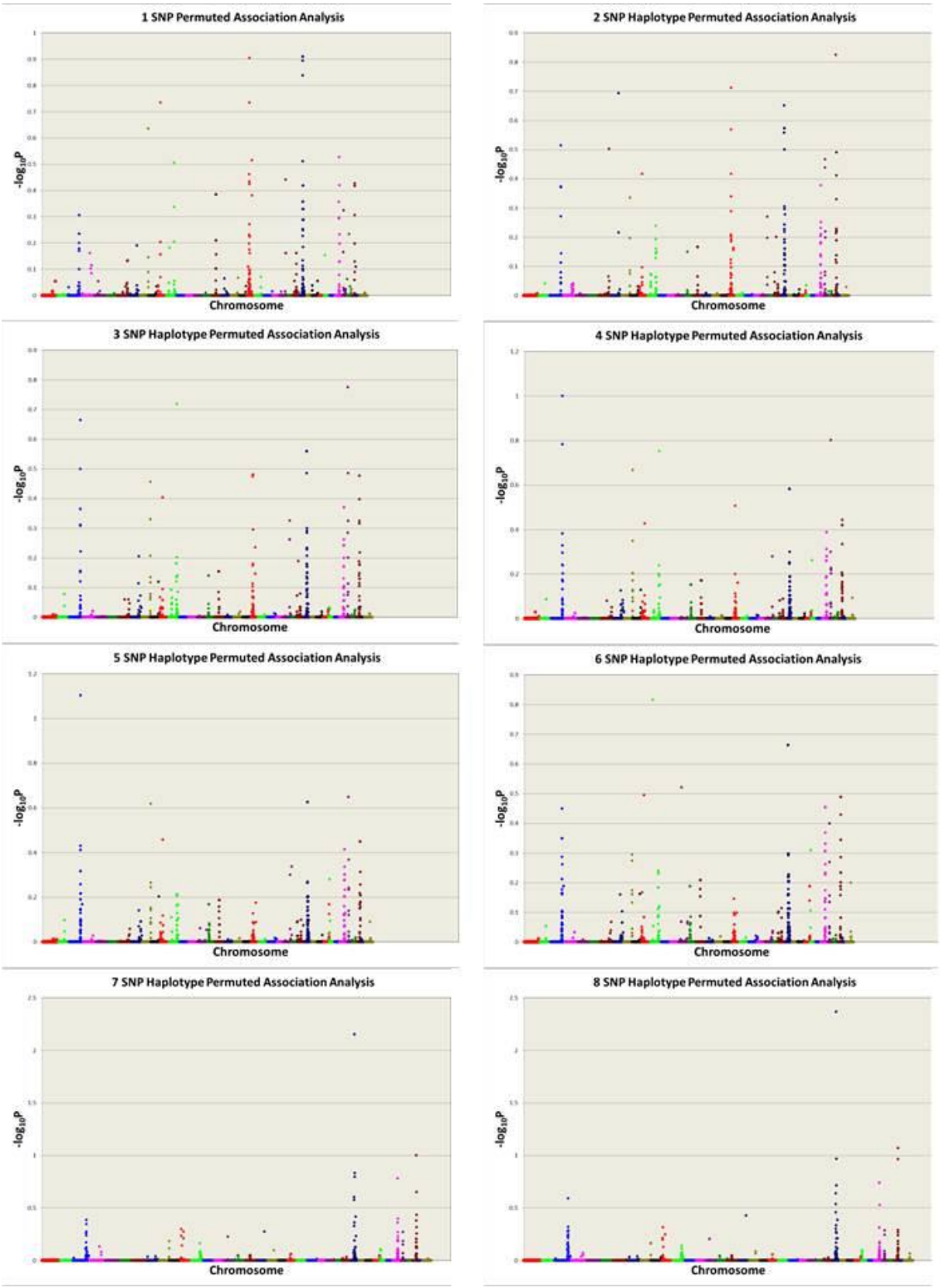

Figure A50. Haplotype permutation association analysis. WSS: PCAG and PLD cases and controls.

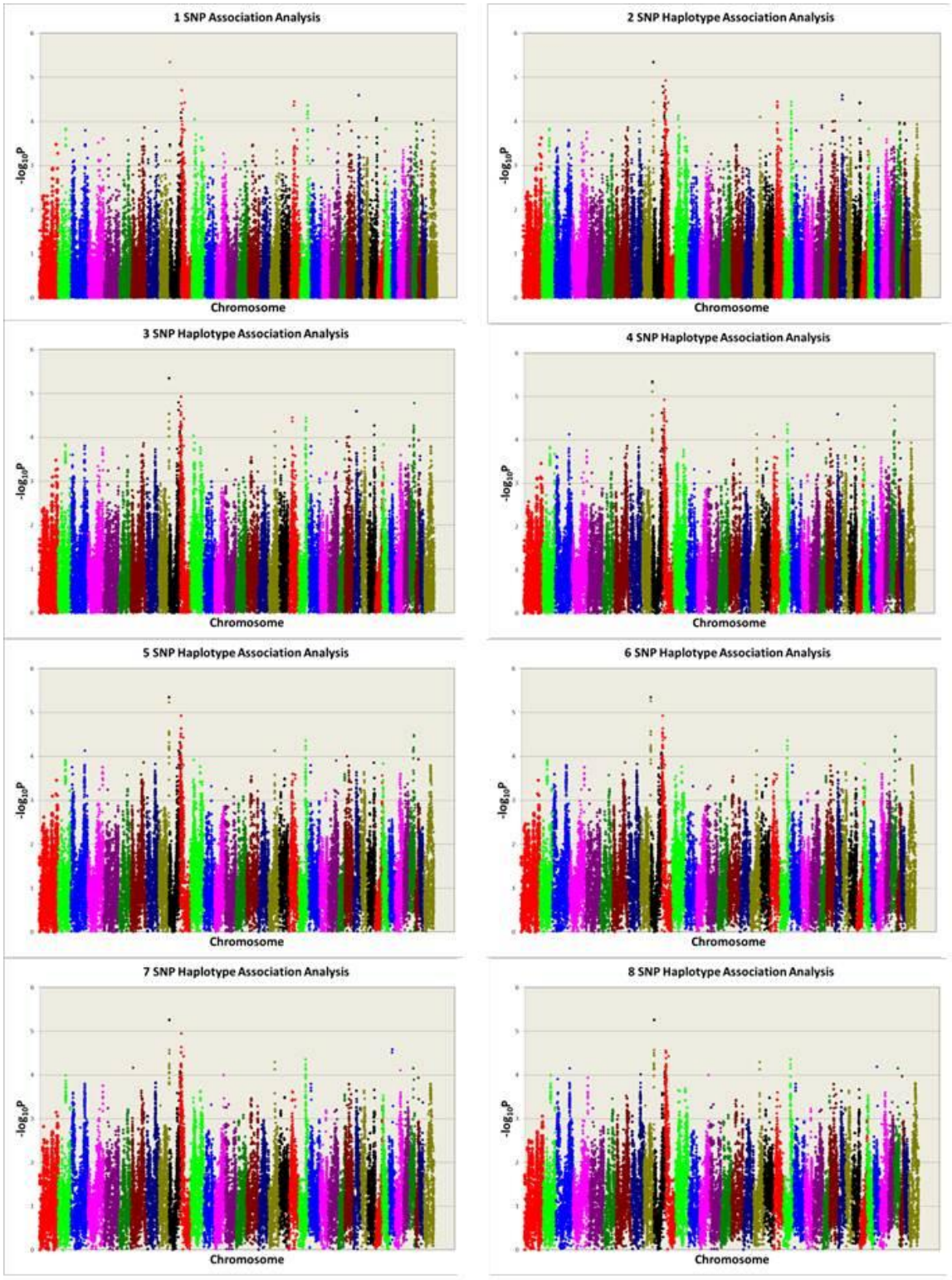

Figure A51. Haplotype association analysis. WSS: PLD cases and controls.

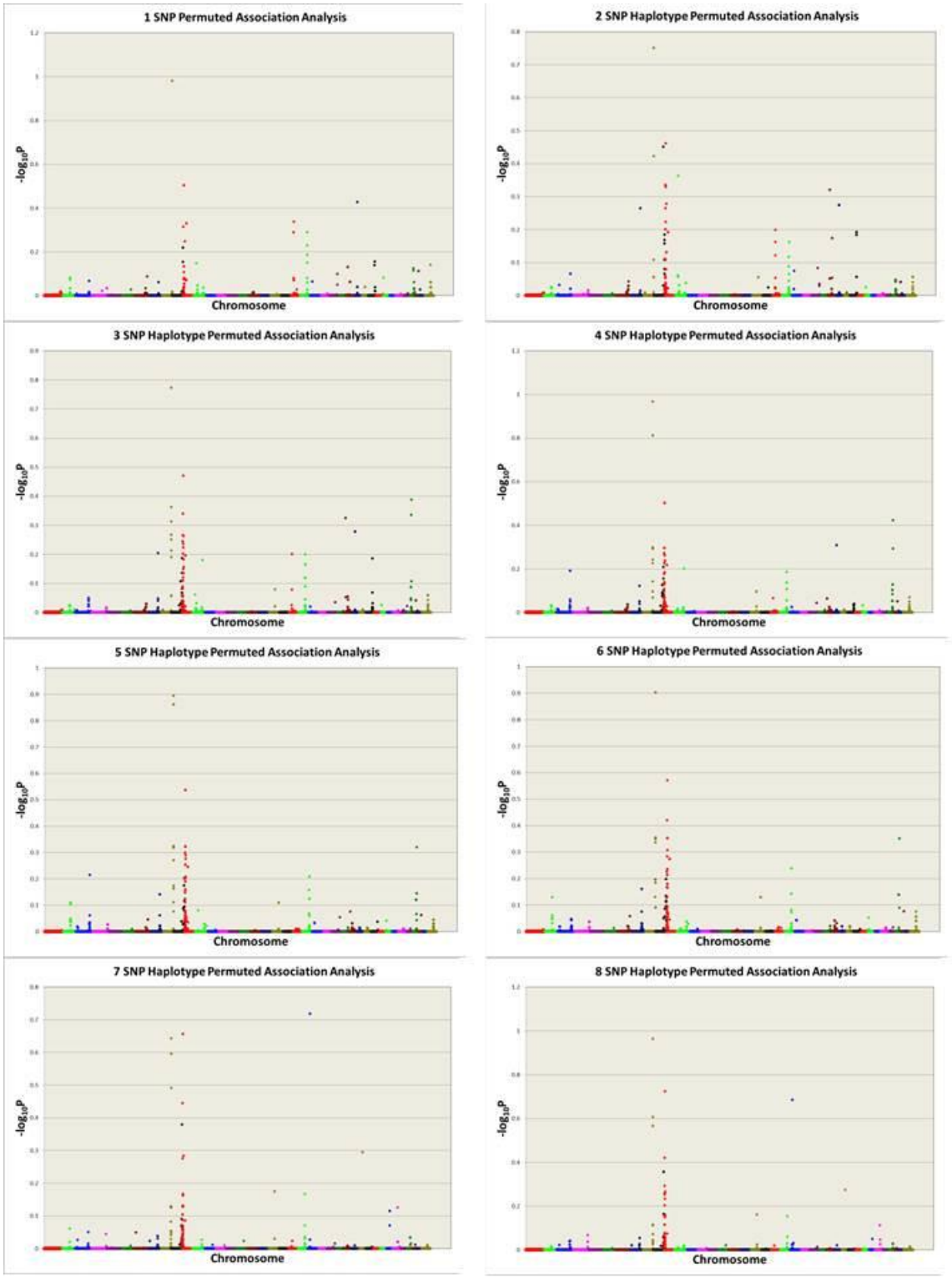

Figure A52. Haplotype permutation association analysis. WSS: PLD cases and controls.

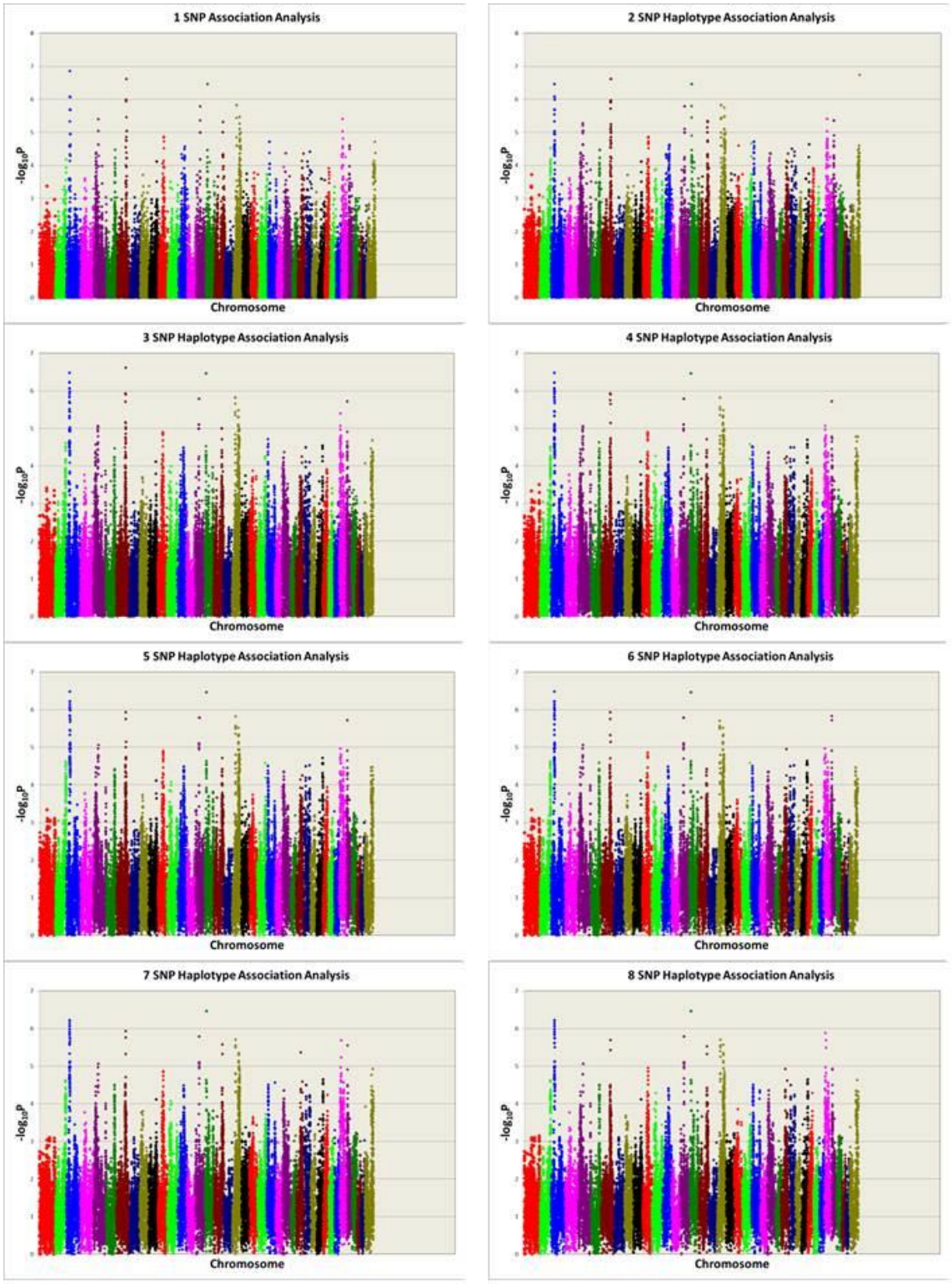

Figure A53. Haplotype association analysis. WSS: PCAG cases and PLD cases.

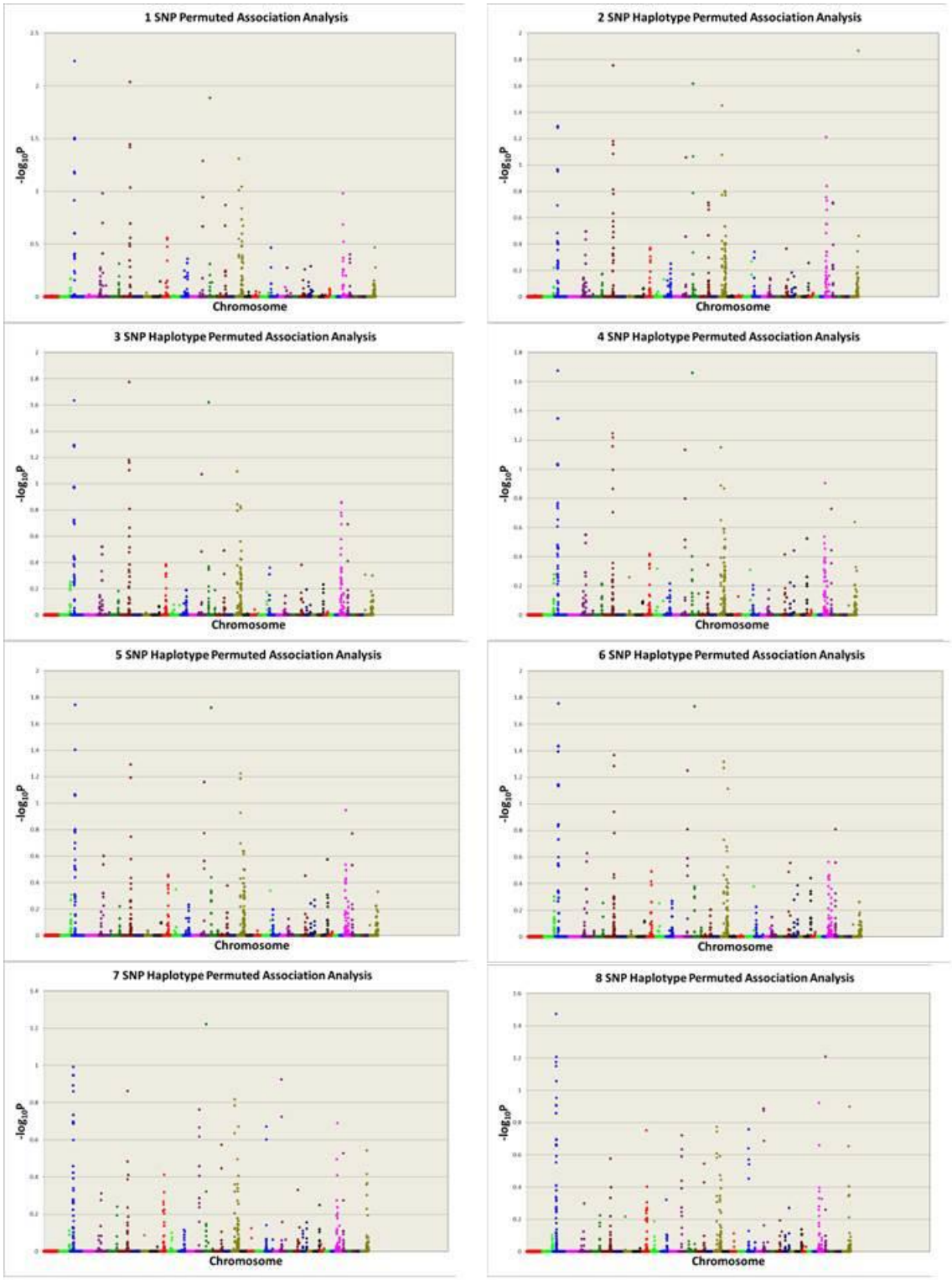

Figure A54. Haplotype permutation association analysis. WSS: PCAG cases and PLD cases.

VIII. Raw genotyping results (CD ROM)

Table A20. Microsatellite genotyping.

Table A22. Microsatellite genotyping.

Table A23. BH PCAG candidate variant genotyping results.

Table A24. FCR PCAG candidate variant genotyping results.

Table A25. DDT PCAG candidate variant genotyping results.

Table A26. WSS PCAG candidate variant genotyping results.